**Global analysis of the transcriptional regulation of *Sinorhizobium meliloti* cell cycle progression and study of cell cycle regulation during symbiosis with *Medicago sativa***

By

Nicole J. De Nisco

B.S. Biology
Massachusetts Institute of Technology, 2007

Submitted to the Department of Biology in Partial Fulfillment of the Requirements for the Degree of

DOCTOR OF PHILOSOPHY IN BIOLOGY
AT THE
MASSACHUSETTS INSTITUTE OF BIOLOGY

September 2013



Signature of Author: _____
Nicole J. De Nisco
Department of Biology
August 28, 2013

Certified by: _____
Graham C. Walker
Professor of Biology
Thesis Supervisor

Accepted by: _____
Stephen P. Bell
Professor of Biology
Co-Chair, Biology Graduate Committee

**Global analysis of the transcriptional regulation of S*inorhizobium meliloti* cell cycle progression and study of cell cycle regulation during symbiosis with *Medicago sativa***

By

Nicole J. De Nisco

Submitted to the Department of Biology
On August 28, 2013 in partial fulfillment of the requirements of the degree of Doctor of Philosophy in Biology at the Massachusetts Institute of Technology

## Abstract

The complex α-proteobacterial cell cycle regulatory network is essential not only for faithful replication and segregation of the genome, but also to coordinate unique cellular differentiation events that have evolved as adaptations to the different lifestyles of this diverse group of bacteria. The soil-dwelling α-proteobacterium, *Sinorhizobium meliloti,* not only has to accurately coordinate the replication of its tripartite genome, but also must undergo a dramatic cellular differentiation in order to form an effective symbiosis with the legume *Medicago sativa.* Preliminary analyses have indicated that plasticity in the *S. meliloti* cell cycle regulatory network may be essential to symbiosis, but cell cycle research in *S. meliloti* has been hindered largely by lack of a method to obtain synchronous populations of *S. meliloti.*

In this thesis, I present the first method to generate synchronous cultures of *S. meliloti.* I performed microarray gene expression analysis on synchronous populations of *S. meliloti* to gain a global view of transcriptional regulation of cell cycle events. This represents the first work of this kind done in an α-proteobacterium besides *Caulobacter crescentus,* which is the current model for α-proteobacterial cell cycle studies. The importance of transcriptional regulation of cell cycle progression was first discovered in *C. crescentus* and the work presented in this thesis highlights the conservation of cell cycle regulated gene expression in *S. meliloti.* I identified 462 cell cycle regulated transcripts in *S. meliloti,* which included genes involved in vital cell processes such as cell division, flagella biogenesis, replication and segregation of its tripartite genome as well as several putative cell cycle regulators. I compared the set of genes with cell cycle regulated transcripts identified in my analysis with the set identified in *C. crescentus* to generate a core set of 128 conserved genes demonstrating cell cycle regulated gene expression in both species. To determine which of the *S. meliloti* genes with cell cycle regulated transcripts might be part of the CtrA and DnaA regulons in *S. meiloti,* I performed CtrA and DnaA binding motif analysis. To understand the evolutionary significance of these CtrA and DnaA binding motifs, I looked at conservation of these motifs in homologous genes from several related α-proteobacteria. The results indicated that the putative CtrA regulon might be more evolutionarily constrained than the

putative DnaA regulon. Organisms more closely related to *S. meliloti* or with more similar lifestyles demonstrated a much greater conservation of the CtrA binding motifs identified in *S. meliloti.* The CtrA binding motifs in *S. meliloti* identified by my analysis were not at all well conserved in *C. crescentus,* which was the most distantly related α-proteobacteria surveyed. These differences in cell cycle regulated transcription and the putative CtrA regulon between *S. meliloti* and *C. crescentus* thus appear to represent specific adaptations to the distinctive genome and unique intracellular symbiotic lifestyle of *S. meliloti* and illustrate the importance of *S. meliloti* as a model for cell cycle regulation in α-proteobacteria with similar intracellular lifestyles.

The work presented in this thesis also describes the importance of CtrA regulation in *S. meliloti* during symbiosis with *M. sativa.* A crucial part of this symbiosis is a striking cellular differentiation (termed bacteroid differentiation), which includes changes in membrane permeability, cell elongation and branching, endoreduplication of the genome and loss of reproductive capacity and therefore a significant deviation from the free-living cell cycle program. Endoreduplication of the genome requires a decoupling of DNA replication and cell division, which could be achieved by down-regulation of the essential master cell cycle regulator CtrA. I tested the effects of CtrA depletion in *S. meliloti* and found that CtrA depletion induces a bacteroid-like state characterized by elongated and branched cells and highly elevated DNA content. I also show that *S. meliloti* CtrA has a comparable half-life to *C. crescentus* CtrA, but regulated proteolysis of CtrA may be different in the two species since we found CtrA proteolysis to be essential in *S. meliloti.* In addition, I demonstrate that the promoter and coding regions of *C. crescentus ctrA* cannot complement an *S. meliloti ctrA* chromosomal deletion during symbiosis even though they can do so in the free-living state. My attempts to identify the defects in the function *C. cresentus ctrA* promoter or coding region within *M. sativa* gave surprising results since *S. melioti* strains expressing *C. crescentus* CtrA from the *S. meliloti ctrA* promoter region and vice versa were able to establish an effective symbiosis with *M. sativa.* I discuss several possibilities to explain this apparent paradox, but further study is required to fully clarify this observation.

Taken as a whole, my thesis work represents a significant advancement to the field of cell cycle research in *S. meliloti* and α-proteobacteria as a whole. The cell synchronization method I developed will greatly facilitate more comprehensive analysis of cell cycle regulation in *S. meliloti.* My microarray gene expression analysis provides a global view of cell cycle regulated transcription in *S. meliloti,* which can be used in more in-depth explorations of specific mechanisms of transcriptional regulation of cell cycle events in *S. meliloti.* Lastly, my study of CtrA function in *S. meliloti* establishes the importance of CtrA regulation during symbiosis with *M. sativa.*

Thesis Advisor: Graham C. Walker
Title: Professor of Biology

**Acknowledgements**

I would like to thank my thesis advisor Graham for giving me the freedom to develop a project that was completely my own and really fostering my development as an independent scientist. Graham's unending zeal and scientific curiosity have been truly exciting and are traits I hope I hope to carry with me throughout my career. I would also like to thank Alan Grossman and Mike Laub who have formed the core of my thesis committee over the ears. Thank you for always making time for me and providing such excellent feedback during committee meetings. Your expertise made it possible for me to peruse the scientific questions that most interested me and develop my thesis project. I would also like to thank Tania Baker for her service on my committee and giving excellent feedback and support, as well as my outside committee member Peter Chien for always being so excited about my project (and science in general) and for giving such excellent suggestions that helped me to think more deeply about my work. I would also like to acknowledge my collaborator Emanuele Biondi for being such a pleasure to work with over the years.

Next I would like to thank the members of Walker lab for being such wonderful co-workers over the years. I would especially like to thank Jon Penterman for being such an awesome baymate and mentor. Our daily discussions contributed greatly to my growth as a scientist and I really admire your generosity and scientific curiosity. Also, thank you to Jon, Dan, Sanjay and Maarten for the perpetual comic relief – you have made the Walker lab a fun, if not extremely sarcastic workplace – never a dull moment. I would like to thank Brenda for organizing so many lab events and Asha for giving me such a wonderful rotation experience. I would also like to acknowledge my amazing UROP Max, who worked with me for 3 years. Teaching while doing science is one of the most fulfilling experiences I have had and Max was truly a joy to work with.

I would also like to thank my very close friends and colleagues Andre and Tracy. Going through graduate school together has made it such a rich experience and our late night philosophical discussions have helped me keep everything in perspective. I would also like to thank the rest of my MIT family (you know who you are) for being such amazing friends. I have truly made some of my best and I know lifelong friends at MIT and I am truly grateful to have y'all in my life.

Lastly I would like to thank my biggest supporters, my parents Tom and Nancy and my boyfriend Ernie. It was very difficult for my mom and dad to send me across the country and give me up to the Tech for 10 years. I am grateful everyday for their constant love and support. Finally, I would like to thank Ernie who is the most kind and supportive partner I could ask for. Thank you for holding my hand throughout all of this (even if from afar). I'm so blessed to have you in my life.

**Table of Contents**


Abstract……2
Acknowledgements……4
Chapter 1: Introduction……8
Rhizobia-legume symbiosis……8
*Nitrogen fixation in the biosphere*……8
*Mechanisms of host invasion in Rhizobia-legume symbiosis*……8
*Nodule development and bacteroid differentiation*……11
Cell cycle regulation in α-proteobacteria……16
*Diversity of the bacterial cell cycle*……16
*Cell cycle regulation in Caulobacter crescentus*……20
*Conservation of C. crescentus cell cycle regulatory network in S. meliloti* and other α-proteobacteria……25
References……29

Chapter 2: A novel method for cell synchronization of the legume symbiont *Sinorhizobium meliloti* and application towards global analysis of cell cycle regulated gene expression……34
Abstract……35
Introduction……36
Results……39
*Synchronization of S. meliloti cell populations via nutrient downshift*……39
*Microarray analysis of synchronized S. meliloti cultures identifies 462 cell cycle regulated transcripts*……40
*Several S. meliloti genes exhibit peak expression corresponding with the timing of their cellular function*……42
*Transcription of most putative cell cycle regulatory genes is activated later in the cell cycle*……46
*Blast and COG analysis reveals a core set of 128 genes with cell cycle regulated expression profiles conserved between C. crescentus and S. meliloti*……48
*Binding site analysis reveals conserved CtrA and DnaA binding sites among genes with cell cycle regulated transcripts*……49
Discussion……53
Experimental procedures……57
Acknowledgements……63
Supplemental tables……64
References……70

Chapter 3: Mechanisms of regulation of CtrA in *Sinorhizobium meliloti* during the free-living cell cycle and symbiosis with *Medicago sativa*……74
Abstract……75
Introduction……76
Results……80

*Depletion of CtrA in S. meliloti results in altered cell morphology and increased DNA content*....80
*The half-life of S. meliloti CtrA is similar to that of C. crescentus CtrA*...83
*A non-degradable allele of CtrA is lethal in S. meliloti*.....84
*C. crescentus ctrA can complement S. meliloti ctrA during free living growth, but not during symbiosis*.....85
*The symbiotic defect of BM146 is not caused by lack of expression of the C. crescentus ctrA promoter during symbiosis or differences in the coding region*.....88
Discussion and Future Directions....92
Experimental Procedures....95
Acknowledgements.....99
Supplemental tables.....100
References.....101

Appendix A: *Sinorhizobium meliloti* CpdR1 is critical for coordinating cell cycle progression and the symbiotic chronic infection.....104

Appendix B: The essential DivJ/CbrA kinase and PleC phosphatase system controls DivK phosphorylation and symbiosis in *Sinorhizobium meliloti*....144

Chapter 4: Conclusions and future work....186
How does CtrA regulate cell cycle progression in S. meliloti?....189
*Does CtrA regulate flagella biogenesis and chemotaxis during the cell cycle?*....189
*How is CtrA involved in regulation of the timing of cell division in S. meliloti?*....191
*Is CtrA a negative regulator of DNA replication initiation in S. meliloti?*....192
Mechanisms of CtrA regulation during the *S. meliloti* free-living cell cycle and during symbiosis....192
*Is CtrA phosphorylation governed by the same mechanism in S. meliloti as in C. crescentus?*.....193
*Is regulated proteolysis of CtrA essential in S. meliloti?*....195
*How is ctrA transcriptionally regulated during the cell cycle and symbiosis?*....195
References....198

**List of Figures and Tables**

Chapter 1: Introduction
Figure 1.1 Stages of Rhizobia-legume symbiosis....10
Figure 1.2 Comparison of the structure of indeterminate and determinate nodules....13
Figure 1.3 Bacteroid differentiation indeterminate vs determinate nodules.14
Figure 1.4 Modification to Rhzobial cell cycle during symbiosis....16
Figure 1.5 Regulation of replication initiation in *E. coli*....18
Figure 1.6 Asymmetric cell division of *C. crescentus* to produce two distinct cell types....19
Figure 1.7 *C. crescentus* Cell cycle Transcription Regulatory Network....22
Figure 1.8 Regulation of Replicative Asymmetry in *C. crescentus*....23
Chapter 2: A novel method for cell synchronization of the legume symbiont *Sinorhizobium meliloti* and application towards global analysis of cell cycle regulated gene expression
Figure 2.1 Synchronization of *S. meliloti* and microarray analysis of cell cycle regulated gene expression....41
Figure 2.2 Heatmaps of cell cycle gene expression of genes involved in various cellular processes....44
Figure 2.3 Expression profiles of *S. meliloti* homologs of *C. crescentus* cell cycle regulators....46
Figure 2.S3 Quantative PCR verification of *ctrA* gene expression during the cell cycle....47
Figure 2.4 Fuzzy clustering of genes with cell cycle regulated transcripts conserved between *S. meliloti* and *C. crescentus*....49
Figure 2.5 Conservation of putative CtrA and DnaA binding sites in cell cycle regulated genes.. ....51
Table 2.1 Samples and corresponding array file names....59
Table 2.S1 List of 462 genes with cell cycle regulated gene expression....64
Table 2.S4 Genes with cell cycle regulated transcripts conserved between *C. crescentus* and *S. meliloti*..... ....67
Table 2.S5A Conservation of CtrA binding motifs with cell cycle regulated transcripts... ....68
Table 2.S5B Conservation of DnaA binding motifs with cell cycle regulated Transcripts....69
Chapter 3: Mechanisms of regulation of CtrA in *Sinorhizobium meliloti* during the free-living cell cycle and symbiosis with *Medicago sativa*
Figure 3.1 Depletion of CtrA in *S. meliloti*....82
Figure 3.2 Flow cytometry analysis of CtrA depletion in *S. meliloti*....83
Figure 3.3 Pulse-chase analysis to determine CtrA half-life in *S. meliloti*....84
Table 3.1 Transduction of *ctrA* deletion in low-copy complemented strains.86
Figure 3.4 Symbiotic efficiency of complemented *ΔctrA* strains....88
Figure 3.5 Analysis of *C. crescentus ctrA* promoter or coding region defects within *M. sativa*....90
Table 3.2 Strains and Plasmids....100

## Chapter 1: Introduction

### Rhizobia-legume symbiosis

#### *Nitrogen fixation in the biosphere*

Nitrogen is one of the most limiting elements for biological growth despite the abundance of di-nitrogen gas ($N_2$) in the atmosphere. The maintenance of levels of biologically available nitrogen depends on the conversion of atmospheric nitrogen to fixed nitrogen (i.e. $NH_3$). Biological nitrogen fixation is by far the largest contributor to the pool of fixed nitrogen in the biosphere (1). All known nitrogen-fixing organisms (diazatrophs) are prokaryotes and their ability to fix nitrogen is dependent on the nitrogenase enzyme system. The chemistry carried out by the nitrogenase enzyme to convert $N_2$ to $NH_3$ is both energetically expensive and oxygen sensitive. For this reason the most efficient diazatrophs are symbionts and their plant hosts provide both the large amounts of energy and microaerobic environment required for nitrogen fixation (2). The three major nitrogen-fixing symbiotic systems include the rhizobia-legume and *Frankia*-actinorhizal symbiosis, which both involve soil bacteria, and the *Nostoc*-*Gunnera* symbiosis, which involves aquatic cyanobacteria. Of these three systems, the symbiosis between rhizobia and their legume hosts is the most thoroughly studied (2).

#### *Mechanisms of host invasion in Rhizobia-legume symbiosis*

*Sinorhizobium meliloti* is an especially important model organism used to study rhizobia-legume symbiosis. *S. meliloti* is a gram-negative α-proteobacterium that forms a nitrogen fixing symbiosis with legumes of the *Medicago, Melilotus and Trigonella* genera (3). *S. meliloti* is peritrichously flagellated and has a tripartite

genome consisting of a 3.6Mb chromosome and two symbiotic megaplasmids, pSymA (1.35Mb) and pSymB (1.68Mb) (4, 5). My thesis work has focused on the symbiosis between *S. meliloti* and agriculturally important *Medicago sativa,* commonly known as alfalfa. A signal interchange between the rhizobial symbiont (*S. meliloti)* and the root cells of the legume host (*M. sativa)* mediates the initiation of this symbiosis (Figure 1.1).

Leguminous plants secrete flavonoid compounds (2-phenyl-1,4-benzopyrone derivatives) into the soil. *M. satvia* specifically secretes the flavonoid luteolin, which binds to and activates the *S. meliloti* Nod protein NodD1 (6). Activated NodD1 stimulates the transcription of *nod* genes, which encode enzymes required for the synthesis of lipochitooligosaccharide Nod factors. The core of the Nod factor structure is encoded by the *nodABC* genes while the *nol* and *noe* genes encode enzymes that make modifications to Nod factors, which determine host specificity (7). These Nod factors are in turn secreted by *S. meliloti* and induce responses required for the invasion of *M. sativa,* such as rearrangement of the root hair cytoskeleton leading to root hair curling and re-initiation of mitosis in root cortical cells forming meristem cells that will comprise the initial nodule primordium (Fig. 1.1) (7, 8).

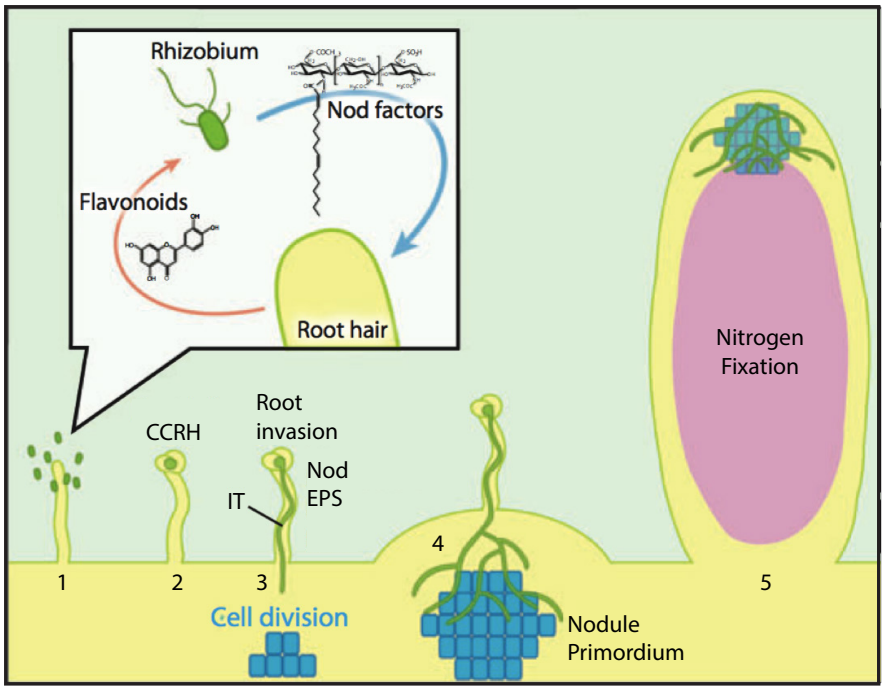


**Figure 1.1 Stages of Rhizobia-legume symbiosis.** From left to right: 1. Signal interchange between rhizobium and legume root hairs initiates infection 2. Root hair curling traps rhizobia 3. Rhizobia invade root hair cells via infection threads (IT) and plant cortical cell division is induced 4. ITs ramify and nodule begins to form 5. Rhizobia are deposited in nodule cells and differentiate into nitrogen fixing bacteroids. Adapted from (9).

Root hair curling facilitates infection by trapping *S. meliloti* in a colonized curled root hair (CCRH). Once inside the CCRH, *S. meliloti* can invade root hair cells by initiating the formation of a host-derived infection thread (IT) (10). This process requires both the secretion of Nod factors and the production of the expolysaccharides, succinoglycan (EPSI) and/or galactoglucan (EPSII) by *S. meliloti* (3). Succinoglcan is a polymer composed of repeating octasaccharide subunits that have acetyl, succinyl and pyruvyl modifications (11). *S. meliloti exo* mutants, which are unable to synthesize genes succinoglycan, cannot induce infection thread formation in *M. sativa* or produce aborted infection threads (12). The nodules produced by plants infected with these *exo* mutants are devoid of bacteroids and unable to fix nitrogen (12). Mutations in the *nod* genes that cause the production of structurally incomplete Nod factors can also yield aberrant, abortive infection threads (13). The exact mechanism by which EPS and Nod factors mediate the

remodeling of the cytoskeleton of the plant cells during infection thread formation has yet to be elucidated.

Once inside the infection thread (IT), *S. meliloti* coordinates cell division with IT extension to invade deeper plant tissues (3). Upon reaching the specialized endoploid plant cortical cells (enlarged cells with an endoreduplicated genome) of the nodule primordium, the IT ramifies substantially (Fig 1.1). This ramification allows for the eventual infection of several endoploid cells by a single infection thread. The endoreduplication of these plant cortical cells is required for symbiosis and it has been postulated that polyploidy allows for increased transcription rates and metabolism necessary to support nitrogen fixation (8). Intracellular infection occurs by a process similar to endocytosis in which the bacterial cells are delivered to the host cytoplasm and are surrounded by the host membrane in a compartment termed the symbiosome (9). An *S. meliloti* gene found to be important for endocytosis is *hemA.* An *S. meliloti hemA* mutant that is defective primarily in heme biosynthesis is released from the infection threads but not encapsulated within symbiosomes (14). Within the symbiosome *S. meliloti* differentiates into a nitrogen-fixing bacteroid.

***Nodule development and bacteroid differentiation***

Two types of nodules are induced in Rhizobia-legume symbioses. Legumes of the inverted repeat-lacking clade (IRLC), such as *M. sativa,* form indeterminate nodules, while non-IRLC legumes form determinate nodules (Fig. 1.2) (9). These nodules differ in both their structure and the fate of their Rhizobial symbionts. Indeterminate nodules are characterized by a persistent meristem that leads to

zonation of the nodule and continued growth during symbiosis (Fig 1.2). In the determinate nodule, meristemic activity is lost and zonation does not occur (15). The zonation of an indeterminate nodule represents specific stages of bacteroid differentiation. Zone I is the bacteroid-free meristemic zone from which the nodule elongates during growth. Rhizobia are delivered to nodule cells via infection threads and endocytosed by these cells in the infection zone (Zone II). Bacteroid differentiation occurs in the interzone between Zone II (infection zone) and Zone III (nitrogen fixation zone). Zone III harbors fully differentiated bacteroids that are able to express the enzymes of the nitrogenase complex and fix nitrogen (16).

Another requirement for nitrogen fixation in differentiated bacteroids is the production of leghaemoglobins by the plant, which gives the pink or red color characteristic of nitrogen fixing bacteroids. These leghaemoglobins are oxygen-binding proteins that help to produce the microaerobic environment in nodules required for the function of the nitrogenase enzyme (17). *S. meliloti* also requires a constant carbon source during bacteroid differentiation and in order to provide the energy for nitrogen fixation. During bacteroid differentiation *S. meliloti* utilizes stores of polyhydroxybutyrate that are synthesized during the time it is in the infection thread, while fixed carbon in the form of dicarboxylic acids is provided to *S. meliloti* by the plant during nitrogen fixation (18, 19). Finally in Zone IV, the senescent zone, bacteroids are no longer metabolically active and do not fix nitrogen (16).

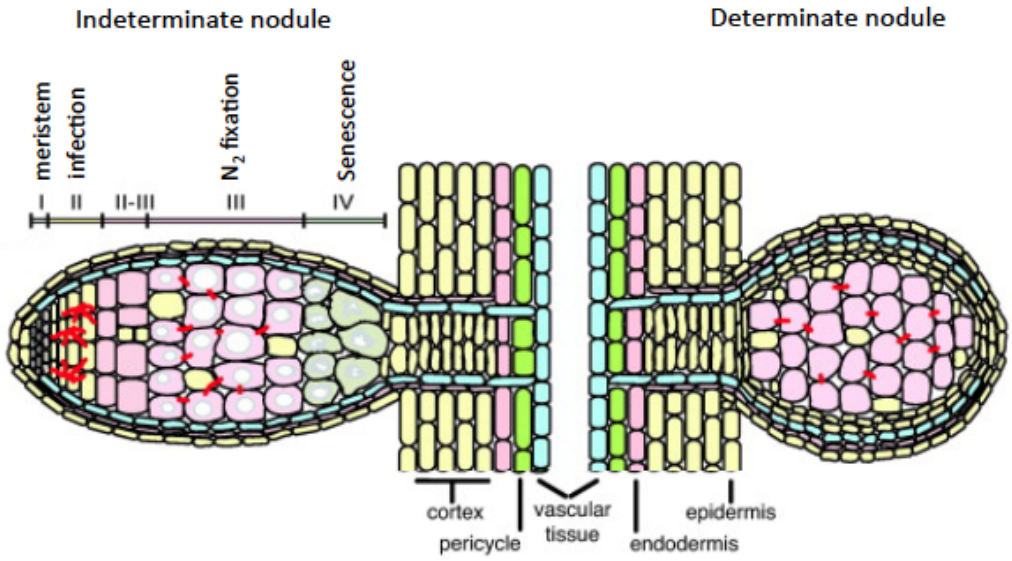


**Figure 1.2 Comparison of the structure of indeterminate and determinate nodules.** Indeterminate nodules (left) continuously grow from a persistent meristem (Zone I) producing a distinct zonation. Rhizobia are delivered into host cells via infection threads (pictured in red) in Zone II. Bacteroid differentiation occurs in interzone II-III and in zone III bacteroids fix nitrogen. The senescent zone (IV) houses bacteroids that are no longer metabolically active. Determinate nodules lack a persistent meristem and do not undergo this zonation, harboring nitrogen-fixing bacteroids in the entire nodule. Adapted from (15).

In addition to their distinct nodule structures, there are striking differences between the bacteroids produced in indeterminate and determinate nodules. In non-IRLC legumes, bacteroids retain the characteristics of free-living bacteria except for the metabolic changes required for nitrogen fixation. Because these bacteroids retain the ability to divide, there are often multiple bacteroids per symbiosome (Fig. 1.3) (20). Bacteroid differentiation in IRLC legumes is mediated by a group of more than 300 nodule specific cysteine rich peptides (NCR), which are very similar to defensin-like antimicrobial peptides (AMPs). In various host-microbe systems, AMPs have been shown to alter membrane permeability and inhibit cell division in the invading microbe (21). The genes encoding NCR peptides are only found in IRLC legumes and their expression is restricted to Rhizobium-infected plant cells (22).

Exposure to NCR peptides within the nodule leads to cell bacteroid enlargement, increased membrane permeability, endoreduplication of the genome and a loss of viability outside the nodule. Bacteroid enlargement often results in branching (Fig. 1.3). Symbiosomes in indeterminate nodules only contain a single bacteroid that is tightly surrounded by the host-derived peribacteroid membrane (PBM) (9). As a result of endoreduplication of the genome, bacteroids can accumulate a DNA content of up to 24N (20). Endoreduplication requires a de-coupling of DNA replication and cell division and therefore a diversion from the normal cell cycle program.

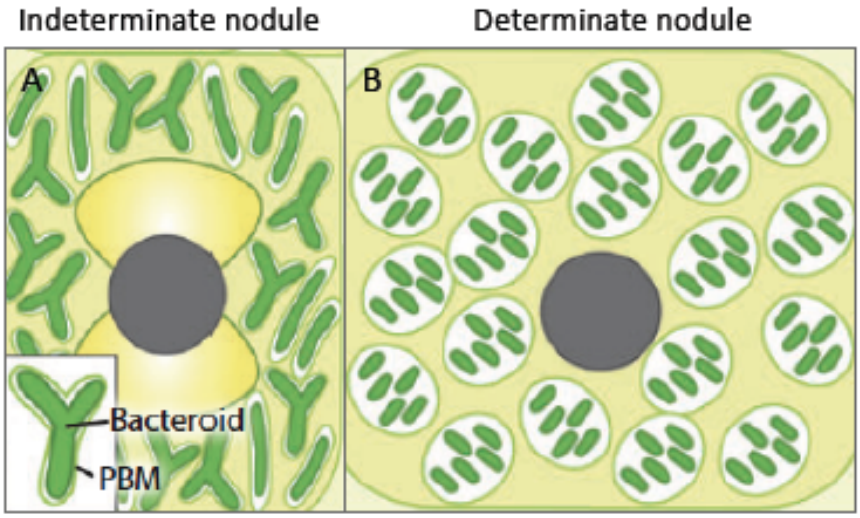


**Figure 1.3 Bacteroid differentiation in indeterminate vs. determinate nodules.** (A) Bacteroids within indeterminate nodules are elongated and sometimes branched. There is a single bacteroid per symbiosome that is tightly surrounded by the host-derived peribacteroid membrane (PBM). (B) Bacteroids within determinate nodules maintain the size and shape of free-living bacteria. There are multiple bacteroids per symbiosome reflecting the ability of bacteroids in indeterminate nodules to keep dividing within the symbiosome. Adapted from (9)

Both legume and rhizobial factors have been identified that are necessary for this NCR peptide mediated bacteroid differentiation. The *M. truncatula* gene *dnf1-1* is required for delivery of NCR peptides to bacteroids and thus bacteroid differentiation. The *dnf1-1* gene encodes a nodule specific component of the signal

peptidase complex and is required to remove the signal peptide from secretory proteins in the endoplasmic reticulum (ER), which is essential for the proper targeting of these proteins (23). Thus NCR peptides are delivered to bacteroids by the secretory pathway in nodule cells. The *S. meliloti* gene *bacA* is also required for bacteroid differentiation. *S. meliloti* mutants lacking functional BacA are able to infect *M. sativa* and *M. truncatula* and are endocytosed into the symbiosome, but lyse within the symbiosome and do not differentiate into functional bacteroids (24). The function of the *bacA* homologs of the mammalian pathogens, *Brucella abortus* and *Mycobacterium tuberculosis* is essential for chronic murine infections (25, 26). The requirement for BacA function during rhizobia-legume symbiosis is due to a protective effect this protein has against the activities of host NCR peptides and it is thought that the homologs of BacA are also protective against mammalian AMPs during *B. abortus* and *M. tuberculosis* pathogenesis (27).

Bacteroid differentiation is mandatory for a functional symbiosis between *S. meliloti* and its legume hosts, *M. truncatula* and *M. sativa.* A crucial part of this differentiation is endoreduplication of this genome, which requires a significant deviation from the normal rhizobial cell cycle program (Figure 1.4). Instead of initiating DNA replication only once per cell cycle, the bacteroid is stuck in an S-phase loop and enlarges and branches instead of dividing (Figure 1.4). This deviation suggests that major regulatory changes to the *S. meliloti* cell cycle network occur during symbiosis, possibly mediated by host NCR peptides. How NCR peptides interfere with specific cell targets to alter the rhizobial cell cycle is an outstanding question in this field. This question has been left unanswered partially because little

is known about the specific regulation of the *S. meliloti* cell cycle. The aim of my thesis work has been to both make *S. meliloti* a more tractable organism for cell cycle research and to further the investigation of cell cycle regulation in *S. meliloti.*

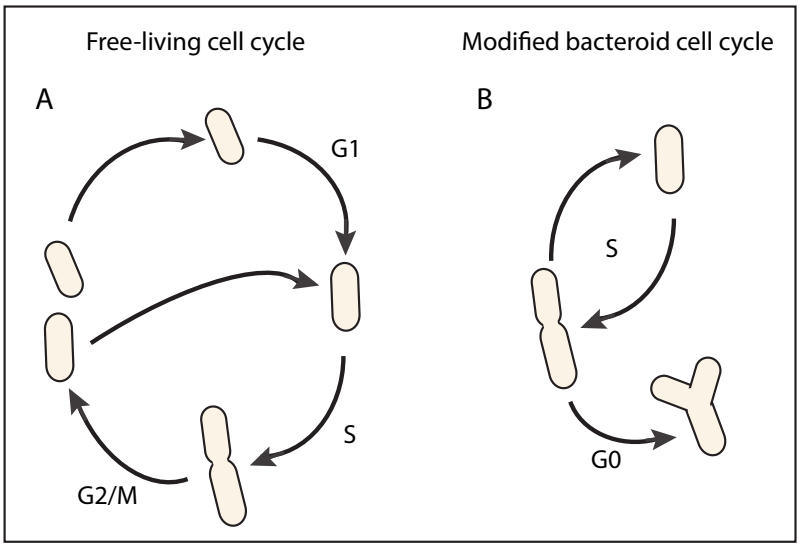


**Figure 1.4 Modification to Rhzobial cell cycle during symbiosis.** (A) During the free-living cell cycle *S. meliloti* replicates its genome(chromosome, pSymA and pSymB) once per division cycle. *S. meliloti* divides asymmetrically producing a larger mother cell that begin S phase immediately and a smaller daughter cell that is in G1 (reviewed below in *Cell Cycle regulation in α-proteobacteria*). (B) *S. meliloti* bacteorids have an altered cell cycle where they undergo subsequent rounds of DNA replication without cell division until a terminally differentiated endoploid cell is produced.

## Cell Cycle Regulation in α-proteobacteria

### *Diversity of the bacterial cell cycle*

Cell cycle regulation in bacteria is as diverse as the organisms that comprise this domain of life. The processes that govern DNA replication, segregation and cytokinesis have only been thoroughly studied in a handful of model organisms including *Escherichia coli, Bacillus subtilis, and Caulobacter crescentus.* A critical point of cell cycle regulation is the initiation of DNA replication. Regulation of this

step can determine the periodicity of DNA synthesis and helps to coordinate DNA replication with cell growth, chromosome segregation and cell cytokinesis (28). In *E. coli,* the initiation of replication occurs at the chromosomal origin of replication termed the *oriC* (29). Initiation of replication depends on transcription by RNA polymerase and the activity of DnaA. DnaA is a highly conserved $AAA^+$ ATPase (ATPase associated with various activities) that is related to eukaryotic Orc initiation proteins (28, 30). DnaA is highly conserved and required for the initiation of DNA replication in several organisms including *E. coli, B. subtilis, C. crescentus* and *S. meliloti* (31). ATP-bound DnaA (DnaA-ATP) initiates replication by binding to the origin or replication and melting the duplex DNA, which allows the loading of the replicative helicase DnaB and the clamp loader DnaC (28).

In *E. coli,* immediate re-initiation of DNA replication is prohibited by the DNA-binding protein SeqA. This is necessary because DnaA-ATP is not immediately hydrolyzed to DnaA-ADP during initiation. SeqA binds to hemimethylated GATC sites in the origin thus inhibiting a second DnaA-ATP binding event and delaying the methylation of the nascent strand by Dam methylase (32, 33). Post initiation levels of DnaA-ATP are kept low by two mechanisms: stimulated hydrolysis to DnaA-ADP by Hda and titration of DnaA-ATP away from the origin by other chromosomal DnaA binding sites (34). These regulatory mechanisms are illustrated in Figure 1.5. In *B. subtilis* re-initiation of DNA replication is prevented by YabA, which is similar to *E. coli* Hda and binds both DnaA and the sliding clamp (DnaN) (35).

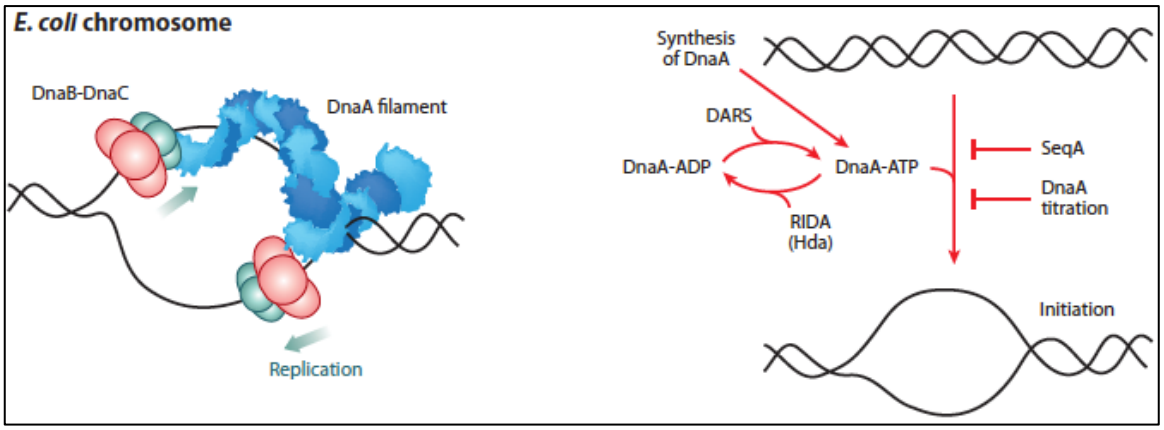


**Figure 1.5 Regulation of replication initiation in *E. coli.*** The loading of two helicase complexes (DnaB-DnaC) directs bidirectional replication at the *oriC* in *E. coli.* Loading of DnaB-DnaC is facilitated by DnaA-ATP which binds and melts the *oriC.* The processes that regulate DnaA-ATP levels and activity are outlined on the right side of the diagram. The synthesis of DnaA and the binding of Dna-ADP to DnaA-reactivation sequences termed DARS cause the accumulation of DnaA-ATP while Hda stimulates conversion of DnaA-ATP to DnaA-ADP and SeqA blocks DnaA binding to the origin by binding to hemimethylated GATC sites. Adapted from (28)

Although both *B. subtilis* and *E. coli* have mechanisms to prevent immediate re-initiation of replication, they can initiate multiple rounds of DNA replication within a single growth cycle in fast-growing conditions. To facilitate fast doubling times, these organisms must initiate new rounds of DNA replication before termination of the first round because the time needed for chromosome replication and cell division is fixed. It is thought that total chromosomal DNA concentration may have a role in regulating the number of re-initiations of DNA replication, but the exact mechanism is unknown (28).

Unlike E. coli *and B. subtilis*, *C. crescentus* and other α-proteobacteria replicate their DNA "once and only once per cell cycle" independent of growth rate. This was first demonstrated molecularly by measuring unmethylated DNA. A second round of DNA replication during a single cell cycle would produce a second completely unmethylated strand of DNA. Unmethylated DNA is nearly undetectable

in *C. crescentus* with only 0.1% unmethylated DNA produced near the replication origin (36). α-proteobacteria also exhibit asymmetric cell division, which is not observed in gamma-proteobacteria such as *E. coli* and gram positive bacteria like *B. subtilis* (37). *C. crescentus* divides asymmetrically to produce two morphologically and functionally different cells (Figure 1.6). The stalked cell is non-motile and displays a polar stalk specialized for attachment. The swarmer cell has a single polar flagellum along with several pili and is motile (38). After cell division, the stalked cell immediately initiates DNA replication while the swarmer cell receives a non-replicating chromosome and remains in G1. In a sufficiently nutrient-rich environment, the swarmer cell differentiates into a stalked cell—ejecting its polar flagellum and developing a stalk its place—and initiates DNA replication (39). During the end of S-phase in a predivisional cell a new flagellum is assembled at the nascent swarmer pole (Figure 1.6) (38).

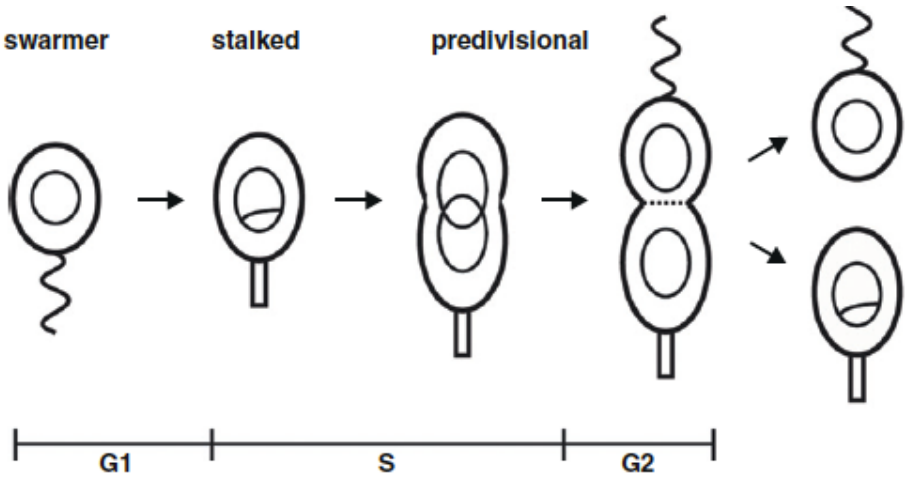


**Figure 1.6 Asymmetric cell division of *C. crescentus* to produce two distinct cell types.** Each divison of *C. crescentus* produces a swarmer and a stalked cell. The stalked cell is able to immediately re-enter the cell cycle and initiate DNA replication while the swarmer cell is stuck in G1 and must differentiate into a stalked cell before initiating DNA replication. Adapted from (40).

Asymmetric cell division has also been demonstrated in the α-proteobacteria *S. meliloti, Agrobacterium tumefaciens* and *Brucella* species. The morphological asymmetry is not as distinct as *C. crescentus,* but each division produces a larger mother cell and a smaller daughter cell (37). Consequently, α-proteobacteria have a specialized network to regulate the "once and only once" initiation of replication and the development of morphological asymmetry, which I will describe in detail below.

***Cell Cycle Regulation in C. crescentus***

The *C. crescentus* cell cycle is controlled by a complex regulatory network. The essential response regulator CtrA coordinates morphological and replicative asymmetry, while DnaA governs the periodicity of replication (41, 42). CtrA belongs to the two-component response regulator class of proteins, which are ubiquitous among bacteria and play important roles in bacterial adaptation (43). In *C. crescentus,* CtrA was first identified as a class I regulator of flagellar biosynthesis (42). CtrA defines replicative asymmetry by binding five sites in the origin of replication (*Cori*) in swarmer cells, which prevents binding of DnaA to the origin and thus initiation of DNA replication (44, 45). During the G1-S transition (differentiation into stalked cells) CtrA is inactivated and cleared from the cell by a combination of dephosphorylation and proteolysis. The absence of CtrA in stalked cells allows for immediate entry into the cell cycle and initiation of replication by DnaA (41, 46).

Following the initiation of DNA replication, CtrA is transcribed and phosphorylated, thereby allowing its action as a transcription factor in pre-

divisional cells. As a transcription factor, CtrA helps to define morphological asymmetry by controlling the temporal expression of 95 genes in *C. crescentus* (47). CtrA tightly coordinates flagella biosynthesis with cell cycle progression by limiting the expression of about 40 genes involved in flagellar biosynthesis to the predivisional cell. The genes encoding the chemotaxis apparatus and pili are also regulated by CtrA and their expression is restricted to the end of the cell cycle (47). In addition, CtrA governs the methylation status of newly synthesized DNA by controlling the expression of the gene encoding the CcrM adenine methylase, thereby restricting its activity until the latter part of the cell cycle (47). This ensures the persistence of hemi-methylated DNA during DNA replication, which helps to prevent re-initiation of DNA replication since methylation of GANTC sites in the promoter region of *dnaA* activates its transcription (48, 49). Among other important genes, CtrA also controls the expression of the cell division genes *ftsZ, ftsA, ftsQ* and *ftsW* and thus helps to govern the timing of cell division during the cell cycle.

Since CtrA controls the transcription of so many genes involved in vital cell processes and can directly repress the initiation of DNA replication, the activity of CtrA in the cell must be tightly regulated. The activity of CtrA as a transcription factor and the ability of CtrA to bind the origin is dependent upon both phosphorylation at a conserved aspartate residue and its stability within the cell. The transcription of *ctrA* is cell cycle regulated with peak activation occurring mid-S phase (50). The regulatory circuit governing *ctrA* transcription is depicted in Figure 1.7, which is adapted from (49, 51). In *C. crescentus,* CcrM-mediated methylation at a GANTC site upstream of *ctrA* P1 promoter represses *ctrA* transcription, while

binding of GcrA to a site upstream of *ctrA* P1 activates transcription (52, 53). GcrA transcription is activated by DnaA during the beginning of S phase and its transcription is repressed by CtrA in late S phase, thus GcrA accumulates out of phase with CtrA (Fig 1.7) (52). CtrA also represses its own transcription early in pre-divisional cells by binding to the P1 promoter and activates its own transcription in late pre-divisional cells by binding the P2 promoter (54).

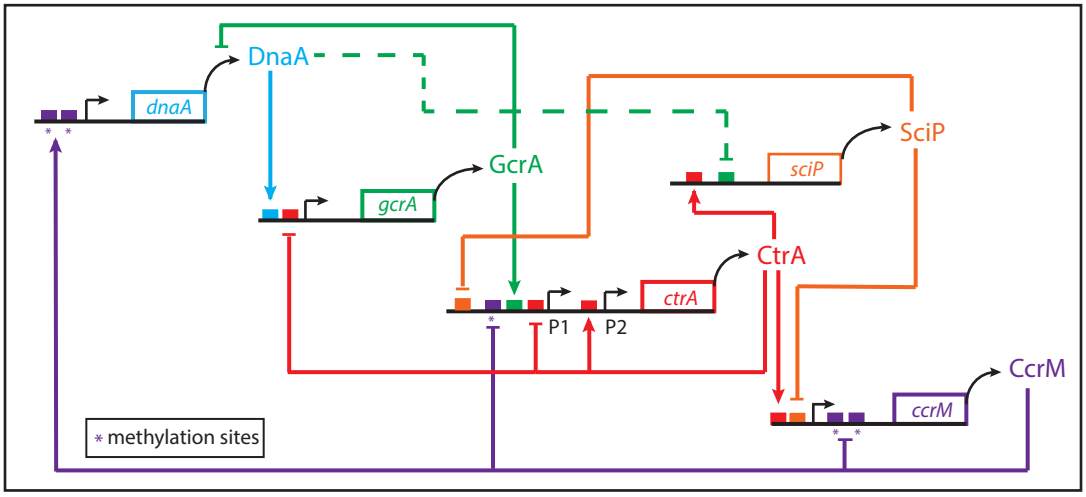


**Figure 1. 7 *C. crescentus* Cell cycle Transcription Regulatory Network.** Schematic of *C. crescentus* transcriptional regulatory network centered around the master cell cycle regulator CtrA. Expression of CtrA from the P1 promoter is activated by the master regulator GcrA and also activated from the P2 promoter by CtrA through autoregulation. CtrA expression from the P1 promoter is repressed by CtrA and SciP and also by methylation of GANTC sites by CcrM. CtrA activates the transcription of *sciP* as well as *ccrM* and represses transcription of *gcrA.* Adapted from (49, 51)

Despite the tight regulation of *ctrA* expression, transcriptional regulation plays a minor role in the regulation of CtrA activity since constitutive expression of *ctrA* does not lead to any major cell cycle defects (46, 55). Instead phosphorylation and regulated proteolysis are the major players in the regulation of CtrA activity (46). The activity of CtrA is specific to cell type with CtrA being absent in stalked cells, but active and abundant in swarmer cells. This cell type specific activity is

controlled by a complex phosphorelay centered around the specific regulation of the activity of the essential hybrid histidine kinase CckA (56). In swarmer cells, CckA autophosphorylates and the phosphoryl group is transferred to either CtrA or CpdR by the histidine phosphotransferase ChpT. This activates CtrA because CtrA-P has a higher affinity for DNA (57) and also stabilizes CtrA because phosphorylation of CpdR prevents CtrA degradation by ClpXP through a complex mechanism (58, 59). CckA is inactivated as a kinase in stalked cells, which results in the dephosphorylation and degradation of CtrA (Figure 1.8).

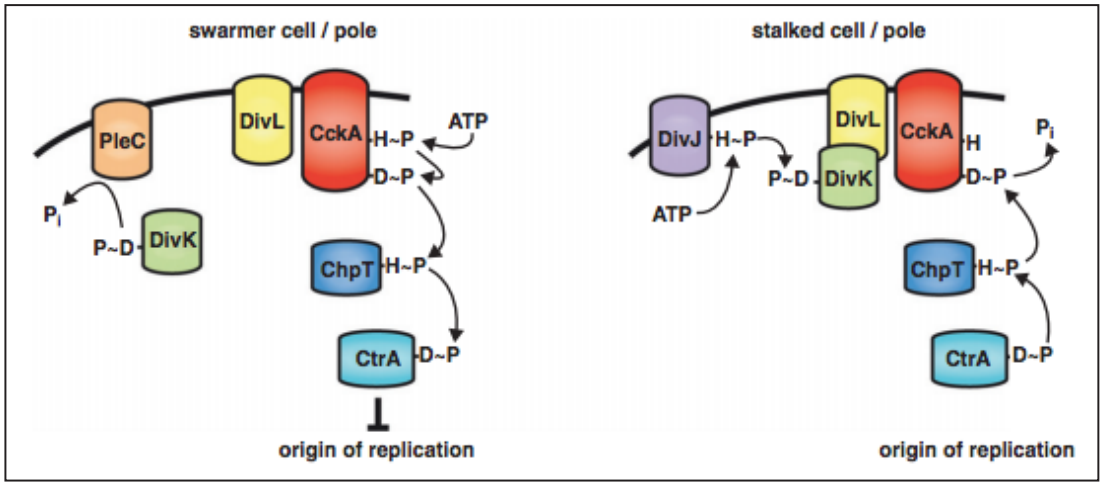


**Figure 1.8 Regulation of Replicative Asymmetry in *C. crescentus.*** Schematic of differential regulation of CtrA activity at the stalked and swarmer poles. At the swarmer pole (right) PleC acts to de-phosphorylate DivK thus allowing DivL to activate CckA kinase activity which leads to the phosphorylation of CtrA through ChpT and allows CtrA to silence the origin of replication. At the stalked pole DivK is phosphorylated by the DivJ histidine kinase, which inhibits DivL activity and converts CckA to a phosphatase. This siphons the phosphoryl group back up the phosphorelay and thus inactivates CtrA allowing initiation of DNA replication to occur at the origin.

Interestingly, CckA is a bi-functional enzyme that acts as a phosphatase when its kinase activity is inhibited and can therefore siphon phosphoryl groups back up the phosphorelay and hydrolyze them (60). The dynamic positioning of two component system signal transduction proteins establishes the cell type specific

activity of CckA (61). The kinase activity of CckA is activated by the atypical histidine kinase DivL, which is in turn regulated by the essential response regulator DivK. Phosphorylated DivK inhibits the ability of DivL to stimulate the kinase activity of CckA, thus converting CckA to a phosphatase. DivK is only phosphorylated at the stalked cell pole due to the activity of its cognate kinase DivJ. At the swarmer cell pole, DivK is unphosphorylated due to the activity of the PleC phosphatase, which allows DivL to activate CckA as a kinase and therefore activate and stabilize CtrA. This complex mechanism of regulation is depicted in Figure 1.8. At the stalked pole where CckA acts as a phosphatase, the response regulator CpdR remains unphosphorylated and therefore active (58). Unphosphorylated CpdR activates the proteolysis of CtrA by promoting the degradation of PdeA, which is a cyclic di-GMP phosphodiesterase. This leads to an accumulation of cyclic di-GMP, which activates CtrA degradation through PopA (58).

This complex regulatory network explains how CtrA activity can be restricted to a specific cell type, but not how CtrA can remain active as a repressor of the origin and target genes, yet be disabled as a transcriptional activator in swarmer cells. Recent work has identified the helix turn helix transcription factor SciP as a mediator of the activity of CtrA as a transcriptional activator of late cell cycle genes, including flagella biosynthesis and chemotaxis genes as well as *ccrM* (Fig 1.7) (51, 62). Transcription of *sciP* is cell cycle regulated and is activated by CtrA specifically in late divisional cells and remains active in swarmer cells (51). SciP is able to bind upstream of CtrA binding motifs in the promoter regions of target genes activated by CtrA thus preventing their expression. SciP also binds to and represses

transcription of *ctrA* from the P1 promoter (51), thus completing the feedback loop (Fig. 1.7). This robust cell cycle regulatory network ensures an ordered progression through the cell cycle and creates the morphological and replicative asymmetry required to produce two distinct cell types at the completion of the *C. crescentus* cell cycle.

***Conservation of C. crescentus cell cycle regulatory network in S. meliloti and other α-proteobacteria.***

Although α-proteobacteria are a highly diverse group of bacteria that lead distinct lifestyles, it has been postulated that the same regulatory network that governs cell cycle progression in *C. crescentus* is also active in most other α-proteobacteria. Most α-proteobacteria do not demonstrate the same extreme dimorphism as *C. crescentus*, but the proteins involved in the *C. crescentus* cell cycle network are well conserved in α-proteobacteria (Brilli 2010). This includes the master cell cycle regulator CtrA, which has homologs that have been studied in other α-proteobacteria, including the legume symbionts *Mesorhizobium loti* and *S. meliloti,* the plant pathogen *Agrobacterium tumefaciens* and the human intercellular pathogens *Brucella* and *Rickettsia prowazekii.* (63-65).

CtrA function was found to be essential in *S. meliloti* and the promoter region of the *ctrA* gene contains five CtrA binding sites suggesting that CtrA may also be autoregulated in *S. meliloti* (63). Bioinformatic analysis has located putative CtrA binding sites in the genomes of many α-proteobacteria and specifically, putative CtrA binding motifs have been identified in the promoter regions of *S. meliloti minC, chpT, rcdA, pleC, ropD,* and *ftsE* genes as well as in the promoter regions of homologs

of direct CtrA targets in *C. crescentus* (*podJ, mraZ, metK, clpP2, ftsK, flaACD, mcpEY*) (66). In *A. tumefaciens,* the conservation of the *ctrA* gene was shown by Southern blot hybridization with a *C. crescentus ctrA* probe (63). In *B. abortus,* the *ctrA* homolog is well-conserved and was found to be a functional response regulator that is phosphorylated on the conserved aspartate residue. *B. abortus* CtrA binds to specific sites *in vitro* including the promoter region of the *B. abortus* homolog of *ccrM*, which is also a target of *C. crescentus* CtrA (64).

Homologs of CcrM have been identified in several α-proteobacteria and shown to be analogously involved in DNA methylation and regulation of cell cycle progression (64, 67). Regulation of *ccrM* expression by CtrA is likely conserved in *B. abortus* because *C. crescentus* CtrA binds to the *B. abortus ccrM* promoter *in vitro*. This result also suggests a conservation of the CtrA binding motif between *C. crescentus* and *B. abortus.* This result suggests that, in *B. abortus*, CtrA also regulates *ccrM* transcription and that the CtrA binding motif might be conserved between the two species (64). *S. meliloti* CcrM was found to be functionally interchangeable with *C. crescentus* CcrM and to have a similar cell cycle regulated activity (67). The homologs of *ccrM* are essential in both *S. meliloti* and *B. abortus*. Furthermore, overexpression of *ccrM* is deleterious in both species, causing a block in cell division (swollen and branched cells) in *S. meliloti* and impairing proper intracellular replication of *B. abortus* in murine macrophages (67, 68).

Components of the phosphorelay responsible for the cell type specific activation of CtrA have also been shown to be important to cell cycle progression in other α-proteobacteria. For example, the *S. meliloti* homolog of the response

regulator DivK is a functional homolog of *C. crescentus* DivK. *S. meliloti* DivK displays a similar phosphorylation dependent polar localization as has been observed in *C. crescentus* (61). DivK is localized specifically to the old pole in *S. meliloti,* which demonstrates the conservation of asymmetric cell division between *C. crescentus* and *S. meliloti* even though *S. meliloti* does not exhibit obvious morphological asymmetry (61). The cell cycle dependent polar localization of the homolog of the *C. crescentus* polarity factor PodJ is also conserved in *S. meliloti* (69). Further supporting the conservation of divisional asymmetry in α-proteobacteria is the finding that *S. meliloti,* along with *B. abortus* and *A. tumefaciens* divides to produce a smaller daughter cell and a larger mother cell (37). In addition, two putative *S. meliloti* cell cycle proteins, CpdR1 and CbrA, were found to be necessary for efficient symbiosis with *M. sativa* (70, 71). CpdR1 is the *S. meliloti* homolog of *C. crescentus* CpdR and loss of CpdR1 activity was shown to lead to serious cell cycle defects including swelling and bloating of cells and increased DNA content (70). CbrA in *S. meliloti* is a putative histidine kinase identified as an ortholog of *C. crescentus* DivJ and PleC and loss of CbrA in *S. meliloti* causes filamentous growth, which indicates a cell division defect (72). It was also found that CbrA is required for the efficient localization of DivK to the cell pole, suggesting that CbrA may be a cognate histidine kinase to DivK, which is further supported by the accumulation of CtrA observed in the absence of CbrA function (72).

It has become more evident that the cell cycle regulatory network in α-proteobacteria is involved in establishing the foundation for cellular differentiation events in this diverse group of bacteria. Disruption of factors postulated to be

involved in the regulation of CtrA is highly detrimental during adaptation events in many α-proteobacteria, including in *S. meliloti* during symbiosis with *M. sativa*, in *B. abortus* during intracellular infection, and also during cyst formation in the photosynthetic bacterium *Rhodospirillum centenum* (70, 71, 73). It is important to expand the investigation of the α-proteobacterial cell cycle to diverse α-proteobacteria, not only to shed light on how this network can be specifically adapted to achieve the cellular differentiation required during the various lifestyles of α-proteobacteria, but also to gain a deeper understanding of the general evolution of this network over time. My thesis work has focused on expanding *S. meliloti* as a model for α-proteobacterial cell cycle research, which has included developing a method to synchronize *S. meliloti*, performing the first global cell cycle gene expression analysis in *S. meliloti,* and elucidating some key mechanisms of cell cycle regulation in *S. meliloti.*

## References


1. *Raymond J, Siefert JL, Staples CR, & Blankenship RE (2004) The natural history of nitrogen fixation. Molecular biology and evolution 21(3):541-554.*
2. *Mylona P, Pawlowski K, & Bisseling T (1995) Symbiotic Nitrogen Fixation. The Plant cell 7(7):869-885.*
3. *Jones KM, Kobayashi H, Davies BW, Taga ME, & Walker GC (2007) How rhizobial symbionts invade plants: the Sinorhizobium-Medicago model. Nature reviews. Microbiology 5(8):619-633.*
4. *Galibert F, et al. (2001) The composite genome of the legume symbiont Sinorhizobium meliloti. Science 293(5530):668-672.*
5. *Pleier E & Schmitt R (1991) Expression of two Rhizobium meliloti flagellin genes and their contribution to the complex filament structure. Journal of bacteriology 173(6):2077-2085.*
6. *Peck MC, Fisher RF, & Long SR (2006) Diverse flavonoids stimulate NodD1 binding to nod gene promoters in Sinorhizobium meliloti. Journal of bacteriology 188(15):5417-5427.*
7. *Oldroyd GE & Downie JA (2004) Calcium, kinases and nodulation signalling in legumes. Nature reviews. Molecular cell biology 5(7):566-576.*
8. *Foucher F & Kondorosi E (2000) Cell cycle regulation in the course of nodule organogenesis in Medicago. Plant molecular biology 43(5-6):773-786.*
9. *Gibson KE, Kobayashi H, & Walker GC (2008) Molecular determinants of a symbiotic chronic infection. Annual review of genetics 42:413-441.*
10. *Gage DJ (2004) Infection and invasion of roots by symbiotic, nitrogen-fixing rhizobia during nodulation of temperate legumes. Microbiology and molecular biology reviews : MMBR 68(2):280-300.*
11. *Reinhold BB, et al. (1994) Detailed structural characterization of succinoglycan, the major exopolysaccharide of Rhizobium meliloti Rm1021. Journal of bacteriology 176(7):1997-2002.*
12. *Leigh JA, Signer ER, & Walker GC (1985) Exopolysaccharide-deficient mutants of Rhizobium meliloti that form ineffective nodules. Proceedings of the National Academy of Sciences of the United States of America 82(18):6231-6235.*
13. *Ardourel M, et al. (1994) Rhizobium meliloti lipooligosaccharide nodulation factors: different structural requirements for bacterial entry into target root hair cells and induction of plant symbiotic developmental responses. The Plant cell 6(10):1357-1374.*
14. *Dickstein R, Scheirer DC, Fowle WH, & Ausubel FM (1991) Nodules elicited by Rhizobium meliloti heme mutants are arrested at an early stage of development. Molecular & general genetics : MGG 230(3):423-432.*
15. *Popp C & Ott T (2011) Regulation of signal transduction and bacterial infection during root nodule symbiosis. Current opinion in plant biology 14(4):458-467.*
16. *Vasse J, de Billy F, Camut S, & Truchet G (1990) Correlation between ultrastructural differentiation of bacteroids and nitrogen fixation in alfalfa nodules. Journal of bacteriology 172(8):4295-4306.*

17. *Ott T, et al. (2005) Symbiotic leghemoglobins are crucial for nitrogen fixation in legume root nodules but not for general plant growth and development. Current biology : CB 15(6):531-535.*
18. *Willis LB & Walker GC (1998) The phbC (poly-beta-hydroxybutyrate synthase) gene of Rhizobium (Sinorhizobium) meliloti and characterization of phbC mutants. Canadian journal of microbiology 44(6):554-564.*
19. *Poole P & Allaway D (2000) Carbon and nitrogen metabolism in Rhizobium. Advances in microbial physiology 43:117-163.*
20. *Mergaert P, et al. (2006) Eukaryotic control on bacterial cell cycle and differentiation in the Rhizobium-legume symbiosis. Proceedings of the National Academy of Sciences of the United States of America 103(13):5230-5235.*
21. *Brogden KA (2005) Antimicrobial peptides: pore formers or metabolic inhibitors in bacteria? Nature reviews. Microbiology 3(3):238-250.*
22. *Van de Velde W, et al. (2010) Plant peptides govern terminal differentiation of bacteria in symbiosis. Science 327(5969):1122-1126.*
23. *Wang D, et al. (2010) A nodule-specific protein secretory pathway required for nitrogen-fixing symbiosis. Science 327(5969):1126-1129.*
24. *Glazebrook J, Ichige A, & Walker GC (1993) A Rhizobium meliloti homolog of the Escherichia coli peptide-antibiotic transport protein SbmA is essential for bacteroid development. Genes & development 7(8):1485-1497.*
25. *Domenech P, Kobayashi H, LeVier K, Walker GC, & Barry CE, 3rd (2009) BacA, an ABC transporter involved in maintenance of chronic murine infections with Mycobacterium tuberculosis. Journal of bacteriology 191(2):477-485.*
26. *LeVier K, Phillips RW, Grippe VK, Roop RM, 2nd, & Walker GC (2000) Similar requirements of a plant symbiont and a mammalian pathogen for prolonged intracellular survival. Science 287(5462):2492-2493.*
27. *Haag AF, et al. (2011) Protection of Sinorhizobium against host cysteine-rich antimicrobial peptides is critical for symbiosis. PLoS biology 9(10):e1001169.*
28. *Reyes-Lamothe R, Nicolas E, & Sherratt DJ (2012) Chromosome replication and segregation in bacteria. Annual review of genetics 46:121-143.*
29. *Oka A, Sugimoto K, Takanami M, & Hirota Y (1980) Replication origin of the Escherichia coli K-12 chromosome: the size and structure of the minimum DNA segment carrying the information for autonomous replication. Molecular & general genetics : MGG 178(1):9-20.*
30. *Baker TA & Wickner SH (1992) Genetics and enzymology of DNA replication in Escherichia coli. Annual review of genetics 26:447-477.*
31. *Moriya S, Kato K, Yoshikawa H, & Ogasawara N (1990) Isolation of a dnaA mutant of Bacillus subtilis defective in initiation of replication: amount of DnaA protein determines cells' initiation potential. The EMBO journal 9(9):2905-2910.*
32. *Bakker A & Smith DW (1989) Methylation of GATC sites is required for precise timing between rounds of DNA replication in Escherichia coli. Journal of bacteriology 171(10):5738-5742.*
33. *Lu M, Campbell JL, Boye E, & Kleckner N (1994) SeqA: a negative modulator of replication initiation in E. coli. Cell 77(3):413-426.*

34. *Katayama T, Ozaki S, Keyamura K, & Fujimitsu K (2010) Regulation of the replication cycle: conserved and diverse regulatory systems for DnaA and oriC. Nature reviews. Microbiology 8(3):163-170.*
35. *Merrikh H & Grossman AD (2011) Control of the replication initiator DnaA by an anti-cooperativity factor. Molecular microbiology 82(2):434-446.*
36. *Marczynski GT (1999) Chromosome methylation and measurement of faithful, once and only once per cell cycle chromosome replication in Caulobacter crescentus. Journal of bacteriology 181(7):1984-1993.*
37. *Hallez R, Bellefontaine AF, Letesson JJ, & De Bolle X (2004) Morphological and functional asymmetry in alpha-proteobacteria. Trends in microbiology 12(8):361-365.*
38. *Shapiro L (1976) Differentiation in the Caulobacter cell cycle. Annual review of microbiology 30:377-407.*
39. *Brun YV, Marczynski G, & Shapiro L (1994) The expression of asymmetry during Caulobacter cell differentiation. Annual review of biochemistry 63:419-450.*
40. *Tsokos CG & Laub MT (2012) Polarity and cell fate asymmetry in Caulobacter crescentus. Current opinion in microbiology 15(6):744-750.*
41. *Jonas K, Chen YE, & Laub MT (2011) Modularity of the bacterial cell cycle enables independent spatial and temporal control of DNA replication. Current biology : CB 21(13):1092-1101.*
42. *Quon KC, Marczynski GT, & Shapiro L (1996) Cell cycle control by an essential bacterial two-component signal transduction protein. Cell 84(1):83-93.*
43. *Stock JB, Ninfa AJ, & Stock AM (1989) Protein phosphorylation and regulation of adaptive responses in bacteria. Microbiological reviews 53(4):450-490.*
44. *Quon KC, Yang B, Domian IJ, Shapiro L, & Marczynski GT (1998) Negative control of bacterial DNA replication by a cell cycle regulatory protein that binds at the chromosome origin. Proceedings of the National Academy of Sciences of the United States of America 95(1):120-125.*
45. *Collier J, Murray SR, & Shapiro L (2006) DnaA couples DNA replication and the expression of two cell cycle master regulators. The EMBO journal 25(2):346-356.*
46. *Domian IJ, Quon KC, & Shapiro L (1997) Cell type-specific phosphorylation and proteolysis of a transcriptional regulator controls the G1-to-S transition in a bacterial cell cycle. Cell 90(3):415-424.*
47. *Laub MT, Chen SL, Shapiro L, & McAdams HH (2002) Genes directly controlled by CtrA, a master regulator of the Caulobacter cell cycle. Proceedings of the National Academy of Sciences of the United States of America 99(7):4632-4637.*
48. *Zweiger G, Marczynski G, & Shapiro L (1994) A Caulobacter DNA methyltransferase that functions only in the predivisional cell. Journal of molecular biology 235(2):472-485.*
49. *Collier J, McAdams HH, & Shapiro L (2007) A DNA methylation ratchet governs progression through a bacterial cell cycle. Proceedings of the National Academy of Sciences of the United States of America 104(43):17111-17116.*

50. *Laub MT, McAdams HH, Feldblyum T, Fraser CM, & Shapiro L (2000) Global analysis of the genetic network controlling a bacterial cell cycle. Science 290(5499):2144-2148.*
51. *Tan MH, Kozdon JB, Shen X, Shapiro L, & McAdams HH (2010) An essential transcription factor, SciP, enhances robustness of Caulobacter cell cycle regulation. Proceedings of the National Academy of Sciences of the United States of America 107(44):18985-18990.*
52. *Holtzendorff J, et al. (2004) Oscillating global regulators control the genetic circuit driving a bacterial cell cycle. Science 304(5673):983-987.*
53. *Reisenauer A & Shapiro L (2002) DNA methylation affects the cell cycle transcription of the CtrA global regulator in Caulobacter. The EMBO journal 21(18):4969-4977.*
54. *Domian IJ, Reisenauer A, & Shapiro L (1999) Feedback control of a master bacterial cell-cycle regulator. Proceedings of the National Academy of Sciences of the United States of America 96(12):6648-6653.*
55. *Biondi EG, et al. (2006) Regulation of the bacterial cell cycle by an integrated genetic circuit. Nature 444(7121):899-904.*
56. *Jacobs C, Domian IJ, Maddock JR, & Shapiro L (1999) Cell cycle-dependent polar localization of an essential bacterial histidine kinase that controls DNA replication and cell division. Cell 97(1):111-120.*
57. *Siam R & Marczynski GT (2000) Cell cycle regulator phosphorylation stimulates two distinct modes of binding at a chromosome replication origin. The EMBO journal 19(5):1138-1147.*
58. *Abel S, et al. (2011) Regulatory cohesion of cell cycle and cell differentiation through interlinked phosphorylation and second messenger networks. Molecular cell 43(4):550-560.*
59. *Duerig A, et al. (2009) Second messenger-mediated spatiotemporal control of protein degradation regulates bacterial cell cycle progression. Genes & development 23(1):93-104.*
60. *Chen YE, Tsokos CG, Biondi EG, Perchuk BS, & Laub MT (2009) Dynamics of two Phosphorelays controlling cell cycle progression in Caulobacter crescentus. Journal of bacteriology 191(24):7417-7429.*
61. *Lam H, Matroule JY, & Jacobs-Wagner C (2003) The asymmetric spatial distribution of bacterial signal transduction proteins coordinates cell cycle events. Developmental cell 5(1):149-159.*
62. *Gora KG, et al. (2010) A cell-type-specific protein-protein interaction modulates transcriptional activity of a master regulator in Caulobacter crescentus. Molecular cell 39(3):455-467.*
63. *Barnett MJ, Hung DY, Reisenauer A, Shapiro L, & Long SR (2001) A homolog of the CtrA cell cycle regulator is present and essential in Sinorhizobium meliloti. Journal of bacteriology 183(10):3204-3210.*
64. *Bellefontaine AF, et al. (2002) Plasticity of a transcriptional regulation network among alpha-proteobacteria is supported by the identification of CtrA targets in Brucella abortus. Molecular microbiology 43(4):945-960.*
65. *Brassinga AK, et al. (2002) Conserved response regulator CtrA and IHF binding sites in the alpha-proteobacteria Caulobacter crescentus and Rickettsia*

*prowazekii chromosomal replication origins. Journal of bacteriology 184(20):5789-5799.*

66. *Schluter JP, et al. (2013) Global mapping of transcription start sites and promoter motifs in the symbiotic alpha-proteobacterium Sinorhizobium meliloti 1021. BMC genomics 14:156.*
67. *Wright R, Stephens C, & Shapiro L (1997) The CcrM DNA methyltransferase is widespread in the alpha subdivision of proteobacteria, and its essential functions are conserved in Rhizobium meliloti and Caulobacter crescentus. Journal of bacteriology 179(18):5869-5877.*
68. *Robertson GT, et al. (2000) The Brucella abortus CcrM DNA methyltransferase is essential for viability, and its overexpression attenuates intracellular replication in murine macrophages. Journal of bacteriology 182(12):3482-3489.*
69. *Fields AT, et al. (2012) The conserved polarity factor podJ1 impacts multiple cell envelope-associated functions in Sinorhizobium meliloti. Molecular microbiology 84(5):892-920.*
70. *Kobayashi H, De Nisco NJ, Chien P, Simmons LA, & Walker GC (2009) Sinorhizobium meliloti CpdR1 is critical for co-ordinating cell cycle progression and the symbiotic chronic infection. Molecular microbiology 73(4):586-600.*
71. *Gibson KE, Campbell GR, Lloret J, & Walker GC (2006) CbrA is a stationary-phase regulator of cell surface physiology and legume symbiosis in Sinorhizobium meliloti. Journal of bacteriology 188(12):4508-4521.*
72. *Sadowski C, Wilson D, Schallies K, Walker G, & Gibson KE (2013) The Sinorhizobium meliloti sensor histidine kinase CbrA contributes to free-living cell cycle regulation. Microbiology.*
73. *Bird TH & MacKrell A (2011) A CtrA homolog affects swarming motility and encystment in Rhodospirillum centenum. Archives of microbiology 193(6):451-459.*

# Chapter 2

## A novel method for cell synchronization of the legume symbiont *Sinorhizobium meliloti* and application towards global analysis of cell cycle regulated gene expression

This manuscript is being prepared for submission to PNAS in August 2013. List of authors: Nicole J De Nisco, Ryan P Abo, Chung-an M Wu and Graham C Walker.

N.J.D developed the synchronization method with the help of C.M.W. N.J.D performed all the wet-lab experiments with the exception of the cDNA synthesis and microarray hybridization which was performed by the BioMicroCenter. R.P.A performed statistical analysis of microarray data and developed the algorithms for the bioinformatic analysis. N.J.D assisted in the development of the bioinformatic methods and performed the manual filtering and annotating of the output data. The manuscript was written by N.J.D and edited by G.C.W.

**Abstract**

Proper regulation of the bacterial cell cycle is crucial for faithful replication and segregation of the genome. In some groups of bacteria, *i.e.* α-proteobacteria, tight regulation of cell cycle progression is also necessary for specific cellular differentiation required for adaptation to their diverse environmental niches. The cell cycle regulated cellular differentiation of the aquatic bacterium *Caulobacter crescentus* has been intensely studied and results in formation of two morphologically distinct cell types, the motile swarmer cell and the sessile stalked cell. The symbiotic lifestyle of the soil bacterium, *Sinorhizobium meliloti* also requires a drastic cellular differentiation that includes changes to the cell envelope, endoreduplication of the genome and loss of reproductive capacity. This differentiation requires a specific re-wiring of the *S. meliloti* cell cycle network to allow for the de-coupling of DNA replication and cell division. The genes encoding the *C. crescentus* cell cycle regulatory network are well conserved in *S. meliloti,* yet cell cycle regulation in *S. meliloti* is poorly understood. The work presented here represents the first global analysis of cell cycle regulated gene expression in an α-proteobacteria besides *C. crescentus.* I developed the first method for cell synchronization of *S. meliloti* and utilized microarray analysis to test the conservation of the transcriptional control of cell cycle progression in α-proteobacteria. I observed both similarities and differences in cell cycle regulated gene expression between *C. crescentus* and *S. meliloti,* which both extend the paradigm of cell cycle regulated transcription to *S. meloliti* as well as highlight specific adaptations to the unique lifestyle and genomic structure of *S. meliloti*.

## Introduction

The diverse lifestyles and unique evolutionary history of α-proteobacteria make them an intriguing model for the study of the bacterial cell cycle. Unlike the intensively studied organisms *Escherichia coli* and *Bacillus subtilis,* which are able to initiate DNA replication many times in a given cell cycle, α-proteobacteria only initiate a single round of replication per cell division (1, 2). The regulatory network controlling the progression of the cell cycle in the aquatic α-proteobacterium *C. crescentus* has been intensely studied and several key regulators have been identified (3). Temporally regulated gene expression allows for coordination of cell cycle progression and cellular differentiation in *C. crescentus*. In fact, the expression of more than 19% of the *C. crescentus* genome varies as a function of the cell cycle (4). This tight transcriptional control of the timing of cell cycle events in *C. crescentus* parallels the temporal patterns of gene expression observed in the yeast cell cycle. These parallels with the cell cycle of lower eukaryotes make the study of the α-proteobacterial cell cycle especially exciting. The *Caulobacter* field has established a rich and exciting model for the cell cycle regulation in α-proteobacteria and many critical regulators of the cell cycle are well conserved among α-proteobacteria. However, the importance of temporal control of gene regulation and the specific functions of these regulators in other α-proteobacteria has yet to be tested (5, 6).

*C. crescentus* divides asymmetrically to produce two morphologically distinct cells. The sessile stalked cell can immediately re-enter the cell cycle, while the motile swarmer cell is arrested in G1 and must differentiate into a stalked cell to

initiate DNA replication (3). The essential response regulator CtrA is the primary regulator of replicative asymmetry in *C. crescentus,* while the AAA+ ATPase DnaA determines the periodicity of DNA replication (3, 7, 8). In *C. crescentus,* activated CtrA-P binds and silences the origin of replication in swarmer cells, while the absence of CtrA allows the initiation of DNA replication by DnaA in stalked cells (9, 10). CtrA and DnaA also function as transcription factors that regulate the transcription of about 95 and 40 genes, respectively (11, 12). In *C. crescentus,* the transcription of CtrA is cell cycle regulated by GcrA, CcrM and CtrA (13), but phosphorylation and regulated proteolysis play a more important role in establishing the differential activity of CtrA in the two different cell types. A phosphorelay involving CckA, ChpT, DivK, DivJ, PleC and DivL regulates both the phosphorylation status of CtrA (3) and the stability of CtrA through the phosphorylation of CpdR, which acts to induce CtrA proteolysis through PdeA, PopA and the second messenger cyclic di-GMP (14).

Nearly all the master regulators of the *C. crescentus* cell cycle are highly conserved in *S. meliloti,* but little is known about their specific functions in *S. meliloti*. Like *C. crescentus, S. meliloti* also divides asymmetrically, but does not produce the same extreme dimorphism in its progeny cells (6). *S. meliloti* is a soil bacterium that is able to form a nitrogen-fixing symbiosis with legumes of the *Medicago, Melilotus and Trigonella* genera (15). In addition to its chromosome, *S. meliloti* has two symbiotic megaplasmids (pSymA and pSymB) forming a tripartite genome (16). Little is known about how *S. meliloti* coordinates the replication and segregation of these three separate replicons. During symbiosis, *S. meliloti* is

exposed to an array of defensin-like nodule-specific cysteine-rich (NCR) peptides that induce a drastic terminal differentiation (2, 17). Bacteroid differentiation occurs once bacteria are encapsulated within the symbiosome compartment of specialized nodule cells and is required for symbiosis (15). This differentiation includes endoreduplication of the bacterial genome, which requires a decoupling of DNA replication and cell division. Altering the expression of certain genes involved in the *S. meliloti* cell cycle (*ftsZ, dnaA, minE, ccrM)* produces bacteroid-like polyploid cells (8, 18-20) and the function of the putative cell cycle regulators CbrA and CpdR1 is required for an efficient symbiosis with *M. sativa* (21, 22). Thus, it is important to understand the role of the *S. meliloti* cell cycle during this symbiosis, which is critical to the global nitrogen cycle.

Due to the conservation of the *C. crescentus* regulatory circuit in other α-proteobacteria, transcriptional control of cell cycle progression has been postulated to be critical in most α-proteobacteria despite their diverse lifestyles and their differences in morphological asymmetry (5, 6). Since it has not been possible to obtain synchronized cultures of *S. meliloti,* cell cycle research in *S. meliloti* has been largely confined to single gene studies and sequence-based bioinformatics analysis. The cell cycle regulators CtrA, DnaA, CcrM are essential and functionally conserved in *S. meliloti*. Nevertheless, a comprehensive analysis is required to determine the extent to which the *C. crescentus* paradigm of cell cycle regulation can be extended to *S. meliloti* and other α-proteobacteria.

In this work I describe an efficient method for the synchronization of *S. meliloti* and application of this method towards global analysis of cell cycle gene

expression. My analysis identifies 462 genes exhibiting strong periods of up-regulation and down-regulation during the cell cycle. Several master cell cycle regulators exhibited strong cell cycle dependent transcriptional regulation as well as large number of genes involved in motility, attachment, and cell division. These data firmly support the extension of the general model of *C. crescentus* cell cycle regulation to other α-proteobacteria. However, comparison of cell cycle regulated transcripts between *S. meliloti* and *C. crescentus* as well as CtrA and DnaA binding motif analysis indicated intriguing differences in the wiring of this network to adapt its function to the specific lifestyle of *S. meliloti.* The differences identified by my analysis exemplify the importance of *S. meliloti* as a model for the study of the evolution of cell cycle regulation as it specifically pertains to α-proteobacterial endosymbionts and intracellular pathogens.

**Results**

**Synchronization of *S. meliloti* cell populations via nutrient downshift.**

Differential centrifugation to isolate G1-arrested cells, which is used to synchronize *C. crescentus,* is not applicable to *S. meliloti* because there is not a large enough density difference between the mother and daughter cells (23). A simple method for synchronizing populations of *E. coli* involves growing cells in conditions that promote the stringent response, which induces a G1 arrest (24). The stringent response in *S. meliloti* is dependent on the bi-functional enzyme $Rel_{Sm}$, which is responsible for both the synthesis and hydrolysis of the alarmone ppGpp (25, 26). In *S. meliloti* ppGpp synthesis is stimulated by both carbon and nitrogen starvation (26). I tested the ability to generate G1 cells in stringent conditions by transferring

early log phase Rm1021 cells to medium lacking a preferred carbon and nitrogen source (25). I monitored DNA content per cell via flow cytometry and found that after 4.5 hours ~95% of the cells had 1C DNA content while 5% of the cells were at 2C (Figure 2.1B). Arrested cells were pelleted and resuspended in rich medium. After 40-50 minutes, *S. meliloti* cells initiate DNA replication in unison and proceed to replicate their genomes (Figure 2.1B). Between 100 and 120 minutes cells reach mid-S phase and by 140 minutes replication is complete. Finally, at 160 minutes the 1N peak re-emerges indicating that the cells are actively dividing. (Figure 2.1B). This cell cycle progression is illustrated in Figure 2.1.

**Microarray analysis of synchronized *S. meliloti* cultures identifies 462 cell cycle regulated transcripts.** To test if the temporally regulated gene expression observed in *C. crescentus* is conserved in *S. meliloti,* I monitored gene expression in synchronized populations of *S. meliloti* as they progressed through the cell cycle (4). RNA was isolated from cultures arrested in G1 (t=0) and at 20-minute intervals starting at the end of G1 (t=40) until cell division (t=160). I directly compared the expression 6046 *S. meliloti* genes in distinct phases of the cell cycle versus early-log phase asynchronous culture via 2-color microarray analysis. Cell cycle regulated transcripts were identified using a standard deviation cutoff to select genes with significant cell cycle variance. Replicate log ratio values for each time point were averaged and then used to calculate the standard deviation for each gene. The standard deviations for each gene were then compared to standard deviations generated from randomly permuted gene expression profiles and genes with statistically significant standard deviations were chosen. To minimize the effect of

the starvation response on variance, only values from the 40-160 time points were used to calculate the standard deviation of each gene. The expression of 462 genes was found to vary as a function of the cell cycle (Table 2.S1). We performed fuzzy c means clustering to identify groups of genes with similar expression patterns (27). This analysis yielded a total of 6 gene clustered that are displayed in Figure 2.1C.

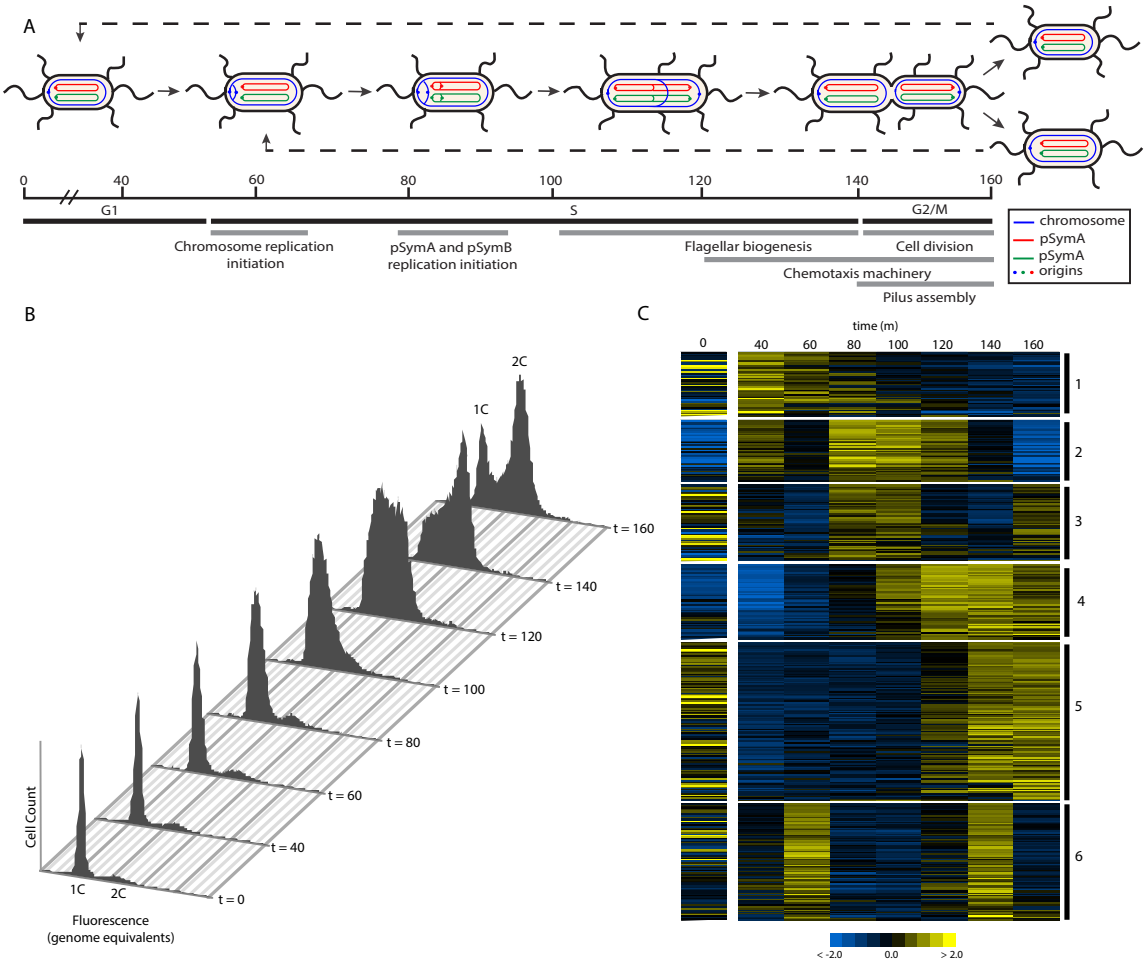


**Figure 2.1. Synchronization of *S. meliloti* and microarray analysis of cell cycle regulated gene expression.** A. Illustration of *S. meliloti* cell cycle progression. *S. meliloti* is peritrichously flagellated and divides asymmetrically (6, 28). FACS profiles from cell synchronization pictured in B. At t=0 95% of cells are arrested in G1. At t=60 replication has initiated and S phase starts (illustrated 2.1A). Cells have completed S phase at t=140 and divide at t=160. C. Heatmap of fuzzy clustering of 462 cell cycle regulated transcripts. Clusters are indicated on the right. Each row represents a single gene.

The majority of these genes are located on the chromosome (320) while 106 are located on pSymB and only 36 located on pSymA. In total 9.5% of chromosomal genes probed demonstrated cell cycle regulated transcription while 6.7% of pSymB genes and 2.7% pSymA genes had cell cycle regulated transcripts, suggesting that the chromosome is enriched for genes with cell cycle regulated expression. This enrichment was verified by a hypergeometric distribution test ($p<0.001$). Many genes with similar functions clustered together, especially the flagellar and chemotaxis machinery, which largely comprise clusters 4 and 5 respectively. Similar to the pattern of cell cycle gene expression observed in *C. crescentus,* each cluster represents a specific period of transcriptional activation during the cell cycle (4). This data clearly demonstrates that temporally regulated gene expression during the cell cycle is conserved between *S. meliloti* and *C. crescentus,* which supports the extension of this paradigm to other α-proteobacteria.

**Several *S. meliloti* genes exhibit peak expression corresponding with the timing of their cellular function.** Figure 2.2A illustrates the expression profiles of genes involved in DNA replication, recombination, repair and chromosome segregation. Genes denoted by an asterisk did not have a strong enough variance in their expression to be included in our list of cell cycle regulated transcripts. Surprisingly, most of the replication machinery did not exhibit strong cell cycle regulated gene expression, which could mean that the activity of these factors is regulated post-transcriptionally or that the cell is sensitive to small differences in the expression of a particular gene. For example, transcription of *dnaA*, which did not have a sufficient standard deviation to meet our cutoff, shows an up-regulation

at 60 minutes corresponding with the start of S-phase observed via flow cytometry (Fig 2.1B, Fig 2.2A). My analysis did reveal that the expression of the *repABC* genes, which govern the replication and segregation of pSymA and pSymB, is clearly cell cycle regulated (29). These genes fall into cluster 3 with peak up-regulation occurring in early S phase between t=80 and t=100 (Fig. 2.1B). Specifically, the expression of *repC1* and *repC2,* which are required for the initiation of replication of pSymB and pSymA respectively, occurs after the observed peak expression of *dnaA*, suggesting that initiation of the megaplasmid origins may follow that of the chromosomal origin instead of occurring simultaneously. This stepwise initiation of origins has been previously observed *Vibrio cholera,* in which initiation of the smaller chromosome II is delayed compared to chromosome I resulting in concurrent termination of replication of the two chromosomes (30). Fig. 2.1A illustrates this initiation pattern as well as the previously observed polar localization of chromosomal and symbiotic plasmid origins, which is consistent with the demonstrated polar localization of the *C. crescentus Cori* (31, 32).

The transcription of nucleotide biosynthesis genes as well as DNA repair genes is strongly cell cycle regulated in *C. crescentus,* but not in *S. meliloti (4)* Only the gene encoding *lexA,* a regulator of the SOS response (33), demonstrated strong cell cycle regulated transcription and it is up-regulated later in the cell cycle putting it in cluster 5 (Fig 2.2A, Fig 2.1C). This is not the same as the expression pattern observed in *C. crescentus* where *lexA* is upregulated from mid-late S phase (4). The role of the transcriptional regulation of *lexA* during the cell cycle is unclear in *S. meliloti* and *C. crescentus* as it is unknown if transcriptional upregulation of *lexA*

corresponds to an increase in LexA protein or activity. In *S. meliloti,* expression of genes involved in chromosome segregation (*parAB, repAB)* peaks prior to that of genes involved in DNA recombination (*ruvA, xerC)*, which is the reverse of the expression patterns observed in *C. crescentus* and might be an adaptation related to the presence of multiple replicons in *S. meliloti* (4).

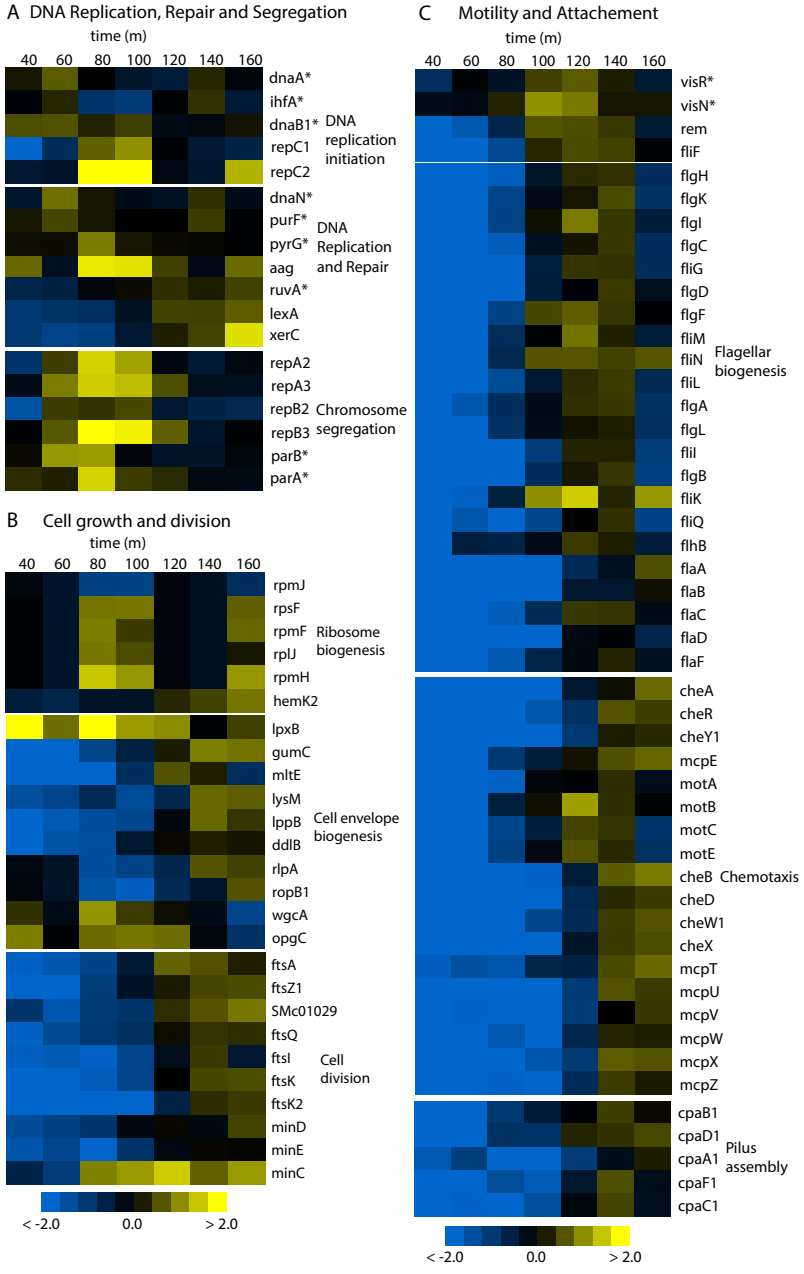


**Figure 2.2. Heatmaps of cell cycle gene expression of genes involved in various cellular processes.** A. Expression of genes involved in DNA processes (replication, repair and segregation) in *S. meliloti.* Not all genes were included in the list of cell cycle regulated transcripts identified in our analysis and are denoted by an asterisk (*). A scale bar corresponding to log-fold expression is included at the bottom of the heatmaps. Values represent raw logfc values (not normalized for clustering as in 2.1C). In B cell cycle expression patterns for genes involved in cell growth and division are illustrated. These include genes required for ribosome and cell envelope biogenesis as well as key cell division genes C. Heatmaps picturing the cell cycle gene expression patterns of genes involved in motility and attachment including flagellar biosynthesis genes (and regulators), chemotaxis machinery and genes required for pili biogenesis.

The *S. meliloti* cell division machinery fell into two separate clusters suggesting the existence of early and late cell division genes in *S.meliloti.* The homologs of *E. coli* division genes *ftsA*, *ftsZ,* and *minC* fell into cluster 4 while *ftsQ, ftsI*, *ftsK, minD* and *minE* fell into cluster 5 (Fig 2.1B). These clusters represent late cell cycle transcription, which directly coincides with the timing of septation and division (Fig 2.1A, Fig 2.2B). The expression pattern of the *minCDE* operon, which is required to restrict the septum to mid-cell was surprising (34). It has been demonstrated that *minCDE* genes are expressed from a promoter directly upstream of *minC* (20), but our data indicate that *minC* expression greatly precedes that of *minDE* during the cell cycle. This phenomenon may be due to a 43bp partial RIME element in the 101bp region between *minC* and *minD.* Repetitive elements such as these have been shown to alter gene expression in polycistronic operons (35).

The most robust set of genes involved in a specific process that demonstrated cell cycle regulated transcription were the motility genes. Flagellar biosynthesis genes dominated cluster 4 while chemotaxis genes were present in cluster 5 (Fig 2.1C, Fig 2.2C). In *S. meliloti,* the restriction of swimming motility to the exponential phase of growth is controlled by a three-class hierarchy of flagellar and chemotaxis genes. Class I regulators VisNR and Rem are at the top of the hierarchy with VisNR controlling the expression of Rem, which in turn controls the expression of class II genes (*flg, flh, fli, mot*). Interestingly, homologs of VisNR and Rem are absent in *C. crescentus*, but are present in several species of the *Rhizobiaceae* group. Following Class II gene expression, the expression of Class III genes (*che, fla*) is activated (36). All motility genes are highly repressed in the

beginning of the cell cycle and the expression of class I and II genes is activated at 100 minutes compared to the activation of class III genes at 140 minutes (Fig 2.2C). This pattern of gene expression is in consensus with the known regulatory hierarchy, but raises the intriguing question of how the expression of these genes is controlled during the cell cycle.

**Transcription of most putative cell cycle regulatory genes is activated later in the cell cycle.** Homologs of the many well-characterized genes involved in the *C. crescentus* cell cycle regulatory network have cell cycle regulated transcripts in *S. meliloti* (Fig 2.3). These putative regulatory genes fell into three clusters, cluster 4 (*pleC, podJ1*), cluster 5 (*ctrA, sciP, divK, divJ, ccrM, chpT*) and cluster 6 (*cpdR1)* (Fig 1B). As indicated by the clustering and heatmap in Figure 2.3, many of these genes are repressed until mid-S phase, which is consistent with their defined role for establishing morphological asymmetry in *C. crescentus* (3). Although it did not make our cutoff, the gene encoding the master regulator GcrA is activated coincidentally with *dnaA,* which is consistent with the transcriptional activation of GcrA by DnaA early in the cell cycle observed in *C. crescentus* (37). The transcription of the essential hybrid histidine kinase CckA, which is at the top of the phosphorelay that phosphorylates the master cell cycle regulator CtrA, is not cell cycle regulated (Fig 2.3). However, the genes encoding the kinases (DivK, DivJ) and phosphatase (PleC) that regulate CckA activity do exhibit cell cycle regulated transcription.

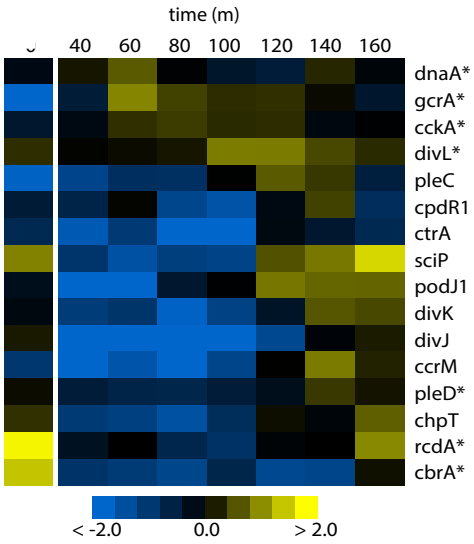


**Figure 2.3. Expression profiles of *S. meliloti* homologs of *C. crescentus* cell cycle regulators.** Values depicted in this heatmap represent raw logfc values (before normalization for clustering). The color scale bar corresponds to log fold expression change in comparison to unsynchronized culture. Gene names with asterisks (*) signify genes that did not show significant cell cycle expression variance to be included in our cell-cycle regulated list.

In addition, the gene encoding SciP is first up-regulated during G1 arrest and then again up-regulated in predivisional cells, which is reflective of its prescribed function in *C. crescentus* (Fig 2.3). In *C. crescentus,* SciP accumulates specifically in swarmer cells to inhibit the activity of CtrA as a transcriptional activator but not its ability to bind the *Cori* and repress the initiation of DNA replication (38). Surprisingly, transcription of *ctrA* is not as strongly activated during the *S. meliloti* cell cycle as it is in *C. crescentus* and its activation is delayed (Fig. 2.3, Fig. 2.S3). However, transcriptional regulation of *ctrA* is not essential in *C. crescentus,* so my data further support the importance of proteolysis and phosphorylation in the regulation of CtrA activity (3). It is also interesting that gene encoding the sensor histidine kinase CbrA, which is not present in *C. crescentus,* is also upregulated in G1 cells. Loss of CbrA activity in *S. meliloti* causes a reduction in the polar localization of the response regulator DivK (39). Thus, CbrA is possibly important for mediating DivK activity in this cell type.

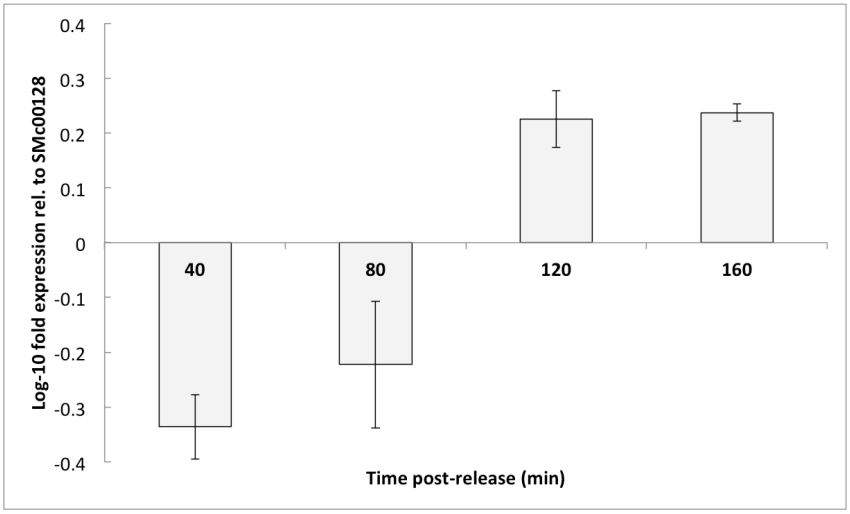


**Figure 2.S3. Quantative PCR verification of *ctrA* gene expression during the cell cycle.** Log-10 change in *ctrA* transcript levels at 40,80.120.160 minutes normalized by levels of *SMc00128* transcript, which are uniform in our expression data. Transcription of *ctrA* is repressed in the beginning of the cell cycle and relieved during late S phase.

**Blast and COG analysis reveals a core set of 128 genes with cell cycle regulated expression profiles conserved between *C. crescentus* and *S. meliloti.*** I directly compared the 462 genes with cell cycle regulated gene expression we identified in *S. meliloti* with the 553 identified in *C. crescentus.* Since I used a completely different method to synchronize *S. meliloti* than is used to synchronize *C. crescentus,* genes with cell cycle regulated transcripts conserved between the two species not only represent a core set of α-proteobacterial cell cycle regulated genes, but represent genes whose expression varies independent of synchronization method. Employing both bi-directional BLAST and COG analysis to identify homologs in the two lists, I discovered 128 genes with cell cycle regulated transcripts that are conserved between *S. meliloti* and *C. crescentus* (annotated list in Table 2.S4). Clustering of the conserved genes yielded four distinct clusters, which correspond with clusters 2, 4, 5 and 6 in Figure 2.1C. Most of the genes in clusters 1 and 3 of Fig 2.1C are not conserved in the *C. crescentus* set of cell cycle regulated genes and are specialized to *S. meliloti*. The genes of the *repABC* operon fall into cluster 3 while *ndvA* which

encodes a putative cyclic β-1,2 glucan ABC transporter is in cluster 1. Cyclic β-glucans are produced by all members of the *Rhizobiacae* family and are involved in adaptation to hypo-osmotic growth and *ndvA* is specifically required for symbiosis *(40).* Conserved genes identified by our analysis include cell division genes (*ftsZ, ftsI, ftsA, ftsQ)*, cell cycle regulators (*ctrA, pleC, divK, divJ, cpdR, chpT)* and many flagellar and chemotaxis genes.

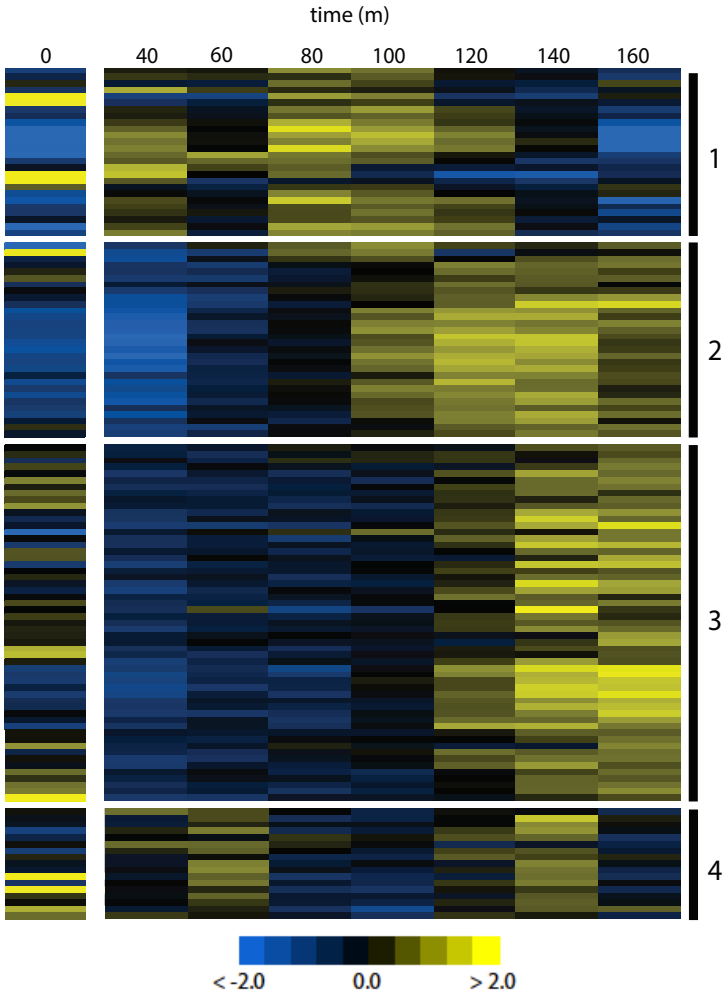


**Figure 2.4. Fuzzy clustering of genes with cell cycle regulated transcripts conserved between *S. meliloti* and *C. crescentus.*** Genes conserved between the *S. meliloti* and *C. crescentus* cell cycle regulated data sets (4) identified by BLAST and COG analysis were subjected to fuzzy c means clustering as in Figure 1C. Conserved genes fell into four clusters with cluster 1,2,3 and 4 here corresponding to clusters 2,4,5 and 6 in Figure 1C.

**Binding site analysis reveals conserved CtrA and DnaA binding sites among genes with cell cycle regulated transcripts.** In *C. crescentus,* CtrA directly controls the transcription of 95 genes in 55 operons and DnaA controls the transcription of

40 genes (11, 12). The genes regulated by CtrA include several chemotaxis and flagellar genes as well as genes required for cell division (*ftsZ, ftsW),* DNA methylation (*ccrM),* and *ctrA* itself (11). The DnaA regulon includes cell polarity factors (*podJ, pleC),* replication machinery (*dnaA, dnaQ, dnaB),* cell envelope and division genes (*ftsZ, mraY)* and the master regulator *gcrA (12).* To determine which *S. meliloti* cell cycle regulated transcripts might be regulated by CtrA and DnaA, I searched for CtrA and DnaA binding motifs within our list of 462 genes. Previously described position weight matrices describing the CtrA and DnaA binding sites were used (5). My analysis revealed 64 genes with CtrA binding sites and 96 with DnaA binding sites with p-values less that $2x10^{-4}$. We analyzed homologs of these genes in 11 representative α-proteobacteria for conserved CtrA and DnaA binding motifs. The results for a selection of genes with the highest scoring motifs are displayed in Figure 2.5 (full list in Table 2.S5A and 2.S5B).

Several CtrA binding motifs previously identified in *S. meliloti* were found by my analysis, including motifs in the promoter regions of *minC, chpT, pleC, ftsK, flaC, flaA, flaD, SMc00651, podJ1* (5, 41). Although *mcpE* and *mcpY* had cell cycle regulated transcripts and have been cited as having putative CtrA binding motifs (41), the p-value of these motifs was not low enough to make the cutoff for our analysis. In all organisms where septum formation regulator *minC* is conserved, the CtrA binding motif is also conserved, suggesting the importance of regulation of the Min system by CtrA in these α-proteobacteria (Fig. 2.5A). *S. meliloti* and *C. crescentus* share a conserved CtrA binding motif in the promoter region of the pili gene *pilA.* An uncharacterized gene with homology to the N terminus of pilus formation genes,

SMc04115, shares a promoter with *pilA* and therefore putative CtrA regulatory sites. SMc04115 has a very strong co-occurrence in the genome with *pilA1* and the pilus assembly genes of the *cpa* operon indicating a likely conserved function in pilus assembly in α-proteobacteria.

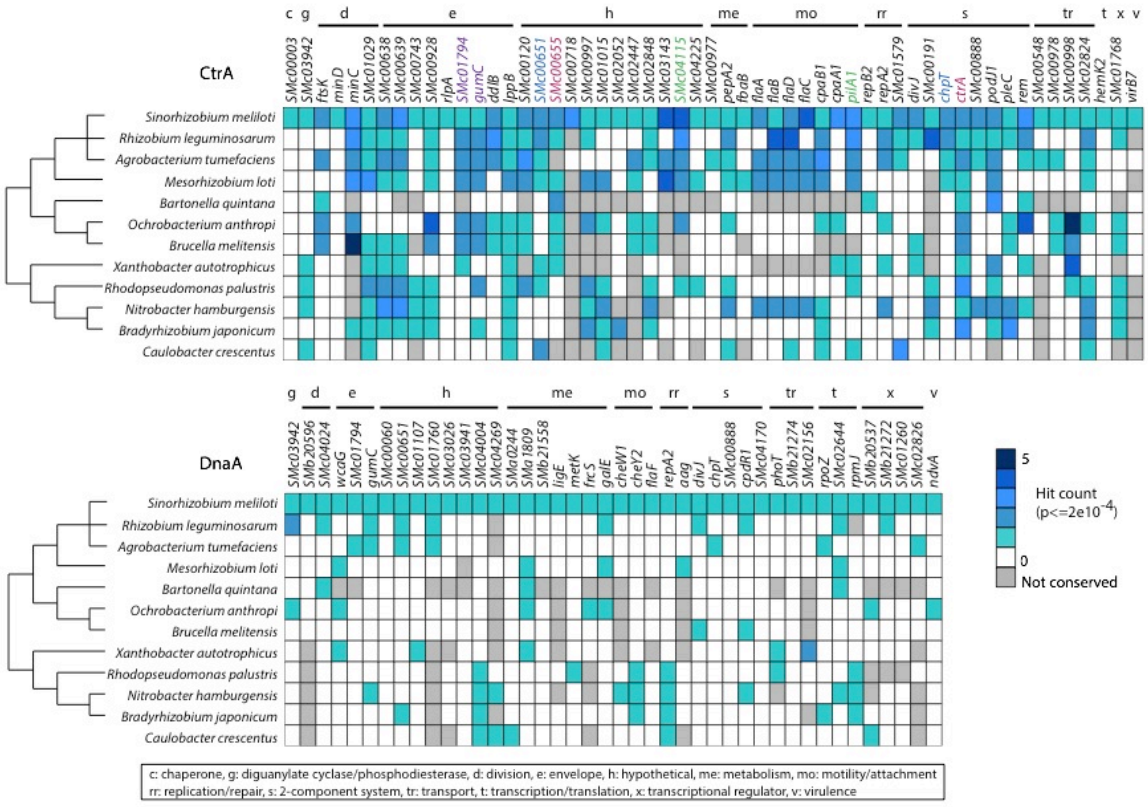


**Figure 2.5. Conservation of putative CtrA and DnaA binding sites in cell cycle regulated genes.** Genes with cell cycle regulated transcripts were scanned for CtrA binding motifs 400bp upstream and 100 bp downstream of their translation start sites. The genomes of 11 related α-proteobacteria were surveyed for homologs of genes with CtrA and DnaA binding sites that we identified in *S. meliloti* and scanned for conserved binding sites. The tree to the left of the organism names represents their evolutionary relationship as described in (5). A. *S. meliloti* cell cycle regulated genes with the highest scoring CtrA binding motifs are displayed and number of hits is denoted by different shades of blue as described in the legend. The conservation of the CtrA binding sites in the homologous genes of various species is also displayed in the same manner. Color-coded genes (i.e. *pilA* and *SMc04115*) share promoter regions and therefore CtrA binding motifs. B. *S. meliloti* cell cycle regulated genes with the highest scoring DnaA binding motifs. Number of binding motifs and conservation of these motifs in other α-proteobacteria is denoted in the same manner as A. A key explaining the putative function of the various genes displayed is provided at the bottom of the figure.

Surprisingly, the numerous CtrA binding sites found in the regulatory regions of the flagellar genes of *C. crescentus* are not conserved in *S.meliloti.* Instead, there are conserved CtrA binding motifs preceding the motility regulator *rem.* This suggests that cell cycle regulation of flagellar and chemotaxis genes may be achieved by regulation of Rem by CtrA instead of through direct regulation of the flagellar and chemotaxis genes by CtrA. The CtrA binding motifs upstream of *rem* are conserved in many α-proteobacteria surveyed in our analysis, including the two organisms most closely related to *S. meliloti, R. leguminosarum* and *A. tumefaciens* (Figure 2.5A). This putative divergence in the mechanism of CtrA mediated cell cycle regulation of motility might have arisen during the evolution to facilitate their distinct morphologies and lifestyles.

Another interesting deviation from the *C. crescentus* cell cycle regulatory network is the absence of CtrA binding motifs upstream of the gene encoding the essential cell cycle regulated methylase, CcrM (5, 19). In *C. crescentus,* CcrM methylates newly replicated DNA at the adenine of GANTC site and the activation of *ccrM* transcription by CtrA at the end of S phase results in the re-methylation of the chromosome (13). My data indicate that the expression of *ccrM* in *S. meliloti* is indeed cell cycle regulated (Fig 2.3), but our analysis did not identify any CtrA binding motifs upstream of *ccrM* (Figure 2.5A). Previous analysis identified GANTC sites upstream of *ccrM* suggesting a method of autoregulation, but it is still unclear how transcription of *ccrM* is up-regulated after completion of S phase in *S. meliloti (5).*

The *dnaA* binding motifs we identified in *S. meliloti* genes with cell cycle regulated transcripts were much less conserved among the α-proteobacteria surveyed (Figure 2.5B). This suggests that the activity of DnaA as a transcriptional regulator in α-proteobacteria might be much less evolutionarily constrained than that of CtrA. There were no genes with both cell cycle regulated transcripts and DnaA binding motifs in *S. meliloti* that were homologs of the 40 genes thought to be regulated by DnaA in *C. crescentus* (12). For example, the CtrA binding motif is conserved upstream of the polarity factor *podJ1,* but the DnaA binding motif is not (12). I identified a previously verified DnaA binding motif in *repA2,* which is involved in segregation of the symbiotic megaplasmid pSymA, and could possibly play a role in coordinating replication of the multiple replicons (8). Interestingly, we also found a well-conserved CtrA binding site 90bp downstream of the DnaA binding site in the *repA2* promoter region. This suggests a possible interplay between CtrA and DnaA in the regulation of expression of this *repABC* operon on pSymA during the cell cycle. It is surprising that neither DnaA motifs nor CtrA motifs were found in the regulatory regions of *repC1* or *repAB3* on pSymB since the expression of these genes is also cell cycle regulated. This suggests that the expression of these genes is coordinated with the cell cycle by a different mechanism.

**Discussion**

In this study, I describe the first published method for efficient cell synchronization of *S. meliloti.* I utilized this method to perform microarray analysis of gene expression during the *S. meliloti* cell cycle, which was also the first analysis

of this kind performed in an α-proteobacterium with multiple replicons. This analysis revealed 462 genes whose expression varies as a function of the cell cycle. Comparing this list to the list of 553 previously identified genes with cell cycle regulated transcripts in *C. crescentus*, I discovered a core set of 128 genes with conserved cell cycle dependent transcription between the two species (4). Despite this conservation, the evidence presented here along with the previous analysis in Brilli *et al*. (5) demonstrates that the regulation of transcription during the cell cycle in α-proteobacteria is as diverse as their unique lifestyles and environmental niches (42). This article highlights key similarities and differences in cell cycle gene expression and the regulation of that expression between *S. meliloti* and *C. crescentus.* Our data indicates a large divergence between the cell cycle dependent regulons of CtrA and DnaA in *C. crescentus* and *S. meliloti,* suggesting unique factors play a role in the regulation of *S. meliloti* cell cycle regulated transcripts.

**Cell cycle regulated gene expression specific to *S. meliloti.*** About 72% of the cell cycle regulated transcripts identified in this analysis were unique to *S. meliloti.* This is representative of the striking differences in morphological asymmetry, genome composition and lifestyle between *S. meliloti* and *C. crescentus.* For example, the Min system for regulation of septation, which acts in *S. meliloti* but not *C. crescentus,* appears to be highly cell cycle regulated in *S. meliloti.* Even more interesting is that strong CtrA binding motifs are present upstream of the *minCDE* operon in every α-proteobacterium we surveyed that contains this operon. The presence of CtrA binding motif in the promoter of *minCDE* represents a possible integration of CtrA-mediated cell cycle control into a very species-specific septation regulation system.

My data also indicate that the replication and segregation of the symbiotic megaplasmids pSymA and pSymB is a cell cycle regulated process in *S. meliloti*. These megaplasmids, which are required for symbiosis, represent a specific adaptation to the symbiotic lifestyle of *S. meliloti,* and how *S. meliloti* coordinates the replication and segregation of these plasmids with that of its chromosome is an especially interesting question. Our data and previous work identified putative CtrA and DnaA binding sites in the promoter region of *repA2,* which may shed light on this subject. More than half of the genes with cell cycle regulated transcripts identified by our analysis encode uncharacterized, hypothetical proteins. Thus, the analysis done in this work revealed a rich pool of completely uncharacterized proteins that may be involved in cell cycle regulated processes.

**The diversity of cell cycle regulation in α-proteobacteria.** One of the most interesting conclusions that can be drawn from the work presented in this article is the diversity of cell cycle regulation schemes between α-proteobacteria. Since CtrA is such an important regulator of morphological and replicative asymmetry in *C. crescentus,* it was quite surprising how few CtrA binding sites were conserved in genes with cell cycle transcripts in *S. meliloti.* This divergence between *S. meliloti* and *C. crescentus* contrasts with the convergence of the putative CtrA regulon in α-protobacteria closely related to or with similar lifestyles as *S. meliloti.* This suggests a specific evolution of CtrA control of the cell cycle based upon the adaptations required for the lifestyles of diverse α-proteobacteria, which can range from cyst cell formation in *Rhodospirillum centenum* to intracellular pathogenesis in *Brucella* (43, 44). The putative regulation of the motility regulator Rem by CtrA is an example

of this. Instead of creating a swarmer cell that can scavenge for nutrient rich environment, *S. meliloti* uses the VisNR and Rem system to limit swimming motility to periods of exponential growth and must integrate this VisNR/Rem system into the cell cycle regulatory network. Our analysis suggests that CtrA likely plays a role in the regulation of *rem* expression. Thus instead of CtrA directly regulating the majority of the flagellar machinery as is the case in *C. crescentus,* CtrA may simply integrate into a pre-existing regulatory hierarchy in *S. meliloti*.

Further research is required to more completely understand the wiring of the cell cycle regulatory circuit in *S. meliloti* and how this regulatory circuit is modified during symbiosis to achieve the specific cellular differentiation required during bacteroid development. For example, putative CtrA and DnaA binding sites must be verified by *in vivo* experiments (i.e. ChIP-seq) and the importance of these binding sites during free-living growth and symbiosis must be determined. In addition, the synchronization method described in this paper is currently being used to assess the cell cycle regulation of protein levels (and phosphorylation status) of some of the major putative cell cycle regulators including CtrA. Determining when these factors are active during the cell cycle will help to elucidate their function. Finally, this new synchronization can also be utilized to help determine the function of NCR peptides during symbiosis. Currently the gene expression profiles of *S. meliloti* cells in distinct cell cycle phases treated with a specific NCR peptide are being assessed to determine the specific functions this NCR peptide may alter or impair. Continued investigation into the regulation of the cell cycle in *S. meliloti* and other α-proteobacteria is crucial to determine how this

intricate cell cycle network has evolved over time and to facilitate specific cellular differentiation events required for the lifestyles of this diverse group of microorganisms.

## Experimental procedures

### *Growth conditions and cell synchronization*

*S. meliloti* strain Sm1021 was grown at 30°C in LBMC (LB supplemented with 2.5 mM $MgSO_4$ and 2.5 mM $CaCl_2$) and modified MOPS-GS medium lacking mannitol (50 mM MOPS (morpholine propane sulfonic acid, pH 7.4), 1 mM $MgSO_4$, 0.25 mM $CaCl_2$, 19 mM glutamic acid, and 0.004 mM biotin). To synchronize *S. meliloti*, 1 L of LBMC was inoculated with 100 µL of saturated Sm1021 liquid culture and grown overnight to $OD_{600}$ = 0.10 - 0.15. Cells were collected by centrifugation, washed twice with 0.85% saline, and re-suspended in modified MOPS-GS. To arrest the cells the culture was incubated in MOPS-GS at 30°C in for 270 min. Following incubation in MOPS-GS lacking mannitol, cells were collected by centrifugation and resuspended in LBMC. At appropriate time points, samples were collected for flow cytometric and RNA transcriptomic analyses.

### *Flow cytometry*

To assess *S. meliloti* DNA content, 200 µL of Sm1021 culture was fixed in 933 µL of 100% ethanol (and optionally stored overnight at 4°C). Cells were collected by centrifugation and incubated in 1 mL of 50 mM sodium citrate containing 3.3 µg/ml RNase A at 50°C for 2 hrs. Samples were then incubated at room temperature with 1 µL of SYTOX Green dye diluted 1:6 in the sodium citrate/RNase solution (to achieve

a working dye concentration of 8.3 μM). Cultures were analyzed with a BD FACScan flow cytometer and data was analyzed with FlowJo 9.6.3 software.

***RNA isolation and Microarray analysis***

RNA was first stabilized in samples of synchronized culture to be used for RNA isolation by treatment with Qiagen RNA protect Bacteria Reagent and then samples were stored at -80C. Control samples were also isolated from early log-phase culture ($OD_{600}$=0.15) and treated with the Qiagen RNA protect Bacteria Reagent before storing at -80C. Once four replicate samples had been collected for each of the eight time points, RNA isolation was performed using the Qiagen RNeasy plus Mini Kit. A total of 600ng of RNA was used for cDNA synthesis (Ambion MessageAmp II-Bacteria kit) and cDNA labeling was carried out using the Ambion Amino Allyl MessageAmp II cRNA Amplification kit. Microarray hybridization was performed using the standard Agilent protocol for two-color microarray-based prokaryote analysis (http://www.genomics.agilent.com/files/Manual/G4813-90010_Prokaryote_Protocol.pdf). A two-color custom Agilent gene expression array (Smexpr1 AMADID: 036667) of 6046 *S. meliloti* ORFs was designed using the previously described Sm6kPCR as a template (45). These are two-color or two-channel microarrays that are hybridized with cDNA prepared from two samples to be compared, a time point specific sample and a control sample in this instance. The cDNA from the two samples are labeled with Cy3 (green) and Cy5 (red) fluorophores. The control and time point experimental sample cDNA are hybridized to a single microarray and the relative intensities of each cDNA fluorophore can be compared to determine up- and down-regulated genes. The two-color system is

mainly designed to determine the relative differences in expression among different spots within a sample and between samples rather than absolute gene expression. **Table 2.1** lists the 8 array file names that were generated with their corresponding samples and the fluorophores used for each sample.

**Table 2.1 Samples and corresponding array file names.**

| SampleNumber | FileName | Cy3 | Cy5 |
|---|---|---|---|
| 1 | 25366710003_SLOT01_S01_GE2_105_Dec08_1_1.txt | time0 | ref |
| 2 | 25366710003_SLOT01_S01_GE2_105_Dec08_1_2.txt | time0 | ref |
| 3 | 25366710003_SLOT01_S01_GE2_105_Dec08_1_3.txt | time0 | ref |
| 4 | 25366710003_SLOT01_S01_GE2_105_Dec08_1_4.txt | time0 | ref |
| 5 | US22502664_SLOT01_S01_GE2_105_Dec08_1_1.txt | time40 | ref |
| 6 | US22502664_SLOT01_S01_GE2_105_Dec08_1_2.txt | time40 | ref |
| 7 | US22502664_SLOT01_S01_GE2_105_Dec08_1_3.txt | time40 | ref |
| 8 | US22502664_SLOT01_S01_GE2_105_Dec08_1_4.txt | time40 | ref |
| 9 | 253666710004_201207171047_S01_GE2_105_Dec08_1_1.txt | time60 | ref |
| 10 | 253666710004_201207171047_S01_GE2_105_Dec08_1_2.txt | time60 | ref |
| 11 | 253666710004_201207171047_S01_GE2_105_Dec08_1_3.txt | time60 | ref |
| 12 | 253666710004_201207171047_S01_GE2_105_Dec08_1_4.txt | time60 | ref |
| 13 | 25366710002_SLOT02_S01_GE2_105_Dec08_1_1.txt | time80 | ref |
| 14 | 25366710002_SLOT02_S01_GE2_105_Dec08_1_2.txt | time80 | ref |
| 15 | 25366710002_SLOT02_S01_GE2_105_Dec08_1_3.txt | time80 | ref |
| 16 | 25366710002_SLOT02_S01_GE2_105_Dec08_1_4.txt | time80 | ref |
| 17 | 25366710002_SLOT02_S01_GE2_105_Dec08_2_1.txt | time100 | ref |
| 18 | 25366710002_SLOT02_S01_GE2_105_Dec08_2_2.txt | time100 | ref |
| 19 | 25366710002_SLOT02_S01_GE2_105_Dec08_2_3.txt | time100 | ref |
| 20 | 25366710002_SLOT02_S01_GE2_105_Dec08_2_4.txt | time100 | ref |
| 21 | US22502664_SLOT01_S01_GE2_105_Dec08_2_1.txt | time120 | ref |
| 22 | US22502664_SLOT01_S01_GE2_105_Dec08_2_2.txt | time120 | ref |
| 23 | US22502664_SLOT01_S01_GE2_105_Dec08_2_3.txt | time120 | ref |
| 24 | US22502664_SLOT01_S01_GE2_105_Dec08_2_4.txt | time120 | ref |
| 25 | 253666710004_201207171047_S01_GE2_105_Dec08_2_1.txt | time140 | ref |
| 26 | 253666710004_201207171047_S01_GE2_105_Dec08_2_2.txt | time140 | ref |
| 27 | 253666710004_201207171047_S01_GE2_105_Dec08_2_3.txt | time140 | ref |
| 28 | 253666710004_201207171047_S01_GE2_105_Dec08_2_4.txt | time140 | ref |
| 29 | 25366710003_SLOT01_S01_GE2_105_Dec08_2_1.txt | time160 | ref |
| 30 | 25366710003_SLOT01_S01_GE2_105_Dec08_2_2.txt | time160 | ref |
| 31 | 25366710003_SLOT01_S01_GE2_105_Dec08_2_3.txt | time160 | ref |
| 32 | 25366710003_SLOT01_S01_GE2_105_Dec08_2_4.txt | time160 | ref |

***Data Normalization***

The array data was processed using the *limma* package in R. First the median red/green signals were background corrected by subtracting the median red/green background signals, and any intensities that are zero or negative are set equal to half the minimum of the positive corrected intensities for that array. Next, the red/green signal log-ratios (M= log2(R/G)) were normalized for each array using loess, so that the log-ratios average to zero within each array. Normalization is intended to remove any systematic trends that arise from the microarray technology rather than from differences between the probes or between the target RNA samples hybridized to the arrays. Normalization between arrays was performed to achieve consistency between arrays. The normalization ensured that the average intensities (A=0.5*log2(RG)) have the same empirical distribution across arrays leaving the log-ratio values (M) unchanged. Sample replicate 4 from time point 140 was removed due to poor correlations with other replicates' normalized gene expression data.

***Selection of significantly varying genes across the time points***

The replicate log ratio values for time points 40-160 were first averaged and used to calculate the standard deviation for each gene. The observed standard deviations were compared to the distribution of standard deviations generated from 10,000 randomly permuted gene expression profiles. Gene's with empirical p-values <= 0.05 were considered for clustering.

***Fuzzy clustering of gene expression***

To identify expression profile patterns among the genes identified to be varying in expression across time points 40-160, a fuzzy c-means clustering approach was applied using R software package e1071 (http://cran.r-project.org/web/packages/e1071/index.html). The gene expression profiles were first mean centered normalized. The 'fuzzy' parameter was estimated by randomizing the datasets and determining the minimum parameter that doesn't result in clustering of random data (27). To establish the number of clusters, a range of cluster numbers were used to compare the minimum centroid distances between clusters as cluster number increased. An optimal cluster number corresponds to a large decrease in minimum centroid distance that slowly decreases as cluster number increases. The 2-norm figure of merit (FOM) measure (46) was also considered to determine the optimal number of clusters.

A bagged clustering wrapper, bclust, was used with the fuzzy c-means algorithm and the parameters estimated. The bagged clustering method reduces the variability in the clustering results by averaging multiple boostrapped runs of the c-means algorithm. The estimated cluster centers from the 500 iterations are then used for a final c-means run using all the data.

***S. meliloti and C. crescentus cell cycle gene comparisons***

The amino acid sequences for 6201 *S. meliloti* 1021 genes were acquired and blasted against 3737 *C. crescentus* protein sequences. The blast results were used to determine which of the 552 *C. crescentus* cell cycle regulated genes identified from Laub et al. (4) were similar to the 462 *S. meliloti* cell cycle regulated genes. The blast

analysis was complemented with the Cluster of Orthologous Groups (COGs) to identify which *C. crescentus* and *S. meliloti* proteins were clustered together using these methods (47). These results were filtered using E-values < 1x10-20 as well as manually filtered to match genes and remove replicates.

***Ctra and DnaA binding motif discovery***

To determine how many of the 462 S. meliloti cell cycle genes have CtrA and DnaA binding sites, the CtrA and DnaA motifs from Brilli et al. (5) were used in FIMO (48) with the 400bp upstream and 100bp downstream the S. meliloti cell cycle gene promoters. FIMO searches within the sequences for the motifs provided. A p-value cutoff of 2x10-4 was used to establish the S. meliloti genes containing the motifs, resulting in 66 and 48 CtrA and DnaA genes, respectively.

The protein sequence for the S. meliloti CtrA and DnaA regulated genes were then reciprocal blasted against all the proteins of 11 closely related species to identify homologous genes that may also contain the motifs. Proteins from the 11 other species that were found to have blastp E-values <= 0.05 in both blastp results were further considered for FIMO analysis using the 400bp upstream and 100bp downstream sequence of their promoters and the corresponding CtrA and DnaA motifs. A 2x10-4 p-value was used as the threshold for significant motif findings.

***qPCR analysis***

Primers were designed to amplify a ~100bp region of the *ctrA* gene (SMc00654) and control gene SMc00128, which demonstrated stable expression across the cell cycle. RNA was isolated from early log phase (OD~0.15) *S. meliloti* unsynchronized culture for primer efficiency testing and standard curve generation. To determine

levels of *ctrA* expression during the cell cycle RNA was isolated from four representative time points in a synchronized *S. meliloti* culture (t=40,80,120,160). All RNA was isolated using the Qiagen RNeasy plus Mini Kit and used to generate cDNA with the BioRad iScript cDNA Synthesis kit (concentration of total RNA was normalized across the samples before used in cDNA synthesis). Quantitative PCR analysis was carried out on a Roche LightCycler 480 using the Roche LightCycler 480 SYBR Green I Master Mix. Standard curves were created using 3:1 serial dilutions of cDNA from unsynchronized *S. meliloti* culture. Standard curves were used to generate the relation between measured $C_p$ values and log-10 concentration. The data for the two technical replicates for each biological replicate was averaged and Log expr. ratio was calculated for each biological replicate (Log expr. ratio = log [ctrA] - log [SMc00128]) and then Log expr. ratios were averaged for biological replicates (standard error represented by error bars in Fig. 2.S3).

**Acknowledgements**

We thank the NIH for their funding and support (GM31010). We also gratefully acknowledge the support and contributions of the Stuart Levine and Manlin Luo from the MIT BioMicro Center for microarray studies. Lastly we thank Jon Penterman and Michael T. Laub for their thoughtful discussion and comments on this manuscript.

# Supplemental Tables

## Table 2.S1. List of 462 clustered genes with cell cycle regulated gene expression.

| cluster | locus | gene | function | cluster | locus | gene | function | cluster | locus | gene | function |
|---|---|---|---|---|---|---|---|---|---|---|---|
| 1 | SMa0126 | cspA8 | ch | 1 | SMb21372 | | txnR | 2 | SMb21272 | | txnR |
| 1 | SMc00141 | | env | 1 | SMc03900 | ndvA | vir | 2 | SMc02141 | phoU | txnR |
| 1 | SMc02089 | lpxB | env | 2 | SMc00033 | | dgc/pde | 3 | SMa0744 | groEL2 | ch |
| 1 | SMa0128 | | hy | 2 | SMa0241 | | env | 3 | SMa2319 | gst14 | ch |
| 1 | SMb20047 | | hy | 2 | SMb21318 | wgcA | env | 3 | SMc00912 | groES1 | ch |
| 1 | SMb20152 | | hy | 2 | SMc00171 | | env | 3 | SMa0412 | | hy |
| 1 | SMb20167 | | hy | 2 | SMc01127 | olsB | env | 3 | SMa1907 | | hy |
| 1 | SMb20278 | | hy | 2 | SMc04381 | opgC | env | 3 | SMa1910 | | hy |
| 1 | SMb21028 | | hy | 2 | SMb20876 | | hy | 3 | SMb20165 | | hy |
| 1 | SMb21282 | | hy | 2 | SMc02491 | | hy | 3 | SMb20684 | | hy |
| 1 | SMb21284 | | hy | 2 | SMa0237 | | me | 3 | SMc00026 | | hy |
| 1 | SMb21357 | | hy | 2 | SMa0244 | | me | 3 | SMc00931 | | hy |
| 1 | SMc00198 | | hy | 2 | SMb20759 | phnG | me | 3 | SMc02052 | | hy |
| 1 | SMc00359 | | hy | 2 | SMb20760 | phnH | me | 3 | SMc02497 | | hy |
| 1 | SMc01586 | | hy | 2 | SMb20761 | phnI | me | 3 | SMc02553 | | hy |
| 1 | SMc02388 | | hy | 2 | SMb20762 | phnJ | me | 3 | SMc02656 | | hy |
| 1 | SMc02389 | | hy | 2 | SMb20765 | | me | 3 | SMc03941 | | hy |
| 1 | SMc02817 | | hy | 2 | SMb21170 | nitR | me | 3 | SMc04435 | | hy |
| 1 | SMc03143 | | hy | 2 | SMb21171 | phnM | me | 3 | SMb20136 | ubiD | me |
| 1 | SMa1809 | | me | 2 | SMb21277 | | me | 3 | SMb20170 | fdh | me |
| 1 | SMa1821 | | me | 2 | SMc00618 | ppk | me | 3 | SMb20171 | | me |
| 1 | SMb20150 | | me | 2 | SMc01847 | btaB | me | 3 | SMb20172 | | me |
| 1 | SMb20205 | pqqB | me | 2 | SMc01848 | btaA | me | 3 | SMb20186 | | me |
| 1 | SMb20207 | pqqD | me | 2 | SMc01907 | | me | 3 | SMb20204 | pqqA | me |
| 1 | SMb20208 | pqqE | me | 2 | SMc03129 | | me | 3 | SMb20251 | xynB | me |
| 1 | SMb20314 | | me | 2 | SMc03243 | | me | 3 | SMb20456 | fabG | me |
| 1 | SMb21179 | | me | 2 | SMc04299 | | me | 3 | SMb21285 | | me |
| 1 | SMb21278 | adeC2 | me | 2 | SMc03130 | | rep | 3 | SMb21286 | xdhA1 | me |
| 1 | SMb21283 | | me | 2 | SMc02147 | phoR | sig | 3 | SMb21300 | deoC | me |
| 1 | SMb21293 | guaD1 | me | 2 | SMb20763 | phnK | tr | 3 | SMb21339 | | me |
| 1 | SMb21373 | | me | 2 | SMb21174 | phoT | tr | 3 | SMb21558 | | me |
| 1 | SMb21374 | | me | 2 | SMb21175 | phoE | tr | 3 | SMc00073 | | me |
| 1 | SMb21494 | ocd | me | 2 | SMb21176 | phoD | tr | 3 | SMc00606 | | me |
| 1 | SMc00673 | | me | 2 | SMb21177 | phoC | tr | 3 | SMc01109 | metK | me |
| 1 | SMc00819 | katA | me | 2 | SMc00620 | | tr | 3 | SMc01270 | adhC1 | me |
| 1 | SMc00977 | | me | 2 | SMc00978 | | tr | 3 | SMc01766 | hemB | me |
| 1 | SMc02349 | asfA | me | 2 | SMc01605 | | tr | 3 | SMc02039 | | me |
| 1 | SMc02874 | murQ | me | 2 | SMc01606 | | tr | 3 | SMc02173 | frcS | me |
| 1 | SMc04384 | | me | 2 | SMc01607 | | tr | 3 | SMc02321 | rhaI | me |
| 1 | SMc04386 | aatB | me | 2 | SMc02143 | pstA | tr | 3 | SMc02503 | | me |
| 1 | SMb20151 | | sig | 2 | SMc02144 | pstC | tr | 3 | SMc03104 | hemA | me |
| 1 | SMb20153 | | tr | 2 | SMc02145 | | tr | 3 | SMa0591 | | ph |
| 1 | SMb21273 | | tr | 2 | SMc02146 | pstS | tr | 3 | SMa2391 | repC2 | rep |
| 1 | SMb21274 | | tr | 2 | SMc02634 | phoX | tr | 3 | SMa2393 | repB2 | rep |
| 1 | SMb21275 | | tr | 2 | SMc03124 | | tr | 3 | SMa2395 | repA2 | rep |
| 1 | SMb21276 | | tr | 2 | SMc03125 | | tr | 3 | SMb20044 | repC1 | rep |
| 1 | SMb21375 | | tr | 2 | SMc03126 | | tr | 3 | SMb20598 | repA3 | rep |
| 1 | SMb21376 | | tr | 2 | SMc03127 | | tr | 3 | SMb20599 | repB3 | rep |
| 1 | SMb21377 | | tr | 2 | SMc03128 | | tr | 3 | SMb20709 | aag | rep |
| 1 | SMc00044 | | tr | 2 | SMc04300 | | tr | 3 | SMa0105 | | tr |
| 1 | SMc00559 | | tr | 2 | SMc04316 | | tr | 3 | SMa2085 | | tr |
| 1 | SMa0246 | | txnR | 2 | SMc04317 | afuA | tr | 3 | SMb20108 | | tr |

| cluster | locus | gene | function |
|---|---|---|---|
| 3 | SMb21536 | | tr |
| 3 | SMc01242 | | tr |
| 3 | SMc02156 | | tr |
| 3 | SMc02283 | | tr |
| 3 | SMc04263 | | tr |
| 3 | SMc00568 | rpsF | tx/tr |
| 3 | SMc01319 | rplJ | tx/tr |
| 3 | SMc03881 | rpmF | tx/tr |
| 3 | SMc04434 | rpmH | tx/tr |
| 3 | SMc02172 | frcR | txnR |
| 3 | SMc04011 | tacA | txnR |
| 3 | SMa1310 | virB7 | vir |
| 3 | SMa0115 | | |
| 4 | SMb21566 | groEL5 | ch |
| 4 | SMb21524 | minC | div |
| 4 | SMc01873 | ftsA | div |
| 4 | SMc01874 | ftsZ1 | div |
| 4 | SMc00638 | | env |
| 4 | SMc00639 | | env |
| 4 | SMc01795 | gumC | env |
| 4 | SMc03045 | | env |
| 4 | SMc00120 | | hy |
| 4 | SMc00291 | | hy |
| 4 | SMc00986 | | hy |
| 4 | SMc01015 | | hy |
| 4 | SMc01793 | | hy |
| 4 | SMc03023 | | hy |
| 4 | SMc03056 | | hy |
| 4 | SMc03057 | | hy |
| 4 | SMc03072 | | hy |
| 4 | SMc03746 | | hy |
| 4 | SMc02825 | pepA2 | me |
| 4 | SMc03004 | mcpE | mo |
| 4 | SMc03009 | cheR | mo |
| 4 | SMc03014 | fliF | mo |
| 4 | SMc03018 | flhB | mo |
| 4 | SMc03019 | fliG | mo |
| 4 | SMc03020 | fliN | mo |
| 4 | SMc03021 | fliM | mo |
| 4 | SMc03022 | motA | mo |
| 4 | SMc03024 | flgF | mo |
| 4 | SMc03025 | fliI | mo |
| 4 | SMc03027 | flgB | mo |
| 4 | SMc03028 | flgC | mo |
| 4 | SMc03029 | fliE | mo |
| 4 | SMc03030 | flgG | mo |
| 4 | SMc03031 | flgA | mo |
| 4 | SMc03032 | flgI | mo |
| 4 | SMc03033 | motE | mo |
| 4 | SMc03034 | flgH | mo |
| 4 | SMc03035 | fliL | mo |
| 4 | SMc03039 | flaD | mo |

| cluster | locus | gene | function |
|---|---|---|---|
| 4 | SMc03040 | flaC | mo |
| 4 | SMc03041 | | mo |
| 4 | SMc03042 | motB | mo |
| 4 | SMc03043 | motC | mo |
| 4 | SMc03044 | fliK | mo |
| 4 | SMc03047 | flgE | mo |
| 4 | SMc03048 | flgK | mo |
| 4 | SMc03049 | flgL | mo |
| 4 | SMc03050 | flaF | mo |
| 4 | SMc03051 | flbT | mo |
| 4 | SMc03052 | flgD | mo |
| 4 | SMc03053 | fliQ | mo |
| 4 | SMc03054 | flhA | mo |
| 4 | SMc03071 | | mo |
| 4 | SMc04110 | cpaD1 | pil |
| 4 | SMc04112 | cpaB1 | pil |
| 4 | SMc02230 | podJ1 | sig |
| 4 | SMc02369 | pleC | sig |
| 4 | SMc03006 | cheY1 | sig |
| 4 | SMc03007 | cheA | sig |
| 4 | SMc03046 | rem | sig |
| 4 | SMc01794 | | tr |
| 4 | SMc02061 | bioS | tr |
| 4 | SMc02824 | | tr |
| 5 | SMc00003 | | ch |
| 5 | SMc00887 | | dgc/pde |
| 5 | SMc00992 | | dgc/pde |
| 5 | SMc03178 | | dgc/pde |
| 5 | SMc03942 | | dgc/pde |
| 5 | SMb20595 | ftsK2 | div |
| 5 | SMb20596 | | div |
| 5 | SMb21522 | minE | div |
| 5 | SMb21523 | minD | div |
| 5 | SMc01029 | | div |
| 5 | SMc01860 | ftsI | div |
| 5 | SMc01872 | ftsQ | div |
| 5 | SMc03808 | ftsK | div |
| 5 | SMc04024 | | div |
| 5 | SMb21091 | lysM | env |
| 5 | SMb21502 | | env |
| 5 | SMb21503 | | env |
| 5 | SMb21505 | wzy | env |
| 5 | SMb21506 | | env |
| 5 | SMc00539 | | env |
| 5 | SMc00604 | ropB1 | env |
| 5 | SMc00743 | | env |
| 5 | SMc00928 | | env |
| 5 | SMc00996 | | env |
| 5 | SMc01187 | rlpA | env |
| 5 | SMc01791 | | env |
| 5 | SMc01796 | | env |
| 5 | SMc01871 | ddlB | env |

| cluster | locus | gene | function |
|---|---|---|---|
| 5 | SMc02060 | lppB | env |
| 5 | SMa0034 | | hy |
| 5 | SMa2239 | | hy |
| 5 | SMb20303 | | hy |
| 5 | SMb21479 | | hy |
| 5 | SMb21512 | | hy |
| 5 | SMb21515 | | hy |
| 5 | SMc00001 | | hy |
| 5 | SMc00060 | | hy |
| 5 | SMc00330 | | hy |
| 5 | SMc00336 | | hy |
| 5 | SMc00651 | | hy |
| 5 | SMc00655 | | hy |
| 5 | SMc00718 | | hy |
| 5 | SMc00742 | | hy |
| 5 | SMc00924 | | hy |
| 5 | SMc00983 | | hy |
| 5 | SMc00997 | | hy |
| 5 | SMc00999 | | hy |
| 5 | SMc01068 | | hy |
| 5 | SMc01107 | | hy |
| 5 | SMc01356 | | hy |
| 5 | SMc01357 | | hy |
| 5 | SMc01433 | | hy |
| 5 | SMc01561 | | hy |
| 5 | SMc01859 | | hy |
| 5 | SMc01933 | | hy |
| 5 | SMc02054 | | hy |
| 5 | SMc02392 | | hy |
| 5 | SMc02447 | | hy |
| 5 | SMc02488 | | hy |
| 5 | SMc02848 | | hy |
| 5 | SMc03013 | | hy |
| 5 | SMc03026 | | hy |
| 5 | SMc03066 | | hy |
| 5 | SMc03174 | | hy |
| 5 | SMc04022 | | hy |
| 5 | SMc04115 | | hy |
| 5 | SMc04117 | | hy |
| 5 | SMc04118 | | hy |
| 5 | SMc04225 | | hy |
| 5 | SMc04359 | | hy |
| 5 | SMa1757 | | me |
| 5 | SMb20650 | | me |
| 5 | SMb20651 | | me |
| 5 | SMc02252 | galE | me |
| 5 | SMc02254 | qxtB | me |
| 5 | SMc02255 | qxtA | me |
| 5 | SMc02524 | fdsG | me |
| 5 | SMc02525 | fdsB | me |
| 5 | SMc02562 | pckA | me |
| 5 | SMc03085 | fdsC | me |

| cluster | locus | gene | function |
|---|---|---|---|
| 5 | SMc03086 | fdsD | me |
| 5 | SMc03983 | fbaB | me |
| 5 | SMc04444 | fdsA | me |
| 5 | SMc00765 | mcpZ | mo |
| 5 | SMc00975 | mcpU | mo |
| 5 | SMc01104 | mcpX | mo |
| 5 | SMc01468 | cheW2 | mo |
| 5 | SMc01469 | mcpW | mo |
| 5 | SMc01719 | mcpT | mo |
| 5 | SMc03005 | cheX | mo |
| 5 | SMc03008 | cheW1 | mo |
| 5 | SMc03010 | cheB | mo |
| 5 | SMc03012 | cheD | mo |
| 5 | SMc03037 | flaA | mo |
| 5 | SMc03038 | flaB | mo |
| 5 | SMc04227 | mcpV | mo |
| 5 | SMc02446 | | pil |
| 5 | SMc02820 | cpaF1 | pil |
| 5 | SMc02822 | | pil |
| 5 | SMc04059 | | pil |
| 5 | SMc04111 | cpaC1 | pil |
| 5 | SMc04113 | cpaA1 | pil |
| 5 | SMc04114 | pilA1 | pil |
| 5 | SMc00021 | ccrM | rep |
| 5 | SMc01183 | lexA | rep |
| 5 | SMc01432 | | rep |
| 5 | SMc01579 | | rep |
| 5 | SMc02489 | xerC | rep |
| 5 | SMc00059 | divJ | sig |
| 5 | SMc00191 | | sig |
| 5 | SMc00652 | chpT | sig |
| 5 | SMc00653 | | sig |
| 5 | SMc00654 | ctrA | sig |
| 5 | SMc00657 | sciP | sig |
| 5 | SMc00888 | | sig |
| 5 | SMc01371 | divK | sig |
| 5 | SMc03011 | cheY2 | sig |
| 5 | SMc04109 | cpaE1 | sig |
| 5 | SMc04170 | | sig |
| 5 | SMc04212 | pdhS2 | sig |
| 5 | SMb20057 | btuC | tr |
| 5 | SMb20902 | | tr |
| 5 | SMc00159 | | tr |
| 5 | SMc00548 | | tr |
| 5 | SMc00991 | | tr |
| 5 | SMc00998 | | tr |
| 5 | SMc01467 | | tr |
| 5 | SMc02171 | frcB | tr |
| 5 | SMc02821 | | tr |
| 5 | SMb21514 | hemK2 | tx/tr |
| 5 | SMc01768 | | txnR |
| 5 | SMc02826 | | txnR |

| cluster | locus | gene | function |
|---|---|---|---|
| 6 | SMc00371 | yciF | ch |
| 6 | SMc01278 | sugE | ch |
| 6 | SMa0369 | | dgc/pde |
| 6 | SMb20523 | | dgc/pde |
| 6 | SMc00404 | | env |
| 6 | SMc01404 | | env |
| 6 | SMc01792 | | env |
| 6 | SMc01846 | | env |
| 6 | SMc02272 | rkpG | env |
| 6 | SMa0333 | | hy |
| 6 | SMa0537 | | hy |
| 6 | SMa0543 | | hy |
| 6 | SMa0629 | | hy |
| 6 | SMa1706 | | hy |
| 6 | SMb20348 | | hy |
| 6 | SMb20411 | | hy |
| 6 | SMb20413 | | hy |
| 6 | SMb20464 | | hy |
| 6 | SMb20862 | | hy |
| 6 | SMb20898 | | hy |
| 6 | SMb20911 | | hy |
| 6 | SMb21036 | | hy |
| 6 | SMb21127 | | hy |
| 6 | SMb21495 | | hy |
| 6 | SMc00014 | | hy |
| 6 | SMc00061 | | hy |
| 6 | SMc00083 | | hy |
| 6 | SMc00084 | | hy |
| 6 | SMc00251 | | hy |
| 6 | SMc00507 | | hy |
| 6 | SMc00591 | | hy |
| 6 | SMc00607 | | hy |
| 6 | SMc00740 | | hy |
| 6 | SMc01315 | | hy |
| 6 | SMc01745 | | hy |
| 6 | SMc01760 | | hy |
| 6 | SMc02112 | | hy |
| 6 | SMc02264 | | hy |
| 6 | SMc02304 | | hy |
| 6 | SMc02842 | | hy |
| 6 | SMc02862 | | hy |
| 6 | SMc03297 | | hy |
| 6 | SMc03747 | | hy |
| 6 | SMc03787 | | hy |
| 6 | SMc03794 | | hy |
| 6 | SMc03986 | | hy |
| 6 | SMc03999 | | hy |
| 6 | SMc04004 | | hy |
| 6 | SMc04164 | | hy |
| 6 | SMc04180 | | hy |
| 6 | SMc04216 | | hy |
| 6 | SMc04269 | | hy |

| cluster | locus | gene | function |
|---|---|---|---|
| 6 | SMc04409 | | hy |
| 6 | SMb20579 | pcaD | me |
| 6 | SMc00594 | ligE | me |
| 6 | SMc01124 | glnD | me |
| 6 | SMc02687 | | me |
| 6 | SMc02761 | trxA | me |
| 6 | SMc04043 | hutG | me |
| 6 | SMc04346 | ilvC | me |
| 6 | SMc03090 | cheW3 | mo |
| 6 | SMa1612 | | ph |
| 6 | SMc03257 | TRm18 | ph |
| 6 | SMb20947 | exoX | sig |
| 6 | SMc02584 | actR | sig |
| 6 | SMc04044 | cpdR1 | sig |
| 6 | SMa2231 | | tox |
| 6 | SMb20412 | | tox |
| 6 | SMc00392 | | tox |
| 6 | SMc00393 | | tox |
| 6 | SMc04332 | ecnB | tox |
| 6 | SMa1945 | | tr |
| 6 | SMb20634 | | tr |
| 6 | SMc00186 | | tr |
| 6 | SMc02279 | | tr |
| 6 | SMc02861 | pit | tr |
| 6 | SMc02981 | | tr |
| 6 | SMc00349 | lepA | tx/tr |
| 6 | SMc00522 | rhlE1 | tx/tr |
| 6 | SMc02408 | rpoZ | tx/tr |
| 6 | SMc02644 | | tx/tr |
| 6 | SMc03151 | | tx/tr |
| 6 | SMc04003 | rpmJ | tx/tr |
| 6 | SMa0738 | cspA6 | txnR |
| 6 | SMa0955 | | txnR |
| 6 | SMa1933 | | txnR |
| 6 | SMb20337 | | txnR |
| 6 | SMb20375 | | txnR |
| 6 | SMb20537 | | txnR |
| 6 | SMb21169 | | txnR |
| 6 | SMc01260 | | txnR |
| 6 | SMc01522 | | txnR |
| 6 | SMc01585 | cspA3 | txnR |
| 6 | SMc03816 | | txnR |
| 6 | SMc03880 | aniA | txnR |
| 6 | SMc04032 | | txnR |
| 6 | SMc04318 | cspA1 | txnR |
| 6 | SMb21110 | | vir |

**Table 2.S4. Genes with cell cyle regulated transcripts conserved between *C. crescentus* and *S. meliloti.***

| Rm 1021 | Cc CB15 | gene | function | E-value |
|---|---|---|---|---|
| SMa0034 | CC2610 | | hy | 1.75E-21 |
| SMa0126 | CC0665 | cspA8 | ch | 9.21E-28 |
| SMa0237 | CC1354 | | me | 2.23E-20 |
| SMa0241 | CC0092 | | env | 4.14E-07 |
| SMa0744 | CC0685 | groEL2 | ch | 0 |
| SMa1757 | CC1675 | | me | 3.25E-20 |
| SMa2319 | CC1316 | gst14 | ch | 4.90E-13 |
| SMb20150 | CC2252 | | me | 9.66E-19 |
| SMb20170 | CC3759 | fdh | me | 5.81E-06 |
| SMb20171 | CC2515 | | me | 2.55E-76 |
| SMb20172 | CC1210 | | me | 1.17E-21 |
| SMb20456 | CC1675 | fabG | me | 1.12E-22 |
| SMb20523 | CC1850 | | dgc/pde | 8.26E-22 |
| SMb20537 | CC3065 | | txnR | 9.51E-21 |
| SMb20763 | CC0361 | phnK | tr | 3.32E-15 |
| SMb20765 | CC2651 | | me | 2.81E-05 |
| SMb21170 | CC1681 | nitR | me | 2.82E-08 |
| SMb21174 | CC0363 | phoT | tr | 5.95E-30 |
| SMb21175 | CC0363 | phoE | tr | 2.55E-28 |
| SMb21176 | CC0362 | phoD | tr | 2.46E-11 |
| SMb21177 | CC0292 | phoC | tr | 3.08E-21 |
| SMb21275 | CC1597 | | tr | 0.000127 |
| SMb21276 | CC3299 | | tr | 1.54E-28 |
| SMb21372 | CC2316 | | txnR | 2.15E-10 |
| SMb21377 | CC0859 | | tr | 3.66E-24 |
| SMb21566 | CC0685 | groEL5 | ch | 0 |
| SMc00003 | CC0011 | | ch | 2.41E-15 |
| SMc00014 | CC3115 | | hy | 6.14E-25 |
| SMc00021 | CC0378 | ccrM | rep | 1.45E-139 |
| SMc00033 | CC0857 | | dgc/pde | 7.05E-16 |
| SMc00059 | CC1063 | divJ | sig | 8.22E-55 |
| SMc00141 | CC0201 | | env | 0.000251 |
| SMc00349 | CC0741 | lepA | tx/tr | 1.99E-32 |
| SMc00539 | CC1872 | nlpD | env | 3.76E-36 |
| SMc00651 | CC1035 | | hy | 2.85E-37 |
| SMc00652 | CC3470 | chpT | sig | 5.48E-21 |
| SMc00653 | CC0432 | | hy | 2.62E-05 |
| SMc00654 | CC3035 | ctrA | sig | 1.02E-110 |
| SMc00765 | CC0504 | mcpZ | mo | 9.26E-86 |
| SMc00887 | CC0857 | | dgc/pde | 1.51E-59 |
| SMc00888 | CC0138 | | sig | 5.34E-15 |
| SMc00912 | CC0686 | groES1 | ch | 1.06E-38 |
| SMc00928 | CC2967 | sleB | env | 3.83E-37 |
| SMc00975 | CC3349 | mcpU | mo | 3.62E-86 |
| SMc00977 | CC2172 | | me | 4.97E-24 |
| SMc00992 | CC0857 | | dgc/pde | 6.72E-56 |
| SMc00998 | CC0167 | | tr | 1.64E-21 |
| SMc01104 | CC0430 | mcpX | mo | 2.29E-101 |
| SMc01109 | CC0050 | metK | me | 4.98E-122 |
| SMc01183 | CC1902 | lexA | rep | 6.89E-82 |
| SMc01319 | CC0496 | rplJ | tx/tr | 1.12E-44 |
| SMc01371 | CC2463 | divK | sig | 6.79E-52 |
| SMc01404 | CC2033 | racX | env | 2.54E-12 |
| SMc01468 | CC0764 | cheW2 | mo | 1.53E-36 |
| SMc01469 | CC1655 | mcpW | mo | 5.04E-75 |
| SMc01522 | CC3343 | | txnR | 0.000203 |
| SMc01579 | CC2165 | | rep | 3.80E-08 |
| SMc01585 | CC0665 | cspA3 | ch | 1.69E-15 |
| SMc01719 | CC2810 | mcpT | mo | 8.00E-28 |
| SMc01792 | CC2384 | | env | 2.85E-39 |
| SMc01794 | CC2432 | | tr | 4.42E-06 |
| SMc01847 | CC2141 | btaB | me | 0.000278 |
| SMc01860 | CC2560 | ftsI | div | 1.59E-89 |
| SMc01872 | CC2542 | ftsQ | div | 2.11E-28 |
| SMc01873 | CC2541 | ftsA | div | 8.15E-78 |
| SMc01874 | CC2540 | ftsZ1 | div | 4.61E-119 |
| SMc02060 | CC3034 | lppB | env | 1.02E-07 |

| Rm 1021 | Cc CB15 | gene | function | E-value |
|---|---|---|---|---|
| SMc02143 | CC0291 | pstA | tr | 6.54E-126 |
| SMc02144 | CC0290 | pstC | tr | 9.05E-90 |
| SMc02147 | CC3102 | phoR | sig | 3.34E-25 |
| SMc02252 | CC0092 | galE | me | 1.56E-60 |
| SMc02369 | CC2482 | pleC | sig | 4.01E-106 |
| SMc02488 | CC2229 | | hy | 0.000115 |
| SMc02524 | CC1950 | fdsG | me | 1.06E-09 |
| SMc02525 | CC1947 | fdsB | me | 2.69E-61 |
| SMc02584 | CC1767 | actR | sig | 7.06E-33 |
| SMc02820 | CC2942 | cpaF1 | mo | 0 |
| SMc02825 | CC0977 | pepA2 | me | 2.49E-44 |
| SMc03004 | CC0428 | mcpE | mo | 5.54E-79 |
| SMc03005 | CC0431 | cheX | mo | 4.31E-12 |
| SMc03006 | CC0432 | cheY1 | sig | 3.96E-44 |
| SMc03007 | CC0433 | cheA | mo | 0 |
| SMc03008 | CC0434 | cheW1 | mo | 5.35E-52 |
| SMc03009 | CC0435 | cheR | mo | 6.80E-85 |
| SMc03010 | CC0436 | cheB | mo | 1.02E-118 |
| SMc03011 | CC0437 | cheY2 | mo | 1.91E-37 |
| SMc03012 | CC0438 | cheD | mo | 1.07E-50 |
| SMc03014 | CC0905 | fliF | mo | 1.39E-49 |
| SMc03019 | CC0906 | fliG | mo | 6.56E-19 |
| SMc03020 | CC0908 | fliN | mo | 2.61E-12 |
| SMc03024 | CC2063 | flgF | mo | 7.99E-34 |
| SMc03025 | CC3040 | fliI | mo | 4.39E-89 |
| SMc03027 | CC0953 | flgB | mo | 2.76E-11 |
| SMc03028 | CC0954 | flgC | mo | 2.78E-32 |
| SMc03030 | CC2064 | flgG | mo | 1.24E-70 |
| SMc03032 | CC2582 | flgI | mo | 2.07E-88 |
| SMc03034 | CC2066 | flgH | mo | 2.49E-40 |
| SMc03037 | CC0792 | flaA | mo | 4.96E-21 |
| SMc03038 | CC0793 | flaB | mo | 3.62E-15 |
| SMc03039 | CC0794 | flaD | mo | 9.04E-14 |
| SMc03040 | CC1460 | flaC | mo | 2.35E-37 |
| SMc03042 | CC1573 | motB | mo | 2.27E-12 |
| SMc03046 | CC1304 | rem | sig | 8.75E-11 |
| SMc03048 | CC0899 | flgK | mo | 6.25E-11 |
| SMc03050 | CC1459 | flaF | mo | 9.82E-09 |
| SMc03051 | CC1458 | flbT | mo | 7.12E-11 |
| SMc03052 | CC0901 | flgD | mo | 3.43E-07 |
| SMc03053 | CC1075 | fliQ | mo | 8.05E-09 |
| SMc03126 | CC1698 | | | 1.47E-12 |
| SMc03178 | CC1850 | | dgc/pde | 1.04E-14 |
| SMc03942 | CC0857 | | dgc/pde | 4.88E-70 |
| SMc03999 | CC3291 | | hy | 1.02E-06 |
| SMc04011 | CC0909 | tacA | txnR | 1.37E-67 |
| SMc04022 | CC0163 | | hy | 1.36E-11 |
| SMc04032 | CC0782 | | txnR | 1.94E-06 |
| SMc04044 | CC0744 | cpdR | sig | 8.45E-37 |
| SMc04109 | CC2943 | cpaE1 | sig | 1.15E-106 |
| SMc04110 | CC2944 | cpaD1 | pil | 1.99E-12 |
| SMc04111 | CC2945 | cpaC1 | pil | 2.14E-72 |
| SMc04112 | CC2946 | cpaB1 | pil | 5.54E-32 |
| SMc04113 | CC2947 | cpaA1 | pil | 2.26E-20 |
| SMc04114 | CC2948 | pilA1 | pil | 4.88E-10 |
| SMc04170 | CC3219 | | sig | 3.36E-06 |
| SMc04212 | CC1062 | | sig | 3.44E-42 |
| SMc04227 | CC2317 | mcpV | mo | 1.81E-72 |
| SMc04300 | CC3373 | | tr | 8.11E-21 |
| SMc04318 | CC0665 | cspA1 | txnR | 2.92E-22 |
| SMc04444 | CC1946 | fdsA | me | 3.12E-35 |

## Table 2.S5A. Conservation of CtrA binding motifs in genes with cell cycle regulated transcripts

| gene | agrobact_tumef | bart_quin | brady_jap | bruc_abort | caul_cres | meso_loti | nitro_hamb | ochro_anthro | rhizo_legum | rhodop_pal | sino_mel | xanth_auto |
|---|---|---|---|---|---|---|---|---|---|---|---|---|
| SMa1310 | 0,0.00161 | 0,0.00176 | - | 0,0.000642 | - | - | - | 0,0.00467 | - | - | 1,0.000131 | 0,0.01 |
| SMa2393 | 0,0.00295 | 1,0.000187 | 0,0.00618 | 0,0.00491 | 0,0.00257 | 0,0.00479 | 0,0.00279 | 0,0.000342 | 0,0.00257 | 0,0.000424 | 1,0.000166 | 0,0.00143 |
| SMa2395 | 2,4.06e-06 | 0,0.000953 | 0,0.00348 | 0,0.000285 | 0,0.00753 | 0,0.000642 | 2,1.13e-07 | 1,3.85e-05 | 2,2.2e-06 | 0,0.000984 | 1,3.81e-06 | 1,2.54e-06 |
| SMb20303 | - | - | - | - | 0,0.0081 | - | - | - | - | - | 1,9e-05 | - |
| SMb21514 | 0,0.00223 | 0,0.00134 | 0,0.00243 | 0,0.00321 | 0,0.00388 | 0,0.00287 | 0,0.00634 | 0,0.00243 | 0,0.00455 | 0,0.0033 | 1,8.62e-05 | 0,0.00479 |
| SMb21523 | 0,0.00126 | 0,0.000953 | 0,0.00139 | 0,0.00264 | 0,0.00753 | 0,0.00147 | 0,0.00204 | 0,0.000274 | 0,0.00545 | 0,0.000984 | 1,0.000102 | 0,0.00559 |
| SMb21524 | 2,1.39e-06 | - | 1,4.48e-07 | 5,2.8e-07 | - | 3,6.57e-07 | - | 2,1.27e-05 | 3,1.82e-07 | - | 3,1.39e-06 | - |
| SMc00003 | 0,0.000561 | 0,0.000505 | 0,0.00126 | 0,0.00229 | 0,0.0033 | 0,0.00517 | 0,0.00134 | 0,0.00081 | 0,0.000409 | 0,0.00849 | 1,4.23e-05 | 0,0.000784 |
| SMc00026 | 0,0.00223 | 0,0.00071 | 0,0.00339 | 0,0.00358 | - | 0,0.0021 | 0,0.00339 | 0,0.00618 | 0,0.00171 | 0,0.00618 | 1,4.86e-05 | 0,0.0079 |
| SMc00059 | 0,0.00081 | 0,0.0013 | 0,0.000285 | 1,7.25e-05 | 0,0.00166 | 0,0.000307 | 0,0.000274 | 0,0.000561 | 1,2.7e-06 | 0,0.000236 | 2,1.84e-05 | 1,4.48e-07 |
| SMc00084 | - | - | - | 0,0.00358 | - | - | - | 0,0.00603 | 0,0.00171 | - | 1,4.86e-05 | - |
| SMc00120 | 3,5.43e-07 | - | 0,0.000381 | 1,6.32e-06 | 0,0.000686 | 2,5.91e-07 | 0,0.000219 | 1,6.32e-06 | 1,7.25e-05 | 2,1.9e-06 | 2,4.34e-06 | - |
| SMc00191 | 0,0.000542 | - | 1,0.000116 | - | 0,0.000784 | - | 2,5.56e-05 | - | 4,2.2e-06 | 1,0.000187 | 1,3.18e-05 | - |
| SMc00548 | 1,5.56e-05 | - | - | 0,0.000837 | - | 0,0.000923 | - | 0,0.000523 | 0,0.000285 | - | 1,5.08e-05 | - |
| SMc00638 | 2,1.57e-05 | 0,0.00304 | 1,0.00012 | 1,7.58e-05 | 0,0.00467 | 1,0.000116 | 3,1.49e-05 | 0,0.000274 | 1,9e-05 | 2,2.37e-05 | 2,7.13e-06 | 1,7.13e-06 |
| SMc00639 | 2,1.57e-05 | - | 1,0.00012 | 1,7.58e-05 | 0,0.00467 | 1,0.000116 | 3,1.49e-05 | 0,0.000274 | 1,9e-05 | 2,2.37e-05 | 3,8.39e-07 | 1,7.13e-06 |
| SMc00651 | 1,5.82e-05 | 0,0.00108 | 0,0.000837 | 0,0.00058 | 2,1.01e-05 | 1,4.06e-06 | 0,0.000642 | 0,0.000953 | 2,5.82e-05 | 1,6.95e-05 | 2,5.82e-05 | 1,8.62e-05 |
| SMc00652 | 1,5.82e-05 | 0,0.00108 | 0,0.00559 | 0,0.00058 | 0,0.00517 | 1,4.06e-06 | 0,0.00358 | 0,0.000953 | 2,5.82e-05 | 0,0.00321 | 2,5.82e-05 | 0,0.0182 |
| SMc00654 | 2,1.2e-05 | 1,0.00018 | 3,1.49e-05 | 2,3.85e-05 | 0,0.00108 | 1,7.91e-05 | 1,9.38e-05 | 2,1.49e-05 | 1,4.03e-05 | 3,5.82e-05 | 2,4.03e-05 | 1,0.000194 |
| SMc00655 | - | 2,0.00018 | 0,0.000664 | 1,3.85e-05 | - | 1,7.91e-05 | 0,0.000318 | 1,1.49e-05 | 1,4.03e-05 | 0,0.000664 | 2,4.03e-05 | 1,0.000194 |
| SMc00718 | 0,0.000227 | - | - | - | - | - | - | - | - | - | 3,2.92e-06 | - |
| SMc00743 | 0,0.000664 | - | 1,0.000116 | - | - | 0,0.00378 | 1,0.000116 | 0,0.00143 | 0,0.000409 | 1,9e-05 | 1,1.27e-05 | 0,0.00156 |
| SMc00888 | 1,6.73e-06 | 0,0.00105 | 0,0.00545 | 0,0.00182 | 0,0.0006 | 0,0.000561 | 2,2.13e-08 | 0,0.0013 | 1,0.00018 | 0,0.00229 | 2,6.08e-05 | 0,0.0025 |
| SMc00928 | 1,0.000148 | 0,0.00156 | 1,0.00016 | 2,9.79e-05 | 0,0.000227 | 1,5.08e-05 | 1,0.000102 | 4,9.97e-07 | 1,0.000194 | 1,9.79e-05 | 1,0.000166 | 0,0.000254 |
| SMc00977 | 1,0.000125 | - | 0,0.000837 | 0,0.000254 | 0,0.000342 | 0,0.00123 | 0,0.000837 | 0,0.00257 | 0,0.00216 | 0,0.00467 | 1,9e-05 | 0,0.00504 |
| SMc00978 | 1,0.000125 | - | 0,0.00829 | 1,8.62e-05 | 0,0.000254 | 0,0.00257 | 0,0.00666 | 1,7.25e-05 | 0,0.00216 | 0,0.00517 | 1,9e-05 | 0,0.00717 |
| SMc00997 | 0,0.00264 | - | 2,3.74e-07 | - | - | 2,6.36e-05 | 1,3.1e-06 | 2,3.5e-05 | 1,1.41e-05 | 2,1.9e-06 | 1,0.00012 | - |
| SMc00998 | 0,0.00198 | - | 0,0.000227 | 2,9.38e-05 | 0,0.00176 | 0,0.0103 | 0,0.00021 | 5,1.42e-07 | 0,0.00139 | 1,6.64e-05 | 1,0.000106 | 4,4.64e-05 |
| SMc01015 | 0,0.000523 | - | 1,2.89e-05 | - | 1,0.000173 | 2,5.91e-07 | 2,4.23e-05 | 1,2.26e-05 | 0,0.00112 | 1,6.64e-05 | 1,3.03e-05 | - |
| SMc01029 | 1,0.000148 | 0,0.000784 | 1,0.000125 | 1,0.000173 | 1,0.000173 | 3,1.33e-05 | 1,6.08e-05 | 0,0.000295 | 1,1.66e-05 | 2,8.39e-07 | 1,4.86e-05 | 1,8.62e-05 |
| SMc01187 | 0,0.000923 | 0,0.00139 | 0,0.00166 | 0,0.00134 | 0,0.000837 | 0,0.000561 | 0,0.000784 | 0,0.000488 | 0,0.000368 | 0,0.00156 | 1,0.000154 | 0,0.00229 |
| SMc01356 | 3,1.27e-05 | - | - | - | - | - | - | - | 1,4.03e-05 | - | 1,4.03e-05 | - |
| SMc01579 | 1,1.49e-05 | 0,0.000953 | 0,0.000505 | 0,0.00229 | 3,6.57e-07 | 0,0.0042 | 0,0.00279 | 0,0.00161 | 1,0.000154 | 0,0.000984 | 2,2.75e-05 | 0,0.00171 |
| SMc01768 | 0,0.000307 | - | 1,0.00018 | 1,0.00016 | - | 0,0.000505 | 1,9.79e-05 | 1,0.00016 | 1,2.15e-05 | 1,0.000154 | 1,0.000187 | - |
| SMc01794 | 2,1.14e-05 | - | 0,0.00934 | 2,6.64e-05 | 0,0.000865 | 2,4.23e-05 | 0,0.00455 | 2,6.64e-05 | 2,4.23e-05 | 0,0.000381 | 1,4.23e-05 | 1,1.07e-05 |
| SMc01795 | 2,1.14e-05 | 0,0.00112 | 1,4.86e-05 | 2,6.64e-05 | 0,0.0033 | 2,4.23e-05 | 0,0.000455 | 2,6.64e-05 | 2,4.23e-05 | 2,9.38e-05 | 1,4.23e-05 | 0,0.000759 |
| SMc01871 | 2,2.89e-05 | 0,0.00187 | 0,0.00147 | 1,4.43e-05 | 0,0.00312 | 0,0.00243 | 0,0.00257 | 1,3.03e-05 | 3,1.41e-05 | 0,0.00182 | 2,1.41e-05 | 0,0.00358 |
| SMc02052 | 0,0.0021 | - | 2,1.2e-05 | 0,0.00171 | - | 0,0.00187 | - | 0,0.00223 | 0,0.00156 | 0,0.00115 | 1,0.000187 | 0,0.00388 |
| SMc02060 | 1,7.25e-05 | 0,0.000953 | 1,0.000166 | 1,8.26e-05 | 1,2.37e-05 | 2,7.13e-06 | 1,5.82e-05 | 1,8.26e-05 | 1,6.08e-05 | 1,6.64e-05 | 1,9.54e-06 | 1,1.07e-05 |
| SMc02230 | 2,1.49e-05 | 3,5.26e-06 | 1,0.000116 | 0,0.000285 | - | 2,1.07e-05 | 2,5.56e-05 | 0,0.000342 | 1,4.03e-05 | 1,0.000187 | 2,1.07e-05 | 2,3.18e-05 |
| SMc02279 | 0,0.00182 | - | - | 0,0.00287 | - | - | - | - | 0,0.00139 | - | 1,3.03e-05 | - |
| SMc02304 | 0,0.00161 | 0,0.00388 | - | 0,0.00368 | - | 0,0.00264 | - | 0,0.00573 | - | - | 1,0.000194 | - |
| SMc02369 | 0,0.000285 | 0,0.0013 | 3,3.55e-06 | 1,1.66e-05 | 0,0.00358 | 0,0.00152 | 2,4.06e-06 | 1,1.66e-05 | 1,6.32e-06 | 0,0.000285 | 1,4.64e-05 | 0,0.000893 |
| SMc02447 | 2,3.85e-05 | - | - | 1,8.26e-05 | - | 1,3.67e-05 | - | 1,0.000142 | 0,0.000542 | - | 1,6.95e-05 | - |
| SMc02824 | 1,0.000106 | 0,0.00264 | 2,2.75e-05 | 0,0.00176 | 1,3.34e-05 | 1,0.000116 | 2,2.75e-05 | 1,3.67e-05 | 2,3.03e-05 | 1,3.81e-06 | 1,0.000106 | 0,0.00479 |
| SMc02825 | 1,0.000106 | 0,0.007 | 0,0.00849 | 0,0.00287 | 1,3.34e-05 | 1,0.000116 | 2,2.75e-05 | 1,3.67e-05 | 2,3.03e-05 | 1,3.81e-06 | 1,0.000106 | 0,0.00573 |
| SMc02848 | 1,2.04e-05 | 0,0.000686 | 1,1.49e-05 | 1,0.000136 | 0,0.00443 | 0,0.00147 | 2,2.03e-06 | 1,0.000136 | 1,0.000131 | 1,3.03e-05 | 1,3.85e-05 | 0,0.00304 |
| SMc02874 | - | - | 0,0.00348 | 0,0.00216 | - | 0,0.000381 | - | 0,0.00229 | - | - | 1,0.000173 | - |
| SMc03037 | 2,9.02e-06 | - | 0,0.00134 | 0,0.00368 | 0,0.00339 | 2,6.23e-09 | 2,2.92e-06 | 0,0.000355 | 0,0.000865 | 0,0.00198 | 2,2.26e-05 | - |
| SMc03038 | 2,9.02e-06 | - | 0,0.00134 | 0,0.00368 | 0,0.00339 | 2,6.23e-09 | 2,2.92e-06 | 0,0.000355 | 4,2.2e-06 | 0,0.00198 | 1,0.000136 | - |
| SMc03039 | 2,9.02e-06 | - | 0,0.00134 | 0,0.00368 | 1,9.54e-06 | 2,6.23e-09 | 2,2.92e-06 | 0,0.000355 | 4,2.2e-06 | 0,0.00198 | 2,4.86e-05 | - |
| SMc03040 | 2,2.8e-07 | - | 0,0.00134 | 0,0.00368 | 0,0.000923 | 2,6.23e-09 | 2,2.92e-06 | 0,0.000355 | 0,0.000865 | 0,0.00198 | 4,2.2e-06 | - |
| SMc03046 | 1,1.27e-05 | 1,0.00018 | 0,0.00279 | 0,0.000409 | 0,0.00108 | 0,0.00272 | 1,9.38e-05 | 4,9.54e-06 | 2,1.9e-06 | 0,0.00182 | 3,2.34e-06 | 1,0.000194 |
| SMc03066 | 0,0.00443 | - | - | - | - | - | - | - | 0,0.000439 | - | 1,0.000142 | - |
| SMc03143 | 2,1.63e-06 | - | 0,0.00517 | - | - | 4,3.41e-07 | - | - | 0,0.000355 | 0,0.0171 | 4,2.92e-06 | 0,0.00443 |
| SMc03243 | - | - | 0,0.00264 | - | 0,0.00229 | 0,0.00304 | - | - | - | - | 1,0.000173 | - |
| SMc03808 | 2,1.29e-06 | 1,3.03e-05 | 0,0.0171 | 2,5.58e-06 | 0,0.000471 | 0,0.000621 | 0,0.000923 | 2,5.58e-06 | 0,0.000542 | 0,0.00934 | 2,3.34e-06 | 0,0.00979 |
| SMc03942 | 0,0.00166 | 0,0.000621 | 0,0.000984 | 0,0.00112 | 1,0.00012 | 0,0.00312 | 1,0.00018 | 0,0.00634 | 0,0.00339 | 1,3.67e-05 | 1,7.25e-05 | 1,0.000173 |
| SMc03983 | 0,0.00081 | 0,0.0042 | 0,0.000368 | - | - | 1,0.000111 | 0,0.019 | 0,0.00161 | 0,0.00112 | 0,0.00431 | 1,1.94e-05 | 0,0.00735 |
| SMc04112 | 3,3.1e-06 | - | 1,0.000136 | - | 1,3.85e-05 | 2,3.85e-05 | 1,6.95e-05 | 1,0.000116 | 2,6.57e-07 | 0,0.000264 | 1,1.66e-05 | - |
| SMc04113 | 0,0.000307 | - | 0,0.00119 | - | 0,0.0042 | 0,0.00033 | 0,0.000686 | 1,0.000131 | 0,0.000471 | 0,0.00272 | 3,2.15e-05 | 1,0.000142 |
| SMc04114 | 2,4.03e-05 | - | 0,0.00187 | - | 1,1.41e-05 | 2,2.34e-06 | 0,0.000318 | 0,0.00123 | 3,2.7e-06 | 1,0.00016 | 3,2.15e-05 | 1,0.000142 |
| SMc04115 | 2,4.03e-05 | - | 0,0.000307 | - | 0,0.01 | 2,2.34e-06 | 0,0.000439 | 2,0.000131 | 3,2.7e-06 | 1,0.00016 | 4,2.15e-05 | - |
| SMc04225 | 0,0.00467 | - | 0,0.000264 | 0,0.0079 | - | 1,6.64e-05 | 0,0.000759 | 0,0.000759 | 0,0.000264 | 1,4.23e-05 | 1,9.79e-05 | 0,0.00517 |

## Table 2.S5B. Conservation of CtrA binding motifs in genes with cell cycle regulated transcripts

| gene | agrobact_tumef | bart_quin | brady_jap | bruc_abort | caul_cres | meso_loti | nitro_hamb | ochro_anthro | rhizo_legum | rhodop_pal | sino_mel | xanth_auto |
|---|---|---|---|---|---|---|---|---|---|---|---|---|
| SMa0241 | 0,0.00133 | - | 0,0.000552 | 0,0.00259 | 0,0.00438 | 1,8.94e-06 | 0,0.00106 | 1,3.17e-05 | 0,0.000437 | 0,0.00348 | 1,0.000175 | 1,8.43e-05 |
| SMa0244 | 0,0.00133 | 0,0.000943 | 0,0.000206 | 0,0.000304 | 1,0.000175 | 0,0.000552 | 0,0.00194 | 0,0.00327 | 0,0.00208 | 0,0.00384 | 1,0.000175 | 0,0.00327 |
| SMa1706 | - | - | - | - | - | - | - | - | 0,0.00144 | - | 1,5.05e-05 | - |
| SMa1809 | 0,0.00223 | 1,2.36e-05 | 0,0.00234 | 0,0.000213 | 0,0.000872 | 1,0.000175 | 0,0.000359 | 1,0.000146 | 0,0.000609 | 0,0.000544 | 1,0.000175 | 1,9.97e-05 |
| SMa2395 | 0,0.00132 | 0,0.0033 | 1,1.7e-05 | 0,0.00132 | 1,8.43e-05 | 0,0.00309 | 1,0.000117 | 0,0.000201 | 0,0.000779 | 1,1.7e-05 | 1,1.3e-05 | 0,0.00223 |
| SMb20537 | 0,0.000406 | - | 0,0.00494 | 0,0.000313 | 1,2.03e-05 | 0,0.000544 | - | 1,0.000146 | 0,0.00133 | - | 1,0.000175 | 0,0.000672 |
| SMb20596 | 0,0.000294 | 0,0.00132 | - | 0,0.000437 | - | 0,0.00254 | - | 0,0.00167 | 0,0.00132 | - | 1,0.000105 | - |
| SMb20709 | 0,0.000779 | - | 0,0.00138 | - | - | 1,1.7e-05 | 0,0.00132 | - | 0,0.00388 | 0,0.000609 | 1,0.000146 | - |
| SMb21036 | - | - | - | - | - | 1,2.36e-05 | - | - | - | - | 1,0.000117 | - |
| SMb21174 | 0,0.000437 | - | 0,0.000576 | 0,0.000672 | 0,0.000437 | 0,0.000872 | - | 0,0.00194 | 0,0.000437 | 1,6.55e-05 | 1,2.03e-05 | 1,2.36e-05 |
| SMb21272 | 0,0.000201 | - | 0,0.00275 | 0,0.000313 | 0,0.00141 | 0,0.00392 | 0,0.000267 | 0,0.000672 | 1,0.000146 | - | 1,1.3e-05 | 0,0.000702 |
| SMb21274 | 0,0.000702 | 0,0.000609 | 0,0.000512 | 0,0.0011 | 0,0.000552 | 0,0.000702 | 0,0.000213 | 0,0.000731 | 0,0.000201 | 0,0.00327 | 1,0.000121 | 0,0.000347 |
| SMb21357 | - | - | - | - | - | 1,0.000175 | - | - | - | 0,0.000406 | 1,8.43e-05 | - |
| SMb21558 | 0,0.000201 | - | 0,0.0024 | 0,0.000779 | 0,0.00215 | 0,0.000672 | 0,0.00132 | 0,0.000852 | 0,0.000359 | 0,0.00254 | 1,0.000175 | 0,0.000628 |
| SMc00059 | 0,0.00327 | 0,0.000459 | 0,0.000872 | 1,0.000175 | 0,0.00029 | 0,0.00208 | 0,0.000313 | 0,0.00234 | 1,0.000175 | 0,0.000852 | 1,0.000175 | 0,0.000235 |
| SMc00060 | 0,0.00254 | 0,0.00307 | 0,0.00208 | 0,0.00096 | 0,0.000201 | 0,0.000437 | 0,0.000437 | 0,0.000201 | 0,0.00125 | 0,0.000437 | 1,9.09e-05 | 0,0.000702 |
| SMc00594 | 0,0.000722 | - | 0,0.000544 | - | 0,0.00141 | 0,0.00037 | - | - | 0,0.000437 | 0,0.000359 | 1,0.000175 | - |
| SMc00651 | 1,0.000134 | 0,0.000504 | 1,0.000146 | 0,0.00103 | 0,0.000235 | 0,0.00254 | 0,0.0011 | 0,0.00103 | 1,0.000175 | 0,0.00234 | 1,0.000175 | 0,0.000702 |
| SMc00652 | 1,0.000134 | 0,0.000504 | 0,0.00254 | 0,0.000852 | 0,0.00254 | 0,0.00384 | 0,0.00121 | 0,0.000852 | 0,0.00341 | 0,0.000702 | 1,0.000175 | 0,0.000235 |
| SMc00888 | 0,0.000235 | 0,0.000649 | 0,0.00307 | 0,0.000576 | 0,0.0024 | 0,0.000628 | 0,0.000235 | 0,0.00138 | 0,0.00106 | 0,0.000406 | 1,0.000105 | 0,0.000576 |
| SMc01107 | 0,0.00144 | 0,0.00234 | 0,0.000437 | 0,0.00144 | 0,0.000406 | 0,0.000437 | 0,0.00103 | 0,0.00254 | 0,0.000201 | 0,0.000437 | 1,0.000146 | 1,9.09e-05 |
| SMc01109 | 0,0.00132 | 0,0.00161 | 0,0.00125 | 0,0.00151 | 0,0.00384 | 0,0.00155 | 0,0.00172 | 0,0.00151 | 0,0.00418 | 1,0.000134 | 1,0.000105 | 0,0.000609 |
| SMc01260 | 0,0.000779 | - | 0,0.00392 | 0,0.000359 | 0,0.00223 | 0,0.000201 | 0,0.000632 | 0,0.00194 | 0,0.000313 | - | 1,6.55e-05 | 0,0.000213 |
| SMc01433 | - | - | - | - | - | 0,0.000852 | - | - | - | - | 1,0.000146 | - |
| SMc01760 | 1,1.3e-05 | - | - | 0,0.000213 | - | 0,0.000852 | - | 0,0.00151 | 1,1.3e-05 | - | 1,3.17e-05 | - |
| SMc01794 | 1,8.03e-05 | - | 0,0.000504 | 0,0.00114 | 0,0.00138 | 0,0.00293 | 0,0.0018 | 0,0.00392 | 0,0.000459 | 0,0.000504 | 1,8.03e-05 | 0,0.00172 |
| SMc01795 | 1,8.03e-05 | 0,0.00103 | 0,0.00132 | 0,0.000201 | 0,0.00121 | 0,0.00293 | 1,0.000175 | 0,0.00392 | 1,5.05e-05 | 0,0.00399 | 1,8.03e-05 | 0,0.000437 |
| SMc02156 | 0,0.00116 | - | - | - | 0,0.000512 | 0,0.000619 | 0,0.000213 | - | 0,0.000672 | 0,0.000437 | 1,4.23e-05 | 2,2.36e-05 |
| SMc02173 | 0,0.0011 | - | 0,0.00254 | 0,0.000722 | - | 0,0.00327 | - | 1,0.000134 | 0,0.00223 | - | 1,9.09e-05 | 0,0.000852 |
| SMc02252 | 0,0.00223 | - | 0,0.00429 | 0,0.000437 | 0,0.00438 | 1,8.94e-06 | 0,0.00106 | 1,3.83e-05 | 1,1.3e-05 | 0,0.000201 | 1,0.000175 | 0,0.000628 |
| SMc02408 | 1,0.000134 | 0,0.000343 | 1,1.3e-05 | 0,0.000544 | 0,0.00384 | 0,0.00254 | 0,0.000406 | 0,0.000558 | 0,0.000448 | 0,0.00132 | 1,7.54e-05 | 0,0.000448 |
| SMc02644 | 0,0.000285 | 1,6.55e-05 | 0,0.00109 | 0,0.00109 | 0,0.000271 | 1,9.97e-05 | 1,0.000149 | 0,0.000347 | 1,2.03e-05 | 0,0.00029 | 1,9.43e-05 | 0,0.000609 |
| SMc02826 | 1,8.94e-06 | - | - | 0,0.000872 | - | 0,0.000702 | - | 0,0.00167 | 0,0.000609 | 0,0.000406 | 1,0.000134 | - |
| SMc03008 | 0,0.00125 | - | 0,0.000722 | - | 0,0.000943 | 0,0.00363 | 1,9.43e-05 | - | 0,0.000406 | 0,0.00363 | 1,2.03e-05 | - |
| SMc03011 | 0,0.000852 | 0,0.000201 | 1,9.43e-05 | 0,0.00194 | 0,0.00161 | 0,0.000628 | 1,0.000175 | 0,0.000576 | 0,0.0011 | 1,0.000175 | 1,5.05e-05 | 0,0.000609 |
| SMc03026 | 0,0.000482 | - | 0,0.000943 | 0,0.000632 | - | 0,0.00194 | 0,0.00138 | 0,0.000943 | 0,0.00127 | 0,0.000359 | 1,5.05e-05 | - |
| SMc03050 | 0,0.000702 | - | 0,0.000672 | 0,0.00307 | 0,0.000872 | 0,0.000437 | 0,0.000437 | 0,0.00374 | 0,0.00254 | 0,0.00109 | 1,6.55e-05 | - |
| SMc03130 | 0,0.0018 | - | - | - | - | 0,0.00161 | - | 0,0.000632 | - | - | 1,0.000149 | 0,0.000672 |
| SMc03900 | 0,0.00399 | 0,0.000307 | 0,0.000894 | 0,0.000213 | 0,0.000779 | 0,0.00307 | 0,0.000406 | 1,6.55e-05 | 0,0.00167 | 0,0.000359 | 1,9.43e-05 | 0,0.000872 |
| SMc03941 | 0,0.00132 | - | 0,0.000722 | 0,0.000406 | 0,0.000852 | - | 0,0.000576 | 0,0.00037 | 0,0.00144 | 0,0.00194 | 1,4.23e-05 | 0,0.00348 |
| SMc03942 | 0,0.00167 | 0,0.000448 | 0,0.00254 | 0,0.0024 | 0,0.00151 | 0,0.00215 | 0,0.000609 | 1,8.03e-05 | 2,1.3e-05 | 0,0.00194 | 1,7.54e-05 | 0,0.0011 |
| SMc04003 | 0,0.000201 | 0,0.00161 | 1,6.55e-05 | 0,0.000609 | 0,0.000201 | 0,0.000201 | 1,6.55e-05 | 0,0.000779 | - | 1,6.55e-05 | 1,0.000175 | 0,0.000201 |
| SMc04004 | 0,0.000201 | 0,0.00161 | 1,6.55e-05 | 0,0.000609 | 1,0.000175 | 0,0.000201 | 1,6.55e-05 | 0,0.00208 | 0,0.000201 | 1,6.55e-05 | 1,0.000175 | 0,0.000201 |
| SMc04024 | 0,0.000343 | 1,5.65e-05 | 0,0.00208 | 0,0.000285 | 0,0.000201 | 0,0.000628 | 0,0.00215 | 0,0.00374 | 1,0.000134 | 0,0.000544 | 1,0.000175 | 0,0.00642 |
| SMc04044 | 0,0.000672 | 0,0.000544 | 0,0.000406 | 1,9.97e-05 | 0,0.000619 | 0,0.00307 | 1,0.000175 | 0,0.000359 | 1,4.23e-05 | 0,0.000609 | 1,0.000146 | 0,0.00132 |
| SMc04170 | 0,0.000406 | 0,0.000201 | 0,0.000313 | 0,0.000576 | 0,0.00161 | 0,0.000852 | 0,0.000304 | 0,0.000649 | 0,0.00132 | 0,0.000313 | 1,2.03e-05 | 0,0.00254 |
| SMc04269 | - | - | - | - | 1,8.94e-06 | 0,0.000235 | 1,8.94e-06 | - | - | 0,0.000285 | 1,8.94e-06 | - |

## References


1. Marczynski GT (1999) Chromosome methylation and measurement of faithful, once and only once per cell cycle chromosome replication in Caulobacter crescentus. *Journal of bacteriology* 181(7):1984-1993.
2. Mergaert P*, et al.* (2006) Eukaryotic control on bacterial cell cycle and differentiation in the Rhizobium-legume symbiosis. *Proceedings of the National Academy of Sciences of the United States of America* 103(13):5230-5235.
3. Tsokos CG & Laub MT (2012) Polarity and cell fate asymmetry in Caulobacter crescentus. *Current opinion in microbiology* 15(6):744-750.
4. Laub MT, McAdams HH, Feldblyum T, Fraser CM, & Shapiro L (2000) Global analysis of the genetic network controlling a bacterial cell cycle. *Science* 290(5499):2144-2148.
5. Brilli M*, et al.* (2010) The diversity and evolution of cell cycle regulation in alpha-proteobacteria: a comparative genomic analysis. *BMC systems biology* 4:52.
6. Hallez R, Bellefontaine AF, Letesson JJ, & De Bolle X (2004) Morphological and functional asymmetry in alpha-proteobacteria. *Trends in microbiology* 12(8):361-365.
7. Barnett MJ, Hung DY, Reisenauer A, Shapiro L, & Long SR (2001) A homolog of the CtrA cell cycle regulator is present and essential in Sinorhizobium meliloti. *Journal of bacteriology* 183(10):3204-3210.
8. Sibley CD, MacLellan SR, & Finan T (2006) The Sinorhizobium meliloti chromosomal origin of replication. *Microbiology* 152(Pt 2):443-455.
9. Jonas K, Chen YE, & Laub MT (2011) Modularity of the bacterial cell cycle enables independent spatial and temporal control of DNA replication. *Current biology : CB* 21(13):1092-1101.
10. Quon KC, Yang B, Domian IJ, Shapiro L, & Marczynski GT (1998) Negative control of bacterial DNA replication by a cell cycle regulatory protein that binds at the chromosome origin. *Proceedings of the National Academy of Sciences of the United States of America* 95(1):120-125.
11. Laub MT, Chen SL, Shapiro L, & McAdams HH (2002) Genes directly controlled by CtrA, a master regulator of the Caulobacter cell cycle. *Proceedings of the National Academy of Sciences of the United States of America* 99(7):4632-4637.
12. Hottes AK, Shapiro L, & McAdams HH (2005) DnaA coordinates replication initiation and cell cycle transcription in Caulobacter crescentus. *Molecular microbiology* 58(5):1340-1353.
13. Collier J, McAdams HH, & Shapiro L (2007) A DNA methylation ratchet governs progression through a bacterial cell cycle. *Proceedings of the National Academy of Sciences of the United States of America* 104(43):17111-17116.
14. Abel S*, et al.* (2011) Regulatory cohesion of cell cycle and cell differentiation through interlinked phosphorylation and second messenger networks. *Molecular cell* 43(4):550-560.

15. Jones KM, Kobayashi H, Davies BW, Taga ME, & Walker GC (2007) How rhizobial symbionts invade plants: the Sinorhizobium-Medicago model. *Nature reviews. Microbiology* 5(8):619-633.
16. Galibert F*, et al.* (2001) The composite genome of the legume symbiont Sinorhizobium meliloti. *Science* 293(5530):668-672.
17. Van de Velde W*, et al.* (2010) Plant peptides govern terminal differentiation of bacteria in symbiosis. *Science* 327(5969):1122-1126.
18. Latch JN & Margolin W (1997) Generation of buds, swellings, and branches instead of filaments after blocking the cell cycle of Rhizobium meliloti. *Journal of bacteriology* 179(7):2373-2381.
19. Wright R, Stephens C, & Shapiro L (1997) The CcrM DNA methyltransferase is widespread in the alpha subdivision of proteobacteria, and its essential functions are conserved in Rhizobium meliloti and Caulobacter crescentus. *Journal of bacteriology* 179(18):5869-5877.
20. Cheng J, Sibley CD, Zaheer R, & Finan TM (2007) A Sinorhizobium meliloti minE mutant has an altered morphology and exhibits defects in legume symbiosis. *Microbiology* 153(Pt 2):375-387.
21. Gibson KE, Campbell GR, Lloret J, & Walker GC (2006) CbrA is a stationary-phase regulator of cell surface physiology and legume symbiosis in Sinorhizobium meliloti. *Journal of bacteriology* 188(12):4508-4521.
22. Kobayashi H, De Nisco NJ, Chien P, Simmons LA, & Walker GC (2009) Sinorhizobium meliloti CpdR1 is critical for co-ordinating cell cycle progression and the symbiotic chronic infection. *Molecular microbiology* 73(4):586-600.
23. Evinger M & Agabian N (1977) Envelope-associated nucleoid from Caulobacter crescentus stalked and swarmer cells. *Journal of bacteriology* 132(1):294-301.
24. Ferullo DJ, Cooper DL, Moore HR, & Lovett ST (2009) Cell cycle synchronization of Escherichia coli using the stringent response, with fluorescence labeling assays for DNA content and replication. *Methods* 48(1):8-13.
25. Wells DH & Long SR (2002) The Sinorhizobium meliloti stringent response affects multiple aspects of symbiosis. *Molecular microbiology* 43(5):1115-1127.
26. Krol E & Becker A (2011) ppGpp in Sinorhizobium meliloti: biosynthesis in response to sudden nutritional downshifts and modulation of the transcriptome. *Molecular microbiology* 81(5):1233-1254.
27. Schwammle V & Jensen ON (2010) A simple and fast method to determine the parameters for fuzzy c-means cluster analysis. *Bioinformatics* 26(22):2841-2848.
28. Pleier E & Schmitt R (1991) Expression of two Rhizobium meliloti flagellin genes and their contribution to the complex filament structure. *Journal of bacteriology* 173(6):2077-2085.
29. Ramirez-Romero MA, Soberon N, Perez-Oseguera A, Tellez-Sosa J, & Cevallos MA (2000) Structural elements required for replication and incompatibility

of the Rhizobium etli symbiotic plasmid. *Journal of bacteriology* 182(11):3117-3124.
30. Rasmussen T, Jensen RB, & Skovgaard O (2007) The two chromosomes of Vibrio cholerae are initiated at different time points in the cell cycle. *The EMBO journal* 26(13):3124-3131.
31. Jensen RB & Shapiro L (1999) The Caulobacter crescentus smc gene is required for cell cycle progression and chromosome segregation. *Proceedings of the National Academy of Sciences of the United States of America* 96(19):10661-10666.
32. Kahng LS & Shapiro L (2003) Polar localization of replicon origins in the multipartite genomes of Agrobacterium tumefaciens and Sinorhizobium meliloti. *Journal of bacteriology* 185(11):3384-3391.
33. Butala M, Zgur-Bertok D, & Busby SJ (2009) The bacterial LexA transcriptional repressor. *Cellular and molecular life sciences : CMLS* 66(1):82-93.
34. Errington J, Daniel RA, & Scheffers DJ (2003) Cytokinesis in bacteria. *Microbiology and molecular biology reviews : MMBR* 67(1):52-65, table of contents.
35. Newbury SF, Smith NH, & Higgins CF (1987) Differential mRNA stability controls relative gene expression within a polycistronic operon. *Cell* 51(6):1131-1143.
36. Rotter C, Muhlbacher S, Salamon D, Schmitt R, & Scharf B (2006) Rem, a new transcriptional activator of motility and chemotaxis in Sinorhizobium meliloti. *Journal of bacteriology* 188(19):6932-6942.
37. Fernandez-Fernandez C, Gonzalez D, & Collier J (2011) Regulation of the activity of the dual-function DnaA protein in Caulobacter crescentus. *PloS one* 6(10):e26028.
38. Gora KG*, et al.* (2010) A cell-type-specific protein-protein interaction modulates transcriptional activity of a master regulator in Caulobacter crescentus. *Molecular cell* 39(3):455-467.
39. Sadowski C, Wilson D, Schallies K, Walker G, & Gibson KE (2013) The Sinorhizobium meliloti sensor histidine kinase CbrA contributes to free-living cell cycle regulation. *Microbiology*.
40. Breedveld MW, Hadley JA, & Miller KJ (1995) A novel cyclic beta-1,2-glucan mutant of Rhizobium meliloti. *Journal of bacteriology* 177(22):6346-6351.
41. Schluter JP*, et al.* (2013) Global mapping of transcription start sites and promoter motifs in the symbiotic alpha-proteobacterium Sinorhizobium meliloti 1021. *BMC genomics* 14:156.
42. Ardissone S & Viollier PH (2012) Developmental and environmental regulatory pathways in alpha-proteobacteria. *Frontiers in bioscience : a journal and virtual library* 17:1695-1714.
43. Berleman JE & Bauer CE (2004) Characterization of cyst cell formation in the purple photosynthetic bacterium Rhodospirillum centenum. *Microbiology* 150(Pt 2):383-390.

44. Roop RM, 2nd, Gaines JM, Anderson ES, Caswell CC, & Martin DW (2009) Survival of the fittest: how Brucella strains adapt to their intracellular niche in the host. *Medical microbiology and immunology* 198(4):221-238.
45. Ruberg S*, et al.* (2003) Construction and validation of a Sinorhizobium meliloti whole genome DNA microarray: genome-wide profiling of osmoadaptive gene expression. *Journal of biotechnology* 106(2-3):255-268.
46. Yeung KY, Haynor DR, & Ruzzo WL (2001) Validating clustering for gene expression data. *Bioinformatics* 17(4):309-318.
47. Tatusov RL, Koonin EV, & Lipman DJ (1997) A genomic perspective on protein families. *Science* 278(5338):631-637.
48. Grant CE, Bailey TL, & Noble WS (2011) FIMO: scanning for occurrences of a given motif. *Bioinformatics* 27(7):1017-1018.

# Chapter 3

## Mechanisms of regulation of CtrA in *Sinorhizobium meliloti* during the free-living cell cycle and symbiosis with *Medicago sativa*

This work is being prepared for submission for publication in October 2013. Author list: Nicole J De Nisco[1*], Lorenzo Ferri [2*], Francesco Pini[2], Graham C Walker[1] and Emanuele G Biondi.
* NJD and LF contributed equally to this work

L.F. constructed all strains with exception of BM557 and BM561, which were constructed by F.P and *ctrADD* cloning, which was performed by NJD. L.F. also performed BM249 microscopy. All symbiotic experiments were performed by NJD as well as pulse-chase analysis. The manuscript was written by NJD and edited by GCW and EGB.

**Abstract**

The intracellular symbiotic lifestyle of the nitrogen-fixing soil bacterium, *Sinorhizobium meliloti* requires a significant cellular differentiation, which includes changes in membrane permeability, cell elongation and branching, endoreduplication of the genome and loss of reproductive capacity. Recent work has suggested that down-regulation of the activity of the master cell cycle regulator, CtrA, may be required for this cellular differentiation to take place. *S. meliloti* mutants in homologs of genes known to negatively regulate CtrA function in *Caulobacter crescentus,* such as CpdR1 and DivJ, are unable to form an efficient symbiosi with the legume host *M. sativa.* In this work we directly probe the role of CtrA during symbiosis. We demonstrate that depletion of CtrA in free-living *S. meliloti* leads to a bacteroid-like state, which is characterized by cell elongation and branching, endoreduplication of the genome and loss of viability. We also show that *S. meliloti* CtrA has a comparable half-life to *C. crescentus* CtrA. However, there may be differences in the proteolytic regulation of CtrA in the two species, since we found that CtrA degradation is likely essential in *S. meliloti.* We demonstrate that the heterologous *C. crescentus ctrA* promoter and coding region cannot complement an *S. meliloti ctrA* chromosomal deletion during symbiosis with *M. sativa,* even though this heterologous DNA can fully complement *S. meliloti ΔctrA* during free living growth. When we tested the symbiotic efficiency of *S. meliloti* strains expressing *S. meliloti ctrA* from the *C. crescentus* promoter and vice versa and we discovered that these strains were able to form an effective symbiosis with *M. sativa* with only minor symbiotic defects. These results present a paradox as to how the full version

of the *C. crescentus ctrA* promoter and coding region cannot function during symbiosis, but individually the *C. crescentus ctrA* promoter and protein seem to be functional.

**Introduction**

Rhizobia are α-proteobacteria with the ability to form a nitrogen-fixing symbiosis with compatible legume hosts (1). The rhizobia-legume symbiosis can be viewed as a chronic infection that is comprised of multiple developmental stages, during which the bacteria must coordinate their cell proliferation with the development of the host plant cells (2, 3). *Sinorhizobium meliloti* progresses through a dramatic differentiation process during symbiosis with the inverted repeat-lacking clade (IRLC) legume, *Medicago sativa* (4). A class of over 300 nodule-specific cysteine rich (NCR) peptides, which are produced by the host legume, are involved in governing bacteroid differentiation (5). One of the hallmarks of bacteroid development is endoreduplication of the genome, which results from successive rounds of DNA replication without subsequent cell division. Endoreduplication results in elongated cells with up to 24N DNA content (4) compared to the small rod-shaped free living *S. meliloti* that have strictly 1N and 2N DNA content (6). The mechanism that leads to endoreduplication of the genome during bacteroid differentiation is unknown, but it is clear that the free-living cell cycle program must be altered.

The involvement of cell cycle regulation in cellular differentiation programs, such as cyst formation in *Rhodospirillum centenum* and the asymmetric division of *Caulobacter crescentus,* is a common theme in α-proteobacteria (7, 8). Although

most of the regulatory mechanisms governing the *S. meliloti* cell cycle have not been elucidated, the cell cycle of the aquatic α-proteobacteria, *C. crescentus,* has been intensely studied. *C. crescentus* divides asymmetrically to produce two morphologically different cells, a motile swarmer cell and a sessile stalked cell (8). The two cell types are also distinct in their replicative capacities. The stalked cell can immediately initiate DNA replication and re-enter the cell cycle, while the swarmer cell is arrested in G1 and must differentiate into a stalked cell before DNA replication can be initiated (9). Morphological and replicative asymmetry are governed primarily by the response regulator CtrA in *C. crescentus* (9). Phosphorylated CtrA binds and silences the origin of replication in swarmer cells and activates the transcription of about 95 genes during the *C. crescentus* cell cycle (10, 11). The expression, activity and stability of CtrA is highly regulated during the cell cycle. Many factors govern the temporally regulated transcription of *ctrA,* but the regulation of CtrA activity via phosphorylation and stability via regulated proteolysis are especially critical to the progression of the *C. crescentus* cell cycle (12). Both the activation and degradation of CtrA are regulated via a complex phosphorelay centered on the bi-functional histidine kinase CckA (9). The kinase activity of CckA is specifically activated at the swarmer cell pole by DivL and this activation leads to the transfer of a phosphoryl group to CtrA and also to the response regulator CpdR via the phosphotransferase ChpT (13). Phosphorylation at a conserved aspartate residue (D51) activates CtrA to bind and silence the origin of replication and to activate the transcription of target genes in pre-divisional cells

(14). Phosphorylation of CpdR inactivates CpdR by targeting the protein for proteolysis (13).

At the swarmer cell pole, the kinase activity of CckA is inhibited by phosphorylated DivK and CckA acts as a phosphatase, such that neither CtrA nor CpdR are phosphorylated. Unphosphorylated CpdR activates the ClpXP mediated proteolysis of the PdeA phosphodiesterase. The degradation of PdeA causes a spike in cyclic di-GMP levels due to the activity of the diguanylate cyclase DgcB, which is able to function in the absence of its antagonist PdeA (15). PleD phosphorylation is also required for the spike in cyclic di-GMP levels observed in stalked cells (16). The increase in cyclic di-GMP levels drives the PopA-mediated proteolysis of CtrA by ClpXP (15, 16). The absence of CtrA in the stalked cell compartment leaves the origin free to be bound by the replication initiation protein DnaA (17).

The genes encoding the essential components of the *Caulobacter crescentus* cell cycle are well-conserved among $\alpha$- proteobacteria (18). Essential functional homologs for many regulators, including CtrA, the replication initiation protein DnaA and the cell cycle regulated methylase CcrM have been identified in *S. meliloti* (19-21). In fact, cell branching and increased DNA content is observed when the DnaA and CcrM are overproduced in *S. meliloti (20, 21).* In addition, cells exhibiting the branching observed in bacteroids can be produced when cell division is inhibited in *S. meliloti* by overproduction of *S. meliloti* homologs the critical septation protein FtsZ (FtsZ1 and FtsZ2 in *S. meliloti*) (22). These results indicate that strict regulation of these factors is crucial for proper cell cycle progression and also suggest that significant cell cycle regulatory changes may occur in *S. meliloti*

during symbiosis. Moreover, loss of function of two proteins (CpdR1 and CbrA) putatively involved in regulation of the *S. meliloti* homolog of CtrA is highly detrimental during symbiosis (23, 24). *S. meliloti* cells without a functional copy of *cpdR1,* which is the homolog of the *C. crescentus cpdR,* display aberrant cell shape, altered DNA content and are not able to survive within the symbiosome (23). Loss of the activity of the histidne kinase CbrA, which is a cognate histidine kinase to the *S. meliloti* homolog of the response regulator DivK, produced cell envelope defects in *S. meliloti* and was highly detrimental during symbiosis with *M. sativa* (25). In *C. crescentus,* phosphorylated DivK has a pivotal role in inhibiting the activity of CtrA at the stalked cell pole (9), so taken together these results indicate that proper regulation of the *S. meliloti* cell cycle may be critical during symbiosis. Following this theme of negative regulation of CtrA being critical to symbiosis, very recent evidence has shown that not only is DivJ, which serves to inactivate CtrA, essential for efficient symbiosis, but CtrA is in fact absent from bacteroids (see Appendix B). The specific regulatory changes that occur in the *S. meliloti* cell cycle that allow for endoreduplication during bacteroid differentiation are not yet known and, even more fundamentally, the regulatory network of the free-living *S. meliloti* cell cycle has yet to be determined.

The work described here further elucidates the role of CtrA in the *S. meliloti* cell cycle both during free-living growth and symbiosis. We report that depletion of CtrA in *S. meliloti* produces significantly enlarged cells with highly elevated DNA content that eventually lose viability. I confirm that CtrA has a comparable half-life to *C. crescentus* CtrA and that putative non-degradable alleles of CtrA are lethal in *S.*

*meliloti.* I also made the interesting observation that, even though, the promoter region and coding region of *C. crescentus ctrA* can complement a *S. meliloti ΔctrA* mutant during free living growth, the same DNA cannot complement a *S. meliloti ΔctrA* mutant during symbiosis. However, I also made the unanticipated observation that an *S. meliloti ΔctrA* strain expressing *C. crescentus ctrA* from the *S. meliloti ctrA* promoter region (*ΔctrAp$_{Sm}$ctrA$_{Cc}$*) and *S. meliloti ΔctrA* expressing *S. meliloti ctrA* from the *C. crescentus ctrA* promoter region (*ΔctrAp$_{Cc}$ctrA$_{Sm}$*) were able form a functional symbiosis with minor defects. The *ΔctrAp$_{Sm}$ctrA$_{Cc}$ S. meliloti* strain seemed to form a more inefficient symbiosis that the *ΔctrAp$_{Cc}$ctrA$_{Sm}$*, which was characterized by a shorter plant height, irregular nodules and less of an ability to compete with wild type *S. meliloti.* The minor symbiotic defects observed in the *ΔctrAp$_{Cc}$ctrA$_{Sm}$* and *ΔctrAp$_{Sm}$ctrA$_{Cc}$* do not explain the profound symbiotic defect in the *S. meliloti* strain carrying the complete heterologous promoter and coding region from *C. crescentus ctrA.* Possibilities to explain this set of unexpected results are discussed.

**Results**

**Depletion of CtrA in *S. meliloti* results in altered cell morphology and increased DNA content.** Since *ctrA* is essential in *S. meliloti,* we tested the effects of depleting CtrA in *S. meliloti* in order to gain more insight into the function of CtrA in *S. meliloti.* Previous work has demonstrated that constitutive expression of CtrA (expression not from the native promoter) produces no cell cycle defects in *C. crescentus* (12). To gain additional insights into the nature of the requirement for CtrA function during the cell cycle, we first placed the *S. meliloti* CtrA ORF under the

control of a tightly regulated IPTG inducible promoter by cloning into the pSRK-Km plasmid (26). The native copy of *ctrA* was then deleted from the chromosomal locus and replaced with a tetracycline resistance cassette in the strain expressing CtrA constitutively on the pSRK plasmid (+IPTG) via a *sacB* suicide vector and sucrose selection. The resulting strain BM249 contains a single copy of *ctrA* under the control of an IPTG inducible promoter. Figure 3.1A shows that BM249 can only grow in the presence of IPTG with optimal growth in 1mM IPTG. CtrA depletion was achieved by growing BM249 to early log phase in the presence of IPTG, pelleting and washing the cells, and then resuspending them in media lacking IPTG and incubating at 30C for several hours. We performed a Western blot to confirm the depletion of the CtrA protein using *C. crescentus* CtrA polyclonal antibodies, which have been previously shown to cross-react with *S. meliloti* CtrA (24). The Western blot in Figure 3.1B shows that after 420 minutes (8 hrs) CtrA is completely absent from *S. meliloti* cells. After 420 minutes depletion of CtrA proved lethal to *S. meliloti* cells as indicated by the results of CFU plating assays displayed in Figure 1C.

Microscopy revealed that depletion of CtrA in *S. meliloti* causes serious morphological defects including bloating, elongation, and branching of *S. meliloti* likely caused by a block in cell division (Fig. 3.1D). The elongation and branching in these cells is very similar to the morphological changes induced during bacteroid differentiation. In addition to causing altered morphologies, bacteroid differentiation includes endoreduplication of the genome, which results in elevated DNA content within bacteroid cells (4). Consistent with this, DAPI staining of CtrA-depleted *S. meliloti* was extremely bright, implying elevated DNA content (Fig. 3.1D).

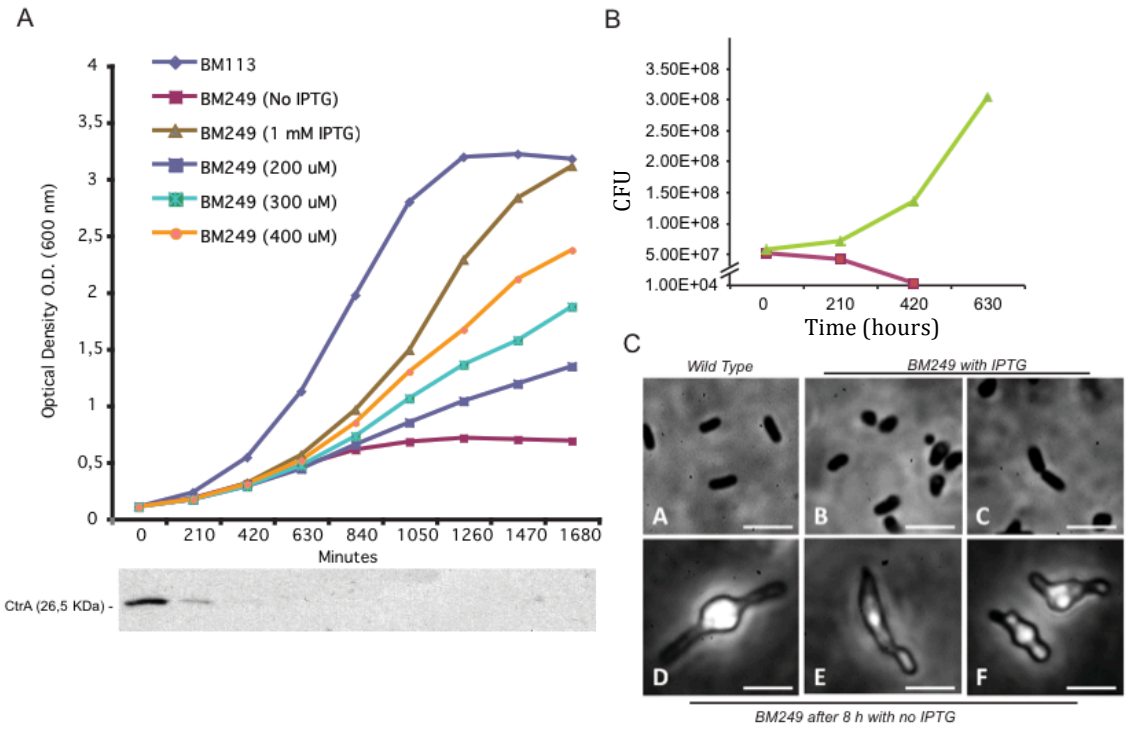


**Figure 3.1. Depletion of CtrA in *S. meliloti.*** A. Growth curve of BM249 cells with differing amounts of IPTG. BM113 is a control strain carrying the pSRK-Km plasmid. Cells grown in 1mM IPTG (brown triangles) exhibit growth dynamic most similar to the control strain. BM249 cells without IPTG do not reach an OD higher than 0.5. The Western blot in B shows the depletion of CtrA protein levels over time when BM249 is grown without IPTG. In C, CFU plating experiments demonstrate that after 420 minutes of CtrA depletion *S. meliloti* cells are no longer viable. In D, microscopy of wild type (top) and CtrA depleted (bottom) *S. meliloti* cells reveals altered morphology in CtrA depleted cells.

To confirm that depletion of CtrA yields *S. meliloti* cells with elevated DNA content, I performed flow cytometry (FACS) analysis on BM249 grown with IPTG (+CtrA) and without IPTG (CtrA deplete) for 8 hours. The FACS analysis reveals that depletion of CtrA leads to greatly elevated DNA content in *S. meliloti* and complete loss of the normal 1N and 2N peaks (Fig. 3.2). The observed increase in DNA content upon CtrA depletion is consistent with the elevated DNA content observed in differentiated *S. meliloti* bacteroids (4). Thus, removal of CtrA causes endoreduplication in *S. meliloti* in the free-living state and this evidence combined with the observation in Pini *et al.* that CtrA is absent in bacteroids (Appendix B.)

suggests that inactivation of CtrA during bacteroid differentiation may be required for endoreduplication of the genome and inhibition of cell division.

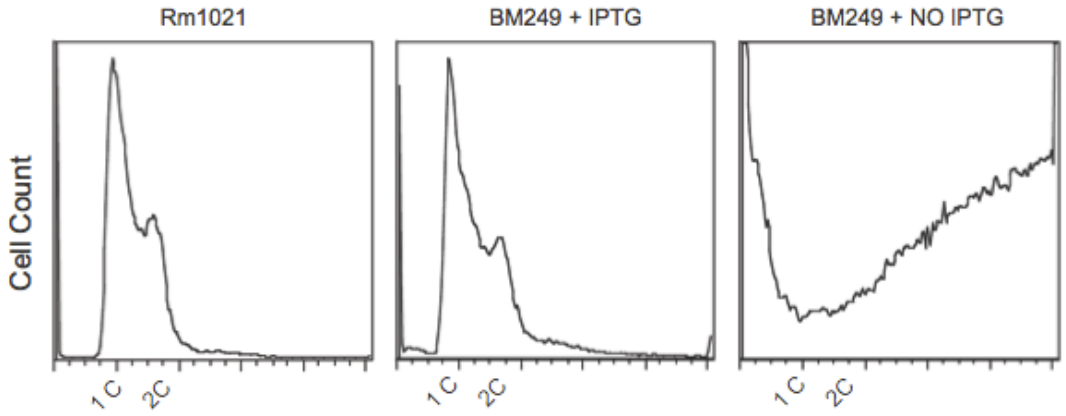


**Figure 3.2. Flow cytometry analysis of CtrA depletion in *S. meliloti*.** FACS profiles of wildtype (Rm1021), control (BM249+IPTG) and CtrA-depleted (after 8 hours without IPTG) *S. meliloti* cells. In wildtype and BM249+IPTG clear 1N and 2N peaks are present while in CtrA-depleted cells there is a growing shoulder right of 2N indicating cells with highly elevated DNA content.

**The half-life of *S. meliloti* CtrA is similar to that of *C. crescentus* CtrA.** The results of CtrA depletion indicate that inactivation or removal of CtrA may be necessary for bacteroid differentiation. Although *S. meliloti* contains a likely C-terminal ClpX targeting tag (C-terminal TA), it has not been demonstrated that *S. meliloti* CtrA is subject to the same regulation by cell cycle regulated proteolysis as observed in *C. crescentus* (12). To test whether *S. meliloti* CtrA may be regulated by proteolysis during the cell cycle I first determined the half-life of CtrA using pulse-chase analysis. I pulsed mid-log phase cultures with $^{35}$S labeled methionine and cysteine, chased with unlabeled methionine and cysteine, and pulled down the *S. meliloti* CtrA protein using a *C. crescentus* CtrA polyclonal antibody that has previously been shown to cross-react with *S. meliloti* CtrA (27). I resolved $^{35}$S-labeled CtrA using SDS-PAGE and autoradiography and observed a 26.5 kDa band corresponding to *S. meliloti* CtrA, which began to disappear after 180 minutes (Fig 3.3A). I directly

measured the signal at each time point and determined the half-life of $^{35}S$ labeled *S. meliloti* CtrA to be 59.2 minutes during a the 216 minute cell cycle (Fig 3.3B), which is comparable to the 53 minute half-life of *C. crescentus* CtrA in unsynchronized culture during a 160 minute cell cycle (28)

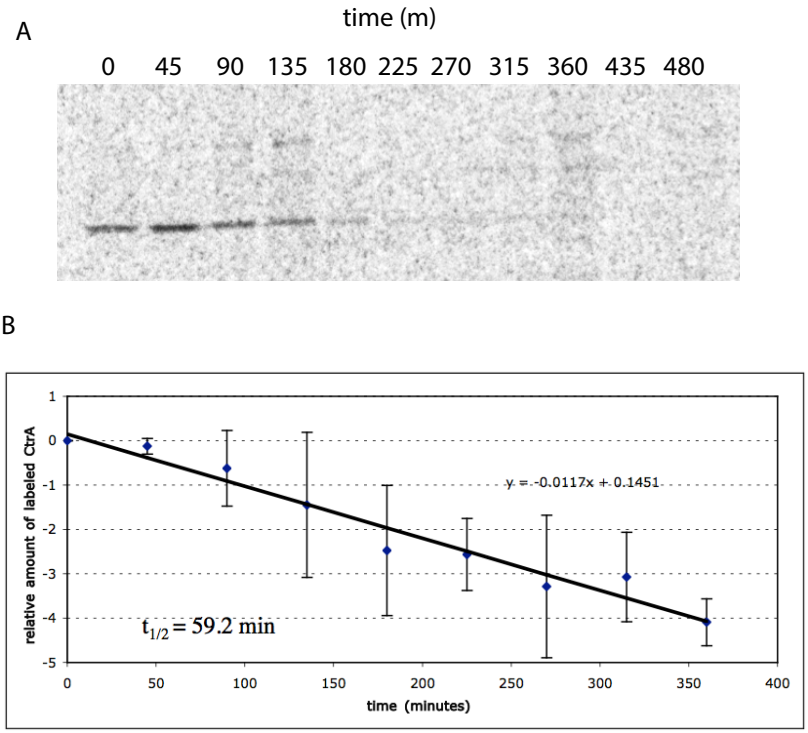


**Figure 3.3. Pulse-chase analysis to determine CtrA half-life in *S. meliloti.*** A. Autoradiograph of 35S labeled CtrA resolved on SDS-PAGE. Signal for CtrA begins to dissipate 180 minutes after chase. In B, the amounts of labeled CtrA at each time point were measured in autoradiographs from three separate experiments were plotted over time. The equation representing the best-fit line is displayed in the graph and the x coefficient was used to calculate the half-life of CtrA in *S. meliloti.*

**A non-degradable allele of CtrA is lethal in *S. meliloti.*** To determine the importance of the proteolytic degradation of CtrA in *S. meliloti,* I tested the effects of a putative non-degradable allele of *S. meliloti* CtrA. In *C. crescentus* it was found that disprupting the final two C-terminal residues of CtrA, which comprise the ClpX recognition tag, stabilized CtrA protein during the cell cycle, but did not cause any major cell cycle defects (12). In *C. crescentus,* both the *ctrADD* allele, in which the C terminal alanines were converterd to aspartates, and the *ctrAΔ3M2* allele, in which the last three amino acids were deleted and replaced with an M2 tag produce

stablized versions of CtrA (12). I therefore constructed a corresponding *ctrADD* allele of *S. meliloti* CtrA by first amplifying the predicted promoter region and coding region and cloning it into a medium copy vector. I then performed site directed mutagenesis to convert the C-terminal TA residues into DD residues and transformed into *E. coli* DH5α. Attempts to mate the medium copy plasmid (pBBR1MCS5) expressing the *ctrADD* allele into *S. meliloti* did not yield any colonies containing the plasmid, while mating the control plasmid yielded hundreds of colonies (data not shown).

I also tried to introduce the *ctrADD* directly into the native *ctrA* locus via a *sacB* suicide vector system, but no transconjugants were obtained. To test if a less severe non-degradable allele was lethal in *S. meliloti,* we constructed a *ctrA* allele missing the last three amino acids (*ctrAΔ3* ), which has been found to produce less severe phenotypes in *C. crescentus* than the *ctrADD* allele. Attempts to indroduce a medium copy plasmid containing this allele into *S. meliloti* also failed and did not yield any colonies containing the plasmid. These results indicate that non-degradable alleles of CtrA such as *ctrADD* and *ctrAΔ3* may be lethal in *S. meliloti.* The deleterious effects of introducing putative non-degradable alleles of *ctrA* to *S. meliloti* suggest that unlike in *C. crescentus,* degradation of CtrA is essential in *S. meliloti.* Conversely, instead of being constitutively active the *ctrADD* and *ctrAΔ3* alleles may be non-functional in *S. meliloti* and their lethality may be due to a dominant negative effect.

***C. crescentus ctrA can complement S. meliloti ctrA during free living growth, but not during symbiosis.*** The bacteroid-like state induced in cells depleted with CtrA

combined with the previously observed symbiotic defects observed in strains lacking the function of putative CtrA regulators (CpdR1 and CbrA) led us to hypothesize that inactivation of CtrA may be critical to symbiosis (23-25). *C. crescentus ctrA* has been shown to complement *S. meliloti ctrA* during free living growth, but the ability to complement during symbiosis had not been tested (19). We constructed two *S. meliloti* strains in which, a chromosomal *ctrA* deletion was transduced into strains complemented with the promoter and coding regions of *C. crescentus ctrA* (BM130) and *S. meliloti ctrA* (BM131) respectively, to create strains BM146 and BM196 (Table 3.1). For each strain, the sole copy of *ctrA* is expressed from its native promoter on the low copy pMR10 plasmid. Neither the strain carrying *S. meliloti ctrA* derivative *(*BM196), nor the strain carrying the *C. crescentus ctrA* derivative (BM146), exhibited any discernable free-living growth defects (data not shown).

**Table 3.1** Transduction of *ctrA* deletion in low-copy complemented strains.

| **Strain** | **Viable cells (cfu/ml)** | **Number of transduced (cfu/ml)** |
|---|---|---|
| BM113 (pMR10) | $5.6 \times 10^{10}$ | 0 |
| BM130 (Cc-ctrA) | $4.5 \times 10^{10}$ | $3.2 \times 10^{2}$ |
| BM132 (Sm-ctrA) | $2.6 \times 10^{10}$ | $3.1 \times 10^{2}$ |

I then tested the ability of strains BM196 and BM146 to nodulate *Medicago sativa.* Seedlings were inoculated with equal numbers of bacteria from saturated cultures of wild type (1021), BM196 and BM146. Wild-type and strain BM196 were able to form an efficient symbiosis with *M. sativa* as characterized by plant height measurements and the production of pink nodules (Figure 3.4). In contrast, the nodules produced by BM146 were white and of varying sizes and the plants were

stunted for growth. Nodule crushing experiments indicated that bacteria were present in the infection thread, so electron microscopy (EM) was used to view bacteroids in nodule cross sections. Nodules of BM196 visualized by EM contained fully differentiated bacteroids closely associated with the peribacteroid membrane (Fig 3.4B). Cross sections of BM146 nodules revealed that very few bacteria had entered into the plant nodule cells and the bacteria present were undifferentiatied, indicating that the bacteria were not able to successfully exit the infection thread and be endocytosed into the symbiosome compartment (Fig. 3.4C).

There are several possibilities that could account for the observation that the *C. crescentus ctrA* promoter and coding regions cannot substitute for *S. meliloti ctrA* during symbiosis even though they can do so during free-living growth. First, the *C. crescentus ctrA* promoter region might not function at all when *S. meliloti* is within *M. sativa* and therefore *ctrA* is not expressed in the infection thread or during the later stages of symbiosis. Second, it is also possible that the *C. crescentus ctrA* promoter region cannot be regulated appropriately when *S. meliloti* is within *M. sativa* to produce the cell cycle changes necessary for bacteroid differentiation and symbiosis. Other possibilities are that the *C. crescentus* CtrA protein is not functional when *S. meliloti* is within in *M. sativa* or that it cannot be down-regulated effectively upon release into the symbiosome to allow for bacteroid differentiation.

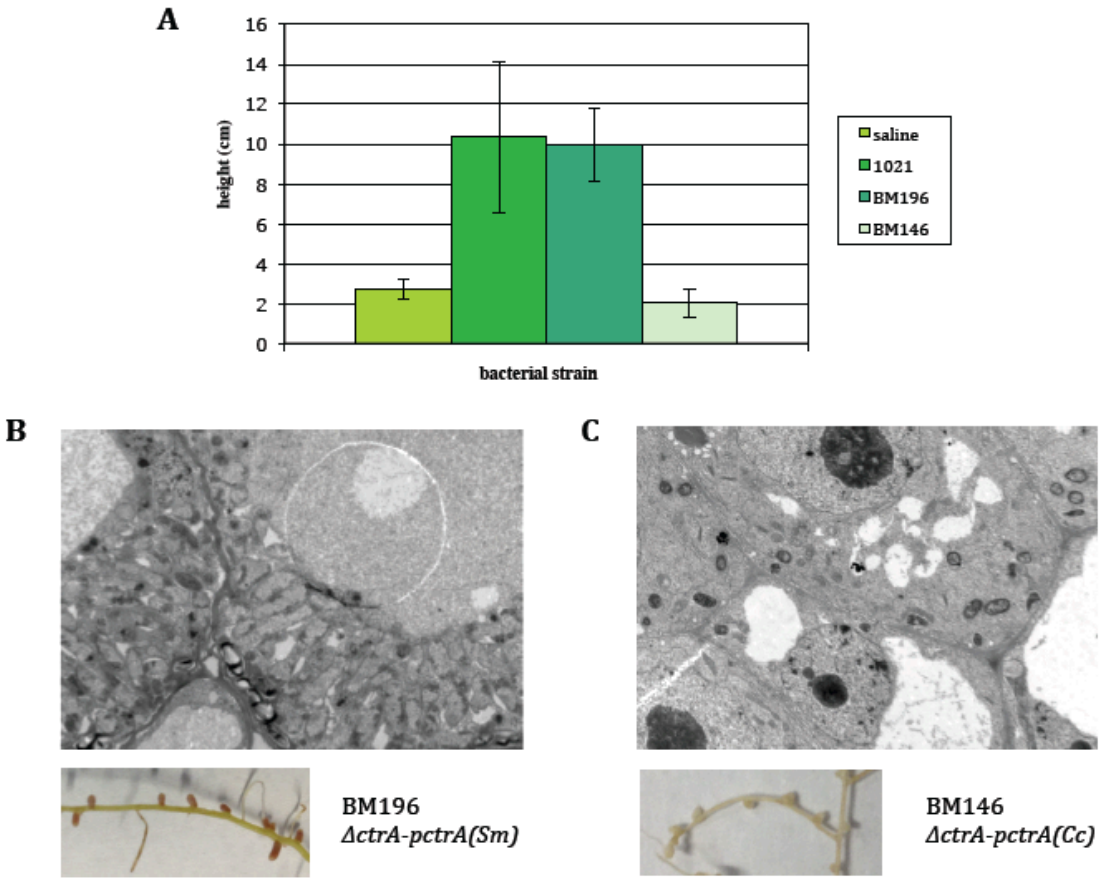


**Figure 3.4 Symbiotic efficiency of complemented *ΔctrA* strains.** A. Plant height measurements of *M. sativa* inoculated for 28 days with various *S. meliloti* strains. B. Representative nodules induced on *M. sativa* infected with BM196 and EM of a nodule cross-section. Symbiosome compartments in nodule cell are full of differentiated bacteroids and induced nodules are elongated and pink. C. Representative nodules induced on *M. sativa* infected with BM146 and EM of a nodule cross-section. Nodules induced by BM146 are white and stunted and nodule cells are nearly devoid of bacteroids.

***The symbiotic defect of BM146 is not caused by lack of expression of the C. crescentus ctrA promoter during symbiosis or differences in the coding region.***

To test whether differences in the promoter regions or the coding regions of *S. meliloti* and *C. crescentus ctrA* were responsible for the symbiotic deficiency of *C. crescentus ctrA,* we constructed two strains, in which the *ctrA* coding region from one organism was under the control of the promoter region of *ctrA* from the other organism. BM557 ($\Delta ctrA p_{Sm} ctrA_{Cc}$) carries the *C. crescentus ctrA* open reading frame on pMR10 under the control of the *S. meliloti ctrA* promoter region while BM561

(*ΔctrA*p$_{Cc}$*ctrA*$_{Sm}$) carries the *S. meliloti ctrA* coding region on pMR10 under the control of the *C. crescentus ctrA* promoter region. Neither of these strains exhibited morphological or growth defects in rich medium (LBMC) indicating that the CtrA was expressed adequately from both plasmids to complement the chromosomal *ctrA* deletion mutant during free-living growth.

To test the symbiotic efficiency of these strains, *M. sativa* seedlings were inoculated with equal amounts of saturated culture from BM557 (*ΔctrA*p$_{Sm}$*ctrA*$_{Cc}$) and BM561 (*ΔctrA*p$_{Sm}$*ctrA*$_{Cc}$), on Jensen agar plates. Surprisingly, neither plants inoculated with BM557 nor plants inoculated with BM561 exhibited the same striking symbiotic phenotypes that were observed in plants inoculated with the BM146 strain (*ΔctrA*p$_{Cc}$*ctrA*$_{Cc}$). BM557 and BM561 were able to form a successful symbiosis with *M. sativa* producing green plants with elongated pink nodules. I did note a shorter than average plant height in plants inoculated BM561 and BM557 (Fig 3.5A). Also, plants inoculated with BM557 (*ΔctrA*p$_{Sm}$*ctrA*$_{Cc}$) displayed a mixture of wild type and irregular nodules (data not shown). These results suggest that these mutant strains may form a less efficient symbiosis than wild type *S. meliloti,* but any defects were not enough to inhibit symbiosis. The lack of a strong symbiotic defect in either of these strains was unexpected since BM146 (*ΔctrA*p$_{Cc}$*ctrA*$_{Sm}$) exhibited such a striking symbiotic defect.

Oftentimes, competition for nodulation assays can be used to distinguish more subtle symbiotic defects. To determine if the symbiotic defect of BM146 was due to a combination of more subtle defects of BM561 and BM557, I performed competition for nodule occupancy assays. *M. sativa* was inoculated with test strains

(BM557 and BM561) mixed with equal amounts of wild type Rm1021. Competition assays were also performed with BM196 and BM146 as controls. Results of the competition for nodulation assays indicated that, as expected, *S. melioti* expressing *C. crescentus ctrA* from the *C. crescentus* promoter region were at profound competitive disadvantage to *S. meliloti* (Fig 3.5B), comprising only 1% recovered from crushed nodules. The control strain BM196, which expresses *S. meliloti ctrA* from the *S. meliloti* promoter region was able to compete well with wild-type and made up 45% of the population in nodules of co-inoculated plants.

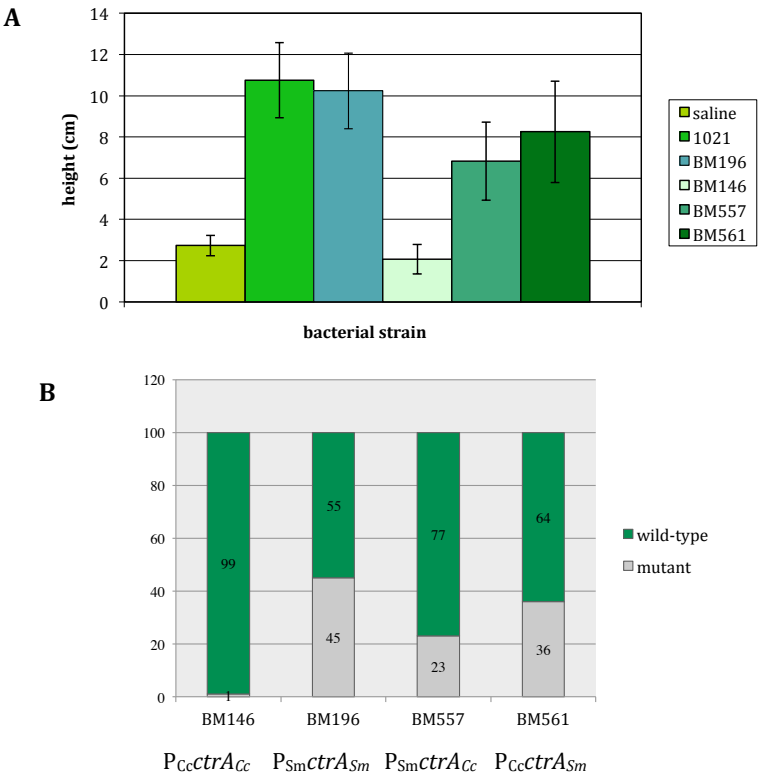


**Figure 3.5. Analysis of *C. crescentus ctrA* promoter or coding region defects within *M. sativa*.** A. Test strains expression *S. meliloti ctrA* from the *C. crescentus ctrA* promoter region (BM561) and vice versa (BM557) were inoculated on *M. sativa* and plant height was measured after 28 days. B. Competition for nodule occupancy assays were performed mixing equal amounts the test strain (i.e. BM557) and wild type Rm 1021 and inoculating *M. sativa.* Nodules were crushed and assayed for the presence of either wild type ($Strep^R$) or mutant ($Neomycin^R$) bacteria. Results are represented as percentage of the bacteria recovered from nodules assayed.

The results of the competition assays for BM557 ($P_{Sm}$-$ctrA_{Cc}$) and BM561 ($P_{Cc}$-$ctrA_{Sm}$) were more difficult to interpret. *S. meliloti* expressing *C. crescentus ctrA* from the *S. meliloti* promoter (BM557) were at a greater competitive disadvantage

to wild-type *S. meliloti* than *S. meliloti* expressing *S. meliloti ctrA* from the *C. crescentus* promoter (BM561). However, neither strain demonstrated a large enough disadvantage to wild type to justify a simple cumulative effect of the *ctrA* coding and promoter regions causing the symbiotic failure of BM146. It is paradoxical that we observed such a strong effect on symbiosis with both the *ctrA* promoter and coding region from *C. crescentus,* but only a very subtle effects when only one of the two regions, *ctrA* promoter or coding region, from *C. crescentus* was present. A more complex mechanism is needed to explain the inability of both the *C. crescentus ctrA* promoter and coding to complement in *S. meliloti* during symbiosis with *M. sativa.*

One possibility is that *S. meliloti* CtrA is regulated by multiple transcriptional and post-transcriptional mechanisms during symbiosis to which *C. crescentus ctrA* cannot respond. Redundancy in the *S. meliloti* CtrA regulatory network during symbiosis may allow for effective symbiosis to continue if only transcriptional or post-transcriptional regulation are broken, but not both. In fact, redundancy of mechanisms CtrA regulation is a common theme during the cell cycle of *C. crescentus* and is thought to add robustness to the regulatory circuit (29). The transcriptional regulation of *ctrA* in *C. crescentus* is extremely complex as *ctrA* mRNA is transcribed from two separate promoters at different times during the cell cycle and subject to transcriptional activation and repression at these promoters by several regulatory factors (30, 31). *S. meliloti ctrA* displays a similar dual promoter structure and although binding of *C. crescentus ctrA* has been demonstrated, the specific timing of

expression from each of the two promoters during the *S. meliloti* cell cycle has not been assessed.

Another possibility is that specialized regulation of *S. meliloti* mRNA may be required during symbiosis, such that when the full *C. crescentus ctrA* mRNA is transcribed (as it is in BM146), it cannot be regulated properly or is not stable. If the *C. crescentus ctrA* mRNA was inappropriately degraded in the infection thread this could lead to defects in replication of *S. meliloti* in the infection thread and explain the lack of bacteoids observed in symbiosomes nodules of plants inoculated with BM146. Undoubtedly a complex mechanism regulates the activity of CtrA in *S. meliloti* during symbiosis and although this mechanism has yet to be elucidated, we have clearly demonstrated the importance of CtrA regulation in *S. meliloti* during symbiosis.

**Discussion and Future Directions**

In this work, we demonstrate that depletion of CtrA in *S. meliloti* leads to a bacteroid-like state characterized by cell elongation, bloating and branching as well as severe endoreduplication of the genome (Fig 3.1C, 3.2). Through pulse-chase analysis we also show that *S. meliloti* CtrA has a comparable half-life to *C. crescentus* CtrA, suggesting that it may also be regulated by proteolysis during the cell cycle (Fig. 3.3). We also show, that unlike in *C. crescentus,* regulated proteolysis of CtrA is likely to be essential in *S. meliloti* as putative non-degradable alleles of *ctrA* were lethal to *S. meliloti.* To confirm this observation, the lethality of a conditional non-degradable *ctrA* allele must be tested in *S. meliloti.* Also to test the activity of the respective plasmid borne *C. crescentus* and *S. meliloti ctrA* promoters in these strains

qPCR analysis should be performed. Finally we show that proper regulation of CtrA during symbiosis is necessary for efficient symbiosis with *M. sativa. S. meliloti* strains carrying *C. crescentus ctrA* under the control of the *C. crescentus ctrA* promoter region (BM146) were not able to enter the symbiosome and differentiate into nitrogen-fixing bacteroids (Fig. 3.4). We uncovered a regulatory paradox when we discovered that *S. meliloti* expressing the *S. meliloti ctrA* coding region from the *C. crescentus ctrA* promoter and vice versa did not exhibit symbiotic defects that were in anyway comparable to the striking defect observed with BM146. This leaves an open question of how *C. crescentus* versions of the *ctrA* promoter region and coding region individually can complement during symbiosis, but when combined lead to a completely ineffective symbiosis. Additional work is clearly required to elucidate the complex regulatory mechanism responsible for CtrA regulation in *S. meliloti* during symbiosis.

Our investigation of the effects of CtrA depletion and the requirements for CtrA regulation during symbiosis strongly suggests that negative regulation of CtrA is crucial during symbiosis, perhaps to allow for endoreduplication of the genome. In *C. crescentus,* CtrA blocks the initiation of DNA replication in swarmer cells so, if CtrA has a similar role in *S. meliloti,* abrogation of CtrA function may be required to allow for endoreduplication. This hypothesis is consistent with symbiotic deficiency exhibited by other *S. meliloti* mutants that are hypothesized to have high CtrA levels, such as the Δ*divJ* (Appendix B) and *ΔcbrA* (24, 25). CbrA is a cognate kinase to DivK responsible for regulation of CtrA activity and stability in *S. meliloti* and loss of CbrA function in *S. meliloti* has been shown to result in increased levels of CtrA (24). The

symbiotic efficiency of the Δ*divJ* mutant is also impaired since *M. sativa* inoculated with Δ*divJ* are stunted for growth and very few Δ*divJ* cells are able to enter the symbiosome, suggesting problems in endocytosis or endoreduplication once they are inside the plant cell cytoplasm (Appendix B). These data further support the hypothesis that CtrA activity must be down-regulated during symbiosis and the discovery that mature bacteroids lack CtrA provides direct support for this hypothesis.

Additional work to elucidate the molecular mechanisms of CtrA regulation during the *S. meliloti* cell cycle is needed to fully understand how CtrA activity is controlled in the free-living state and during symbiosis. Now that a synchronization method has been developed for *S. meliloti* CtrA protein levels over the course of the cell cycle can be assessed and compared to the oscillation observed in *C. crescentus.* Synchronized cultures can also be used to look at the cell cycle stage specific phosphorylation of CtrA and other regulators including *S. meliloti* CpdR1, DivK, DivJ and CbrA to help elucidate their regulatory functions during the the *S. meliloti* cell cycle. The *S. meliloti* cell synchronization method can also be used to asses the transcription from each of the two promoters present in the *S. meliloti ctrA* upstream regulatory region during the cell cycle (32). In *C. crescentus,* transcription of *ctrA* occurs at different points in the cell cycle from two promoters. CtrA is expressed at low levels from the P1 promoter early in the cell cycle and then activates its own transcription at much higher levels from the P2 promoter later in the cell cycle (30). RNAse protection assays or transcriptional *lacZ* fusions can be

used on synchronized cultures to determine if the *C. crescentus ctrA* transcriptional regulatory scheme is conserved in *S. meliloti* (19).

**Experimental Procedures**

***Bacterial strains, media, cloning and growth conditions***

The bacterial strains and plasmids used in this are described in Table 3.2. *Escherichia coli* strains were grown in Luria-Bertani (LB) broth (Sigma Aldrich) at 37°C supplemented with appropriate antibiotics: kanamycin (50 μg/ml), tetracycline (10μg/ml). For most experiments *S. meliloti* was grown at 30C in either LB with 2.5 mM $MgSO_4$ and 2.5 mM $CaCl_2$ (LBMC) or TY broth supplemented when necessary with kanamycin (200 μg/ml), streptomycin (500 μg/ml), tetracycline (1 μg/ml in liquid broth, 2 μg/ml in agar). For creating *ctrA* deletion constructs two 1000bp fragments upstream and downstream of the *ctrA* locus were amplified and a deletion cassette was constructed as previously described (33). For sacB selection 10% sucrose was added to agar plates and two step recombination of the deletion cassette was conducted as previously described to BM146 (33).

For construction of the complementation plasmids (pMR10-ctrA(Cc) and pMR10-ctrA(Sm)), the putative promoter regions and coding regions of *C. crescnetus* and *S. meliloti ctrA* were amplified by PCR using the Rm1021 genomic DNA as template and primers specific to those regions. Fragments were gel purified and cloned into the low copy vector pMR10 (34). To construct the "promoter swap" plasmids, promoter regions of *S. meliloti* and *C. crescentus ctrA* were PCR amplified and ligated to the coding regions of *C. crescentus* and *S. meliloti ctrA,* respectively and cloned into pMR10. For conjugation experiments, $1\times10^9$ *S. meliloti* and $0.5\times10^9$

*E. coli* S17-1 cells were combined on LB agar plates and incubated 24h at 30° C. For transduction, phage and bacteria (in LB containing 2.5 mM $CaCl_2$ and 2.5 mM $MgSO_4$) were mixed to give a multiplicity of infection 1:2 (phage/cell) and the mixture was incubated at 30°C for 30 min.

To construct the non-degradable alleles of *ctrA,* the entire *ctrA* promoter region and open reading frame were amplified from the *S. meliloti* genome and cloned into pBBR1MCS5. Site-directed mutagenesis was used to replace the C-terminal alanines (AA) with aspartates (DD) and introduced to *S. meliloti* via conjugation. For *ctrAΔ3M2* an M2 tag replaced the final three amino acids of CtrA as previously described (12). For pulse-chase analysis *S. meliloti* 1021 was grown in SMM (11mM $KH_2PO_4$, 13mM $K_2HPO_4$, 15mM $NH_4Cl$, 15mM NaCl, 2mM $MgSO_4.7H_2O$, 200ng/mL CoCl2, 200g/mL biotin, 0.3% sucrose) media without methionine (35). The CtrA depletion strain (BM249) was grown in LBMC supplemented with 1mM IPTG. All *S. meliloti* strains constructed were derivatives of Rm 1021.

***Pulse-chase analysis***

Pulse-chase analysis was performed as described in (36). *S. meliloti* 1021 was grown in SMM media without antibiotics to mid-log phase ($OD_{600}$ ~0.6-0.7). About 25-30mLs of culture were transferred to a disposable baffled flask and incubated at 30C shaking at 200rpm for 5 minutes. Cultures were pulsed for 5 minutes with 20uCi of $^{35}$[S]met and cys EasyTagEXPRESS protein labeling mix (Perkin Elmer). Then cultures were chased with appropriate volumes of of 100x chase solution (0.4% methionine, 0.3% cysteine). Time points were taken and pelleted at 10,000xg for 3 minutes every 45 minutes including 0 minutes after chase. Each 1mL time point was

resuspended in 10x TEN (100mM Tris pH8, 10mM EDTA pH8, 0.25 $NaN_3$), pelleted and resuspended in 1X TEN and put on ice. Once all time points were collected each sample was pelleted again and then resuspended in 50uL TES (10mM Tris pH8, 1mM EDTA pH8, 1% SDS). All samples were incubated at 100C for 10 minutes and then flash spun to bring down condensation. After adding 1mL of IP buffer (50mM Tris, pH7.5, 150mM NaCl, 1% Triton X-100) plus Sigma protease inhibitors (1:250) were added to each tube the pellet was resuspended and the samples were pelleted again. Next, 850uL of the supernatant was transferred to a new tube (50 uL was kept for TCA) and 25uL of equilibrated 50% slurry Protein A agarose (Pierce) was added to each tube and samples were rotated at 4C for 20 minutes. Then 750uL of supernatant was transferred to a new tube and 1uL of un-diluted CtrA antibody (*C. crescentus* CtrA antibody R308 gift of Michael Laub) and 25uL of 50% slurry Protein A agarose was added to each tube and rotated for 4 hours at 4C. Samples were washed 3x with IP buffer and 1x with IP buffer without Triton using an aspirator to remove the supernatant. Samples were resuspended in 12.uL of 2x sample buffer and stored at -80C. Samples were thawed an boiled for 5 minutes and flash spun before loading onto a 4-20% Tris-HCl gel. Gels were run for ~40 minutes at 180V and then dried in Saran wrap using a gel dryer. Dried gels were exposed for at least 12hrs to an Amersham Biosciences Storage Phosphor Screen, which was developed using a Typhoon imager.

***Depletion of CtrA in S. meliloti***

For CtrA depletion experiments *S. meliloti* BM249 cells were grown to early log phase ($OD_{600}$=0.1-0.2) at 30C in rich medium (either LB/MC or TY) with 1mM IPTG.

Cells were pelleted at 6000rpm for 5 minutes and resuspended in rich medium without IPTG and grown at 30C. For the efficiency-of-plating (EOP) assays, samples were taken from BM249+IPTG and CtrA depleted BM249 cultures and various time points and then diluted to an $OD_{600}$ of 0.1 of LB. For each time point control and CtrA depleted samples were serially diluted up to $10^{-6}$ in LB, and spread onto LB agar. After 4 to 5 days of growth at 30°C, the number of CFUs were determined.

***Microscopy***

For microscopy of CtrA-depleted and wild-type *S. meliloti* cells, samples were taken from Rm1021 mid-log phase culture as well as from BM249 culture after 8 hours of depletion, fixed in 70% ethanol, washed, and concentrated with saline solution (0.85% NaCl). Samples were incubated with DAPI to stain DNA, deposited on microscope slides coated with 0.1% poly-L-lysine and imaged using an alpha Plan-Apochromat 100x/1.46 OilDIC objective and Zeiss AxiocamMR3 camera.

***Flow Cytometry***

Wild-type (1021), BM249+IPTG, and cells depleted of CtrA for 8hrs (BM249-IPTG) were collected in early log phase and fixed in 100% ethanol (200 µL culture in 933uL ethanol) and stored overnight at 4°C. Cells were collected by centrifugation and incubated in 1 mL of 50 mM sodium citrate containing 3.3 µg/ml RNase A at 50°C for 2 hrs. Samples were then incubated at room temperature with 1 µL of SYTOX Green dye diluted 1:6 in the sodium citrate/RNase solution. Fluorescence per cell was measured by a BD FACScan flow cytometer and data was analyzed with FlowJo 9.6.3 software.

***Nodulation assays and Competition assays***

Three day-old alfalfa seedlings (*Medicago sativa* cv. Iroquois: Agway, Plymouth IN, USA) were inoculated with Rm1021 and Rm1021 derivatives on Petri dishes containing Jensen agar as previously described (37, 38). After 4 weeks plants were analyzed for symbiotic phenotypes. For competition assays an $OD_{600}$-normalized 1:1 mix of Rm1021 and the mutant strain (BM146, BM196…) was inoculated onto *M. sativa* seedlings. After 4 weeks ~12 representative nodules were collected per plant and were surface sterilized in 50% bleach, washed three times in sterile dd$H_2O$ and crushed in LBMC+0.3M glucose. Samples were diluted to 1:100 or 1:200 and plated simultaneously on LB + Streptomycin and LB + Neomycin to determine the presence of wild-type versus mutant bacteria in each nodules. After 2-3 days of incubation at 30C, CFUs were quantified on each plate. Plants were also assessed for symbiotic phenotypes.

**Acknowledgements**

We gratefully acknowledge support and funding from the NIH (grant GM31010) for work done in the lab of G.C.W. N.J.D. was also supported by the Massachusetts Institute of Technology NIH training grant. We also acknowledge support from the Ente Cassa di Risparmio di Firenze, Accademia dei Lincei, Fondazione Buzzati-Traverso and ANR (JCJC-CASTACC), the Region Nord-Pas-de-Calais for work done by E.G.B, F.P. and L.P. G.C.W. is an American Cancer Society Professor.

**Supplemental tables**

**Table 3.2 Strains and Plasmids**

| Organism | Strain/Plasmid | Description | Resistance | Source |
|---|---|---|---|---|
| *S. meliloti* | Rm1021 | SU47 str-21 | Sm | (39) |
| | BM146 | Rm1021Δ*ctrA*+pMR10-p$ctrA_{CC}ctrA_{CC}$ | Sm, Tc, Km | This work |
| | BM196 | Rm1021Δ*ctrA*+pMR10-p$ctrA_{Sm}ctrA_{Sm}$ | Sm, Tc, Km | This work |
| | BM557 | Rm1021Δ*ctrA*+pMR10-p$ctrA_{Sm}ctrA_{Cc}$ | Sm, Tc, Km | This work |
| | BM561 | Rm1021Δ*ctrA*+pMR10-p$ctrA_{Cc}ctrA_{Sm}$ | Sm, Tc, Km | This work |
| | BM249 | Rm1021Δ*ctrA*+pSRKKm-$ctrA_{Sm}$ (CtrA depletion) | Sm, Tc, Km | This work |
| *E. coli* | DH5α | *huA2 lac(del)U169 phoA glnV44 Φ80' lacZ(del) M15 gyrA96 recA1 relA1 endA1 thi-1 hsdR17* | | (40) |
| General Plasmids | pMR10 | Broad host range cloning vector low copy number | Km | (34) |
| | pSRKKm | pBBR1MCS-2 derived broad host range vector containing *lac* promoter, $lacI^q$, $lacZ^+$ | Km | (26) |
| | pBBR1MCS5 | Broad host range medium copy vector | Gm | (41) |
| Deletion plasmids | pNTPS138 | Suicide vector *oriT, sacB* | Km | D. Alley |
| | Δ*ctrA* | pNTPS138-Tc deletion cassette for *ctrA* | Km, Tc | This work |
| Phage | ΦM12 | Transducing phage | | (42) |
| Expression plasmids | p*ctrADD* | pBBR1MCS5-p$ctrA_{Sm}ctrADD_{Sm}$ | Gm | This work |

## References


1. Jones KM, Kobayashi H, Davies BW, Taga ME, & Walker GC (2007) How rhizobial symbionts invade plants: the Sinorhizobium-Medicago model. *Nature reviews. Microbiology* 5(8):619-633.
2. Oke V & Long SR (1999) Bacteroid formation in the Rhizobium-legume symbiosis. *Current opinion in microbiology* 2(6):641-646.
3. Foucher F & Kondorosi E (2000) Cell cycle regulation in the course of nodule organogenesis in Medicago. *Plant molecular biology* 43(5-6):773-786.
4. Mergaert P*, et al.* (2006) Eukaryotic control on bacterial cell cycle and differentiation in the Rhizobium-legume symbiosis. *Proceedings of the National Academy of Sciences of the United States of America* 103(13):5230-5235.
5. Van de Velde W*, et al.* (2010) Plant peptides govern terminal differentiation of bacteria in symbiosis. *Science* 327(5969):1122-1126.
6. Gibson KE, Kobayashi H, & Walker GC (2008) Molecular determinants of a symbiotic chronic infection. *Annual review of genetics* 42:413-441.
7. Bird TH & MacKrell A (2011) A CtrA homolog affects swarming motility and encystment in Rhodospirillum centenum. *Archives of microbiology* 193(6):451-459.
8. Shapiro L (1976) Differentiation in the Caulobacter cell cycle. *Annual review of microbiology* 30:377-407.
9. Tsokos CG & Laub MT (2012) Polarity and cell fate asymmetry in Caulobacter crescentus. *Current opinion in microbiology* 15(6):744-750.
10. Laub MT, McAdams HH, Feldblyum T, Fraser CM, & Shapiro L (2000) Global analysis of the genetic network controlling a bacterial cell cycle. *Science* 290(5499):2144-2148.
11. Quon KC, Yang B, Domian IJ, Shapiro L, & Marczynski GT (1998) Negative control of bacterial DNA replication by a cell cycle regulatory protein that binds at the chromosome origin. *Proceedings of the National Academy of Sciences of the United States of America* 95(1):120-125.
12. Domian IJ, Quon KC, & Shapiro L (1997) Cell type-specific phosphorylation and proteolysis of a transcriptional regulator controls the G1-to-S transition in a bacterial cell cycle. *Cell* 90(3):415-424.
13. Biondi EG*, et al.* (2006) Regulation of the bacterial cell cycle by an integrated genetic circuit. *Nature* 444(7121):899-904.
14. Siam R & Marczynski GT (2000) Cell cycle regulator phosphorylation stimulates two distinct modes of binding at a chromosome replication origin. *The EMBO journal* 19(5):1138-1147.
15. Abel S*, et al.* (2011) Regulatory cohesion of cell cycle and cell differentiation through interlinked phosphorylation and second messenger networks. *Molecular cell* 43(4):550-560.
16. Duerig A*, et al.* (2009) Second messenger-mediated spatiotemporal control of protein degradation regulates bacterial cell cycle progression. *Genes & development* 23(1):93-104.

17. Collier J (2012) Regulation of chromosomal replication in Caulobacter crescentus. *Plasmid* 67(2):76-87.
18. Brilli M*, et al.* (2010) The diversity and evolution of cell cycle regulation in alpha-proteobacteria: a comparative genomic analysis. *BMC systems biology* 4:52.
19. Barnett MJ, Hung DY, Reisenauer A, Shapiro L, & Long SR (2001) A homolog of the CtrA cell cycle regulator is present and essential in Sinorhizobium meliloti. *Journal of bacteriology* 183(10):3204-3210.
20. Sibley CD, MacLellan SR, & Finan T (2006) The Sinorhizobium meliloti chromosomal origin of replication. *Microbiology* 152(Pt 2):443-455.
21. Wright R, Stephens C, & Shapiro L (1997) The CcrM DNA methyltransferase is widespread in the alpha subdivision of proteobacteria, and its essential functions are conserved in Rhizobium meliloti and Caulobacter crescentus. *Journal of bacteriology* 179(18):5869-5877.
22. Latch JN & Margolin W (1997) Generation of buds, swellings, and branches instead of filaments after blocking the cell cycle of Rhizobium meliloti. *Journal of bacteriology* 179(7):2373-2381.
23. Kobayashi H, De Nisco NJ, Chien P, Simmons LA, & Walker GC (2009) Sinorhizobium meliloti CpdR1 is critical for co-ordinating cell cycle progression and the symbiotic chronic infection. *Molecular microbiology* 73(4):586-600.
24. Sadowski C, Wilson D, Schallies K, Walker G, & Gibson KE (2013) The Sinorhizobium meliloti sensor histidine kinase CbrA contributes to free-living cell cycle regulation. *Microbiology*.
25. Gibson KE, Campbell GR, Lloret J, & Walker GC (2006) CbrA is a stationary-phase regulator of cell surface physiology and legume symbiosis in Sinorhizobium meliloti. *Journal of bacteriology* 188(12):4508-4521.
26. Khan SR, Gaines J, Roop RM, 2nd, & Farrand SK (2008) Broad-host-range expression vectors with tightly regulated promoters and their use to examine the influence of TraR and TraM expression on Ti plasmid quorum sensing. *Applied and environmental microbiology* 74(16):5053-5062.
27. Fields AT*, et al.* (2012) The conserved polarity factor podJ1 impacts multiple cell envelope-associated functions in Sinorhizobium meliloti. *Molecular microbiology* 84(5):892-920.
28. Iniesta AA, McGrath PT, Reisenauer A, McAdams HH, & Shapiro L (2006) A phospho-signaling pathway controls the localization and activity of a protease complex critical for bacterial cell cycle progression. *Proceedings of the National Academy of Sciences of the United States of America* 103(29):10935-10940.
29. Collier J, McAdams HH, & Shapiro L (2007) A DNA methylation ratchet governs progression through a bacterial cell cycle. *Proceedings of the National Academy of Sciences of the United States of America* 104(43):17111-17116.
30. Domian IJ, Reisenauer A, & Shapiro L (1999) Feedback control of a master bacterial cell-cycle regulator. *Proceedings of the National Academy of Sciences of the United States of America* 96(12):6648-6653.

31. Tan MH, Kozdon JB, Shen X, Shapiro L, & McAdams HH (2010) An essential transcription factor, SciP, enhances robustness of Caulobacter cell cycle regulation. *Proceedings of the National Academy of Sciences of the United States of America* 107(44):18985-18990.
32. Schluter JP*, et al.* (2013) Global mapping of transcription start sites and promoter motifs in the symbiotic alpha-proteobacterium Sinorhizobium meliloti 1021. *BMC genomics* 14:156.
33. Skerker JM, Prasol MS, Perchuk BS, Biondi EG, & Laub MT (2005) Two-component signal transduction pathways regulating growth and cell cycle progression in a bacterium: a system-level analysis. *PLoS biology* 3(10):e334.
34. Roberts RC*, et al.* (1996) Identification of a Caulobacter crescentus operon encoding hrcA, involved in negatively regulating heat-inducible transcription, and the chaperone gene grpE. *Journal of bacteriology* 178(7):1829-1841.
35. Griffitts JS & Long SR (2008) A symbiotic mutant of Sinorhizobium meliloti reveals a novel genetic pathway involving succinoglycan biosynthetic functions. *Molecular microbiology* 67(6):1292-1306.
36. Chen EJ, Sabio EA, & Long SR (2008) The periplasmic regulator ExoR inhibits ExoS/ChvI two-component signalling in Sinorhizobium meliloti. *Molecular microbiology* 69(5):1290-1303.
37. Leigh JA, Signer ER, & Walker GC (1985) Exopolysaccharide-deficient mutants of Rhizobium meliloti that form ineffective nodules. *Proceedings of the National Academy of Sciences of the United States of America* 82(18):6231-6235.
38. Pellock BJ, Cheng HP, & Walker GC (2000) Alfalfa root nodule invasion efficiency is dependent on Sinorhizobium meliloti polysaccharides. *Journal of bacteriology* 182(15):4310-4318.
39. Galibert F*, et al.* (2001) The composite genome of the legume symbiont Sinorhizobium meliloti. *Science* 293(5530):668-672.
40. Taylor RG, Walker DC, & McInnes RR (1993) E. coli host strains significantly affect the quality of small scale plasmid DNA preparations used for sequencing. *Nucleic acids research* 21(7):1677-1678.
41. Kovach ME*, et al.* (1995) Four new derivatives of the broad-host-range cloning vector pBBR1MCS, carrying different antibiotic-resistance cassettes. *Gene* 166(1):175-176.
42. Finan TM*, et al.* (1985) Symbiotic mutants of Rhizobium meliloti that uncouple plant from bacterial differentiation. *Cell* 40(4):869-877.

## Appendix A.

## *Sinorhizobium meliloti* CpdR1 is critical for coordinating cell cycle progression and the symbiotic chronic infection

This work was published in Molecular Microbiology, 2009. **73**(4): p. 586-600 by Hajime Kobayashi, Nicole J. De Nisco, Peter Chien, Lyle A. Simmons and Graham C. Walker.

H.K. performed all molecular cloning experiments and FACS analysis**.** N.J.D and H.K. took all mutant strain microscopy images, set up all symbiotic assays and obtained EM nodule images. P.C. made invaluable intellectual contributions. Microscopy of GFP labeled proteins was performed by L.A.S. Manuscript was written and revised by P.C, H.K., N.J.D and G.C.W.

**Abstract**

ATP-driven proteolysis plays a major role in regulating the bacterial cell cycle, development and stress responses. In the nitrogen-fixing symbiosis with host plants, *Sinorhizobium meliloti* undergoes a profound cellular differentiation, including endoreduplication of the genome. The regulatory mechanisms governing the alterations of the *S*. *meliloti* cell cycle *in planta* are largely unknown. Here, we report the characterization of two *cpdR* homologues, *cpdR1* and *cpdR2*, of *S.meliloti* that encode single-domain response regulators. In *Caulobacter crescentus*, CpdR controls the polar localization of the ClpXP protease, thereby mediating the regulated proteolysis of key protein(s), such as CtrA, involved in cell cycle progression. The *S*. *meliloti cpdR1*-null mutant can invade the host cytoplasm, however, the intracellular bacteria are unable to differentiate into bacteroids. We show that *S*. *meliloti* CpdR1 has a polar localization pattern and a role in ClpX positioning similar to *C*. *crescentus* CpdR, suggesting a conserved function of CpdR proteins among α-proteobacteria. However, in *S*. *meliloti*, free-living cells of the cpdR1-null mutant show a striking morphology of irregular coccoids and aberrant DNA replication. Thus, we demonstrate that CpdR1 mediates the co-ordination of cell cycle events, which are critical for both the free-living cell division and the differentiation required for the chronic intracellular infection.

**Introduction**

Rhizobia are α-proteobacteria with the remarkable ability to form a nitrogen-fixing symbiosis with compatible legume hosts (reviewed in Broughton *et al*., 2000; Jones *et al*., 2007; Gibson *et al*., 2008). The symbiosis is based on chronic infection co-ordinated by the exchange of signal molecules between the

symbiotic partners (reviewed in Perret *et al*., 2000; Jones *et al*., 2007; Kobayashi and Broughton, 2008). The process of infection of a plant host by rhizobia is comprised of multiple develop- mental stages, in which the bacteria modulate their cell proliferation in concert with the development of host cells (reviewed in Oke and Long, 1999; Foucher and Kon- dorosi, 2000). In the free-living stage, rhizobia cells divide in an asymmetric manner, producing two daughters of different sizes (Lam *et al*., 2003; Hallez *et al*., 2004). Upon recognition of a compatible host plant, rhizobia enter the root through host-derived tubes called infection threads (reviewed in Gage and Margolin, 2000; Gage, 2004). The extension of infection threads is synchronized with the colonization of rhizobia by the restriction of bacterial cell division and the collective movement of bacteria (Gage, 2002; Fournier *et al*., 2008). At the tip of the infection thread, the bacteria are released into the nodule cell by a process analogous to phagocytosis (reviewed in Brewin, 1998; Jones *et al*., 2007): the bacteria are engulfed with host-derived membranes (called peri-bacteroid membranes) and sealed off into membrane- bound vesicles (called symbiosomes) within the host cytoplasm, where the oxygen tension is reduced by leghemoglobin. The microoxic condition induces expression of genes encoding the nitrogenase and genes essential for microoxic respiration in rhizobia (reviewed in Kaminski *et al*., 1998). At the same time, the bacteria that have been newly released from the infection thread generally divide several times and then cease to divide upon initiation of nitrogen fixation (reviewed in Oke and Long, 1999). At this stage, the bacteria chronically infecting the host cytoplasm are referred to as bacteroids and act like plant organelles, where metabolites from both partners are interchanged (reviewed in Prell and Poole, 2006).

*Sinorhizobium meliloti* induces nodules of an indeterminate type on plants of *Medicago, Melilotus* and *Trigonella* genera (reviewed in Jones *et al*., 2007). In such indeterminate nodules, the bacterial symbionts undergo an even more striking cellular differentiation (Mergaert *et al*., 2006). In the process of the bacteroid development, DNA replication is repeated several times without cell division, resulting in the formation of elongated cells containing up to 24 copies of the genome. Fully differentiated bacteroids possess permeabilized cell envelopes and lose their ability to resume growth (Kobayashi *et al*., 2001; Mergaert *et al*., 2006). Although genes required for the symbiotic chronic infection have been actively studied in *S. meliloti* (reviewed in Jones *et al*., 2007; Gibson *et al*., 2008), the mechanism(s) governing the differentiation processes is largely unknown.

In several bacterial species, regulated proteolysis by ClpXP has been shown to control vital cellular processes (reviewed in Dougan *et al*., 2002; Jenal and Hengge- Aronis, 2003), including cell division (Jenal and Fuchs, 1998), cell differentiation (Liu *et al*., 1999) and nitrogen fixation (Rodriguez *et al*., 2006). ClpXP is an AAA+ pro- tease, which is composed of the ClpX ATPase and the ClpP peptidase (reviewed in Sauer *et al*., 2004; Baker and Sauer, 2006). Substrates are initially recognized by ClpX and are subsequently unfolded and transferred to ClpP for degradation. In *Caulobacter crescentus*, a non-symbiotic member of α-proteobacteria, ClpXP proteolytically modulates the cellular level of CtrA (Jenal and Fuchs, 1998; Gorbatyuk and Marczynski, 2005; McGrath *et al*., 2006; Chien *et al*., 2007), an essential response regulator that regulates DNA replication and cell division (collectively, the progression of the cell cycle) (Quon *et al*., 1996; 1998; Laub *et al*., 2000; 2002). At least partially due to this role, ClpXP is essential for

viability in *C. crescentus* (Jenal and Fuchs, 1998). *C. crescentus* shares several regulatory components (such as CtrA) involved in cell cycle progression and differentiation with *S. meliloti* and its pathogenic relative *Brucella* species (Barnett *et al*., 2001; Bellefontaine *et al*., 2002; Hallez *et al*., 2004). It is therefore plausible that the ClpXP-mediated proteolysis might play a critical role in *S. meliloti* and its chronic infection.

Interestingly, during *C. crescentus* cell cycle, ClpXP dynamically localizes to the cell pole and the cell-division plane, providing temporal and spatial specificity to the proteolysis of substrates (McGrath *et al*., 2006). The proper localization of ClpXP is directed by another response regulator CpdR, which physically interacts with ClpXP, and is dependent on the phosphorylation state of CpdR (Iniesta *et al*., 2006). When CpdR is unphosphorylated, it localizes to the cell pole, thereby mediating ClpXP localization to the cell pole. When CpdR is phosphorylated, it and ClpXP are not localized to the cell pole and consequently CtrA is not degraded. The phosphorylation (thus, inactivation) of CpdR is mediated by the CckA- ChpT phosphorelay, in which the histidine kinase CckA phosphorylates the histidine phosphotransferase ChpT, which in turn phosphorylates CpdR (Biondi *et al*., 2006). The same phosphorelay also phosphorylates CtrA, which is in this case activated by the phosphorylation. Thus, CpdR mediates the fine-tuning of the cell cycle progression in *C. crescentus* by modulating the ClpXP-mediated proteolysis of CtrA (Biondi *et al*., 2006; Iniesta *et al*., 2006; Iniesta and Shapiro, 2008).

In this report, we investigated the role of CpdR in *S. meliloti* and present the first indication that proteolytic regulation and cell cycle progression is critical for the chronic intracellular infection. The *S. meliloti* chromosome

encodes two *cpdR* homologues (SMc04044 and SMc00720), designated *cpdR1* and *cpdR2*. SMc04044 and SMc00720 do not appear to be in operons containing other open reading frames (ORFs) (a tRNA-Val gene is located 285 bp downstream of SMc04044 and the insertion sequence ISRm22 is located downstream of SMc00720 in the opposite direction). Putative single domain-response regulators encoded by *cpdR1* and *cpdR2* share 61% and 46% amino-acid sequence identity with the CpdR protein of *C*. *crescentus* in the two pairwise comparisons, respectively, and share 42% amino-acid sequence identity with each other. We found that both *cpdR* homologues could be disrupted, while the *clpX* homologue was essential in *S*. *meliloti*. Only the *cpdR1* mutant was symbiotically defective. Our examination of these mutants revealed that CpdR1 function is required for proper morphogenesis in free-living cells and for differentiation into bacteroids. We also found that CpdR1 functions to couple DNA replication to cell division in *S*. *meliloti*. In contrast to the *C*. *crescentus cpdR* mutant, which is poised at the G1 phase of the cell cycle, the *S. meliloti cpdR1* mutant accumulates more than two copies of genomic DNA, demonstrating the plasticity of this regulatory network among α-proteobacteria. Thus, in *S*. *meliloti*, cell division in the free-living stage and the bacteroid differentiation are controlled, in part, by CpdR1.

**Results**

**Expression profiles of *cpdR* and *clpX* homologues in free-living and *in planta* cells of *S. meliloti*.** To examine the role of the CpdR homologues in *S*. *meliloti*, we first determined their transcriptional expression during free-living growth and symbiosis. We also compared the expression profiles of the *cpdR* homologues and *clpX* by measuring their transcriptional expression in parallel.

Chromosomal loci of *cpdR* genes (*cpdR1* and *cpdR2*) and *clpX* were transcriptionally fused with *uidA* by inserting pJH104, an integration vector carrying promoter-less *uidA* (for *cpdR1* and *cpdR2*) (Ferguson *et al*., 2005) or a *uidA*-Nmr cassette (for *clpX*) (Metcalf and Wanner, 1993), downstream of each ORF (ATG of *uidA* were located 23, 23 and 59 bp downstream of the stop codons of *cpdR1*, *cpdR2* and *clpX* respectively), yielding strains Rm1021*cpdR1uidA*, Rm1021*cpdR2uidA* and Rm1021*clpXuidA*.

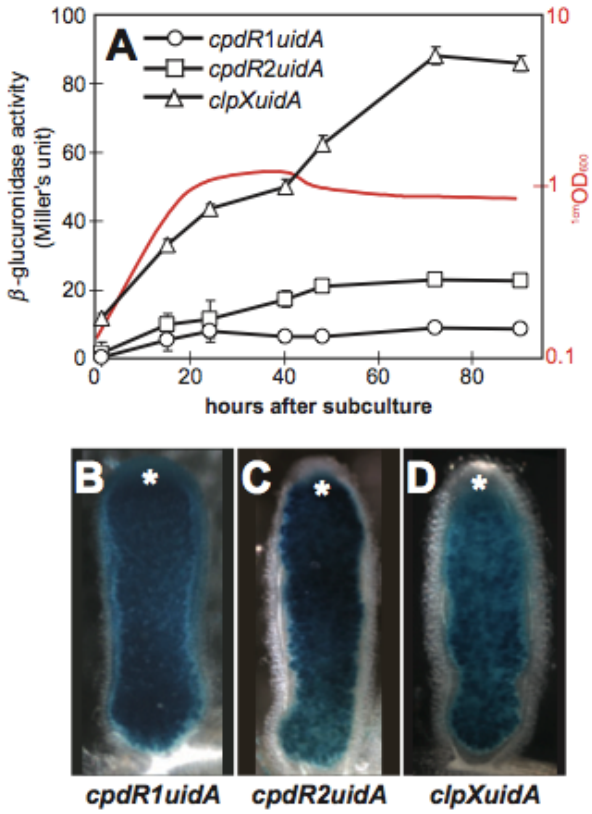


**Figure 1**. Expression of *S. meliloti cpdR* and *clpX* homologues in free-living cells and bacteroids. A. The levels of β-glucuronidase activity (given in Miller's units) for the transcriptional level of *cpdR1*, *cpdR2* and *clpX* transcriptionally fused to *uidA* respectively. The wild-type Rm1021 showed no β-glucuronidase activity (data not shown). Assays were performed at 1, 16, 24, 40, 48, 72 and 90 h after subculture. The values reported represent the means of three independent experiments with standard errors (error bars). A growth curve of a representative strain (monitored by $OD_{600}$) is also shown (red curves). B–D. Histochemical localization of b-glucuronidase activity in nodule hand-sections. Nodules were harvested from alfalfa plants infected with *S. meliloti* strains used in (A). β-Glucuronidase activity was visualized as blue precipitates of the chromogenic substrate 5-bromo-4-chloro-3-indolyl glucuronide (X-Gluc). A total of 30–40 nodules from five plants were examined for each fusion. The meristematic zone of nodule is marked with white asterisks.

To measure expression in the free-living state, exponentially growing cells were inoculated into fresh M9 minimal media and β-glucuronidase activities of *S. meliloti* strains were monitored 1, 16, 24, 40, 48, 72 and 90 h post subculture (Fig. 1A). Both *cpdR1* and *cpdR2* fusions were expressed weakly throughout the growth phases. On the other hand, the expression of the *clpX* fusion was enhanced when cells entered stationary phase.

In order to study gene expression during symbiosis, nodules elicited on alfalfa by the strains carrying *uidA* fusions were sectioned and stained for β -glucuronidase activity (Fig. 1B and C). *S. meliloti* induces formation of indeterminate-type nodules with persistent meristems (which are marked with asterisks in Fig. 1B–D). Expression of *clpX* and the *cpdR* fusions occurs throughout the nodule. This is consistent with the possibility that the CpdR proteins as well as ClpX are present throughout symbiotic development and could potentially play a role in multiple stages of symbiosis.

**CpdR1 localizes to cell poles.** Since our assay with *uidA*-transcriptional fusions indicated that two *cpdR* homologues are transcribed (albeit at a low level) in *S. meliloti*, we asked if both of the CpdR proteins share the same function with *C. crescentus* CpdR; localization to the cell pole and recruitment of ClpXP. To this end, localization of CpdR1 and CpdR2 was examined. We fused *yfpmut2A206K* (encoding a monomeric derivative of YFP, and referred to herein as *yfp*) to *cpdR1* and *cpdR2* under the control of their native promoters on the low-copy vector pTH1227 (Cheng *et al*., 2007). Resulting plasmids, p-*cpdR1–yfp* and p-*cpdR2– yfp*, carrying *cpdR–yfp* fusion genes were introduced into the wild-type *S. meliloti* strain Rm1021.

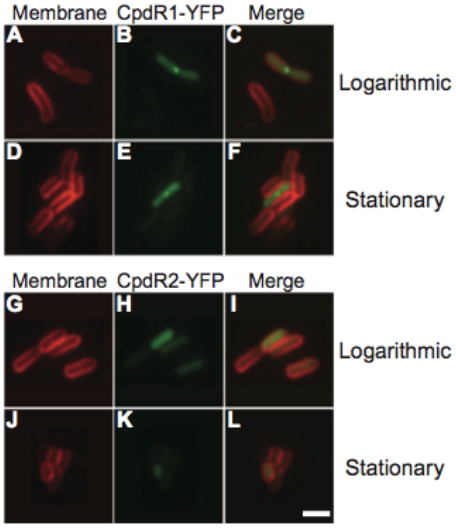


**Figure 2.** Subcellular localization of CpdR1 and CpdR2 in free-living *S. meliloti* cells. Subcellular localization of CpdR1–YFP (A–F) and CpdR2–YFP (G–L) fusion proteins in free-living *S. meliloti* by epi-fluorescence microscopy. *S. meliloti* strains carrying fusion genes were grown in M9 medium supplemented with succinate. Cells were examined in the logarithmic phase (A–C and G–I) or the stationary phase (D–F and J–L). Localization of YFP fusion proteins was visualized in living cells as represented in green (B, E, H and K). The cell membrane was stained by FM4-64 as represented in red (A, D, G and J). Epi-fluorescence views of different filters were merged to analyse relative localization (C, F, I and L). No focus was observed in cells of the wild-type *S. meliloti* strain Rm1021 (data not shown). Scale bar represents 2 μm.

In the log-phase cells, a single CpdR1–YFP focus was visible above the background fluorescence in ~6% of cells ($n$ = 1399) (Fig. 2A–C; Table 1). In *C. crescentus*, it has been reported that the CpdR focus only appears at particular stages of the cell cycle (the swarmer-to-stalked cell transition and the predivisional stage) (Iniesta *etal*., 2006). Since the *S. meliloti* cultures were not synchronized, it is reasonable to speculate that the cultures consisted of a heterogeneous cell population, where ~6% of cells were at the cell cycle stage(s) specific for polar localization of CpdR1. The formation of CpdR1–YFP foci was also observed in ~5% ($n$ = 1273) of cells in stationary phase, although the YFP foci signal was faint compared with the foci intensity of cells in log phase (Fig. 2D–F; Table 1). Of the foci that formed, ~100% ($n$ = 245) of the CpdR1–YFP foci were localized at the cell poles and we did not detect any cells with more than one focus (this is similar to *C. crescentus*) (Table 1).

**Table 1.** Formation of CpdR–YFP foci in *S. meliloti* Rm1021.

| | Growth phase | No. of cells | % of cells with *n* foci | | |
|---|---|---|---|---|---|
| | | | 0 | 1 | 2 ≤ |
| CpdR1–YFP | Logarithmic | 1399 | 94 | 6 | ND |
| | Stationary | 1273 | 95 | 5 | ND |
| CpdR2–YFP | Logarithmic | 534 | 100 | ND | ND |
| | Stationary | 561 | 99 | < 1 | ND |

ND, not detected.

We also investigated the localization of CpdR2–YFP in *S. meliloti.* We found that the formation of CpdR2–YFP foci was observed in only a small subpopulation of stationary-phase cells (~0.4% of cells, $n$ = 561; Table 2). In both log- and stationary-phase cultures, some of cells have brighter CpdR2–YFP signals throughout the cell than other cells (Fig. 2G–L). It should be noted that each YFP fusion was transcribed from the native promoters of *cpdR1* and *cpdR2*, respectively, supporting our results with *uidA* fusions, showing that *cpdR1* and

*cpdR2* were expressed throughout the growth phases. The active localization of CpdR1 to cell poles suggested that CpdR1 shares a similar function with *C. crescentus* CpdR, while the significance of CpdR2 localization remains unclear.

**Table 2.** Formation of highly branched cells in *S. meliloti* Rm1021 strains.

| Strains | No. of cells | % of cells with morphology | | |
|---|---|---|---|---|
| | | Rod | Elongated | Highly branched |
| Rm1021(pTH1227) | 413 | 99 | < 1 | ND |
| Rm1021*minCDE*⁻(pTH1227) | 453 | 99 | < 1 | ND |
| Rm1021(p-*cpdR1*D53A) | 551 | 82 | 12 | 6 |
| Rm1021*minCDE*⁻(p-*cpdR1*D53A) | 405 | 90 | 10 | ND |

'rod', 1–3 μm rod-shape with two poles; 'elongated', cells longer than 4 μm with two to three poles; 'highly branched', cells with more than three poles.
ND, not detected.

***S. meliloti cpdR1* and *cpdR2* are not essential, while *clpX* provides an essential function.** To further examine the function of *cpdR1* and *cpdR2* in *S.meliloti*, both were disrupted by inserting a spectinomycin/streptomycin resistance gene (for *cpdR1*) (Fellay *et al*., 1987) or a *uidA*-Cm$^r$ cassette (for *cpdR2*) (Metcalf and Wanner, 1993), generating strains Rm1021Ω*cpdR1* and Rm1021*cpdR2*::*uidA*. The *cpdR1*- null mutant grew much slower than the parental strain, while the growth of the *cpdR2*-null mutant was virtually indistinguishable from that of the parental strain (data not shown). This further supports the idea that the two *cpdR* homologues have non-identical roles in *S. meliloti*. In addition, we found that *clpX* is essential for viability of *S. meliloti*, as is the case for *C. crescentus* (Jenal and Fuchs, 1998). We attempted to generate a *clpX*-null allele in *S. meliloti*. The plasmid, pJQ-*clpX*$^-$, a suicide vector pJQ200-SK (Quandt and Hynes, 1993) derivative, in which the *clpX* ORF was disrupted by insertion of a neomycin resistance (Nm$^r$) marker (Fellay *et al*., 1987), was integrated into the chromosomal *clpX* locus by single cross-over. Counter-selection for the double cross-over in the resulting strain was performed with derivatives that contained either a plasmid carrying the functional copy of *clpX*

(p-*clpX*$^{+}$) or the empty vector pTH1227. The disruption of chromosomal *clpX* occurred only in the presence of p-*clpX*$^{+}$ (data not shown), indicating that *clpX* encodes an essential function in *S. meliloti*. Similar procedures were employed to show that *ctrA* and *ccrM*, genes encoding proteins critical for cell cycle progression, are also essential in *S. meliloti* (Wright *et al*., 1997; Barnett *et al*., 2001). We conclude that CpdR1 has an important role during the free-living growth of *S. meliloti* and that *clpX* is essential under the growth conditions examined in this study. We speculate that the role of CpdR in free-living *S. meliloti* likely involves the regulation of ClpXP protease as reported for *C. crescentus* CpdR (Iniesta *et al*., 2006).

**CpdR1 is critical for the bacteroid differentiation.** To test whether the *cpdR* homologues are important for symbiosis, alfalfa seedlings were inoculated with the *cpdR1*- or *cpdR2*-null mutants. Four weeks post inoculation, alfalfa plants infected with the wild-type grew to a shoot length of 11.4 ± 0.3 cm with pink-coloured and elongated nodules on the roots (Fig. 3A). In contrast, plants inoculated with the *cpdR1*-null mutant appeared to be starved of nitrogen, having short shoots (2.9 ± 0.1 cm) with yellowed leaves (Fig. 3A). Nodules induced by the *cpdR1*-null mutant were white-coloured, small and non-elongated globular shape. The size and appearance of the shoots of the plants were indistinguishable from those of the mock-inoculated plants, which had no nodules on their roots. This could indicate that the nodules induced by the *cpdR1*-null mutant lacked nitrogen-fixing activity (Fig.3A). No significant difference was observed in nodule number or in plant growth between plants infected with the wild-type and the *cpdR2*-null mutant (Fig. 3A).

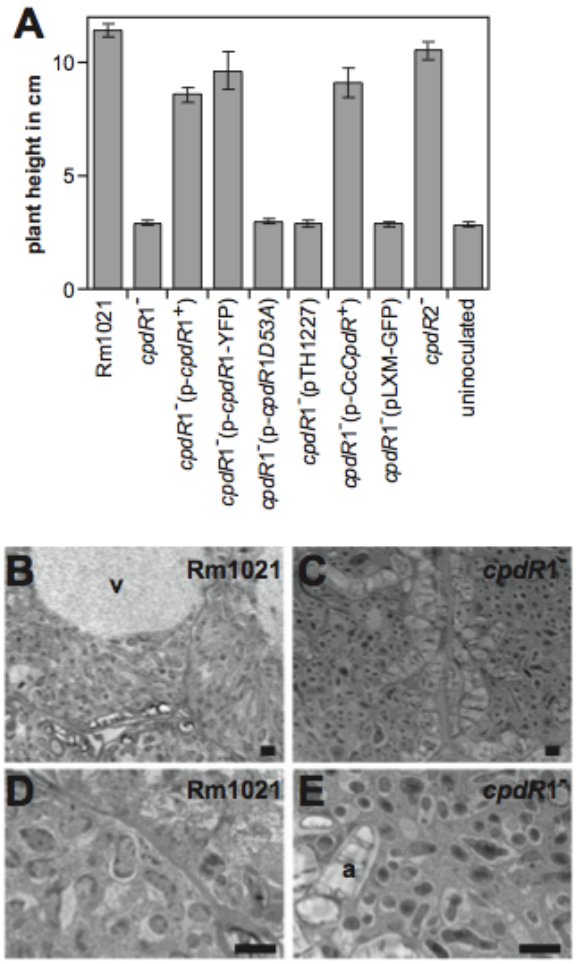


**Figure 3.** CpdR1 is critical for symbiosis between *S. meliloti* and alfalfa. A. The *cpdR1*-null mutant elicits ineffective nodules on alfalfa roots. The symbiotic defect can be complemented by plasmid-born *cpdR1*$^{+}$, the *cpdR1–yfpmut2* fusion gene and *C. crescentus cpdR* but not by *cpdR1D53A* or vector controls (pTH1227 and pLXM-GFP). The disruption of *cpdR2* has neither a positive nor a negative effect on growth of plants relative to that of the wild-type *S. meliloti* strain Rm1021. Growth of alfalfa plants were examined 4 weeks after inoculation. The plant heights are the lengths of shoots (cm). Error bars indicate standard errors. At least 20 plants were examined for each strain. B–E. In nodules elicited by the wild-type *S. meliloti* strain Rm1021 viewed by transmission electron microscopy (B and D), cells from the nitrogen fixing zone are packed with bacteroids and contained a large central vacuole (v). Nodules elicited by the *cpdR1*-null mutant (C and E) contain plant cells filled with bacteria of irregular-coccoid morphology and have large amyloplasts (a). Scale bars represent 2 μm.

A more striking phenotype of the *cpdR1*-null mutant was observed by electron microscopy. Figure 3B and D shows a plant cell from the nitrogen-fixing zone of a nodule containing the wild-type *S. meliloti* strain Rm1021. These bacteroids generally have elongated or Y-shaped morphology and are 5–10 times longer than the free-living cells. Figure 3C and E shows the corresponding region of a nodule containing the *cpdR1*-null mutant. The host cells contain numerous intracellular bacteria, indicating that the *cpdR1*-null mutant is not especially impaired in the early stages of nodule invasion through the root hair or in invading the cytoplasm of the host cell. However, the morphology of these intracellular bacteria is diverse. Although some cells are abnormally enlarged, most of the bacteria appear to be highly irregular spherically shaped (coccoid) cells much smaller than the bacteroids of the wild-type *S. meliloti* Rm1021 and

have refractory cytoplasm indicative of aborting bacteroids (Campbell *et al*., 2002). The host cells also contained large amyloplasts. Amyloplasts are starch deposits that are normally present in nodule cells early in development and are absorbed upon *S. meliloti* infection of alfalfa. Thus, in *S. meliloti*, CpdR1 is critical for establishing the chronic intracellular infection, particularly, at the stage of bacteroid differentiation.

The symbiotic deficiency of the *cpdR1*-null mutant was fully complemented by p-*cpdR1*$^{+}$, a plasmid carrying the wild-type *cpdR1*$^{+}$, and also by p-*cpdR1–yfp*, but not by the empty vector pTH1227. In *C. crescentus*, it has been shown that the activity of CpdR is regulated by phosphorylation (Iniesta *et al*., 2006). Only the unphosphorylated CpdR localizes to the cell pole and is capable of directing the polar localization of ClpXP. To understand the role of CpdR phosphorylation status in symbiosis, we generated an allele of *cpdR1*, *cpdR1D53A*, which codes for an alanine at position 53 instead of the conserved aspartic acid. In *C.crescentus*, CpdRD51A, the analogue of *S. meliloti* CpdR1D53A, was shown to prevent phosphorylation of the protein, resulting in a constitutively active form that directs ClpXP to the cell pole throughout the cell cycle (Iniesta *et al*., 2006). Introduction of the *cpdR1D53A* allele did not restore the symbiotic deficiency of the *cpdR1*-null mutant (Fig. 3A), indicating that the fine-tuning of CpdR1 phosphorylation status is important for symbiosis. Heterologous expression of *C. crescentus cpdR* in the *S. meliloti cpdR1*-null background complements the symbiotic deficiency as well as the growth defect of the free-living cells, indicating that the CpdR function is conserved between *S.meliloti* and *C. crescentus*. We conclude that *S. meliloti* CpdR1 phosphorylation is critical for its function and that *C. crescentus cpdR* can complement the *S.*

*meliloti cpdR1* defect indicating a conserved role of CpdR among α-proteobacteria.

**CpdR1 is required for proper morphogenesis of *S. meliloti.*** The abnormal morphology of the intracellular cells of the *cpdR1*-null mutant in alfalfa led us to examine the cell morphology in the free-living stage. As free-living cells, the wild-type *S. meliloti* are rod shaped (Fig. 4A). Strikingly, free-living cells of the *cpdR1*-null mutant are highly irregular swollen or coccoid shape with the size generally three to four times larger than the size of wild- type *S. meliloti* cells (Fig. 4B). Some cells were further enlarged and branched with single or multiple asymmetric septa (data not shown). The morphology, and the size of the free-living cells of the *cpdR1*-null mutant, was similar to those of the *in planta* intracellular cells. This suggests that the *cpdR1*-null mutant could not initiate the differentiation process into bacteroid form. Introduction of the wild-type *cpdR1*$^{+}$ to the *cpdR1*-null mutant restored normal morphology (Fig. 4C), while introduction of the *C. crescentus cpdR* only partially rescued the morphological defect (Fig. 4D). The *S. meliloti cpdR1*-null mutant expressing *C.crescentus* CpdR appeared to be rod shaped with, occasionally, single or multiple small branches (Fig. 4D). Introduction of the *cpdR1D53A* allele into the *cpdR1*-null mutant failed to rescue the morphology of the mutant and exacerbated slow growth phenotype (Fig. 4F; data not shown). Moreover, expression of *cpdR1D53A* in the wild-type *S. meliloti* Rm1021 transformed ~6% ($n$ = 551) of the cells into highly branched cells with more than three poles (Fig. 4G; Table 2). Such cells were not detected in the wild-type *S. meliloti* carrying the empty vector ($n$ = 413) or in the wild-type *S. meliloti* alone (Table 2). Thus, CpdR1 function is critical for the proper morphogenesis during both free-living growth and during bacteroid

differentiation. The morphology of the *cpdR2*-null mutant was indistinguishable from the wild- type *S. meliloti* Rm1021 (Fig. 4E), indicating that *cpdR2* is not important for cell morphogenesis in the free-living form.

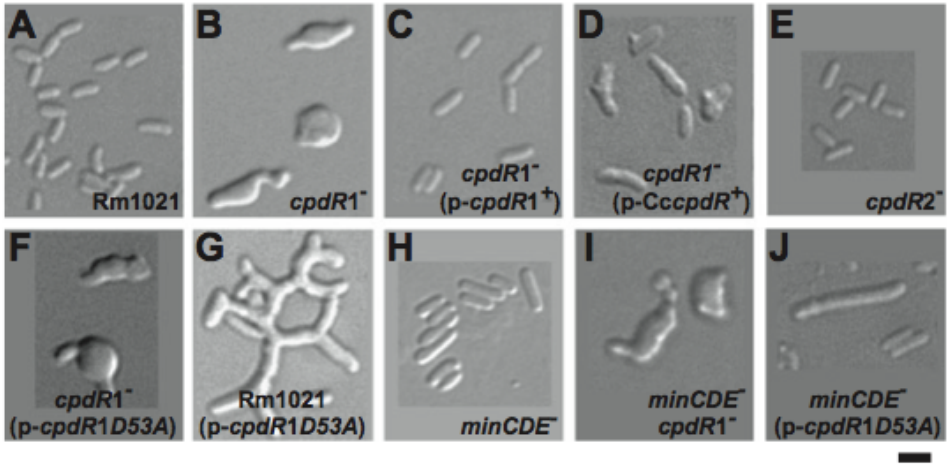


**Figure 4.** Cell morphology of *S. meliloti* strains. DIC view of the wild-type *S. meliloti* stain Rm1021 (A), the *cpdR1*-null mutant (B), the *cpdR1*-null mutant carrying p-*cpdR1*$^{+}$ (C) or p-C*cpdR*$^{+}$ (D), the *cpdR2*-null mutant (E), the *cpdR1*-null mutant (F) or the wild-type strain (G) carrying p-*cpdR1D53A*, the *minCDE*-null mutant (H), the *minCDEcpdR1* double mutant (I) and the *minCDE*-null mutant carrying p-*cpdR1D53A* (J). Cells were grown in LBMC medium to logarithmic phase and processed for DIC microscopy. Scale bars represent 2 μm.

**The morphological phenotype caused by CpdR1D53A is Min dependent.**

During the examination of morphology of free-living cells, we noticed that the morphology of the *cpdR1*-null mutant is similar to the morphology of the *minE*-disrupted mutant of *S. meliloti* (Cheng *et al*., 2007). The MinE protein forms, together with MinC and MinD, the Min cell-division inhibitor system. The Min system is well studied in *Escherichia coli*, where it directs cell division to the mid-cell by negatively regulating the formation of the Z ring (reviewed in Margolin, 2005). MinC is the inhibitor of Z-ring formation, which is recruited to the membrane by MinD and induced to oscillate by MinE. Although the *minE* single mutant shows a morphological defect, the *minCDE* triple mutant has wild-type morphology in *S. meliloti*, indicating that the phenotype of the *minE* mutant is likely due to the non- specific action of MinC and MinD (Cheng *et al*., 2007; Fig.

4H; Table 2). Overexpression of MinD or MinCDE in *S. meliloti* generates highly branched cells (Cheng *et al*., 2007), which is also similar to the morphology we observe with *S. meliloti* Rm1021 expressing CpdR1D53A (Fig. 4G). The similarity in morphology between the *cpdR1*-null mutant and the *minE*-null mutant, as well as between the CpdR1D53A-expressing strain and Min-overexpressing strains, led us to hypothesize that *cpdR* affects proper activity of the Min system. To test this hypothesis, *minCDE* were disrupted in the *cpdR1*-null and *cpdR1D53A* backgrounds. Disruption of *minCDE* did not restore the morphology of the *cpdR1*-null mutant (Fig. 4I), indicating that the morphological defect of the *cpdR1*-null mutant is independent of the Min system. However, when *minCDE* was disrupted in *S. meliloti* Rm1021(p-*cpdR1D53A*), highly branched cell (with more than three poles) was not detected any longer, while elongated cells (with two or three poles) were still observed (Fig. 4J; Table 2). Thus, the morphogenesis of highly branched cells by CpdR1D53A appears to depend, in part, on the Min system.

**CpdR1 affects the formation of ClpX–YFP foci.** *Caulobacter crescentus cpdR* can partially complement the *S. meliloti cpdR1*-null mutant, suggesting that the molecular function is conserved for both gene products. In *C. crescentus*, the role of CpdR in directing ClpX to the cell pole has been demonstrated (Iniesta *et al*., 2006). To examine the role of CpdR1 in the ClpX localization, we fused *yfp* to the genomic copy of *clpX* in *S. meliloti*. The strain, Rm1021*clpX-yfp*, which carries the *clpX-yfp* fusion gene as the only copy of *clpX*, is viable. The growth rate and the cell morphology of the *clpX-yfp* strain was indistinguishable from the wild-type *S. meliloti* strain Rm1021, indicating that the ClpX–YFP fusion protein is functional. In logarithmic-phase growth, ~9% ($n$ = 1005) of cells had one focus of ClpX–YFP

visible above the background fluorescence (Fig.5A–C; Table3). In stationary-phase cells, ClpX–YFP foci formed in ~88% (*n* = 594) of cells (Fig. 5D–F; Table 3). Most of the cells containing ClpX– YFP foci had one focus per cell (Table 3). This observation is interesting, since CpdR1–YFP foci were observed in ~5% (*n* = 1273) of cells in stationary phase (Table 1). Thus, in stationary-phase cells, most of the population of cells with ClpX–YFP foci do not correspond to the population of cells with CpdR1–YFP foci. In both growth phases, ClpX–YFP foci were preferentially formed at the cell poles. We found that ~78% (*n*=134) and ~97% (*n*=150) of ClpX–YFP foci were located at the poles in logarithmic- and stationary-phase cells respectively (Table S2). Interestingly, ClpX–YFP foci were observed in less than ~1% of mature bacteroids (*n* = 579). Taken together, these observations indicate that ClpX–YFP foci formation is growth-phase regulated.

**Table 3.** Growth phase-dependent formation of ClpX–YFP foci in *S. meliloti* strains.

| *S. meliloti* strain | Growth phase | No. of cells | Percentage of cells with *n* foci | | |
|---|---|---|---|---|---|
| | | | 0 | 1 | 2 ≤ |
| Rm1021 | Logarithmic | 1005 | 90 | 9 | 1 |
| | Stationary | 594 | 12 | 84 | 4 |
| | Bacteroid | 579 | 99 | 1 | ND |
| Rm1021 *cpdR1*ΩSp$^r$ | Logarithmic | 545 | 94 | 5 | < 1 |
| | Stationary | 1004 | 88 | 11 | < 1 |
| Rm1021 *cpdR2*::*uidA*-Cm$^r$ | Logarithmic | 938 | 91 | 8 | < 1 |
| | Stationary | 869 | 21 | 76 | 3 |
| Rm1021(p-*cpdR1*D53A) | Logarithmic | 798 | 91 | 8 | 1 |
| Rm1021(p-*cpdR2*D52A) | Logarithmic | 677 | 88 | 11 | 1 |

To assess the role of two CpdR homologues in directing ClpX to the cell pole, the localization of ClpX–YFP was examined in the *cpdR1*- and *cpdR2*-null mutants. Compared with the wild-type, a smaller population of the *cpdR1*-null cells showed ClpX–YFP foci (Fig. 5J–O; Table 3). We found that the percentage of stationary- phase cells with ClpX–YFP foci was reduced approximately eightfold in the *cpdR1*-null mutant (Table 3). In *C. crescentus*, it has been reported that ClpX localization to the cell-division plane is independent of CpdR function

(Iniesta *et al*., 2006). It has to be noted that, since we cannot distinguish the cell-division plane of *S. meliloti* (it is difficult to determine by DIC microscopy whether two proximal cells are currently dividing or just placed side by side), we can only score the location of foci as 'polar' when they are located at the fully formed pole of a cell (Table S2). The decreased formation of ClpX foci in the *cpdR1*-null mutant further supports the hypothesis that CpdR1 plays a conserved role in the polar localization of ClpX in *S. meliloti*. We could not score the location of ClpX foci in the *cpdR1*-null mutant, because the 'poles' were not obvious in the irregular coccoid cells. In the *cpdR1*- null mutant, we also noticed that the foci intensity of ClpX–YFP was reduced relative to that of the foci formed in the wild-type background. In the wild-type background, ClpX–YFP foci were readily captured by an exposure for 240 ms, while an exposure of 6000 ms was necessary to capture distinct foci in the *cpdR1*-null mutant. This observation suggests that the loss of CpdR1 function pleiotropically affects the ClpX expression and/or the accumulation of ClpX–YFP at the cell poles.

We also examined the effect of CpdR1D53A on ClpX localization in *S. meliloti*. In the wild-type *S. meliloti* Rm1021 expressing CpdR1D53A, cell morphologies are abnormal (see Fig. 4G), but the formation and the localization of ClpX–YFP foci nonetheless showed common features with background Rm1021: a minority of cells formed a ClpX focus, and of those that did, the foci were at cell poles (Fig. 5P–R). These observations differ from results in *C. crescentus* (Iniesta *et al*., 2006), where the expression of CpdRD51A resulted in ~100% polar localization of ClpX foci. This difference is probably because we expressed plasmid-born *cpdR1D53A* under the control of a *tac* promoter in the wild-type *S. meliloti* Rm1021, where the wild-type *cpdR* gene is also present. In

the *C. crescentus* strain, however, *cpdRD51A* replaces the wild-type *cpdR* locus and was expressed from the native *cpdR* promoter (Iniesta *et al*., 2006). We did not examine localization of ClpX–YFP in the *cpdR1*-null mutant expressing CpdR1D53A, since the morphology of the cells was severely defective (data not shown). In the *cpdR2*-null mutant or the wild-type *S. meliloti* expressing CpdR2D53A, cells formed ClpX–YFP foci of intensity indistinguishable from the foci in wild-type cells, although the population of cells with ClpX–YFP foci was slightly affected compared with the wild-type *S. meliloti* background (Table 3). We conclude that CpdR1 is important for proper subcellular localization of ClpX–YFP in *S. meliloti*.

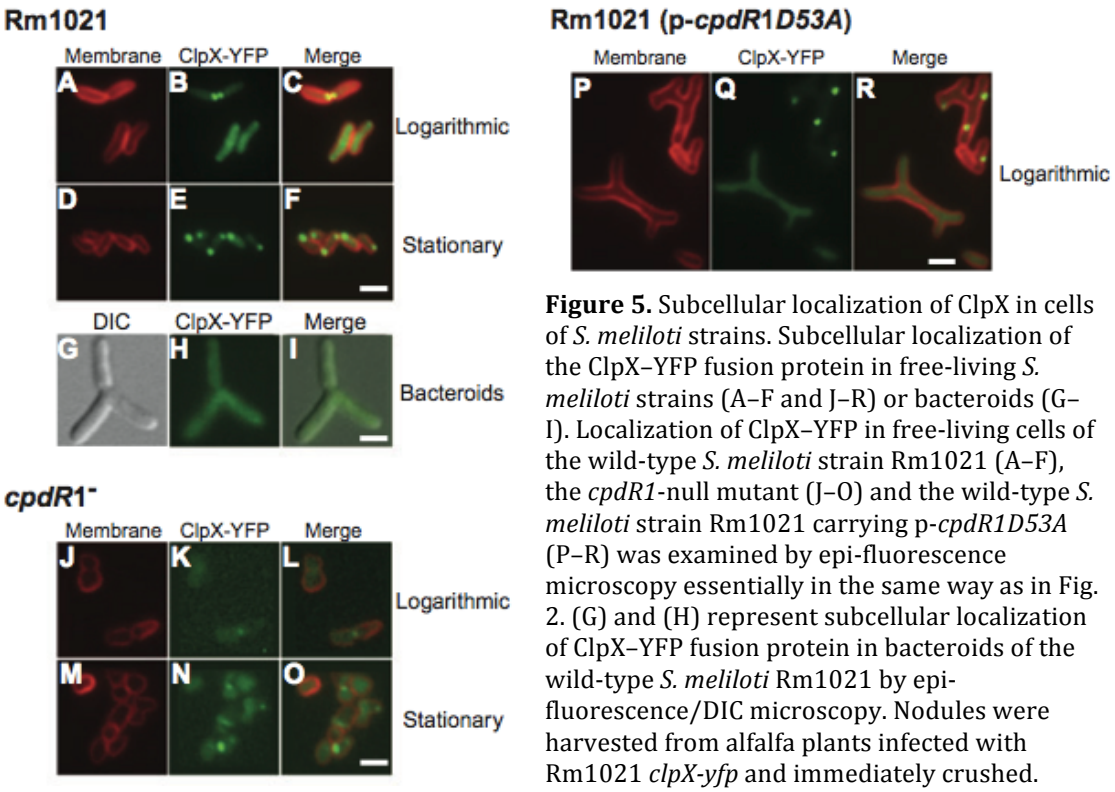


**Figure 5.** Subcellular localization of ClpX in cells of *S. meliloti* strains. Subcellular localization of the ClpX–YFP fusion protein in free-living *S. meliloti* strains (A–F and J–R) or bacteroids (G–I). Localization of ClpX–YFP in free-living cells of the wild-type *S. meliloti* strain Rm1021 (A–F), the *cpdR1*-null mutant (J–O) and the wild-type *S. meliloti* strain Rm1021 carrying p-*cpdR1D53A* (P–R) was examined by epi-fluorescence microscopy essentially in the same way as in Fig. 2. (G) and (H) represent subcellular localization of ClpX–YFP fusion protein in bacteroids of the wild-type *S. meliloti* Rm1021 by epi-fluorescence/DIC microscopy. Nodules were harvested from alfalfa plants infected with Rm1021 *clpX-yfp* and immediately crushed. Long, blanched bacteroid cells were visually distinguished from non-differentiated *S. meliloti* cells or plant-derived materials (G). In contrast to the free-living cells, the membrane of bacteroids could not be stained by FM4-64 (data not shown). Localization of ClpX–YFP was visualized in bacteroids as represented in green (H). Epi-fluorescence view and DIC view were merged to analyse relative localization (I). Scale bars represent 2 μm.

**CpdR1 functions to co-ordinate initiation of DNA replication with cell cycle progression.** In *S. meliloti*, it has been shown that the larger cell volume correlates with the polyploid state of the cell (Mergaert *et al*., 2006). The enlarged cell volume of the *cpdR1*-null mutant led us to examine the DNA content of *S. meliloti* cells. Flow cytometry is a well-established tool for studying the cell cycle in synchronized cultures of *C. crescentus* (Winzeler and Shapiro, 1995). It has also been used in *S. meliloti* to examine the state of chromosomal replication in cell populations (Wright *et al*., 1997; Mergaert *et al*., 2006). As reported previously (Mergaert *et al*., 2006), in the wild-type *S. meliloti* strain Rm1021, DNA content distribution of an exponentially growing cell population is composed of two peaks (Fig. 6A). The first (left) peak indicates the number of cells with 1C DNA content (marked with blue-dotted line). The second peak is positioned around twice the relative fluorescence intensity of the first peak and represents the cells with 2C DNA content (marked with red-dotted line). In the *cpdR1*-null mutant, one broad peak representing cells with more than one genome (mainly 2~5C) equivalents were observed (Fig. 6B), indicating that most cells had multiple copies of the genome. Thus, in the *cpdR1*-null mutant, aberrant DNA replication uncoupled from cell division seems to have occurred. Introduction of the wild-type *cpdR1*+ restored proper progression of cell cycle in the *cpdR1*-null mutant (Fig. 6C). The profile of DNA content distribution of the *cpdR1*-null mutant expressing *C. crescentus* CpdR was similar to the profile in the wild-type, although the population with 2C DNA content was larger than the population with 1C DNA content (Fig. 6D).

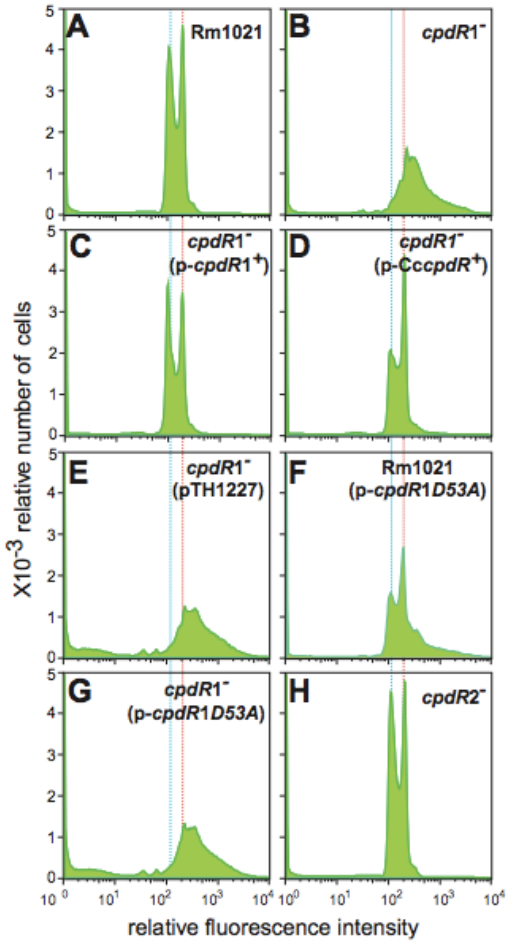


**Figure 6.** Flow cytometry analyses of *S. meliloti* strains. The DNA contents of *S. meliloti* strains were measured in a population of 50 000 cells with a Becton Dickinson FACScan machine at 530 nm. Relative cell number (*y*-axis) is plotted against the Cytox Green fluorescence signal (arbitrary units). 1C and 2C of the genome equivalents were marked with blue- and red-dotted lines respectively.

This observation, together with the partially rescued morphology of the *S.meliloti cpdR1*-null mutant by *C. crescentus cpdR*, suggests that *C. crescentus* CpdR is partially functional in *S. meliloti*. *C. crescentus* CpdR likely has a different affinity for *S. meliloti* ChpT and ClpX, causing a slight perturbation in progression of the *S. meliloti* cell cycle. In the wild-type *S. meliloti* expressing CpdR1D53A, the population with 2C DNA content was also larger than the population with 1C DNA content (Fig. 6F). In this strain, moreover, populations with 2~5C DNA content were also detected, likely corresponding to the cells with elongated or highly branched morphology. The DNA content profile of the *cpdR1*-null mutant expressing CpdR1D53A was indistinguishable from the *cpdR1*-null mutant with the empty vector or the mutant alone (Fig. 6E and G). Thus, expression of CpdR1D53A also causes aberrant cell cycle progression and the effect of

CpdR1D53A expression requires the presence of wild- type *cpdR1*$^{+}$. The *cpdR2*-null mutant showed DNA content profile indistinguishable from the wild-type *S. meliloti* Rm1021 (Fig. 6H). These data suggest that the function of CpdR1 is critical for proper coupling of DNA replication with cell division in *S. meliloti*.

**Discussion**

In this study, we demonstrate that CpdR plays a critical role in *S. meliloti.* In the free-living stage, cells of the *cpdR1*-null mutant showed an irregular coccoid morphology instead of the rod shape of the parental strain. The cells are generally three to four times larger in volume than wild-type cells. In *S. meliloti*, it has been shown that the larger cell volume correlates with the polyploid state of a cell (Mergaert *et al*., 2006). Strikingly, the *cpdR1*-null mutant tends to accumulate higher copies (generally 2∼5C) of genomic DNA. Thus, in *S. meliloti*, the loss of CpdR1 function results in uncoupling between DNA replication and cell division, causing a higher genomic content and enlarged spherical morphology of the mutant cells.

Moreover, we demonstrate that CpdR1 is required for symbiosis between *S. meliloti* and the host plant alfalfa. Upon inoculation in alfalfa, the *cpdR1*-null mutant is capable of inducing the formation of nodules on the root and capable of invading the cytoplasm of nodule cells. However, it appears that nitrogen fixation does not occur in the resulting nodules. In these nodules, the intracellular bacteria remain morphologically similar to the free-living cells of the *cpdR1*-null mutant and do not differentiate into wild-type bacteroids, which are normally larger and elongated. In wild-type *S. meliloti*, elongation of the bacteria during bacteroid maturation is a result of repeated DNA replication without cell division (endoreduplication) (Mer- gaert *et al*., 2006). The inability

of intracellular cells to differentiate into bacteroids indicates that, in the *cpdR1*-null mutant, normal endoreduplication required for bacteroid differentiation is not initiated. Thus, in the *cpdR1*- null mutant, the loss of proper cell cycle control is likely a common cause of both the aberrant morphology in the free-living stage and a defect in bacteroid differentiation. In other words, the same regulatory mechanism involving CpdR1, which couples initiation of DNA replication to cell division in free-living stage, also affects the endoreduplication during bacteroid development.

What is the molecular function of CpdR1 critical for co-ordinating cell cycle progression? In *C. crescentus*, CpdR directs ClpXP complex to the cell pole, thereby mediating regulated proteolysis of ClpXP substrates (Iniesta *et al*., 2006). The cross-species complementation of *S. meliloti* CpdR1 with *C. crescentus* CpdR strongly suggests a conserved role for CpdR homologues between α-proteobacterial species. In agreement with this idea, we observed that loss of CpdR1 function attenuates the polar localization of ClpX–YFP.

It is therefore likely that the phenotype of the *cpdR1*-null mutant is caused by a lack of proper proteolysis by ClpXP. In *C. crescentus*, CtrA is an important substrate of ClpXP (Jenal and Fuchs, 1998; Gorbatyuk and Marczynski, 2005; Chien *et al*., 2007). CtrA controls, directly or indirectly, critical cell cycle regulated genes including those involved in polar morphogenesis, DNA replication initiation, DNA methylation, cell division and cell wall metabolism (Laub *et al*., 2002). CtrA is conserved in *S. meliloti* and it has been shown that *C. crescentus ctrA* can substitute for *S. meliloti ctrA* for viability (Barnett *et al*., 2001). CtrA protein of *S.meliloti* has a conserved ClpX-recognition signal at the C-terminus (Flynn *et al*., 2003; Chien *et al*., 2007), suggesting that CtrA is also a

substrate for ClpXP in *S. meliloti*. Modified abundance of CtrA affects cell cycle progression (Quon *et al*., 1998) and at least partially accounts for aberrant cell cycle progression in the absence of *cpdR1* in *S. meliloti*.

Regarding cell cycle progression, the phenotype of the *cpdR1*-null mutant fundamentally differs in *S. meliloti* from the phenotype reported in the *C. crescentus cpdR*-null mutant. In *C. crescentus*, the *cpdR*-null mutant also showed an aberrant morphology; an abnormal location of the cell-division plane and straight-cell morphology rather than the crescentoid morphology of the wild-type (Iniesta *et al*., 2006). It has also been reported that disruption of *C. crescentus cpdR* results in decreased motility, a longer generation time and, in a subpopulation, elongation of the cell (Skerker *et al*., 2005). In *S. meliloti*, on the other hand, we found that a disruption of *cpdR1* results in significant enlargement of the cell size and spherical cell shape in most of the cells. More importantly, the loss of CpdR function does not cause polyploidy in *C.crescentus* (Duerig *et al*., 2009).

The different phenotypes resulted from loss of CpdR function on DNA replication likely reflects the plasticity of the regulation network involving CtrA in α-proteobacterial species (Hallez *et al*., 2004). In *C. crescentus*, phosphorylated CtrA (CtrA~P) binds to five distinct sites in the origin of replication to repress replication initiation by blocking the access of proteins for DNA replication initiation (Quon *et al*., 1998; Siam and Marczynski, 2000). CpdR directs ClpXP to the pole, where ClpXP degrades the CtrA~P, allowing for de-repression of DNA replication initiation. In the absence of CpdR, the ClpXP protease is not positioned at the pole and, consequently, CtrA~P is not degraded, keeping the replication origin physically blocked and DNA replication initiation

repressed. Yet, CpdR is not essential for viability most likely because CtrA~P could still be inactivated by dephosphorylation.

In *S. meliloti*, on the other hand, no conserved CtrA- binding site has been detected in the replication origin (Hallez *et al*., 2004). In *Brucella abortus*, an intracellular pathogen closely related to *S. meliloti*, the replication origin also lacks a functional CtrA-binding site and was shown not to be bound by *B. abortus* CtrA *in vitro* (Belle- fontaine *et al*., 2002). From these observations, it has been proposed that, in *S. meliloti* and *B. abortus*, DNA replication initiation is not regulated by the binding of CtrA to the replication origin (Bellefontaine *et al*., 2002; Hallez *et al*., 2004). It is therefore likely that, in the absence of CpdR function, the replication origin is available for DNA replication initiation even though CtrA is not proteolytically regulated. In agreement with this model, we found that, in *S. meliloti*, the loss of CpdR1 function does not result in repression of DNA replication initiation and can even provoke DNA replication in an unregulated manner.

We find it likely that genes regulated by CtrA are misregulated by the stabilization of CtrA and at least partially responsible for the aberrant cell cycle progression in the *cpdR1*-null mutant. In *S. meliloti* and *C. crescentus*, it has been reported that overexpression of *ccrM*, a CtrA-target gene encoding a DNA methyltransferase, results in the loss of control of DNA replication and aberrant cell morphology, phenotypes similar to the *cpdR1*-null mutant (Zweiger *et al*., 1994; Wright *et al*., 1996; 1997). Although the accumulation of CcrM protein was not observed in the *C. crescentus cpdR* mutant (Iniesta *et al*., 2006), it is possible that *ccrM* is overexpressed in the *S. meliloti cpdR1* mutant, contributing to its phenotype. In the *S. meliloti* symbiotic plasmid pSymA, putative CtrA-binding

sites have been detected in promoter regions of *repA*2 (Hallez *et al*., 2004), which encodes a putative replication protein A. Unregulated expression of *repA2* could also be the cause of the aberrant DNA replication in the *cpdR1*-null mutant.

In *S. meliloti* and *B. abortus*, two and four CtrA-binding motifs were detected in an upstream region of the *minCDE* operon, respectively, while *minCDE* is absent in *C. crescentus* genome (Bellefontaine *et al*., 2002; Hallez *et al*., 2004; Cheng *et al*., 2007). When CpdR1D53A, the constitutively active variant of CpdR1, is expressed in *S. meliloti*, *minCDE* is probably de-repressed, causing the over-branched cell morphology of the strain. The over- branched cell phenotype was only seen in cells expressing CpdR1D53A in the presence of wild-type *cpdR1*$^{+}$. It is unclear how the effect of CpdR1D53A expression requires the wild-type *cpdR1*$^{+}$ in *S. meliloti*.

In addition to the perturbation in cell cycle progression, abundance of other ClpXP substrates as a consequence of reduced ClpXP localization may contribute to the phenotype of the *cpdR1*-null mutant. It has been shown that ClpXP plays a major role in protein quality control by degrading SsrA-tagged proteins (Keiler *et al*., 1996; Gottesman *et al*., 1998; Herman *et al*., 1998). The SsrA tag is a peptide that is added cotranslationally to the C-termini of nascent polypeptides in stalled translation complexes, and targets these proteins for degradation by ClpXP and other proteases (Keiler *et al*., 1996). It is possible that SsrA-tagged proteins are not properly degraded by ClpXP in the absence of CpdR1, contributing to the pleiotropic phenotype of the *cpdR1*-null mutant. In agreement with this idea, the *Bradyrhizobium japonicum sra* locus, which encodes an *ssrA* homologue, is essential for symbiosis with the host plant (Ebeling *et al*., 1991).

We observed that the majority (~88%) of cells contain ClpX–YFP foci in stationary-phase cells, while ClpX–YFP foci were observed in around ~10% of cells in logarithmic phase. Such increased formation of ClpX foci in stationary phase has not been reported in other organisms. The localization of ClpX has been examined in *C. crescentus* and the Gram-positive bacteria *Bacillus subtilis* (McGrath *et al*., 2006; Kain *et al*., 2008; Kirstein *et al*., 2008; Simmons *et al*., 2008). In the case of *C. crescentus*, however, the localization was not examined in stationary phase. In *B. subtilis*, a *cpdR* homologue has not been identified, and ClpX-GFP forms foci preferentially at the poles in approximately half of cells (Simmons *et al*., 2008). The percentage of cells with ClpX foci remains constant from logarithmic phase to stationary phase (L.A. Simmons, unpublished). Thus, our observation suggests that, in *S. meliloti*, ClpXP-dependent proteolysis plays an important role during stationary phase, in addition to its role in the cell cycle progression. In *E. coli*, it has been reported that cultures of the strains lacking functional ClpP or ClpX displayed a more rapid loss of viability during extended stationary phase than the wild-type (Wei- chart *et al*., 2003). It is interesting to note that the *cpdR1*- null mutant displays decreased foci formation of ClpX also in stationary-phase cells, suggesting that CpdR1 function is required for the ClpX localization in both growth phases.

Thus, further study is required to determine the molecular function of CpdR1 and ClpXP in *S. meliloti*. Moreover, the genome of *S. meliloti* encodes the second homologue of *cpdR*, *cpdR2*, and three *clpP* homologues. Although we could not detect a phenotype of the *cpdR2*-null mutant, CpdR, ClpX and ClpP proteins may form a network, which regulates various physiological processes in the complex life cycle of *S. meliloti*. As we discussed above, since the regulatory

network involving CtrA in *S. meliloti* and *Brucella* species share a similar structure (Hallez *et al*., 2004), the CpdR protein may also have a critical role in co-ordinating cell cycle progression in *Brucella* species. It would be interesting to examine whether CpdR is also critical for the chronic infection of *Brucella* species.

**Experimental Procedures**

***Microbiological techniques*.** Strains and plasmids used in this study are listed in Table S3. *E. coli* recombinants were grown at 37°C on Luria–Bertani (LB) media/medium (Sambrook *et al*., 1989). *S. meliloti* strain Rm1021 (Meade *et al.*, 1982) and its derivatives were raised at 30°C in/on M9 succinate medium with biotin or LBMC (LB supplemented with 2.5 mM $MgSO_4$ and 2.5 mM $CaCl_2$). Gentamycin (Gm), neomycin (Nm), streptomycin (Sp), streptomycin (Sm) and tetracycline (Tet) were added at concentrations of 50, 200, 50, 500 and 15 μg $ml^{-1}$ respectively. Plasmids were mobilized into *S. meliloti* strain Rm1021 and derivative strains by tri-parental mating using pRK600 as the helper plasmid (Ditta *et al*., 1980). Pfu turbo (Stratagene) was used in all PCR reaction followed by cloning. The amplified products were cloned into pCR-Blunt II-TOPO (Invitrogen) and verified by sequencing the inserts.

***Construction of insertional disruptions of* clpX *and* cpdR *homologues.*** To construct the insertional disruption of *cpdR1* (SMc04044), *cpdR2* (SMc00720) and *clpX*, we amplified each full-length ORF with flanking regions by PCR using Rm1021 genomic DNA and the following primer pairs: for *cpdR1* (5′- CTCGAGAA ACGTGGCGCTGCGGAACAGTTCATCGACGAAAT-3′/5′-CTGCAGTTCCGTCGAGCGCG CTAAGGCGTTGAAATAACGAA-3′); for *cpdR2* (5′-CCCGGGACCGAATCCAAGGGCG TCAGGATCACCAAGGATAT-3′/5′-TCTAGAGCGC TACGGCCTTGCGGATGTCGGGCA

GTGAAAAT-3′); for *clpX* (5′-TTGCGGCAAGAGCCAGCATGAAGTCCGC-3′/5′-ATGCT GTTGCAGACCTTGCGACCTGCCC-3′). Underlined nucleotides correspond to mismatches introduced to create selected restriction sites. To disrupt *cpdR1*, *cpdR2* and *clpX*, a $Sm^r/Sp^r$ cassette (from pHP45Ω; Fellay *et al.*, 1987), an *uidA*-$Cm^r$ cassette (from pWM4; Metcalf and Wanner, 1993) and a $Km^r/Nm^r$ cassette (from pHP45Ω-Km; Fellay *et al.*, 1987) were inserted into the internal NruI, SalI and BglII sites respectively. DNA fragments containing disrupted *cpdR* and *clpX* homologues were subcloned into pJQ200-SK (Quandt and Hynes, 1993), and the resulting plasmids were mobilized into Rm1021 or its derivatives by tri-parental mating. Transconjugants were first selected on LBMC plates containing Sm and Gm, then on LBMC plates containing appropriate antibiotics to select the antibiotic-resistance markers in the disrupted genes and 5% (w/v) sucrose to select for double cross-overs. Replacement of wild-type *clpX* and *cpdR* genes with its disrupted loci was confirmed by PCR.

***Construction of plasmids for expression of CpdR proteins, ClpX and CpdR variants.*** The *cpdR1*, *cpdR2* and *clpX* genes were PCR amplified by using Rm1021 genomic DNA and the following primer pairs: for *cpdR1* (5′-CTCGAGAAGAAGTAG CCACGGCCAGATATGACTGCGAAAAT-3′/5′-CTGCAGATATGTTCGCTGCTCAGGCG GCCAGCATCTTGTT-3′); for *cpdR2* (5′-CTCGAGAAAAAATACGGGAGGCCATGAT GGCGAAAATCCTGATCA-3′/5′- CTGCAGCTATGCATGAATTTTCCCCGGACAGCCCTG CCG CTT-3′); for *clpX*; (5′-GGATCCGGAAGGAAGTGGAAATGAGCAAGGTCAGCGGT A-3′/5′-GCATGCTGTGGCCTCAAGCCGAAACGTTGGTCTTCTCCT-3′). The cloned fragments were subcloned in pTH1227, the low-copy-number vector for *S. meliloti* carrying $lacI^q$ and the *tac* promoter (Cheng *et al*., 2007). The resulting plasmids, carrying *cpdR* homologues or *clpX* under the control of *tac* promoter,

were mobilized into Rm1021 by tri-parental mating. The cloned *cpdR1* and *cpdR2* were converted into *cpdR1*D53A and *cpdR2*D52A by site-directed mutagenesis (Stratagene) with following primer pairs: for *cpdR1*D53A (5′-CCCTT TTCGCTTCTCCTGACCGCCATCGTCATGCCGGAGATGGAC-3′/ 5′-GTCCATCTCCGGC ATGACGATGGCGGTCAGGAGAAGCGAAAAGGG-3′); for *cpdR2*D52A (5′-CCGTTCGA CCTCTTGCTATCCGCCATCCGGATGCCGGTCATGGAC-3′/5′- GTCCATGACCGGCATC CGGATGGCGGATAGCAAGAGGTCGAACGG-3′). Underlined nucleotides correspond to mismatches introduced to create the site-directed mutation. The mutated genes were verified by sequencing and cloned in pTH1227 as the same way for the wild-type genes.

***Construction of chromosomal* uidA*-transcriptional fusions.*** To construct *cpdR-uidA* transcriptional fusions, ORFs of *cpdR1* and *cpdR2* were amplified by PCR using the following primer pairs: *cpdR1uidA* (5′-ACTAGTTCCCCCATCGGAAC CCTTTTTACCATGTCCGGTTCTT-3′/5′-CTCGAGTCAGGCGGCCAGCATCTTGTTGAC CTCGTTGACGAGGT-3′); *cpdR2uidA* (5′-ACTAGTAGTGGTGACGGGCGACGCAACCT AACTTGGCTCGT-3′/5′-CTCGAGTCAGGCGGCCAGTGCGAGCGCTACGGCCTTGCGGA -3′). The cloned fragments were subcloned into the suicide *uidA* reporter vector pJH104. Resulting plasmids were mobilized into Rm1021 by tri- parental mating. Transconjugants were selected on LBMC plates containing Sm and Nm. It should be noted that derivatives of pJH104 were inserted into directly downstream of native gene loci by single cross-over recombination without disrupting the genes (ATG of the *uidA* gene is located 23 bp downstream of the stop codon of each *cpdR* homologue). Although the insertion of pJH104 derivatives results in an additional copy of *cpdR1* and *cpdR2*, the second copy of *cpdR* genes lack an upstream promoter. Insertions of pJH104 were confirmed by PCR. To construct a

*clpX-uidA* transcriptional fusion, the *clpX* ORF and the downstream region of *clpX* were amplified separately by PCR using following primer pairs: *clpXuidA* (5′-TCT AGAGGAAGGAAGTGGAAATGAGCAAGGTCAGCGGTA-3′/5′-GGATCCTGTGGCCTCA AGCCGAAACGTTGGTCTTCTCCT-3′); the downstream region of *clpX* (5′-CCCGGG AGGAGAAGACCAACGTTTCGGCTTGA GGCCACA-3′/5′-CTCGAGTCTCGGCACGCGA CCGTCCTTCGACCAGAACCT-3′). Two fragments were subcloned together in pJQ200-SK and combined with *uidA*-Nm$^r$ cassette from pWM6 (Metcalf and Wanner, 1993). The resulting pJQ200-SK derivative carries *clpX* followed by *uidA*-Nm$^r$ cassette and the downstream sequence of native *clpX* locus (ATG of the *uidA* gene is located 59 bp downstream of the stop codon of *clpX*). The resulting plasmid was integrated into Rm1021 by double cross-over as described above. Thus, in resulting strains, *uidA* is inserted downstream of the stop codons of chromosomal *cpdR1*, *cpdR2* and *clpX*, being transcribed as the single transcriptional units with *cpdR* homologues and *clpX*.

***β-Glucuronidase assay in free-living Rm1021 strains.*** The relative expression level of each *uidA* transcriptional fusion was determined by assaying β -glucuronidase activity as previously described (Jefferson *et al*., 1986) with the following modifications. The assay buffer was supplemented with 10 mM EDTA (pH 8.0) and 0.1% sarcosyl, and the enzyme assays were performed with 5 mM p-nitrophenyl β -D- glucuronide substrate (Sigma). The β-glucuronidase activity was normalized to the cell density ($OD_{600}$) and represented in Miller's unit (Miller, 1972).

***Nodulation assay and β-glucuronidase assay in nodules.*** Seedlings of alfalfa (*Medicago sativa* cv. Iroquois: Agway, Plymouth IN, USA) were inoculated with Rm1021 derivatives on Petri dishes containing Jensen agar as described previ-

ously (Leigh *et al*., 1985; Pellock *et al*., 2000). Four-week-old plants were examined for the symbiotic phenotypes. For β-glucuronidase assay, 4-weeks-old nodules were excised, hand-sectioned longitudinally in half, and incubated in X-gluc staining buffer [1 mM 5-bromo-4-chloro-3-indoyl-β-d-glucuronide, 0.1 M Na-phosphatebuffer (pH 7), 10 mM EDTA, 0.5 mM K-ferricyanide, 0.5 mM K-ferrocyanide, 0.1% Triton X-100] at 37°C for overnight. Plants inoculated with Rm1021 derivatives containing pJH104 insertions showed a wild-type phenotype for nodulation.

***Construction for tagging CpdR1, CpdR2 and ClpX with YFP.*** For tagging CpdR1 and CpdR2 with YFP, we fused plasmid- born *cpdR1* and *cpdR2* with *yfpmut*2*A206K*, encoding the *A206K* missense mutation generating monomeric YFP, of pKL183 (Lemon and Grossman, 2000). *cpdR* homologues (including the promoter region and the entire ORF except the stop codon) were amplified by PCR using the following primer pairs: *cpdR1–yfpmut*2 (5′-AAGCTTGATCGAGGCG CGACTGGTCGAGAAAGAACTGGGGA-3′/5′-CTCGAGGGCGGCCAGCATCTTGTTGAC CTCGTTGACGAGGT-3′); *cpdR2– yfpmut*2 (5′-AAGCTTAGTGGTGACGGGCGACGCA ACCTAACTTGGCTCGT-3′/5′-CTCGAGGGCGGCCAGTGCGAGCGCTACGGCCTTGCGG ATGT-3′). The cloned fragments were subcloned into the HindIII-XhoI sites of pTH1227, removing *lacI*q and the *tac* promoter from pTH1227, and combined with the XhoI-PstI fragment containing *yfpmut*2*A206K*. The resulting pTH1227 derivatives, carrying the *cpdR1*– or *cpdR2– yfpmut*2*A206K* fusion gene under the control of native promoters of *cpdR1* or *cpdR2*, were mobilized into the wild-type Rm1021 by tri-parental mating. For tagging ClpX with YFP, we fused chromosomal *clpX* with *yfpmut*2*A206K*. The 3′ region of *clpX* coding sequence was amplified by PCR using the following primer pair: *clpX–yfpmut*2 (5′-GGGCCC

TCGACAAGATTTCCCGTAAGTCCGACAACCCGT-3′/5′-GTCGACAGCCGAAACGTTGG TCTTCTCCTCGGAACGCT-3′). The cloned fragments was subcloned in pJQ200-SK and combined with the XhoI-PstI fragment containing *yfpmut*2*A206K*. The resulting pJQ200-SK derivative, carrying the 3′ region of *clpX* fused to *yfpmut*2*A206K*, was integrated into the native *clpX* locus by single cross-over, disrupting the wild-type *clpX* locus. The resulting *S.meliloti* strain carries the *clpX*– *yfpmut*2 fusion gene as only one copy of functional *clpX*. We noticed that *S. meliloti* carrying *sacB* gene is symbiotically defective and therefore isolated a spontaneous *sacB*$^-$ strain for *in planta* assay.

***Live cell microscopy.*** Aliquots of cells grown in M9 medium supplemented with succinate were stained with the vital membrane dye FM4-64 (Molecular Probes). The following Chroma filter sets were used: 41029 for YFP and 41002C for FM4-64. Exposure time for CpdR1–YFP, CpdR2–YFP and ClpX–YFP fusion protein was 1000, 1000 and 250 ms respectively. In the case of ClpX–YFP in the *cpdR1*-null background, 6000 ms of exposure was required to capture the distinctive foci. Images were acquired, colorized, and merged using OpenLab software (Improvision). To assess the effect of the growth phases in free-living cells, aliquots of M9 cultures of stationary phase ($OD_{600}$ of > 1.5) or log-phase ($OD_{600}$ of 0.4–0.6) were observed under the microscope. For bacteroids, whole alfalfa plants on Petri dishes containing Jensen agar were harvested 4 weeks after inoculation. Nodules were immediately harvested, crushed and bacteroids were observed by microscopy. Positions of foci were scored after colorization and merging of microscopic images. All data presented here are cumulative from at least two independent experiments, each of which gave nearly identical results.

***Flow cytometry.*** For flow cytometry analyses, *S. meliloti* strains were grown to the mid-logarithmic phase in LBMC. The cells were fixed in 90% ethanol for 16 h at 4°C, incubated in the sodium citrate buffer (50 mM sodium citrate with 3.3 μg $ml^{-1}$ RNase H) for 3 h at 50°C and stained by Cytox Green (1:6000 diluted in the sodium citrate buffer) (Molecular Probes). For each flow cytometry experiment, the DNA content was measured in a population of 50 000 cells with a Becton Dickinson FACScan machine at 530 nm. The data were collected and analysed by using the FlowJo software (Tree Star).

**Acknowledgements**

We are indebted to Mary Lou Pardue (Massachusetts Institute of Technology) and Alan D. Grossman (Massachusetts Institute of Technology) for the use of their microscopes. We are grateful to Jiujun Cheng and Turlough M. Finan (McMaster University) for providing us pTH1218 and pTH1227. We wish to thank Judith Carlin and Marianne White for their help. The authors thank Mary Ellen Wiltrout for insightful discussions and kind suggestions; Celeste Peterson, Glenn Paradis and Michiko E. Taga for help with flow cytometry; Melanie Barker-Berkmen for help with the microscopy.

This work was supported by National Institutes of Health grant GM31010 (to G.C.W.), National Cancer Institute (NCI) Grant CA21615-27 (to G.C.W.), MIT Center for Environmental Health Sciences NIEHS P30 ES002109, JSPS Postdoctoral Fellowships for Research Abroad (to H.K.) and a postdoctoral fellowship from the NCI (to L.A.S.), a Jane Coffin Childs Memorial Fund Fellowship (to P.C.) and NIH Grant 5K99GM084157-01 (to P.C.). G.C.W. is an American Cancer Society Research Professor.

## References


Baker, T.A., and Sauer, R.T. (2006) ATP-dependent pro- teases of bacteria: recognition logic and operating principles. *Trends Biochem Sci* **31:** 647–653.

Barnett, M.J., Hung, D.Y., Reisenauer, A., Shapiro, L., and Long, S.R. (2001) A homolog of the CtrA cell cycle regula- tor is present and essential in *Sinorhizobium meliloti*. *J Bacteriol* **183:** 3204–3210.

Bellefontaine, A.F., Pierreux, C.E., Mertens, P., Vanden- haute, J., Letesson, J.J., and De Bolle, X. (2002) Plasticity of a transcriptional regulation network among alpha- proteobacteria is supported by the identification of CtrA targets in *Brucella abortus*. *Mol Microbiol* **43:** 945–960.

Biondi, E.G., Reisinger, S.J., Skerker, J.M., Arif, M., Perchuk, B.S., Ryan, K.R., and Laub, M.T. (2006) Regulation of the bacterial cell cycle by an integrated genetic circuit. *Nature* **444:** 899–904.

Brewin, N.J. (1998) Tissue and cell invasion by *Rhizobium*: the structure and development of infection threads and symbiosis. In *The Rhizobiaceae*. Spaink, H.P., Kondorosi, A., and Hooykaas, P.J.J. (eds). Dordrecht: Kluwer Aca- demic Press, pp. 417–429.

Broughton, W.J., Jabbouri, S., and Perret, X. (2000) Keys to symbiotic harmony. *J Bacteriol* **182:** 5641–5652.

Campbell, G.R.O., Reuhs, B.L., and Walker, G.C. (2002) Chronic intracellular infection of alfalfa nodules by *Sinorhizobium meliloti* requires correct lipopolysaccharide core. *Proc Natl Acad Sci USA* **99:** 3938–3943.

Cheng, J., Sibley, C.D., Zaheer, R., and Finan, T.M. (2007) A *Sinorhizobium meliloti minE* mutant has an altered morphology and exhibits defects in legume symbiosis. *Micro- biology* **153:** 375–387.

Chien, P., Perchuk, B.S., Laub, M.T., Sauer, R.T., and Baker, T.A. (2007) Direct and adaptor-mediated substrate recog- nition by an essential AAA+ protease. *Proc Natl Acad Sci USA* **104:** 6590–6595.

Ditta, G., Stanfield, S., Corbin, D., and Helinski, D.R. (1980) Broad host range DNA cloning system for gram-negative bacteria: construction of a gene bank of *Rhizobium meliloti*. *Proc Natl Acad Sci USA* **77:** 7347–7351.

Dougan, D.A., Mogk, A., Zeth, K., Turgay, K., and Bukau, B. (2002) AAA+ proteins and substrate recognition, it all depends on their partner in crime. *FEBS Lett* **529:** 6– 10.

Duerig, A., Abel, S., Folcher, M., Nicollier, M., Schwede, T., Amiot, N., *et al.* (2009) Second messenger-mediated spa- tiotemporal control of protein degradation regulates bacte- rial cell cycle progression. *Genes Dev* **23:** 93–104.

Ebeling, S., Kundig, C., and Hennecke, H. (1991) Discovery of a rhizobial RNA that is essential for symbiotic root nodule development. *J Bacteriol* **173:** 6373–6382.

Fellay, R., Frey, J., and Krisch, H. (1987) Interposon mutagenesis of soil and water bacteria: a family of DNA fragments designed for *in vitro* insertional mutagenesis of Gram-negative bacteria. *Gene* **52:** 147–154.

Ferguson, G.P., Datta, A., Carlson, R.W., and Walker, G.C. (2005) Importance of unusually modified lipid A in *Sinorhizobium* stress resistance and legume symbiosis. *Mol Microbiol* **56:** 68–80.

Flynn, J.M., Neher, S.B., Kim, Y.I., Sauer, R.T., and Baker, T.A. (2003) Proteomic discovery of cellular substrates of the ClpXP protease reveals five classes of ClpX-recognition signals. *Mol Cell* **11:** 671–683.

Foucher, F., and Kondorosi, E. (2000) Cell cycle regulation in the course of nodule organogenesis in *Medicago*. *Plant Mol Biol* **43:** 773–786.

Fournier, J., Timmers, A.C.J., Sieberer, B.J., Jauneau, A., Chabaud, M., and Barker, D.G. (2008) Mechanism of infec- tion thread elongation in root hairs of *Medicago truncatula* and dynamic interplay with associated rhizobial colonization. *Plant Physiol* **148:** 1985–1995.

Gage, D.J. (2002) Analysis of infection thread development using Gfp- and DsRed-expressing *Sinorhizobium meliloti*. *J Bacteriol* **184:** 7042–7046.

Gage, D.J. (2004) Infection and invasion of roots by symbi- otic, nitrogen-fixing rhizobia during nodulation of temperate legumes. *Microbiol Mol Biol Rev* **68:** 280–300.

Gage, D.J., and Margolin, W. (2000) Hanging by a thread: invasion of legume plants by rhizobia. *Curr Opin Microbiol* **3:** 613–617.

Gibson, K.E., Kobayashi, H., and Walker, G.C. (2008) Molecular determinants of a symbiotic chronic infection. *Annu Rev Genet* **42:** 413–441.

Gorbatyuk, B., and Marczynski, G.T. (2005) Regulated degradation of chromosome replication proteins DnaA and CtrA in *Caulobacter crescentus*. *Mol Microbiol* **55:** 1233–1245.

Gottesman, S., Roche, E., Zhou, Y., and Sauer, R.T. (1998) The ClpXP and ClpAP proteases degrade proteins with carboxy-terminal peptide tails added by the SsrA-tagging system. *Genes Dev* **12:** 1338–1347.

Hallez, R., Bellefontaine, A.F., Letesson, J.J., and De Bolle, X. (2004) Morphological and functional asymmetry in alpha-proteobacteria. *Trends Microbiol* **12:** 361–365.

Herman, C., Thevenet, D., Bouloc, P., Walker, G.C., and D'Ari, R. (1998) Degradation of carboxy-terminal-tagged cytoplasmic proteins by the *Escherichia coli* protease HflB (FtsH). *Genes Dev* **12:** 1348–1355.

Iniesta, A.A., and Shapiro, L. (2008) A bacterial control circuit integrates polar localization and proteolysis of key regula- tory proteins with a phospho-signaling cascade. *Proc Natl Acad Sci USA* **105:** 16602–16607.

Iniesta, A.A., McGrath, P.T., Reisenauer, A., McAdams, H.H., and Shapiro, L. (2006) A phospho-signaling pathway con- trols the localization and activity of a protease complex critical for bacterial cell cycle progression. *Proc Natl Acad Sci USA* **103:** 10935–10940.

Jefferson, R.A., Burgess, S.M., and Hirsh, D. (1986) beta- Glucuronidase from *Escherichia coli* as a gene-fusion marker. *Proc Natl Acad Sci USA* **83:** 8447–8451.

Jenal, U., and Fuchs, T. (1998) An essential protease involved in bacterial cell-cycle control. *EMBO J* **17:** 5658–5669.

Jenal, U., and Hengge-Aronis, R. (2003) Regulation by pro- teolysis in bacterial cells. *Curr Opin Microbiol* **6:** 163–172.

Jones, K.M., Kobayashi, H., Davies, B.W., Taga, M.E., and Walker, G.C. (2007) How rhizobial symbionts invade plants: the *Sinorhizobium-Medicago* model. *Nat Rev Micro-biol* **5:** 619–633.

Kain, J., He, G.G., and Losick, R. (2008) Polar localization and compartmentalization of ClpP proteases during growth and sporulation in *Bacillus subtilis*. *J Bacteriol* **190:** 6749– 6757.

Kaminski, P.A., Batut, J., and Boistard, P. (1998) A survey of symbiotic nitrogen fixation by rhizobia. In *The Rhizobi- aceae*. Spaink, H.P., Kondorosi, A., and Hooykaas, P.J.J. (eds). Dordrecht: Kluwer Academic Press, pp. 431–460.

Keiler, K.C., Waller, P.R., and Sauer, R.T. (1996) Role of a peptide tagging system in degradation of proteins synthe- sized from damaged messenger RNA. *Science* **271:** 990– 993.

Kirstein, J., Strahl, H., Molière, N., Hamoen, L.W., and Turgay, K. (2008) Localization of general and regulatory proteolysis in *Bacillus subtilis* cells. *Mol Microbiol* **70:** 682–694.

Kobayashi, H., and Broughton, W.J. (2008) Fine-tuning of symbiotic genes in rhizobia: Flavonoid signal transduction cascade. In *Nitrogen Fixation: Origins, Applications, and Research Progress Volume 7: Nitrogen-Fixing Legume Symbiosis.* Dilworth, M.J., James, E.K., Sprent, J.I., and Newton, W.E. (eds). Dordrecht: Springer Netherlands, pp. 117–152.

Kobayashi, H., Sunako, M., Hayashi, M., and Murooka, Y. (2001) DNA synthesis and fragmentation in bacteroids during *Astragalus sinicus* root nodule development. *Biosci Biotechnol Biochem* **65:** 510–515.

Lam, H., Matroule, J.Y., and Jacobs-Wagner, C. (2003) The asymmetric spatial distribution of bacterial signal transduc- tion proteins coordinates cell cycle events. *Dev Cell* **5:** 149–159.

Laub, M.T., McAdams, H.H., Feldblyum, T., Fraser, C.M., and Shapiro, L. (2000) Global analysis of the genetic network controlling a bacterial cell cycle. *Science* **290:** 2144–2148.

Laub, M.T., Chen, S.L., Shapiro, L., and McAdams, H.H. (2002) Genes directly controlled by CtrA, a master regula- tor of the *Caulobacter* cell cycle. *Proc Natl Acad Sci USA* **99:** 4632–4637.

Leigh, J.A., Signer, E.R., and Walker, G.C. (1985) Exopolysaccharide-deficient mutants of *Rhizobium meliloti* that form ineffective nodules. *Proc Natl Acad Sci USA* **82:** 6231–6235.

Lemon, K.P., and Grossman, A.D. (2000) Movement of rep- licating DNA through a stationary replisome. *Mol Cell* **6:** 1321–1330.

Liu, J., Cosby, W.M., and Zuber, P. (1999) Role of Lon and ClpX in the post-translational regulation of a sigma subunit of RNA polymerase required for cellular differentiation in *Bacillus subtilis*. *Mol Microbiol* **33:** 415–428.

McGrath, P.T., Iniesta, A.A., Ryan, K.R., Shapiro, L., and McAdams, H.H. (2006) A dynamically localized protease complex and a polar specificity factor control a cell cycle master regulator. *Cell* **124:** 535–547.

Margolin, W. (2005) FtsZ and the division of prokaryotic cells and organelles. *Nat Rev Mol Cell Biol* **6:** 862–871.

Meade, H.M., Long, S.R., Ruvkun, G.B., Brown, S.E., and Ausubel, F.M. (1982) Physical and genetic characterization of symbiotic and auxotrophic mutants of *Rhizobium meliloti* induced by transposon Tn5 mutagenesis. *J Bacteriol* **149:** 114–122.

Mergaert, P., Uchiumi, T., Alunni, B., Evanno, G., Cheron, A., Catrice, O., *et al.* (2006) Eukaryotic control on bacterial cell cycle and differentiation in the *Rhizobium*-legume symbiosis. *Proc Natl Acad Sci USA* **103:** 5230–5235.

Metcalf, W.W., and Wanner, B.L. (1993) Construction of new beta-glucuronidase cassettes for making transcriptional fusions and their use with new methods for allele replacement. *Gene* **129:** 17–25.

Miller, J.F. (1972) *Experiments in Molecular Genetics*. Cold Spring Harbor, NY: Cold Spring Harbor Laboratory.

Oke, V., and Long, S.R. (1999) Bacteroid formation in the *Rhizobium*-legume symbiosis. *Curr Opin Microbiol* **2:** 641– 646.

Pellock, B.J., Cheng, H.P., and Walker, G.C. (2000) Alfalfa root nodule invasion efficiency is dependent on *Sinorhizo- bium meliloti* polysaccharides. *J Bacteriol* **182:** 4310– 4318.

Perret, X., Staehelin, C., and Broughton, W.J. (2000) Molecular basis of symbiotic promiscuity. *Microbiol Mol Biol Rev* **64:** 180–201.

Prell, J., and Poole, P. (2006) Metabolic changes of rhizobia in legume nodules. *Trends Microbiol* **14:** 161–168.

Quandt, J., and Hynes, M.F. (1993) Versatile suicide vectors which allow direct selection for gene replacement in Gramnegative bacteria. *Gene* **127:** 15–21.

Quon, K.C., Marczynski, G.T., and Shapiro, L. (1996) Cell cycle control by an essential bacterial two-component signal transduction protein. *Cell* **84:** 83–93.

Quon, K.C., Yang, B., Domian, I.J., Shapiro, L., and Marczynski, G.T. (1998) Negative control of bacterial DNA replication by a cell cycle regulatory protein that binds at the chromosome origin. *Proc Natl Acad Sci USA* **95:** 120–125.

Rodriguez, H., Mendoza, A., Cruz, M.A., Holguin, G., Glick, B.R., and Bashan, Y. (2006) Pleiotropic physiological effects in the plant growth-promoting bacterium *Azospiril- lum brasilense* following chromosomal labeling in the *clpX* gene. *FEMS Microbiol Ecol* **57:** 217–225.

Sambrook, J., Fritsch, E.F., and Maniatis, T. (1989) *Molecular Cloning: A Laboratory Manual*, 2nd edition. Cold Spring Harbor, NY: Cold Spring Harbor Laboratory.

Sauer, R.T., Bolon, D.N., Burton, B.M., Burton, R.E., Flynn, J.M., Grant, R.A., *et al.* (2004) Sculpting the proteome with AAA(+) proteases and disassembly machines. *Cell* **119:** 9–18.

Siam, R., and Marczynski, G.T. (2000) Cell cycle regulator phosphorylation stimulates two distinct modes of binding at a chromosome replication origin. *EMBO J* **19:** 1138–1147.

Simmons, L.A., Grossman, A.D., and Walker, G.C. (2008) Clp and Lon proteases occupy distinct subcellular positions in *Bacillus subtilis*. *J Bacteriol* **190:** 6758–6768.

Skerker, J.M., Prasol, M.S., Perchuk, B.S., Biondi, E.G., and Laub, M.T. (2005) Two-component signal transduction pathways regulating growth and cell cycle progression in a bacterium: a system-level analysis. *PLoS Biol* **3:** e334.

Weichart, D., Querfurth, N., Dreger, M., and Hengge-Aronis, R. (2003) Global role for ClpP-containing proteases in stationary-phase adaptation of *Escherichia coli*. *J Bacteriol* **185:** 115–125.

Winzeler, E., and Shapiro, L. (1995) Use of flow cytometry to identify a *Caulobacter* 4.5 S RNA temperature-sensitive mutant defective in the cell cycle. *J Mol Biol* **251:** 346–365.

Wright, R., Stephens, C., Zweiger, G., Shapiro, L., and Alley, M.R. (1996) *Caulobacter* Lon protease has a critical role in cell-cycle control of DNA methylation. *Genes Dev* **10:** 1532–1542.

Wright, R., Stephens, C., and Shapiro, L. (1997) The CcrM DNA methyltransferase is widespread in the alpha sub- division of proteobacteria, and its essential functions are conserved in *Rhizobium meliloti* and *Caulobacter crescentus*. *J Bacteriol* **179:** 5869–5877.

Zweiger, G., Marczynski, G., and Shapiro, L. (1994) A *Cau- lobacter* DNA methyltransferase that functions only in the predivisional cell. *J Mol Biol* **235:** 472–485.

## Appendix B.

## The essential DivJ/CbrA kinase and PleC phosphatase system controls DivK phosphorylation and symbiosis in *Sinorhizobium meliloti*

This has been submitted for pulication to *Mol Micro* on June 2, 2013 (currently under review) by Francesco Pini, Benjamin Frage, Lorenzo Ferri, Nicole J. De Nisco, Saswat S. Mohapatra, Lucilla Taddei, Antonella Fioravanti, Frederique Dewitte, Marco Galardini, Matteo Brilli, Vincent Villeret, Marco Bazzicalupo, Alessio Mengoni, Graham C. Walker, Anke Becker and Emanuele G. Biondi.

F.P. and L.F. constructed the strains used in this paper. F.P. did all experiments with exception of: *in silico* Pdh analysis by M.B., symbiotic assays by B.F. Flow cytometry analysis by N.J.D. and Model development by E.G.B., N.J.D. and G.C.W. The manuscript was written and reviewed by E.G.B, F.P., N.J.D., G.C.W and A.B.

**Abstract**

*Sinorhizobium meliloti* is a soil bacterium that invades the root nodules it induces on *Medicago sativa*, whereupon it undergoes an alteration of its cell cycle and differentiates into nitrogen-fixing, elongated and polyploid bacteroid with higher membrane permeability. In *Caulobacter crescentus,* a related alphaproteobacterium, the principal cell cycle regulator, CtrA, is inhibited by the phosphorylated response regulator DivK. The activation of DivK depends on the histidine kinase DivJ, while PleC is the principal phosphatase for DivK. Despite the importance of the DivJ in *C. crescentus,* the mechanistic role of this kinase has never been elucidated in other *Alphaproteobacteria.*

We show here that the histidine kinases DivJ together with CbrA and PleC participate in a complex phosphorylation system of the essential response regulator DivK in *S. meliloti*. In particular, DivJ and CbrA are involved in DivK phosphorylation and in turn CtrA inactivation, thereby controlling correct cell cycle progression and the integrity of the cell envelope. In contrast, the essential PleC presumably acts as a phosphatase of DivK. Interestingly, we found that a DivJ mutant is able to elicit nodules and enter plant cells, but fails to establish an effective symbiosis suggesting that proper envelope and/or low CtrA levels are required for symbiosis.

**Introduction**

*Caulobacter crescentus* and *Sinorhizobium meliloti* belong to the class of *Alphaproteobacteria*, which includes plant endosymbionts (e.g., *Rhizobium*, *Sinorhizobium*, *Mesorhizobium* and *Azorhizobium*), animal pathogens (e.g., *Brucella*, *Rickettsia*) and plant pathogens (e.g., *Agrobacterium*). *Sinorhizobium meliloti,* one of the most intensively studied of these organisms, is able to elicit

the formation of nodules on the roots of plants of the genera *Medicago*, *Melilotus* and *Trigonella* (Horvath *et al.*, 1986). *S. meliloti* induces nodule formation, invades plant cells in the interior of the nodule and then undergoes a cellular differentiation process in order to become a nitrogen-fixing bacteroid. In this differentiation, the cells become elongated and polyploid as a result of endo-reduplication of the genome, which suggests that a cell cycle change may be inherent to the differentiation process (Mergaert *et al.*, 2006; Kobayashi *et al.*, 2009; Van de Velde *et al.*, 2010; Wang *et al.*, 2010).

The cell cycle machinery responsible for DNA replication, cell division, and morphogenesis of polar structures is the engine of every organism and has been extensively studied in *C. crescentus* (Curtis and Brun, 2010). Many factors are known to regulate cell cycle progression, most of which are members of the family of two-component signal transduction proteins, which is comprised of histidine kinases and their response regulator substrates. Among these, the essential response regulator CtrA is the master regulator and its activity varies as a function of the cell cycle (Quon *et al.*, 1996; Laub *et al.*, 2002).

In *C. crescentus,* CtrA regulates gene expression of key players in the cell cycle and other processes, and it also blocks DNA replication by binding the origin of replication and thus making it inaccessible to the replication initiation factors. The regulon directly controlled by CtrA comprises genes involved in cell division (*ftsZ*, *ftsA*, *ftsQ* and *ftsW*), proteolysis (*clpP)*, DNA methylation (*ccrM)*, flagellar biogenesis (e.g. *flgBC, fliE* and *fliLM*), stalk biogenesis (*tacA*), pili biogenesis (*pilA)*, and chemotaxis (Skerker and Shapiro, 2000; Wortinger *et al.*, 2000; S E Jones *et al.*, 2001; Laub *et al.*, 2002; Biondi, Jeffrey M Skerker, *et al.*, 2006; Collier *et al.*, 2007). The essential role of CtrA has also been demonstrated

in other *Alphaproteobacteria*, such as *Brucella* (Bellefontaine *et al.*, 2002) and *S. meliloti* (Barnett *et al.*, 2001), while in several other species, cells can survive without CtrA. In these cases, this protein only controls dispensable functions, such as motility and chemotaxis (e.g. in *Rhodospirillum* and *Magnetospirillum*) (Bird and MacKrell, 2011; Greene *et al.*, 2012).

In *C. crescentus,* CtrA activity peaks only at the predivisional stage (Domian *et al.*, 1997), thanks to a combination of transcriptional, proteolytic and phosphorylation control. CtrA is activated through phosphorylation in a cell-cycle dependent fashion; this is accomplished by an essential phosphorelay, comprised of the hybrid histidine kinase CckA and the histidine phosphotransferase ChpT (Biondi, Reisinger, *et al.*, 2006). ChpT can also shuttle the phosphate from CckA to CpdR, a second response regulator that, together with RcdA, is involved in CtrA proteolysis mediated by the ClpP-ClpX protease (Jenal and Fuchs, 1998; Hung and Shapiro, 2002; Ryan *et al.*, 2002; Ryan *et al.*, 2004; McGrath *et al.*, 2006; Iniesta *et al.*, 2006). The phosphorylated response regulator DivK promotes cell cycle progression because it acts at the top of the phosphorelay, interrupting the phosphate flow towards CtrA and thus promoting DNA replication (Hecht *et al.*, 1995; Wu *et al.*, 1998).

Two histidine kinases, DivJ and PleC, are known to interact with DivK. DivJ plays a role in controlling the length and location of the stalk and the cell division plane (Ohta *et al.*, 1992), while a null *Caulobacter pleC* mutant produces almost symmetric cells at division and shows abnormal polar development (Burton *et al.*, 1997). Phosphorylated DivK also acts as an allosteric activator for DivJ and PleC, triggering PleD-dependent production of cyclic-di-GMP, which ultimately modulates CtrA proteolysis in the stalked compartment (Paul *et al.*,

2008; Abel *et al.*, 2011). In *Caulobacter*, DivJ and PleC are the principal kinase and phosphatase of DivK, respectively (Wheeler and Shapiro, 1999). It should be noted that, although DivK has an essential role and its activation by phosphorylation is crucial, the non-essentiality of DivJ and PleC in *C. crescentus* is still inexplicable.

In other *Alphaproteobacteria*, histidine kinases similar to DivJ/PleC have been described, such as CbrA and PleC in *S. meliloti* and PdhS in *B. abortus* (Gibson *et al.*, 2006; Hallez *et al.*, 2007; Gibson *et al.*, 2007; Mignolet *et al.*, 2010; Fields *et al.*, 2012; Sadowski *et al.*, 2013). Although two-hybrid experiments have shown that PdhS binds DivK in *Brucella*, no direct biochemical demonstration have been provided yet for the other species. Recently, CbrA has been connected to the positive control of DivK phosphorylation in *S. meliloti* (Sadowski *et al.*, 2013), as it is positively responsible for the control of DivK localization, which in turn depends on its phosphorylation state. The investigation of the cell cycle's genetic architecture in *Alphaproteobacteria* has been recently explored using bioinformatics, revealing the conservation of the regulatory network of CtrA and DivK in *Caulobacterales* and the *Rhizobiales* (Brilli *et al.*, 2010), although no direct experimental evidence has been provided.

Here we studied the *S. meliloti* phosphorylation system, consisting of several putative kinases, that controls the essential cell cycle factor DivK. We integrated both *in vivo* and *in vitro* approaches to dissect its architecture and understand its function. Our results indicate that the kinases involved in phosphorylation/dephosphorylation of DivK are essential in *S. meliloti*, a major difference with respect to *Caulobacter* despite the similarities concerning their cell cycle networks. In addition to the defects in the cell cycle caused by loss of

DivJ, we show that the absence of DivJ strongly affects the ability of *Sinorhizobium meliloti* to function as an efficient symbiont of *M. sativa*, suggesting a link between cell cycle regulators and symbiosis.

**Results and Discussion**

**DivJ in *S. meliloti* is involved in cell cycle regulation.** In *S. meliloti,* the putative DivJ is a histidine kinase that is anchored to the membrane and it has a sensor region that is divergent from that of the *C. crescentus* DivJ. Instead of having several membrane spanning domains, the sensor region of *S. meliloti* DivJ only contains one (Fig. 1A). In order to study its function, we constructed a *S. meliloti* strain carrying the deletion of the gene SMc00059, encoding DivJ (Hallez *et al.*, 2004; Brilli *et al.*, 2010). The Δ*divJ* (BM253) mutant was viable, but it showed a severe reduction of its doubling time (Fig. 1B). We confirmed the deletion by PCR and excluded the possibility that the phenotypes were caused by polar mutations by using the phage ΦM12 (Finan *et al.*, 1984) to transduce the deletion cassette from BM253 into a strain carrying a plasmid-borne *divJ*$^{+}$ and showing that the *divJ*$^{+}$ plasmid is indeed able to fully complement all the mutant phenotypes (Fig. 1C). Most of the cells of BM253 were abnormally shaped (long, branched or short morphologies > 60 %) and in particular we observed a branched phenotype in 10% of the cells (Fig. 1C), which usually suggests cell division and polarity defects. As in *C. crescentus*, the *S. meliloti* Δ*divJ* was still motile (Fig. 1D). The slightly smaller halo of the *divJ* mutant in the soft agar could be due to the slower growth of the mutant and/or the branched phenotype of cells, which usually retards the motility. Confirming the functional annotation, the putative *divJ* of *S. meliloti* was able to complement deletion of *divJ* in *C. crescentus*. In particular, the growth defect was rescued by expressing *S. meliloti*

DivJ, which resulted in a change from a doubling time in rich medium of 140 ± 10 min. to 102 ± 8 min. - the same as the wild type doubling time of ca. 100 ± 5 min.

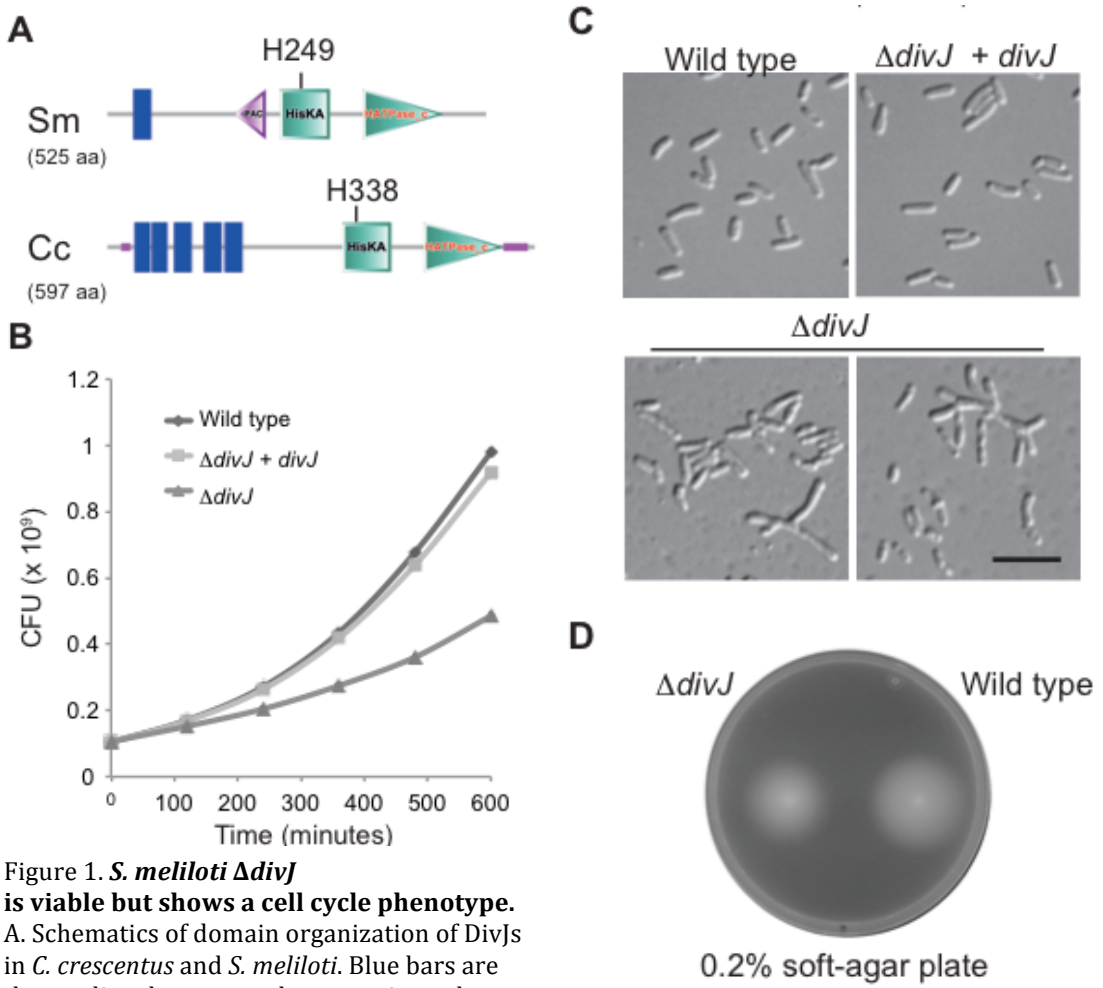


Figure 1. ***S. meliloti* Δ*divJ* is viable but shows a cell cycle phenotype.** A. Schematics of domain organization of DivJs in *C. crescentus* and *S. meliloti*. Blue bars are the predicted transmembrane regions, the pink triangle is a predicted PAC domain, green squares are the HisKA domains that include the phosphorylated histidine residue, purple horizontal lines are intrinsically disordered regions and finally the HATPase_c domains are the green triangles (analysis performed using SMART database) (Letunic et al., 2102). B. Colony Forming Units (CFU) of wild type, Δ*divJ* (BM253), Δ*divJ* + *divJ* (BM224). Doubling time (30˚C, 180rpm) of BM224 is 200 ± 15 min (similar to wild type cells, 190 ± 13 min), while BM253 doubling time is 284 ± 21 min. C. Cell morphology of the *S. meliloti* wild type, *divJ* mutant and Δ*divJ* + *divJ*. Black bar corresponds to 4 mm. D. Soft agar swarmer assay (wild type is 5.6 ± 0.2 cm, while Δ*divJ* is 5.4 ± 0.3 cm after 5 days).

Moreover the overall morphology of this complemented strain (Fig. 2A) closely resembled that of the wild type cells (cell length corresponding to 90% ± 10% of wild type cells), as compared to *ΔdivJ* cell (180% ± 20% of wild type) and stalk length (120% ± 15% of wild type), as compared to *ΔdivJ* (240% ± 20% of normal stalks). Next we tested the effect of *divJ* overexpression in *S. meliloti* by

constructing a strain in which *divJ* was under the control of an IPTG inducible $P_{lac}$ promoter (Khan *et al.*, 2008) (BM317). Overexpression of *divJ* caused a severe growth defect as implied by the absence of colony forming units in medium with IPTG (Fig. 2B). The strain overexpressing DivJ also showed an elongated cell morphology suggesting a negative effect on cell division (Fig. 2C). Finally, we checked alterations of the DNA content by using flow cytometry analysis (Fig. 2D). This investigation revealed that, after 4 h of overexpression of *divJ,* cells with two genome copies accumulated in comparison with wild type, suggesting a block of cell division at the G2 stage.

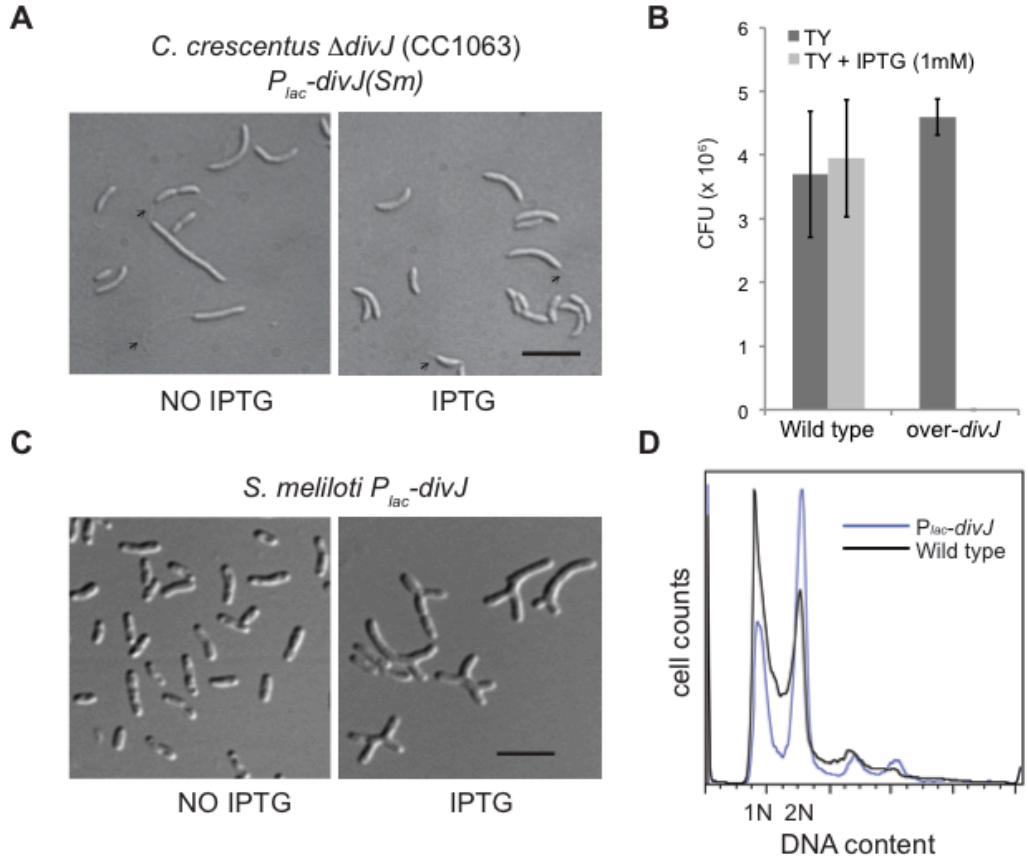


Figure 2. **Complementation of *C. crescentus* Δ*divJ* by the *S. meliloti* gene.** A. Morphology of *C. crescentus* Δ*divJ* (Skerker *et al.*, 2005) (BM331) and Δ*divJ* complemented (BM333) by an IPTG-inducible copy of *S. meliloti divJ* (100 µM IPTG). Black bar corresponds to 4 mm. Small black arrows indicate stalks. The presence of *S. meliloti divJ* was indeed able to partially rescue the growth defect and the abnormal morphology of *C. crescentus* Δ*divJ* (see text for details). B. CFUs of over-*divJ* (BM317) in comparison with wild type cells containing the empty over-expression vector; $10^6$ cells of cultures grown for 4 hours with or without IPTG, were plated without IPTG in order to measure the viability (CFU). Clearly the overexpression of *divJ* (IPTG) shows a CFU < $10^6$; C. Morphology of over-*divJ*. D. FACS analysis of over-*divJ* in comparison with wild type cells.

Overexpression of *divJ(H249A)* (EB775), which is mutated in the conserved histidine putatively required for phosphorylation showed no over-expression phenotypes, suggesting that the histidine in position 249 is responsible for DivJ activity (data not shown). *divJ(H249A)* was also unable to complement the deletion phenotype of the *divJ* mutant (data not shown). As we were unable to obtain a good preparation of DivJ antibodies, we cannot exclude the formal possibility that that instability of the DivJH249A mutant protein may be responsible for the absence of an overexpression phenotype, but we consider this to be very unlikely.

The observation that PleC, the phosphatase that dephosphorylates DivK in *C. crescentus*, is essential in *S. meliloti* (Fields *et al.*, 2012) suggests that severity of *divJ* overexpression may be because higher levels of DivK phosphorylation are not well-tolerated in *S. meliloti*. We speculated then that deletion of *pleC* should be similar to overexpression of *divJ*, and that the over-expression of *divJ* is lethal in *S. meliloti* due to the high levels of DivK-P. This explanation requires that DivJ would be able to transfer phosphate groups to DivK.

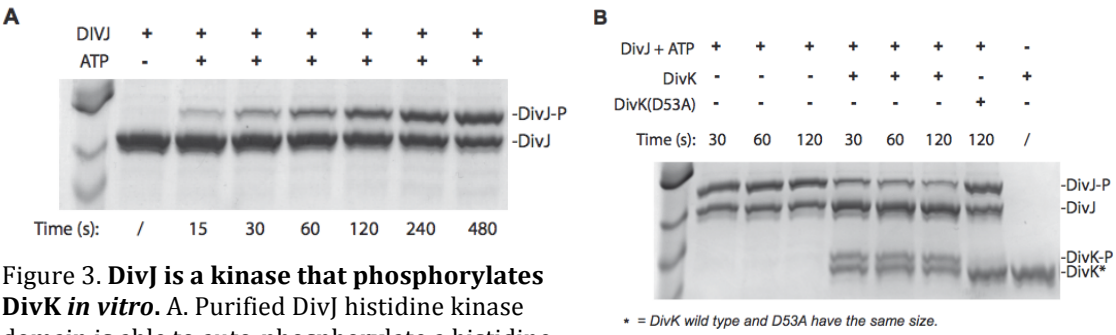


Figure 3. **DivJ is a kinase that phosphorylates DivK *in vitro*.** A. Purified DivJ histidine kinase domain is able to auto-phosphorylate a histidine residue using ATP as the phosphate source. DivJ in presence of ATP gives two distinct bands in a SDS-PAGE Phos-tag™ gel. In particular the amount of phosphorylated band (upper band) increases over time. B. DivJ-P transfers the phosphate to the aspartate in position 53 of DivK, as the mutant D53A is not able to receive the phosphate from DivJ.

In order to confirm that DivJ is in fact a histidine kinase (HK) able to phosphorylate DivK, we purified its HK domain, as predicted by SMART database and used it for phosphorylation biochemical assays. After incubating the DivJ HK domain with ATP, we were able to separate the phosphorylated form of DivJ-HK by Phos™-Tag SDS-PAGE electrophoresis. The phosphorylated form of DivJ-HK accumulated over time indicating auto-kinase activity (Fig. 3A). This auto-phosphorylation is dependent on the presence of the histidine residue H249 since mutation of this residue abolished the autokinase activity (Fig. S1). In order to test the ability of DivJ-P to transfer phosphate to DivK, we removed ATP after DivJ-P had accumulated and added purified DivK or DivK(D53A), incubating at different time points. Results in Fig. 3B clearly showed that only wild type DivK received the phosphate from DivJ, while the point mutant at the predicted aspartate receiver residue did not. These *in vitro* phosphortransfer experiments indicate that purified DivJ-HK is able to auto-phosphorylate its histidine catalytic residue H249 using ATP and then transfer the phosphate to the aspartate D53 of DivK.

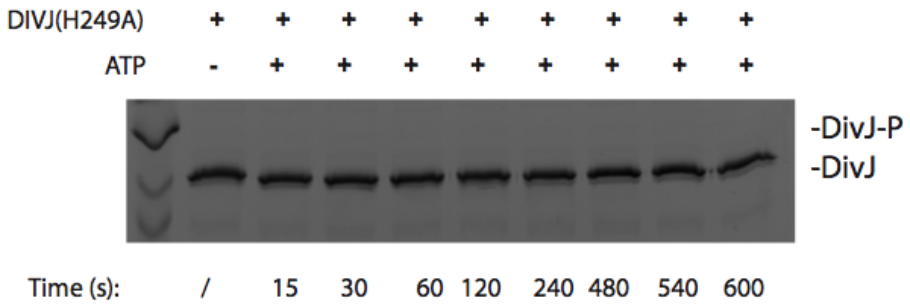


Figure S1. ***In vitro* phosphorylation assay using DivJ_HK (H249A).** DivJ(H249A) was incubated with ATP as described in the text and then loaded on a Phos-Tag polyacrylamide gel. No detectable DivJ(H249A)-P is produced over time. For positive phosphorylation refers to fig. 3.

**DivJ represses CtrA phosphorylation and activity in *S. meliloti*.** In *C. crescentus,* DivK inhibits CtrA via DivL/CckA (Biondi, Reisinger, *et al.*, 2006; Tsokos *et al.*, 2011) and triggers c-di-GMP production via PleD (Paul *et al.*, 2008;

Abel *et al.*, 2011). If DivJ/DivK also inhibit CtrA activity in *S. meliloti*, the combination of a mutation that increases CtrA levels and the deletion of *divJ* should lead to a severe/lethal phenotype. Using an M12 phage lysate of strain BM253 (Δ*divJ* carrying the resistance cassette for tetracycline), we attempted to transduce the *divJ* deletion, into a strain with *ctrA* under the inducible promoter (BM240), creating the strain BM264. Transductants were recovered only without IPTG in the selective medium (Fig. 4A) indicating that a strain carrying a deletion of *divJ* does not tolerate high levels of CtrA. We further analyzed the strain BM264 grown first without IPTG and then switched to a medium supplemented with IPTG; the strain developed a phenotype highly branched and elongated, confirming its severe cell cycle defect(s) when CtrA is overproduced (Fig. 4B).

**A**

| Recipient strain | Number of transduced colonies (CFU/ml) |
|---|---|
| Wild Type | 210 |
| Wild Type IPTG | 180 |
| $P_{lac}$ - *ctrA NO IPTG* | 230 |
| $P_{lac}$ - *ctrA* IPTG | 0 |
| *cbrA*::Tn5 $P_{lac}$-*divJ* NO IPTG | 0 |
| *cbrA*::Tn5 $P_{lac}$-*divJ* IPTG | 76 |

**B**

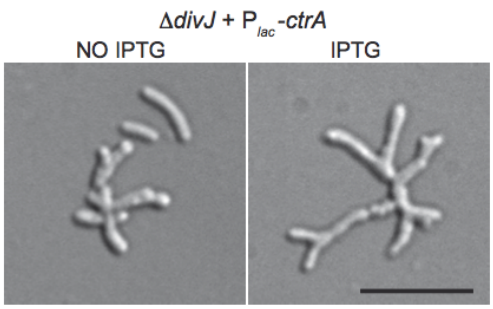


Figure 4. **High CtrA levels are lethal in combination with** Δ*divJ* A. Transduction table, in which over-expression of *ctrA* (IPTG) in combination with the Δ*divJ* is lethal; B. Morphology of *S. meliloti* strain BM264 (Δ*divJ* + over-*ctrA*) with and without induction by 1 mM IPTG. The black bar is 3 mm.

To investigate this further, we measured the expression levels of the *pilA* promoter in a Δ*divJ* strain in comparison with wild type cells. In *C. crescentus, pilA* expression is directly controlled by CtrA (Skerker and Shapiro, 2000). We measured the expression by fusing a *pilA* promoter to the b-galactosidase gene and measuring b-galactosidase activity. Our results (Fig. 5A) demonstrate that the *pilA* is expressed at higher levels in the *divJ* mutant (EB638), suggesting that

CtrA is also more active, which fits the model of DivJ and DivK inhibiting CtrA activity.

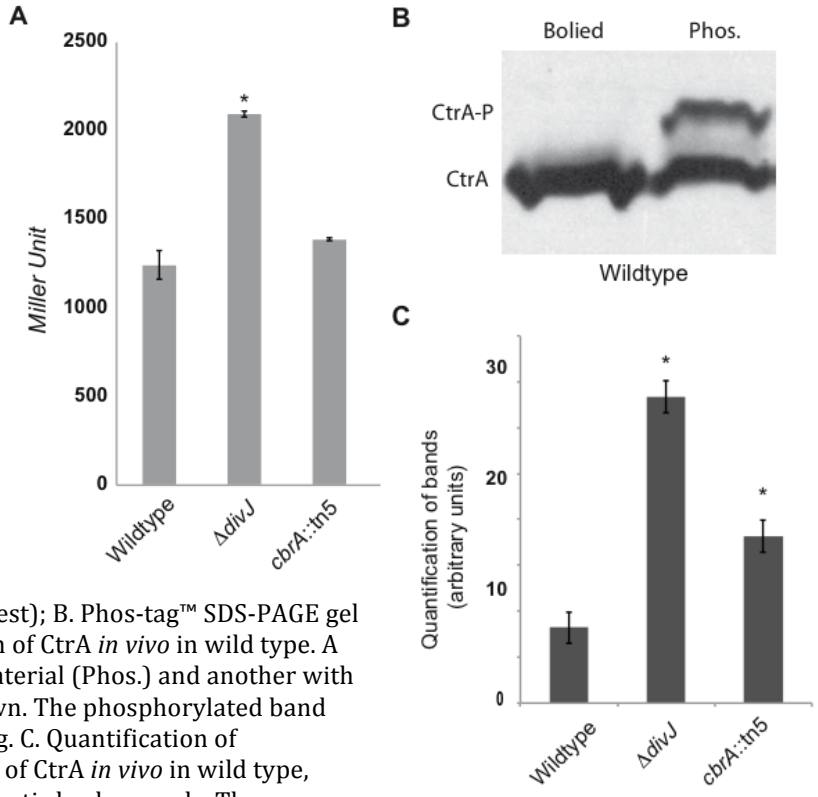


Figure 5. **DivJ and CbrA are inhibiting CtrA phosphorylation and activity *in vivo*.** A. b-galactosidase activity of a CtrA-controlled promoter in wild type (EB594), Δ*divJ* (EB638) and *cbrA*::Tn5 (EB593) genetic backgrounds. Experiments were performed in biological triplicates. Asterisk corresponds to significant statistical difference with wild type conditions (Student's test); B. Phos-tag™ SDS-PAGE gel shows phosphorylation of CtrA *in vivo* in wild type. A lane with SDS-lysed material (Phos.) and another with boiled sample are shown. The phosphorylated band disappears after boiling. C. Quantification of phosphorylation levels of CtrA *in vivo* in wild type, Δ*divJ* and *cbrA*::Tn5 genetic backgrounds. The average of three experiments using samples at the same $OD_{600}$ is showed. The amount of CtrA-P was normalized for the number of cells. Asterisk corresponds to significant statistical difference with wild type conditions (Student's test).

We further tested this model by measuring phosphorylation levels of CtrA in different genetic backgrounds. In order to quantify CtrA-P levels *in vivo*, we used the Phos-Tag system in combination with immunoblots with anti-CtrA antibodies (Fig. 5B). To the best of our knowledge, is the first time in the *S. meliloti* field that in vivo measurements of phosphorylation of a protein have been successfully performed. Cell lysates are loaded on SDS-Page electrophoresis gels and, in contrast to measurements using radioactivity, no specific culture medium is required, as Phos-Tag detects unlabeled wild type proteins. We measured levels of CtrA-P (Figure 5C) in three biological replicates of wild type, Δ*divJ* and *cbrA*::Tn5 cells (this latter case is discussed in the

following sections). Consistent with the increased activity of the CtrA-controlled promoter of *pilA*, levels of phosphorylated CtrA were significantly increased in the Δ*divJ* strain compared to wild type.

In summary, the results discussed in this section show that DivJ, which is able to phosphorylate DivK *in vitro*, is also required, through DivK-P, for down-regulation of CtrA phosphorylation and subsequently its activity as transcriptional activator. However, this raises the question of whether DivJ is the only histidine kinase controlling DivK phosphorylation in *S. meliloti*.

***In silico* analysis of histidine kinases predicted to interact with DivK in *S. meliloti*.** We employed an *in silico* strategy to identify other genes in *S. meliloti* and other *Alphaproteobacteria* that encode for proteins that belong to the family of histidine kinases that controls DivK phosphorylation and dephosphorylation. This family was named *pleC*/*divJ* homolog sensor family (PdhS) as previously suggested (Hallez *et al.*, 2004). In order to predict the kinases interacting with a response regulator, we took advantage of a previous analysis that defined the regions of the histidine kinase that make contact with the response regulator and that are responsible for the specificity of this interaction (Skerker *et al.*, 2008). This approach was integrated with the hypothesis that all *Alphaproteobacterial* DivK and PleC proteins are able to interact with DivK (Brilli *et al.*, 2010). The fragment of the HK responsible for the specific interaction with the response regulator DivK comprises helix 1 and helix 2 of the two-helix bundle that surrounds the histidine residue (Ohta and Newton, 2003; Skerker *et al.*, 2008). Helix 1 of the *C. crescentus* DivJ corresponds to residues 332 to 351 and helix 2 corresponds to 369 to 395. Results of the alignment of all DivJs and PleCs are shown in figure S2.

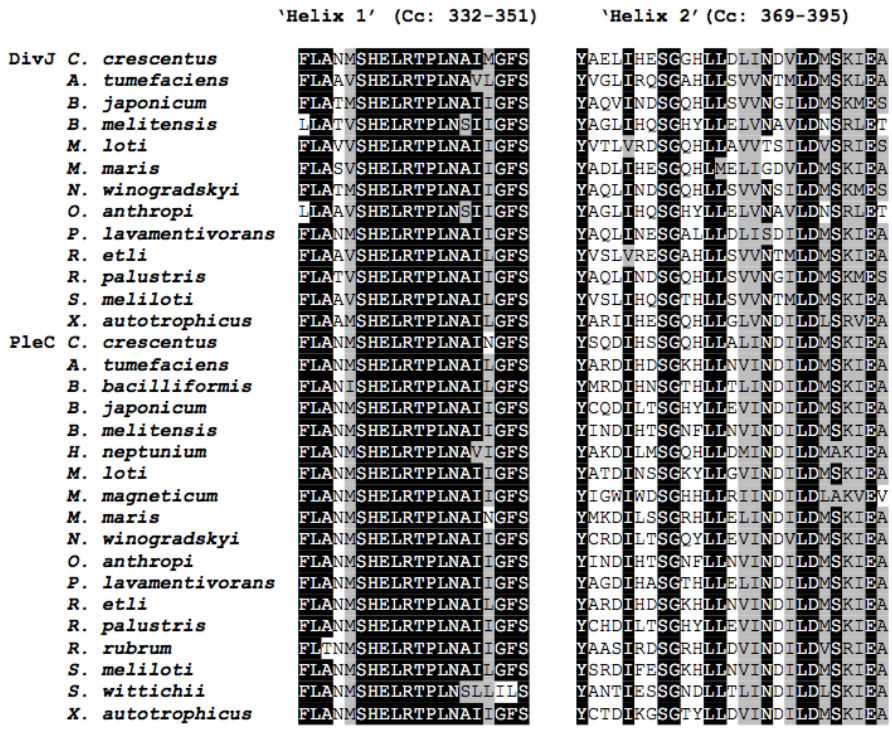


Figure S2 Alignment of DivJs and PleCs in *Alphaproteobacteria* using ClustalW. Accession numbers of othologs of DivJ and PleC are in bottom table. The consensus sequence is shown in figure 6A.

From this alignment, in which we used both helices, we derived a probability model describing the variability at each position of the most conserved helix (helix 1) in DivJ and PleC proteins from organisms possessing DivK (Fig. 6A). We scanned for HKs in *Alphaproteobacteria* genomes using a probability matrix that allowed us to assign a score to each of them, while a threshold chosen to include known DivK partners allowed identifying additional putative DivK interactors. Notably, *S. meliloti* CbrA (Gibson *et al.*, 2007) and the *B. abortus* PdhS (Hallez *et al.*, 2007), which have been hypothesized to interact with DivK, were in fact detected with this bioinformatic analysis (available as table S1 on the *Mol Micro* website). *S. meliloti* showed five Pdh kinases including CbrA (Gibson *et al.*, 2006), DivJ and PleC (Fields *et al.*, 2012) and two other

histidine kinases putatively belonging to the PdhS family that we named PdhSA and PdhSB (Fig. 6B), SMc04212 and SMc01128 respectively.

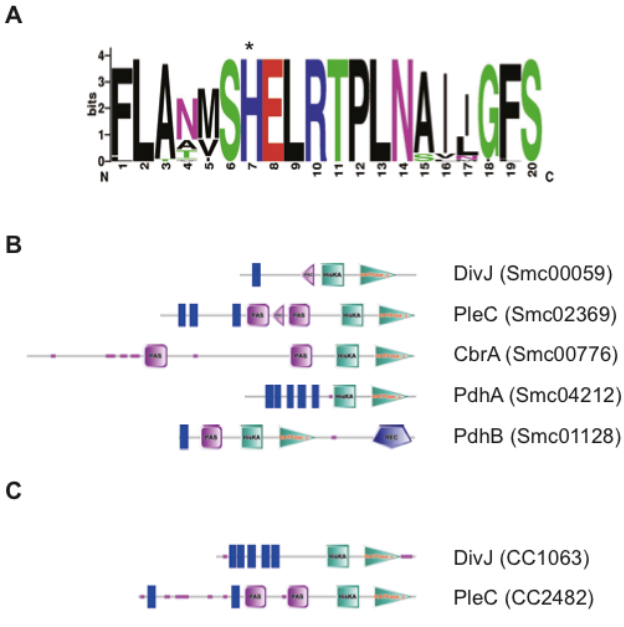


Figure 6. ***In silico* analysis of histidine kinases of the Pdh family interacting with.** A. PdhS (PleC DivJ Homolog) family specificity consensus based on the alignment in figure S2. Asterisk corresponds to the phosphorylated histidine; B. Pdh-family members in *S. meliloti*; domains were predicted by SMART (Letunic *et al.*, 2012); C. Domains organization of DivJ and PleC in *C. crescentus* predicted by SMART (Letunic *et al.*, 2012). Blue bars are the predicted transmembrane regions, the pink squares are predicted PAS domains, the pink triangles are predicted PAC domains, green squares are the HisKA domains that include the phosphorylated histidine residue, purple horizontal lines are intrinsically disordered regions and finally the HATPase_c domains are the green triangles (analysis performed using SMART database) (Letunic et al., 2102).

**DivJ and CbrA are *in vivo* kinases of DivK while PleC acts as a phosphatase.**

Our prediction identified 5 putative histidine kinases able to interact with DivK, but are those proteins really involved in control of DivK phosphorylation? Previous studies showed that CbrA controls DivK localization by controlling the phosphorylation of DivK (Sadowski *et al.*, 2013). Several other altered phenotypes of the *cbrA* null mutant were reported, such as abnormal EPS production and nodulation defects in alfalfa plants (Gibson *et al.*, 2006; Gibson *et al.*, 2007). PleC is essential in *S. meliloti*, influencing the septum localization and interactions with PodJ (Fields *et al.*, 2012), but no evidence of DivK control by PleC has ever been provided. Mutants of PdhSA and PdhSB, previously generated by mini Tn5 mutagenesis, were viable and did not show any abnormal growth or cell cycle phenotype (Pobigaylo *et al.*, 2006). Hence these two latter factors were

not analyzed further and we focused on the putative interactions of DivJ, PleC and CbrA with DivK *in vivo*.

First we compared the phenotypes of the *cbrA* mutant and the *divJ* deletion. We tested the ability to bind calcofluor (Gibson *et al.*, 2006), revealing that like the *cbrA*::Tn5 strain (KEG2016), the Δ*divJ* strain is brighter than wild type; in fact, the *divJ* deletion is much brighter than the *cbrA*::Tn5 strain (Fig. 7A). Since calcofluor is an indicator of alterations in envelope composition we tested the integrity of the cell envelope /resistance to osmotic stresses of Δ*divJ* by assaying the sensitivity of Δ*divJ* to the hydrophobic dye crystal violet in comparison with the *cbrA*::Tn5 and wild type cells. Both mutant strains were unable to form single colonies in LB supplemented with the crystal violet, while wild type cells could survive, suggesting an alteration of in the cell envelope composition (Fig. 7B). This is interesting because permeability of membranes and resistance to oxidative stress are important factors during the infection of legume hosts (Sharypova *et al.*, 2003; Campbell *et al.*, 2003).

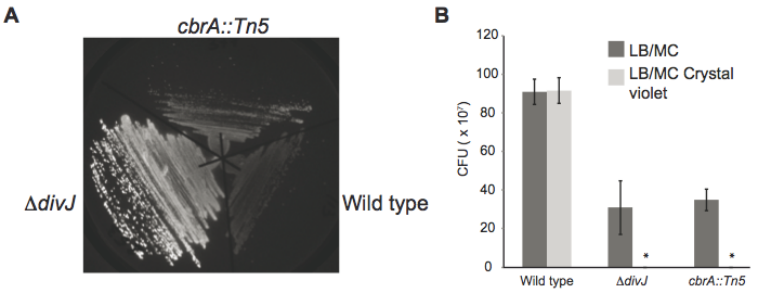


Figure 7 **Envelope-related phenotypes of Δ*divJ* and *cbrA*::Tn5.** A. Calcofluor staining of deletion of *divJ* in comparison with wild type and *cbrA*::Tn5 reveals that both *cbrA* and *divJ* mutants are brighter than wild type cells; B. Viable counts of the deletion of *divJ* in comparison with wild type and *cbrA*::Tn5 with Crystal violet dye revealed that both *divJ* and *cbrA* mutants are sensitive to crystal violet. $10^7$ cells were plated in LB/MC or LB/MC plus crystal violet.

In order to gain more information about the functions controlled by DivJ, transcriptome profile analysis of the *divJ* mutant was performed and compared with the transcriptome profile of *cbrA*::Tn5 (Gibson *et al.*, 2007). We first determined genes differentially expressed in the *divJ* mutant compared to the

wild type (Table 1). The analysis revealed genes that had altered expression in the *divJ* mutant compared with wild type cells; log ratios of the mutant vs. wild type are shown. A total of 16 genes were downregulated, including several flagellar genes (*fliE*, *flgG*, *flaA* and *flab*), as well as chemotactic genes (*mcpU*, *mcpZ* and *cheR*) and genes encoding putative manganese transporters (*sitB* and *sitC*). Also four genes encoding conserved hypothetical proteins, a putative transcription factor gene of the family of *merR,* and *gcvT*, possibly involved in catabolism of glycine were down regulated. Eighteen genes appeared to be up regulated, ten of which code for hypothetical proteins. Among the genes with an assigned function, *feuP* and five FeuP-controlled genes (Smb20838, SMc00198, Smc01557, SMc01586 and *ndvA*), and the *exoN2* and *pilA* genes, the latter encoding a pilin subunit, were upregulated. The upregulated gene encoding FeuP has previously been shown to control several genes such as SMc00198, SMc03900 (*ndvA*), SMc01586, SMc01557 that are required for cyclic glucan export and symbiosis (Griffitts *et al.*, 2008).

The differential expression of several genes in wild type versus Δ*divJ* that we observed in our microarray analysis was verified by creating *lacZ* fusions to the promoter regions of these genes and assaying beta-galactosidase activity. The results of the beta-galactocidase assays confirmed our microarray expression results. Since we had discovered that CtrA activity is higher in a Δ*divJ* strain, (Fig. 5), it was interesting to find that several genes upregulated in this mutant are preceded by a putative CtrA binding site (Brilli *et al.*, 2010). This included the *pilA* promoter whose expression levels are higher in the Δ*divJ* strain. This observation is consistent with the discovery that CtrA is upregulated

in the Δ*divJ* mutant, although the presence of the consensus CtrA site does not establish a regulatory role.

The limited number of genes discovered by the transcriptomic analysis could be explained by multiple post-translational regulatory controls that prevent the over-activity of CtrA; moreover it is possible to hypothesize that DivJ may have a role in preparing the raising of DivK-P levels, but it may not be present when CtrA is activated. Finally, the presence of multiple cell types in Δ*divJ* in which presumably transcriptomic profiles are antithetic may buffer differences in gene expression, suggesting that the window of activity of DivJ, although important, could be very limited in time.

Many of the genes (19 genes out of 34) putatively controlled by DivJ were also found to be influenced by CbrA (Gibson *et al.*, 2007), indicating a common pathway between the two histidine kinases possibly involving DivK. This observation is also consistent with the observation that both DivJ and CbrA appear to be involved in CtrA activity repression (Figure 5). Additionally, *cbrA*::Tn5 showed significantly higher levels of CtrA-P (Fig. 5C) suggesting that both DivJ and CbrA participate in similar functions.

Since in *C. crescentus* DivK is essential, we investigated whether DivK was also essential in *S. meliloti*. Using a two-step recombination strategy, we first constructed an *S. meliloti* strain in which *divK* coding sequence was replaced by tetracycline resistance cassette, complemented by the *divK* locus including the promoter. We then selected for excision of the integrative plasmid by plating on sucrose medium. We were able to select sucrose resistant colonies only when the complementing plasmid was present, suggesting the essentiality of DivK (data not shown). To gain additional support for the conclusion that DivK is essential

in *S. meliloti,* we also attempted to transduce the *divK* deletion into several genetic backgrounds as reported in Table S2. Again, we were only successful in introducing the *divK* deletion when an extra copy of *divK* was present. These data confirm that is *divK* is essential in *S. meliloti*. We confirmed *in vivo* the importance of the putative phosphorylated site of DivK, the aspartate in position 53 (D53), by overexpressing *divK* and *divK(D53A).* Overexpression of *divK*, but not overexpression of *divK(D53A)* caused cell cycle defects in *S. meliloti* (Fig. S4B). DivK overexpression produced cells with abnormal morphologies, resembling the morphological phenotype produced by DivJ overexpression (Fig. S4A).

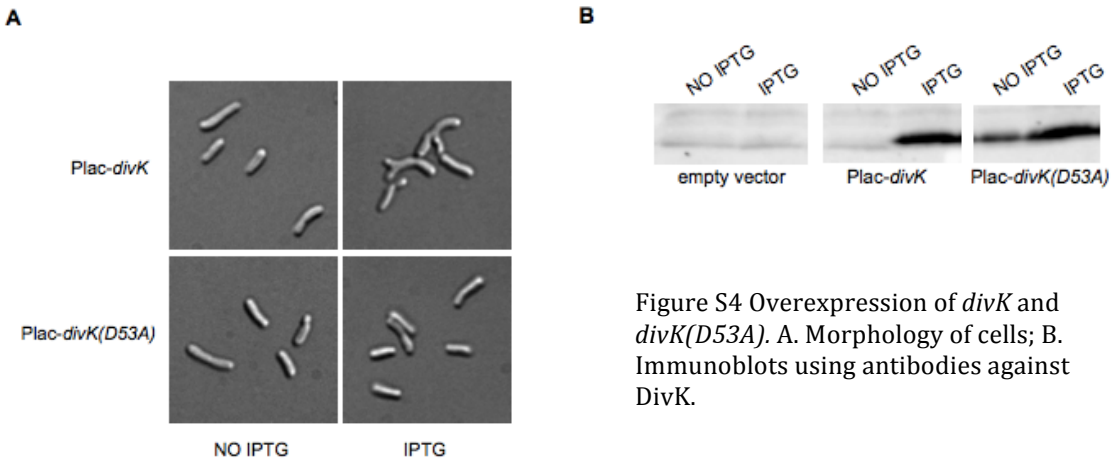


Figure S4 Overexpression of *divK* and *divK(D53A).* A. Morphology of cells; B. Immunoblots using antibodies against DivK.

Next we tested the hypothesis that DivJ and CbrA were synergic, by attempting to combine the deletion of *divJ* with the *cbrA::*Tn5 mutant, using a phage lysate produced by infection of BM253. Although *cbrA*::Tn5 is sensitive to phage infection (data not shown), allowing transduction, we could not recover any colonies when we attempted to transduce the *divJ* deletion strain, while the same transduction with wild type as recipient yielded hundreds of colonies (Fig. 4A). This result suggests that the combination of the *divJ* and *cbrA* mutations is lethal in *S. meliloti*. However, we were able to create a double conditional mutant

Δ*divJ* and *cbrA*::Tn5 that was able to survive by expressing *divJ* from an inducible promoter ($P_{lac}$) in the presence of IPTG, while the transduction without IPTG did not yield any colonies, thereby confirming the lethality of the *divJ cbrA* double mutation (EB602).

To determine the *in vivo* activity of each predicted DivK kinase/phosphatase we measured the DivK phosphorylation levels in different backgrounds (Δ*divJ, cbrA*::Tn5, Δ*pleC*+$P_{lac}$-*pleC*), as described for CtrA, this time using anti-DivK antibodies raised in rabbit. The anti-DivK antibodies were able to detect two bands in Phos-Tag SDS-Page gels, one of which corresponded to the phosphorylated form that disappeared by boiling the sample, which destroys the labile phosphate bond (Fig. 8A) (Barbieri and Stock, 2008).

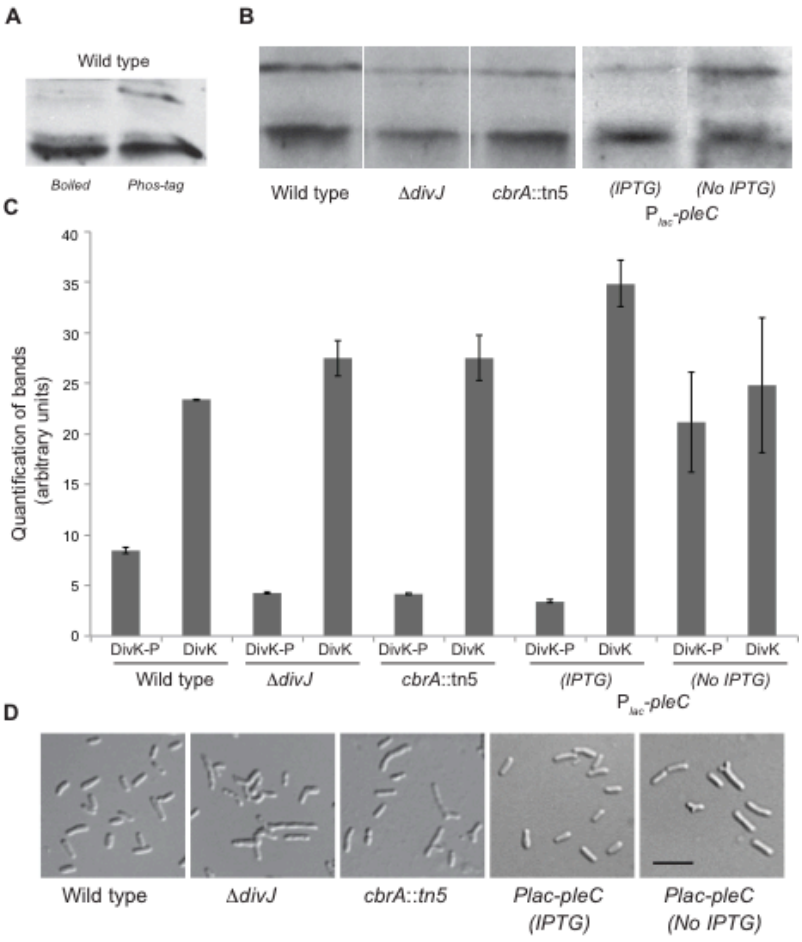


Figure 8. **DivJ and CbrA are required for DivK phosphorylation, while PleC acts as a phosphatase** A. SDS-PAGE Phos-tag™ gel detects phosphorylation of DivK *in vivo* in wild type; boiling step ("boiled"), which breaks the phosphate bond, specifically affected the upper band; B. SDS-PAGE Phos-tag™ gel shows phosphorylation of DivK *in vivo* in wild type, D*divJ, cbrA*::Tn5 and *pleC* depletion (After 7 h) genetic backgrounds; C. Quantification of phosphorylation levels of DivK *in vivo* in wild type, D*divJ, cbrA*::Tn5 and *pleC* depletion genetic backgrounds. The average of three experiments is shown. D. Morphologies of cells of D*divJ, cbrA*::Tn5 and *pleC* depletion genetic backgrounds. This latter condition is shown with 1mM IPTG and after washes, without IPTG for 7 hours. The black bar corresponds to 3 mm.

Phosphorylation of DivK *in vivo* (Fig. 8B), together with previous results, demonstrated that DivJ is a kinase of DivK and also that CbrA is involved in this DivK phosphorylation, as the level of DivK-P dropped by about half in both strains (Fig. 8C). This result is consistent with analyses showed in the previous sections for DivJ and similar to the conclusion recently published for CbrA (Sadowski *et al.*, 2013). It also suggests that, as the combination of DivJ and CbrA mutations is lethal, phosphorylation of the essential factor DivK is also essential in *S. meliloti* cells. We also measured *in vivo* phosphorylation of DivK in the *pleC* depletion strain (EB601). Using 100 uM IPTG, the *pleC* depletion strain showed a mild overexpression of PleC, but had DivK phosphorylation levels similar to D*divJ* (Fig 8C). After 6 hours of *pleC* depletion DivK-P levels were 2 fold higher than wild type, demonstrating that in *S. meliloti* PleC plays an opposite role of DivJ and is involved in maintaining low levels of DivK-P, as observed in *C. crescentus.*

Next we tested whether it was possible to rescue the lethal phenotype of Δ*pleC* by transducing this deletion in *cbrA*::Tn5 or Δ*divJ* backgrounds (Table S3). We found that it was only possible to transduce the *pleC* deletion into a strain carrying the *cbrA* mutation (EB630). The observation that only CbrA mutation (not DivJ) is able to rescue the lethality of *pleC* deletion is puzzling but it could be explained by introducing other regulatory levels of these kinases besides the simple contribution to the chemical equilibrium of DivK/DivK-P. For example DivJ, CbrA and PleC could be expressed at different times and/or present in different subcellular locations during the cell cycle. This regulation in time and space could suggest that DivJ is never together PleC while the soluble kinase

CbrA could be co-localized with PleC therefore influencing DivK/DivK-P levels at the same time/space as PleC.

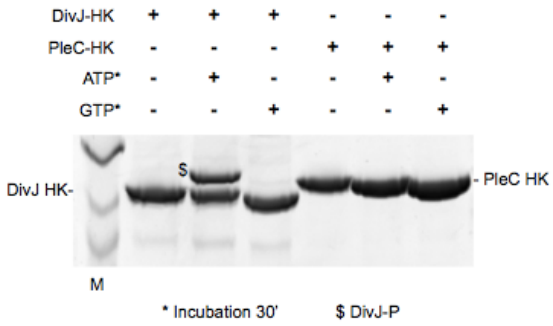


Figure S5 Comparison between DivJ and PleC kinase domains in a phosphorylation assay. Purified DivJ histidine kinase domain is able to auto-phosphorylate a histidine residue using ATP (not GTP) as the phosphate source. DivJ in presence of ATP gives two distinct bands in a SDS-PAGE Phos-tag™ gel. PleC preparation is not able to autophosphorylate using ATP or GTP.

In order to test the enzymatic capability of PleC and CbrA to phosphorylate DivK *in vitro*, as we did for DivJ, we attempted to purify both HK domains. We cloned the HK domains of both PleC and CbrA and expressed them in *E. coli* cells. PleC was soluble and purified well, as shown in Fig. S5. In contrast, several preparations of CbrA were all insoluble; therefore no *in vitro* experiments were performed with CbrA. In contrast to the DivJ HK, the preparation of PleC HK did not show any autokinase activity with either ATP or GTP, suggesting that for PleC the sensor part of the protein and/or specific signals are required to activate this kinase *in vitro*. Nevertheless, taken together the in vivo results, the genetic experiments, the high degree of homology of PleC-CbrA-DivJ, and the recent results with CbrA (Sadowski *et al.*, 2013) strongly support a direct role of CbrA and PleC in controlling DivK-P levels.

**DivJ activity is required for the symbiotic process.** The alteration of the cell cycle that occurs during bacteroid differentiation in the symbiotic process suggests a possible role for cell cycle regulators, a conjecture supported by previous experiments on the cell cycle regulators CbrA (Gibson *et al.*, 2006) and CpdR (Kobayashi *et al.*, 2009). We therefore tested the ability of the *divJ* mutant (BM253) to nodulate and fix nitrogen in *M. sativa* (Fig. 9). Plants inoculated with

the Δ*divJ* mutant had similar appearance and dry weight to non-infected plants, suggesting that nitrogen fixation was impaired (Fig. 9A). The Δ*divJ* mutant was able to induce nodule formation but, compared to the nodules elicited by the wild type strain, these were more abundant, smaller, white, and abnormal in shape (Fig. 9B). Therefore we tested if cells lacking DivJ were able to invade the nodule cells. We infected alfalfa plants using GFP-tagged wild type and Δ*divJ* strains (Fig. 9C). Both nodules of wild type and Δ*divJ* showed GFP signal inside the internal part of the nodule tissue, suggesting infection by bacteria. Sections of nodules containing wild type or Δ*divJ* cells were also stained with the bacteria-specific Toluidine blue and observed under the microscope (Fig. 9C) in order to understand if mutants were able to enter the plant cells and their ability to proliferate inside. It was evident that bacteria of Δ*divJ* were able to infect plant cells inside the nodule, however starch accumulation was present, which is usually a sign of inefficient symbiosis. Normally, starch accumulates in root cells before the infection and then when symbiosis is established the granules are quickly metabolized (Hirsch *et al.*, 1983). As expected, the Δ*divJ* strain complemented with wild type *divJ* (BM224) gave a normal symbiotic phenotype.

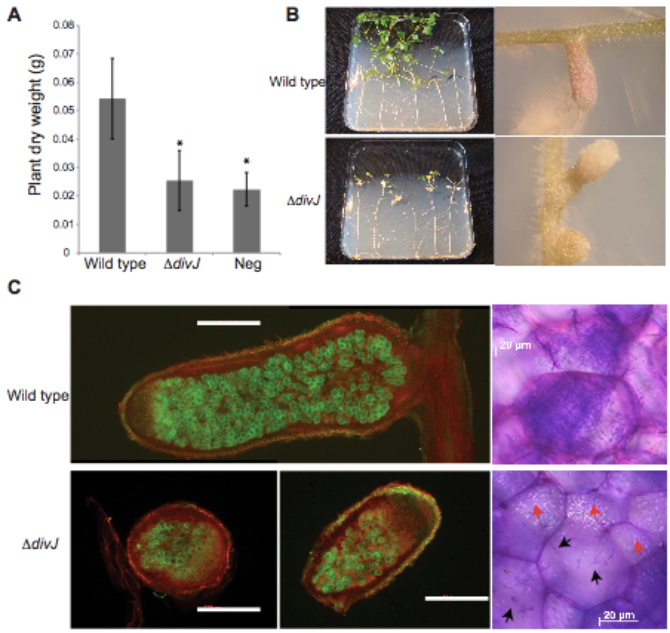


Figure 9. **Symbiotic efficiency of Δ*divJ*.** A. Histogram with the dry weight of alfalfa plants infected by *S. meliloti* wild type and Δ*divJ* (neg = un-inoculated control); B. Pictures of five plants and details on nodules. C. Nodules from an infection of alfalfa plants using GFP-tagged strains (green), wild type is strain Rm1021G and Δ*divJ* is BM253G (Table S4); on the left (white bars correspond to 500 mm) and Toluidine blue staining on the right. Black arrows indicate bacteria inside plants cells, red arrows indicate starch granules.

This result suggests that Δ*divJ* is not able to infect efficiently alfalfa plants possibly due to high CtrA levels in Δ*divJ* cells that may be responsible for the severe symbiotic defects, impairing the ability of the cell to grow, differentiate, or survive in plant cells, as CtrA protein and phosphorylation levels are both high in D*divJ*. Similar results involving a strain with putative high levels of CtrA, were also documented for the null mutant of CpdR, a response regulator required for proper CtrA proteolysis in *C. crescentus* (Kobayashi *et al.*, 2009).

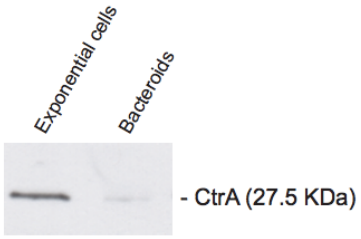


Figure S6 Immunoblot using antibodies against CtrA on normal culture cells and bacteroids isolated form mature nodules of alfalfa (see Experimental Procedures).

In order to test the hypothesis that CtrA levels or activity should be low in bacteria infecting plant cells, we isolated bacteroids from mature nitrogen fixing nodules and measured CtrA protein levels by immunoblot (Figure S6). The same number of bacteroids and wild type cells was loaded in the SDS-Page gel. Our results clearly showed that CtrA in bacteroids, although more protein content was loaded, was absent. This observation may explain why the deletion mutant of *divJ,* the *cbrA*::Tn5 mutant, and also the null mutant of *cpdR,* which have all high CtrA levels, are compromised in the establishment of an efficient symbiosis.

**Conclusions**

Our biochemical and genetic investigation of the histidine kinase DivJ, and its relationship with CbrA and PleC, sheds light on the DivK cell cycle regulatory module in *S. meliloti* and unveils an association between cell cycle regulation and symbiosis. We propose here a model (Fig. 10) in *S. meliloti* where DivJ is a kinase of the essential response regulator DivK. CbrA is also involved in DivK

phosphorylation, while PleC, as in *C. crescentus,* may act as phosphatase. Although the putative cell cycle regulated activity (regulation in time) of CbrA, DivJ and PleC and their subcellular localization (regulation in space) have not been completely investigated, we can hypothesize that these kinases create a complex sensory module that is able to coordinate the phosphorylation levels of the essential factor DivK in time and space.

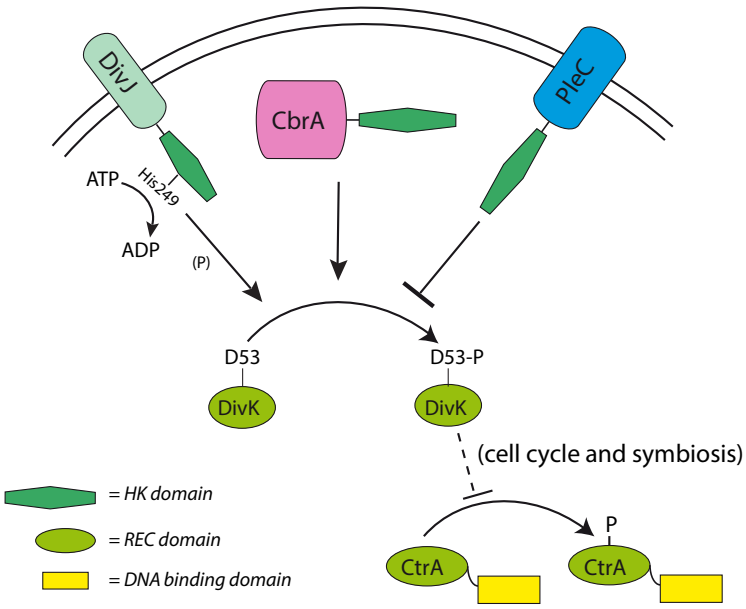


Figure 10. **Functional scheme of DivK control system of CtrA.** DivK is phosphorylated on the aspartate 53 by the membrane histidine kinase DivJ (conserved residue H249 and ATP) and presumably by the soluble histidine kinase CbrA. The absence of both kinases from *S. meliloti* is a lethal condition, presumably abolishing DivK phosphorylation. Also the deletion of the membrane histidine kinase PleC is lethal (Fields *et al.*, 2012); results presented here show that PleC is involved in de-phosphorylation of DivK. Finally we showed here that DivJ is negatively acting on CtrA and apparently CtrA inactivation is required for an efficient symbiosis, presumably through degradation of the protein. In fact, mature bacteroids do not show detectable CtrA levels, suggesting that one of the symbiotic problems of Δ*divJ* is the high level of activity of CtrA.

As in *C. crescentus* the phosphorylated DivK acts negatively on CtrA, which in turn plays a positive role for the biogenesis of polar structures and cell division. Unlike in *C. crescentus,* both DivK phosphorylation and dephosphorylation are essential in *S. meliloti*. This essentiality is indicated by the lethality of both the *divJ-cbrA* double mutant and the *pleC* deletion mutant and our *in vivo* phosphorylation data. The comparison between *S. meliloti* and *C. crescentus* suggests that the genetic architecture that controls cell cycle regulation in *Alphaproteobacteria*, although similar in all *Alphaproteobacteria*,

also exhibits certain differences, possibly due to different levels of redundancy of feedbacks and regulatory connections. This has been recently observed in *Agrobacterium tumefaciens,* in which cell cycle regulation shows specific characteristics despite being generally similar to the other *Alphaproteobacteria* (Kim *et al.*, 2013).

An interesting feature of the cell cycle defects discovered in *S. meliloti* is the high degree of branching that has been observed when levels of phosphorylated DivK are low. This feature, which is absent in *C. crescentus* cell cycle mutants, may be related to the polar asymmetric growth of peptidoglycan observed in *Rhizobiales* (Brown *et al.*, 2012).

Our investigation of the role of the DivK module during symbiosis revealed that bacteroids are deficient of CtrA and strains with putative high CtrA levels, as the Δ*divJ* in this study, *ΔcbrA* (Sadowski *et al.*, 2013) or the CpdR mutant (Kobayashi *et al.*, 2009) are directly impaired in establishing an efficient symbiosis. As mentioned in the introduction, CpdR is a response regulator that is required for CtrA proteolysis in *C. crescentus*. The *S. meliloti cpdR* mutant showed the ability to penetrate into the nodule and infect plant cells, but it failed to differentiate in bacteroids. Previous studies indicated that bacteroids have an interrupted cell cycle, associated with the multiplication of the chromosome number, a block of cell division, inducing enlargement of cell bodies, and the consequent loss of the ability to multiply (Mergaert *et al.*, 2006).

The ability of the Δ*divJ* mutant to infect alfalfa plant cells and enter the cytoplasm of nodule cells suggest that DivJ is not required in early steps of the infection process outside the roots or inside the infection thread. The symbiotic efficiency, however, is impaired since plants infected by the Δ*divJ* mutant are

similar in size to non-inoculated ones and the histology of the nodule tissue revealed many starch granules, typical of inefficient nitrogen fixation. Also the low number of bacteria inside plant cells in comparison with plants infected by wild type suggests problems in the inside the infection thread or endocytosis or multiplication inside the plant cell cytoplasm or problems in the differentiation process. Those problems may be related to the growth defects of the *divJ* mutant observed in the free-living state. Also this symbiotic defect of the *divJ* mutant could be associated to the phenotypes correlated to envelope integrity we observed in this work, such as increased envelope material detected by calcofluor staining or increased sensitivity to oxidative stresses (Fig. 7). However, combined with previous studies, our results suggest that mutations in the cell cycle factors that play a negative role on CtrA (CpdR, DivJ, CbrA) result in a symbiotic defect. Since, DivJ and CbrA, are involved in the inhibition of CtrA, it appears that a high level of CtrA may interfere negatively with the symbiotic process leading to the speculation that bacteroid differentiation requires the down-regulation of CtrA. Direct support for this hypothesis is provided by our discovery that that mature bacteroids have no CtrA. Perhaps plants are able to block cell cycle of infectious rhizobia by affecting the master regulator CtrA. Proper regulation of CtrA may be required to respond to plant inhibitory activity. Alternatively, one could speculate that strains with lower CtrA activities may show a higher symbiotic activity that could be exploited to increase symbiosis efficiency.

**Experimental Procedures**

***Bacterial strains, plasmids, cloning and growth conditions*.** The bacterial strains and plasmids used in this study are described in Table S4. *Escherichia coli*

strains were grown in liquid or solid Luria-Bertani (LB) broth (Sigma Aldrich) (Sambrook *et al.*, 1989) at 37°C supplemented with appropriate antibiotics: kanamycin (50 µg/ml in broth and agar), tetracycline (10µg/ml in broth and agar). *S. meliloti* strains were grown in broth or agar TY (Beringer, 1974) supplemented when necessary with kanamycin (200 µg/ml in broth and agar), streptomycin (500 µg/ml in broth and agar), tetracycline (1 µg/ml in liquid broth, 2 µg/ml in agar), nalidixic acid (10 µg/ml in broth and agar) as necessary. For negative selection 10% sucrose was added to agar plates. For calcofluor analyses, LB agar was buffered with 10 mM MES (morpholine-ethane-sulfonic acid), pH 7.5, and calcofluor white MR2 Tinopal UNPA-GX (Sigma Aldrich) was added at a final concentration of 0.02%.

For conjugation experiments, $1\times10^9$ *S. meliloti* and $0.5\times10^9$ *E. coli* S17-1 cells (Simon *et al.*, 1983) were used and incubated 24h at 30° C. For creating the deletion of *divJ, divK* and *pleC*, two fragments of about 1000-bp long amplifying the upstream (P1-P2) and downstream (P3-P4) regions respectively of the target genes were amplified by PCR. For *divJ* the deletion cassette was constructed as previously described (Skerker *et al.*, 2005). For *pleC* and *divK*, instead, restriction enzymes sites for directional forced cloning with the tetracycline resistance cassette were used. All plasmids were then sequenced for verification. The first six and last 12 codons of each gene deleted were left intact to protect against disruption of possible regulatory signals for adjacent genes. Two-step recombination of deletion cassettes was conducted as previously described using integrative plasmid pNPTS138 (Skerker *et al.*, 2005). Deletion of genes was verified by PCR using primers pSmc00059_P1tris, pSmc00059_P4tris,

pSmc02369_Pext_fw, pSmc02369_Pext_rv and pSmc02369_Pint_fw, pSmc01371_P1ext and pSmc01371_P4ext.

For transduction, phage and bacteria (in LB containing 2.5 mM $CaCl_2$ and 2.5 mM $MgSO_4$) were mixed to give a multiplicity of infection 1/2 (phage/cell). The mixture was incubated at 30°C for 30 min.

For construction of the complementation plasmid, *divJ* and *pleC* and their putative promoter regions were amplified by PCR using the Rm1021 genomic DNA as template and primers specific to those regions. Fragments were gel purified and cloned into the low copy vector pMR10 (Roberts *et al.*, 1996). Plasmids obtained were introduced in *S. meliloti* strains by electroporation (Ferri *et al.*, 2010).

The *divJ* gene for overexpression *in vivo* was amplified from genomic DNA of *S. meliloti* Rm1021 by PCR using pSmc00059_P0 and pSmc00059_P6, digested by restriction (NdeI and XhoI) and ligated in pSRKKm (previously restricted with the same enzymes), generating pSRKKm*divJ*, which was transferred to Rm1021 by electroporation. Similarly pSRKGm-*divJ*, pSRKKm*pleC,* pSRKKm*ctrA* and pSRKKm*divJ*(D249A), pSRKKm*divK* and pSRKKm*divk* (D53A) were constructed. The *divJ* H249A mutant was constructed on the plasmid pSRKKm*divJ* using PfuTurbo DNA polymerase (Stratagene) as previously described (Biondi, Reisinger, *et al.*, 2006).

For β-galactosidase assay, plasmids were constructed by directional forced cloning of pRKlac290 (Alley *et al.*, 1991) digested with BamHI and XbaI with fragments (600bp) of the Smc0360 and Smc0949 promoter regions amplified with the primers pSmc0360_prom_XbaI, pSmc0360_prom_BamHI,

pSmc0949_prom_XbaI and pSmc0949_prom_BamHI. β-galactosidase assay was performed as previously described (Fioravanti *et al.*, 2013).

For the efficiency-of-plating (EOP) assays, cultures were grown to exponential phase ($OD_{600}$, ≈0.5) in LB/MC medium and then diluted to an $OD_{600}$of 0.1 of LB. Each sample was serially diluted up to $10^{-6}$ in LB, and spread onto LB agar containing either crystal violet (Sigma) or IPTG (1mM). After 4 to 5 days of growth at 30°C, the number of CFU was determined, with the exception of the *ΔdivJ* and *cbrA*::Tn*5* mutant, which required an additional 48 h of growth at 30°C for colonies to appear. The average and standard deviation for each strain were derived from two independent cultures.

***FACS analysis*.** Cells were cultured into LB/MC and grown to OD600 ca. 0.1-0.2 with the appropriate antibiotic. Samples were taken and fixed in 70% ethanol overnight. Fixed cells were centrifuged at and resuspended in 1mL of 50mM sodium citrate buffer plus 100 mg/mL RNaseA and then incubated for two hours at 50° C. After the RNaseA treatment 1uL of a 1:6 dilution of Sytox Green dye (Invitrogen) was added to each sample. Each sample was then read using a FACScan flow cytometer and results were plotted using Flojo software.

***Transcriptome analysis: microarray-based gene expression profiling*.** In this study, we applied the Sm14kOLI microarray carrying 50mer to 70 mer oligonucleotide probes directed against coding and intergenic regions of the *S. meliloti* Rm1021 genome (Galibert *et al.*, 2001). Each of the 6208 coding regions predicted by Galibert et al. (2001) were represented by a single oligonucleotide whereas both strands of the intergenic regions were covered by 8080 oligonucleotides. Intergenic oligonucleotides mapped at distances of ~50 to 150

nucleotides to the intergenic regions. The microarray layout and oligonucleotide sequences are available at ArrayExpress accession no. A-MEXP-1760.

Production and processing of microarrays were done as described in (Brune *et al.*, 2006). Four biological replicates of control strain 1021 or experiment strain BM253 were grown in 100 ml TY supplemented with nalidixic acid medium to an OD600 of 0.6. RNA isolation, cDNA synthesis, labeling, hybridization, image acquisition and data analysis were done as described in (Serrania *et al.*, 2008). To identify significant up- or down-regulated genes, EMMA 2.2 microarray data analysis software (Dondrup *et al.*, 2003) was used for LOWESS normalization and t statistics. Genes were classified as differentially expressed if $p \leq 0.05$ and $M \geq 0.5$ or $\leq -0.5$. The M value represents the $\log_2$ ratio between both channels. Microarray data were submitted to ArrayExpress (Accession number).

***In vitro and in vivo phosphorylation*.** We use Phos-tag™ Acrylamide (Nard Chemicals, LTD, Japan) in order to separate and visualize in SDS-Page gels the phosphorylated form (on histidine and aspartate residues) of CtrA, DivJ and DivK as previously described (Barbieri and Stock, 2008). Bands corresponding to the phosphorylated forms of CtrA and DivK were empirically recognized by a simple boiling step that affects specifically the stability of phosphate. Due to this instability all samples were lysed and directly loaded on gels unless specifically indicated.

For biochemical assays (Fig. 3), *S. meliloti* DivJ (just the kinase domain), DivJ H249A (the kinase domain), PleC (the kinase domain), DivK and Divk D53A were PCR amplified, expressed in *E. coli* BL21 and purified as previously described (Fioravanti *et al.*, 2012). The *divK* D53A mutant was prepared from a

plasmid containing wild-type *divK* performing a site-directed mutagenesis using PfuTurbo DNA polymerase (Stratagene) as previously described (Biondi, Reisinger, *et al.*, 2006). Several clones were sequence verified to confirm the presence of the mutation.

Phos-tag™ Acrylamide SDS-PAGE gels (29:1 acrylamide:N,N''-methylene-bis-acrylamide) were prepared with 50 µM Phos-tag™ acrylamide and 100 µM $MnCl_2$ for *in vitro* phosphorylation assays (figure 3) or 25 µM Phos-tag™ acrylamide and 50 µM $MnCl_2$ for *in vivo* phosphorylation analysis (Figures 5 and 8). All gels were run at 4˚C under constant voltage (100 V). In vitro phosphorylation assays were performed using HK 10 mM, ATP 1 mM, $MgCl_2$ 5 mM in HKEDG buffer (10 mM HEPES-KOH pH 8.0, 50 mM KCl, 10% glycerol, 0.1 mM EDTA, 2 mM DTT). Incubation was performed RT and removal of ATP was done by filtration 4 times with HKEDG/Mg buffer using Amicon Ultra 0.5 10 KDa (Millipore).

For *in vivo* analysis, strains were grown to mid-log phase, and then 2ml of the cells were pelleted and stored at -80˚C. Pellets were resuspended using a lysis buffer with 10 mM Tris-Cl, pH 7.5 and 4% SDS and incubated at RT for 5 min, then the loading dye was added. Samples were stored on ice for a short time (<10 min) prior to loading onto Phos-tag™ acrylamide gels. Gels were fixed for 10 min in transfer buffer (50 mM Tris-Cl, 40 mM glycine, 15% (v/v) ethanol,) with 1 mM EDTA to remove $Mn^{2+}$ from the gel. Gels were washed 3 times in transfer buffer without EDTA to remove the chelated metal. Immunoblots were performed using Western Blot Signal Enhancer (Thermo Pierce) with rabbit anti-CtrA (1:5000) or anti-DivK (1:2500) primary antibodies. Chemiluminescent detection was performed using Super Signal West Pico Chemiluminescent

Substrate (Thermo-Pierce). Bands intensities were analyzed using ImageJ (Schneider *et al.*, 2012).

***Nodulation assays and GFP Strains construction.*** To observe infected cells using eGFP-expressing bacteroids, a mutated constitutive *S. meliloti sinR* promoter region was amplified by PCR from the pSRmig (McIntosh *et al.*, 2009) derivative pSRmigPsinR171mutcc (Matthew McIntosh) using primer pairs psinRmut_fwd and psinRmut_rev. The fragment was inserted into KpnI and XbaI sites of the integrating pG18mob derivative pGEE upstream of EGFP, resulting in vector pGECE. The construct was transferred by *E. coli* S17-1-mediated conjugation to *S. meliloti* Rm1021 or BM253 and integrated into the chromosome by homologous recombination.

*Medicago sativa* seeds (cv. Eugenia seeds, Samen-Frese, Osnabrück) were surface sterilized and germinated as described (Müller *et al.*, 1988). 48h-old seedlings were transferred to square petri plates containing buffered nodulation medium (BNM) agar (Ehrhardt *et al.*, 1992). The seedlings were inoculated with 200ul bacteria culture, which was grown to logarithmic phase in TY medium supplemented with nalidixic acid and washed in BNM medium. Plant growth and nodule development were screened over the duration of four weeks. After 28 days, plant height, plant dry weight and number of nodules per plant were measured. Images of plant plates and nodules were acquired, and microscopy images of nodule thin cuts were taken. Bacteroids were extracted from alfalfa mature nodules as previously described (Finan *et al.*, 1983).

***Microscopy.*** *S. meliloti* cells were grown to mid-log phase, fixed in 70% ethanol, washed, and concentrated with saline solution (0.85% NaCl). Samples were deposited on microscope slides coated with 0.1% poly-L-lysine. Differential

interference contrast and fluorescence imaging of nodules was done on a Zeiss Observer Z1 inverted microscope using Zeiss Axiovision software. Exponential phase bacteria were immobilized on 1% agarose slides and imaged using an alpha Plan-Apochromat 100x/1.46 OilDIC objective and Zeiss AxiocamMR3 camera. Nodule thin sections (100 mm) were stained with 16 mM FM4-64 membrane stain, and imaged using an EC Plan-Neofluar 5x/0.16 Ph1 objective and AxiocamMR3 camera, or using a Plan-Apochromat 40x/0.95 DICII objective and AxiocamHRc color camera. Images were processed with ImageJ (Schneider *et al.*, 2012).

**Acknowledgements**

We gratefully acknowledge support from the Ente Cassa di Risparmio di Firenze, Accademia dei Lincei and Fondazione Buzzati-Traverso (Italy). This project was also supported by ANR (JCJC-CASTACC), the Region Nord-Pas-de-Calais (France) and the LOEWE program of the State of Hesse, Germany. G.C.W. and N.J.D. were supported by NIH grant GM31010. G.C.W. is an American Cancer Society Professor.

**Table 1.** Transcriptome profile of the *S. meliloti divJ* deletion vs. wild type

| Gene code | Annotation | Log-Ratio | CbrA array* | CtrA bs[$] |
|---|---|---|---|---|
| *Down-regulated* | | | | |
| SMa0281 | Putative regulator, MerR family | -0.61 | | |
| SMc00888 | Response regulator | -0.99 | y (-) | y |
| SMc00765 | *mcpZ* | -0.65 | y (-) | |
| SMc00975 | *mcpU* | -0.52 | y (-) | |
| SMc03009 | *cheR* | -0.63 | y (-) | |
| SMc02047 | *gcvT* | -0.51 | | |
| SMc02507 | *sitC* | -0.54 | | |
| SMc02508 | *sitB* | -0.64 | | |
| SMc03029 | *fliE* | -0.58 | y (-) | |
| SMc03030 | *flgG* | -0.72 | y (-) | |
| SMc03037 | *flaA* | -0.51 | y (-) | y |
| SMc03038 | *flaB* | -0.78 | y (-) | |
| SMc02104 | Conserved hypothetical protein | -0.57 | | |
| SMc00360 | Conserved hypothetical protein | -0.62 | y (-) | y |
| SMc03013 | Conserved hypothetical protein | -0.66 | y (-) | |
| SMc03057 | Conserved hypothetical protein | -0.51 | y (-) | |
| *Up-regulated* | | | | |
| SMb20838 | putative secreted Ca2+-binding protein | 0.57 | y (+) | |
| SMc00949 | Conserved hypothetical protein | 0.76 | y (+) | |
| SMc01557 | Hypothetical signal peptide protein | 0.74 | y (+) | |
| SMa1043 | Hypothetical protein | 1.45 | | |
| SMb21069 | Hypothetical protein | 2.16 | | |
| SMb21440 | Hypothetical protein | 1.16 | y (+) | |
| SMc00198 | Hypothetical protein | 0.59 | y (+) | |
| SMc01586 | Hypothetical protein | 0.75 | y (+) | |
| SMc03999 | Hypothetical protein | 0.65 | | |
| SMc02051 | Conserved hypothetical protein | 0.56 | | y |
| SMc02052 | Conserved hypothetical protein | 0.56 | | |
| SMc02266 | Conserved hypothetical protein | 0.83 | y (+) | |
| SMc02900 | Conserved hypothetical protein | 0.96 | | |
| SMc03100 | Conserved hypothetical protein | 0.66 | | |
| SMc00458 | *feuP* | 1.48 | | |
| SMc03900 | *ndvA* | 0.54 | y (+) | |
| SMc04023 | *exoN2* | 0.55 | | |
| SMc04114 | *pilA1* | 0.54 | | y |

**Table S2.** Transduction of tetR deletion of *divK* in different genetic backgrounds.

| Recipient strain | Number of transduced colonies (cfu/ml) |
|---|---|
| Rm1021 + pMR10 | 0 |
| Rm1021 + pMR10-*divK* | 87 |

**Table S3.** Transduction of tetR deletion of *pleC* in different genetic backgrounds.

| Recipient strain | Number of transduced colonies (cfu/ml) |
|---|---|
| Wild type | 0 |
| cbrA::Tn5 | 51 |
| DdivJ | 0 |
| 1021 + pMR10 *pleC* | 122 |

**Table S4.** Strains and Plasmids

| Organism or plasmid | Strain or plasmid name | Description | Resistence | Source |
|---|---|---|---|---|
| Strains | | | | |
| *S. meliloti* | Rm1021 | SU47 *str-21* | Sm | (Galibert, *et al.*, 2001) |
| | Rm1021G | Rm1021 + pGECE | | This work |
| | KEG2016 | *cbrA*::Tn*5* | Sm, Km | (Gibson, *et al.*, 2006) |
| | BM224 | Rm1021 Δ*divJ* ::tc + pMR10 *divJ* | Sm, Km, Tc | This work |
| | BM253 | Rm1021 Δ*divJ* ::tc pMR10 (deletion transduced from BM224) | Sm, Km, Tc | This work |
| | BM253G | BM253 + pGECE | | This work |
| | BM317 | Rm1021 + pSRKKm*divJ* (S.mel) | Sm, Km | This work |
| | EB775 | Rm1021 + pSRKKm*divJ* H249A (*S.meliloti*) | Sm, Km | This work |
| | BM240 | Rm1021 + pSRKKm*ctrA* (S.mel) | Sm, Km | This work |
| | BM264 | Rm1021Δ*divJ*::tc+ pSRKKm*ctrA* (*S.meliloti*) | Sm, Km, Tc | This work |
| | EB594 | Rm1021 + pJS70 | Sm, Tc | This work |
| | EB638 | Rm1021Δ*divJ*::tc + pJS70 | Sm, Tc | This work |
| | EB593 | Rm1021*cbrA*::tn5 + pJS70 | Sm, Km, Tc | This work |
| | EB602 | Rm1021Δ*divJ*::tc + *cbrA*::tn5 +pSRK Gm *divJ* | Sm, Km, Tc, Gm | This work |
| | EB601 | Rm1021Δ*pleC* + pSRKKm *pleC* | Sm, Km, Tc | This work |
| | EB630 | Rm1021Δ*pleC* + *cbrA*::tn5 | Sm, Km, Tc | This work |
| | EB704 | Rm1021 + pMR10 *divK* | Sm, Km | This work |
| | EB705 | Rm1021 + pSRK Km *divK* | Sm, Km | This work |
| | EB710 | 1021Δ*divK* + pMR10 *divK* | Sm, Km, Tc | This work |
| | EB775 | Rm1021 + pSRKKmdivJ H249A | Sm, Km | This work |
| | EB841 | Rm1021 + pSRK Km divK D53A | Sm, Km | This work |
| | EB864 | Rm1021 + pFP01 | Sm, Tc | This work |
| | EB865 | Rm1021 + pFP02 | Sm, Tc | This work |
| | EB866 | Rm1021Δ*divJ* + pFP01 | Sm, Tc | This work |
| | EB868 | Rm1021Δ*divJ* + pFP02 | Sm, Tc | This work |
| | EB825 | Rm1021 pdhA plasmid insertion | Sm, Km | (Pobigaylo *et al.*, 2006) |
| | EB826 | Rm 2011 pdhB::Tn5_1 | Sm, Km | (Pobigaylo *et al.*, 2006) |
| | EB826 | Rm 2011 pdhB::Tn5_2 | Sm, Km | (Pobigaylo *et al.*, 2006) |
| | EB827 | Rm 2011 pdhB::Tn5_3 | Sm, Km | (Pobigaylo *et al.*, 2006) |
| | EB827 | Rm 2011 pdhB::Tn5_4 | Sm, Km | (Pobigaylo *et al.*, 2006) |
| *C. crescentus* | BM328 | CB15 + pSRKKm | Km, Tc | This work |
| | BM330 | CB15 + pSRKKm *divJ* (S.mel) | Km, Tc | This work |
| | BM331 | CB15 ΔdivJ-tet from (Skerker et al 2005) + pSRKKm (S.mel) | Km, Tc | This work |
| | BM333 | CB15 ΔdivJ-tet from (Skerker et al 2005) + pSRKKm divJ (S.mel) | Km, Tc | This work |
| *E. coli* | S17-1 | *recA*, *pro*, *hsdR*, *RP4-2-Tc::Mu-km::Tn7* | - | (Simon, *et al.*, 1983) |
| Bacteriophage | ΦM12 | Transducing phage | | (Finan, *et al.*, 1984) |
| Plasmids | | | | |
| General purpose vectors | pNTPS138 | Suicide vector, *oriT*, *sacB* | Km | D. Alley |
| | pMR10 | Broad host-range cloning vector, low copy number | Km | (Roberts, *et al.*, 1996) |
| | pSRKKm | pBBR1MCS-2-derived broad-host-range expression vector containing *lac* promoter and *lacI*$^q$, *lacZ*$^+$ | Km | (Khan, *et al.*, 2008) |
| | pSRKGm | pBBR1MCS-5-derived broad-host-range expression vector containing *lac* promoter and *lacI*$^q$, *lacZ*$^+$ | Gm | (Khan, *et al.*, 2008) |
| Deletion plasmids | pΔ*divJ* | pNPTS138-Tc deletion cassette for *divJ* | Km, Tc | This work |
| | pΔ*divJ* markerless | pNPTS138 deletion cassette for *divJ* | Km | This work |
| | pΔ*pleC* | pNPTS138-Tc deletion cassette for *pleC* | Km, Tc | This work |
| | pΔ*divK* | pNPTS138-Tc deletion cassette for *divK* | Km, Tc | This work |
| Overexpression plasmids | pSRKKm*ctrA* | pSRKKm containing *ctrA* inserted between NdeI and KpnI sites | Km | This work |
| | pSRKKm*divJ* | pSRKKm containing *divJ* inserted between NdeI and XhoI sites | Km | This work |
| | pSRKGm*divJ* | pSRKGm containing *divJ* inserted between NdeI and XhoI sites | Gm | This work |
| | pSRKKm*pleC* | pSRKKm containing *pleC* inserted between NdeI and KpnI sites | | |
| | pSRKKm *divK* | pSRKKm containing *divK* inserted between NdeI and KpnI sites | Km | This work |
| | pSRKKm *divK* D53A | pSRKKm containing *divK* D53A inserted between NdeI and KpnI sites | Km | This work |
| | pSRKKm *divJ* H249A | pSRKKm containing *divJ* H249A inserted between NdeI and XhoI sites | Km | This work |
| GFP-tagging plasmids | pGEE | pG18mob derivative; promoterless *eGFP* gene, it integrates between the *exoP* terminator and the *thiD* gene | Gm | Elizaveta Krol (unpublished) |
| | pSRmig | pSRPP18 derivative; promoterless *lacZ* replaced with promoterless *egfp* | Km | (McIntosh *et al.*, 2009) |
| | pSRmigPsinR171mutcc | pSRmig derivative; containing a mutated constitutive sinR promoter | Km | Matthew McIntosh (unpublished) |
| | pGECE | integrative vector overexpressing EGFP | Gm | This work |
| Reporter plasmid | pJS70 | *pilA* promoter–*lacZ* fusion in pRKlac290 | Tc | (Skerker & Shapiro 2000) |
| | pRKlac290-$P_{Smc00360}$ | *SMc0360* promoter–*lacZ* fusion in pRKlac290 | Tc | This work |
| | pRKlac290-$P_{Smc00949}$ | *SMc0949* promoter–*lacZ* fusion in pRKlac290 | Tc | This work |

## References


Abel, S., Chien, P., Wassmann, P., Schirmer, T., Kaever, V., Laub, M.T., *et al.* (2011) Regulatory cohesion of cell cycle and cell differentiation through interlinked phosphorylation and second messenger networks. *Mol Cell* **43**: 550–560.

Alley, M.R., Gomes, S.L., Alexander, W., and Shapiro, L (1991) Genetic analysis of a temporally transcribed chemotaxis gene cluster in Caulobacter crescentus. *Genetics* **129**: 333–341.

Barbieri, C.M., and Stock, A.M. (2008) Universally applicable methods for monitoring response regulator aspartate phosphorylation both in vitro and in vivo using Phos-tag-based reagents. *Anal Biochem* **376**: 73–82.

Barnett, M J, Hung, D Y, Reisenauer, A, Shapiro, L, and Long, S R (2001) A homolog of the CtrA cell cycle regulator is present and essential in Sinorhizobium meliloti. *J Bacteriol* **183**: 3204–3210.

Bellefontaine, A.-F., Pierreux, C.E., Mertens, P., Vandenhaute, J., Letesson, J.-J., and Bolle, X. De (2002) Plasticity of a transcriptional regulation network among alpha-proteobacteria is supported by the identification of CtrA targets in Brucella abortus. *Mol Microbiol* **43**: 945–960.

Biondi, E.G., Reisinger, S.J., Skerker, Jeffrey M, Arif, M., Perchuk, B.S., Ryan, K.R., and Laub, M.T. (2006) Regulation of the bacterial cell cycle by an integrated genetic circuit. *Nature* **444**: 899–904.

Biondi, E.G., Skerker, Jeffrey M, Arif, M., Prasol, M.S., Perchuk, B.S., and Laub, M.T. (2006) A phosphorelay system controls stalk biogenesis during cell cycle progression in Caulobacter crescentus. *Mol Microbiol* **59**: 386–401.

Bird, T.H., and MacKrell, A. (2011) A CtrA homolog affects swarming motility and encystment in Rhodospirillum centenum. *Arch Microbiol* **193**: 451–459.

Brilli, M., Fondi, M., Fani, R., Mengoni, A., Ferri, L., Bazzicalupo, M., and Biondi, E.G. (2010) The diversity and evolution of cell cycle regulation in alpha-proteobacteria: a comparative genomic analysis. *BMC Syst Biol* **4**: 52.

Brown, P.J.B., Pedro, M.A. de, Kysela, D.T., Henst, C. Van der, Kim, J., Bolle, X. De, *et al.* (2012) Polar growth in the Alphaproteobacterial order Rhizobiales. *Proc Natl Acad Sci USA* **109**: 1697–1701.

Brune, I., Becker, Anke, Paarmann, D., Albersmeier, A., Kalinowski, J., Pühler, Alfred, and Tauch, A. (2006) Under the influence of the active deodorant ingredient 4-hydroxy-3-methoxybenzyl alcohol, the skin bacterium Corynebacterium jeikeium moderately responds with differential gene expression. *J Biotechnol* **127**: 21–33.

Burton, G.J., Hecht, G.B., and Newton, A (1997) Roles of the histidine protein kinase pleC in Caulobacter crescentus motility and chemotaxis. *J Bacteriol* **179**: 5849–5853.

Campbell, G.R.O., Sharypova, L.A., Scheidle, H., Jones, K.M., Niehaus, K., Becker, Anke, and Walker, Graham C (2003) Striking complexity of lipopolysaccharide defects in a collection of Sinorhizobium meliloti mutants. *J Bacteriol* **185**: 3853–3862.

Collier, J., McAdams, H.H., and Shapiro, Lucy (2007) A DNA methylation ratchet governs progression through a bacterial cell cycle. *Proc Natl Acad Sci USA* **104**: 17111–17116.

Curtis, P.D., and Brun, Yves V (2010) Getting in the loop: regulation of development in Caulobacter crescentus. *Microbiol Mol Biol Rev* **74**: 13–41.

Domian, I.J., Quon, K.C., and Shapiro, L (1997) Cell type-specific phosphorylation and proteolysis of a transcriptional regulator controls the G1-to-S transition in a bacterial cell cycle. *Cell* **90**: 415–424.

Dondrup, M., Goesmann, A., Bartels, D., Kalinowski, J., Krause, L., Linke, B., *et al.* (2003) EMMA: a platform for consistent storage and efficient analysis of microarray data. *J Biotechnol* **106**: 135–146.

Ehrhardt, D.W., Atkinson, E.M., and Long, S R (1992) Depolarization of alfalfa root hair membrane potential by Rhizobium meliloti Nod factors. *Science* **256**: 998–1000.

Ferri, L., Gori, A., Biondi, E.G., Mengoni, A., and Bazzicalupo, M. (2010) Plasmid electroporation of Sinorhizobium strains: The role of the restriction gene hsdR in type strain Rm1021. *Plasmid* **63**: 128–135.

Fields, A.T., Navarrete, C.S., Zare, A.Z., Huang, Z., Mostafavi, M., Lewis, J.C., *et al.* (2012) The conserved polarity factor podJ1 impacts multiple cell envelope-associated functions in Sinorhizobium meliloti. *Mol Microbiol* **84**: 892–920.

Finan, T.M., Hartweig, E., LeMieux, K., Bergman, K., Walker, G C, and Signer, E.R. (1984) General transduction in Rhizobium meliloti. *J Bacteriol* **159**: 120–124.

Finan, T.M., Wood, J.M., and Jordan, D.C. (1983) Symbiotic properties of C4-dicarboxylic acid transport mutants of Rhizobium leguminosarum. *J Bacteriol* **154**: 1403–1413.

Fioravanti, A., Fumeaux, C., Mohapatra, S.S., Bompard, C., Brilli, M., Frandi, A., *et al.* (2013) DNA Binding of the Cell Cycle Transcriptional Regulator GcrA Depends on N6-Adenosine Methylation in Caulobacter crescentus and Other Alphaproteobacteria. *PLoS Genet* **9**: e1003541.

Galibert, F, Finan, T.M., Long, S R, Puhler, A., Abola, P., Ampe, F., *et al.* (2001) The composite genome of the legume symbiont Sinorhizobium meliloti. *Science* **293**: 668–672.

Gibson, K.E., Barnett, Melanie J, Toman, C.J., Long, Sharon R, and Walker, Graham C (2007) The symbiosis regulator CbrA modulates a complex regulatory network affecting the flagellar apparatus and cell envelope proteins. *J Bacteriol* **189**: 3591–3602.

Gibson, K.E., Campbell, G.R., Lloret, J., and Walker, Graham C (2006) CbrA is a stationary-phase regulator of cell surface physiology and legume symbiosis in Sinorhizobium meliloti. *J Bacteriol* **188**: 4508–4521.

Greene, S.E., Brilli, M., Biondi, E.G., and Komeili, A. (2012) Analysis of the CtrA pathway in Magnetospirillum reveals an ancestral role in motility in alphaproteobacteria. *J Bacteriol* **194**: 2973–2986.

Griffitts, J.S., Carlyon, R.E., Erickson, J.H., Moulton, J.L., Barnett, Melanie J, Toman, C.J., and Long, Sharon R (2008) A Sinorhizobium meliloti osmosensory two-component system required for cyclic glucan export and symbiosis. *Mol Microbiol* **69**: 479–490.

Hallez, R., Bellefontaine, A.-F., Letesson, J.-J., and Bolle, X. De (2004) Morphological and functional asymmetry in alpha-proteobacteria. *Trends Microbiol* **12**: 361–365.

Hallez, R., Mignolet, J., Mullem, V. Van, Wery, M., Vandenhaute, J., Letesson, J.-J., *et al.* (2007) The asymmetric distribution of the essential histidine kinase PdhS indicates a differentiation event in Brucella abortus. *EMBO J* **26**: 1444–1455.

Hecht, G.B., Lane, T., Ohta, N, Sommer, J.M., and Newton, A (1995) An essential single domain response regulator required for normal cell division and differentiation in Caulobacter crescentus. *EMBO J* **14**: 3915–3924.

Hirsch, A.M., Bang, M., and Ausubel, F.M. (1983) Ultrastructural analysis of ineffective alfalfa nodules formed by nif::Tn5 mutants of Rhizobium meliloti. *J Bacteriol* **155**: 367–380.

Horvath, B., Kondorosi, E, John, M., Schmidt, J., Török, I., Györgypal, Z., *et al.* (1986) Organization, structure and symbiotic function of Rhizobium meliloti nodulation genes determining host specificity for alfalfa. *Cell* **46**: 335–343.

Hung, Dean Y, and Shapiro, Lucy (2002) A signal transduction protein cues proteolytic events critical to Caulobacter cell cycle progression. *Proc Natl Acad Sci USA* **99**: 13160–13165.

Iniesta, A.A., McGrath, P.T., Reisenauer, Ann, McAdams, H.H., and Shapiro, Lucy (2006) A phospho-signaling pathway controls the localization and activity of a protease complex critical for bacterial cell cycle progression. *Proc Natl Acad Sci USA* **103**: 10935–10940.
Jenal, U, and Fuchs, T. (1998) An essential protease involved in bacterial cell-cycle control. *EMBO J* **17**: 5658–5669.

Jones, S.E., Ferguson, N.L., and Alley, M.R. (2001) New members of the ctrA regulon: the major chemotaxis operon in Caulobacter is CtrA dependent. *Microbiology (Reading, Engl)* **147**: 949–958.

Khan, S.R., Gaines, J., Roop, R.M., 2nd, and Farrand, S.K. (2008) Broad-host-range expression vectors with tightly regulated promoters and their use to examine the influence of TraR and TraM expression on Ti plasmid quorum sensing. *Appl Environ Microbiol* **74**: 5053–5062.

Kim, J., Heindl, J.E., and Fuqua, C. (2013) Coordination of Division and Development Influences Complex Multicellular Behavior in Agrobacterium tumefaciens. *PLoS ONE* **8**: e56682.

Kobayashi, H., Nisco, N.J. De, Chien, P., Simmons, L.A., and Walker, Graham C (2009) Sinorhizobium meliloti CpdR1 is critical for co-ordinating cell cycle progression and the symbiotic chronic infection. *Mol Microbiol* **73**: 586–600.

Laub, M.T., Chen, S.L., Shapiro, Lucy, and McAdams, H.H. (2002) Genes directly controlled by CtrA, a master regulator of the Caulobacter cell cycle. *Proc Natl Acad Sci USA* **99**: 4632–4637.

Letunic, I., Doerks, T., and Bork, P. (2012) SMART 7: recent updates to the protein domain annotation resource. *Nucleic Acids Res* **40**: D302–305.

McGrath, P.T., Iniesta, A.A., Ryan, K.R., Shapiro, Lucy, and McAdams, H.H. (2006) A dynamically localized protease complex and a polar specificity factor control a cell cycle master regulator. *Cell* **124**: 535–547.

McIntosh, M., Meyer, S., and Becker, Anke (2009) Novel Sinorhizobium meliloti quorum sensing positive and negative regulatory feedback mechanisms respond to phosphate availability. *Mol Microbiol* **74**: 1238–1256.

Mergaert, P., Uchiumi, T., Alunni, Benoît, Evanno, G., Cheron, A., Catrice, O., *et al.* (2006) Eukaryotic control on bacterial cell cycle and differentiation in the Rhizobium-legume symbiosis. *Proc Natl Acad Sci USA* **103**: 5230–5235.

Mignolet, J., Henst, C. Van der, Nicolas, C., Deghelt, M., Dotreppe, D., Letesson, J.-J., and Bolle, X. De (2010) PdhS, an old-pole-localized histidine kinase, recruits the fumarase FumC in Brucella abortus. *J Bacteriol* **192**: 3235–3239.

Müller, P., Hynes, M., Kapp, D., Niehaus, K., and Pühler, Alfred (1988) Two classes of Rhizobium meliloti infection mutants differ in exopolysaccharide production and in coinoculation properties with nodulation mutants. *Mol Gen Genet* **211**: 17–26.

Ohta, N, Lane, T., Ninfa, E.G., Sommer, J.M., and Newton, A (1992) A histidine protein kinase homologue required for regulation of bacterial cell division and differentiation. *Proc Natl Acad Sci USA* **89**: 10297–10301.

Ohta, Noriko, and Newton, Austin (2003) The core dimerization domains of histidine kinases contain recognition specificity for the cognate response regulator. *J Bacteriol* **185**: 4424–4431.

Paul, R., Jaeger, T., Abel, S., Wiederkehr, I., Folcher, M., Biondi, E.G., *et al.* (2008) Allosteric regulation of histidine kinases by their cognate response regulator determines cell fate. *Cell* **133**: 452–461.

Pobigaylo, N., Wetter, D., Szymczak, S., Schiller, U., Kurtz, S., Meyer, F., *et al.* (2006) Construction of a large signature-tagged mini-Tn5 transposon library and its application to mutagenesis of Sinorhizobium meliloti. *Appl Environ Microbiol* **72**: 4329–4337.

Quon, K.C., Marczynski, G.T., and Shapiro, L (1996) Cell cycle control by an essential bacterial two-component signal transduction protein. *Cell* **84**: 83–93.

Roberts, R.C., Toochinda, C., Avedissian, M., Baldini, R.L., Gomes, S.L., and Shapiro, L (1996) Identification of a Caulobacter crescentus operon encoding hrcA, involved in negatively regulating heat-inducible transcription, and the chaperone gene grpE. *J Bacteriol* **178**: 1829–1841.

Ryan, K.R., Huntwork, S., and Shapiro, Lucy (2004) Recruitment of a cytoplasmic response regulator to the cell pole is linked to its cell cycle-regulated proteolysis. *Proc Natl Acad Sci USA* **101**: 7415–7420.

Ryan, K.R., Judd, E.M., and Shapiro, Lucy (2002) The CtrA response regulator essential for Caulobacter crescentus cell-cycle progression requires a bipartite degradation signal for temporally controlled proteolysis. *J Mol Biol* **324**: 443–455.

Sadowski, C., Wilson, D., Schallies, K., Walker, G., and Gibson, K.E. (2013) The Sinorhizobium meliloti sensor histidine kinase CbrA contributes to free-living cell cycle regulation. *Microbiology (Reading, Engl)* .

Sambrook, J., Fritsch, E.F., and Maniatis, T. (1989) *Molecular cloning: a laboratory manual*. Cold Spring Harbor Laboratory.

Schneider, C.A., Rasband, W.S., and Eliceiri, K.W. (2012) NIH Image to ImageJ: 25 years of image analysis. *Nat Methods* **9**: 671–675.

Serrania, J., Vorhölter, F.-J., Niehaus, K., Pühler, Alfred, and Becker, Anke (2008) Identification of Xanthomonas campestris pv. campestris galactose utilization genes from transcriptome data. *J Biotechnol* **135**: 309–317.

Sharypova, L.A., Niehaus, K., Scheidle, H., Holst, O., and Becker, Anke (2003) Sinorhizobium meliloti acpXL mutant lacks the C28 hydroxylated fatty acid moiety of lipid A and does not express a slow migrating form of lipopolysaccharide. *J Biol Chem* **278**: 12946–12954.

Simon, R., Priefer, U., and Pühler, A. (1983) A Broad Host Range Mobilization System for In Vivo Genetic Engineering: Transposon Mutagenesis in Gram Negative Bacteria. *Nat Biotech* **1**: 784–791.

Skerker, J M, and Shapiro, L (2000) Identification and cell cycle control of a novel pilus system in Caulobacter crescentus. *EMBO J* **19**: 3223–3234.

Skerker, Jeffrey M, Perchuk, B.S., Siryaporn, A., Lubin, E.A., Ashenberg, O., Goulian, M., and Laub, M.T. (2008) Rewiring the specificity of two-component signal transduction systems. *Cell* **133**: 1043–1054.

Skerker, Jeffrey M, Prasol, M.S., Perchuk, B.S., Biondi, E.G., and Laub, M.T. (2005) Two-component signal transduction pathways regulating growth and cell cycle progression in a bacterium: a system-level analysis. *PLoS Biol* **3**: e334.

Tsokos, C.G., Perchuk, B.S., and Laub, M.T. (2011) A dynamic complex of signaling proteins uses polar localization to regulate cell-fate asymmetry in Caulobacter crescentus. *Dev Cell* **20**: 329–341.

Velde, W. Van de, Zehirov, G., Szatmari, A., Debreczeny, M., Ishihara, H., Kevei, Z., *et al.* (2010) Plant peptides govern terminal differentiation of bacteria in symbiosis. *Science* **327**: 1122–1126.

Wang, D., Griffitts, J., Starker, C., Fedorova, E., Limpens, E., Ivanov, S., *et al.* (2010) A nodule-specific protein secretory pathway required for nitrogen-fixing symbiosis. *Science* **327**: 1126–1129.

Wheeler, R.T., and Shapiro, L (1999) Differential localization of two histidine kinases controlling bacterial cell differentiation. *Mol Cell* **4**: 683–694.

Wortinger, M., Sackett, M.J., and Brun, Y V (2000) CtrA mediates a DNA replication checkpoint that prevents cell division in Caulobacter crescentus. *EMBO J* **19**: 4503–4512.

Wu, J., Ohta, N, and Newton, A (1998) An essential, multicomponent signal transduction pathway required for cell cycle regulation in Caulobacter. *Proc Natl Acad Sci USA* **95**: 1443–1448.

# Chapter 4

# Conclusions and Future Work

In this thesis I describe my development of the first method to synchronize cell populations of the alpha-proteobacterial legume symbiont, *S. meliloti* (Chapter 2). I also demonstrate the overall conservation of cell cycle regulated gene expression between *C. crescentus* and *S. meliloti* through microarray analysis (1). However, analysis of cell cycle gene expression also revealed intriguing divergences in cell cycle regulation between the two alpha-proteobacterial species. Of the 462 cell cycle regulated transcripts identified in *S. meliloti,* 72% were not conserved between *C. crescentus* and *S. meliloti.* This indicates that the cell cycle regulation of transcription has specially evolved in *S. meliloti,* perhaps to fit its unique dual soil-dwelling and symbiotic lifestyle. Indeed, analysis of CtrA and DnaA binding motif conservation in genes with cell cycle regulated transcripts in *S. meliloti* revealed a large divergence between the putative regulons of CtrA and DnaA in *S. meliloti* and *C. crescentus.* Although most DnaA binding sites were not well conserved between the 11 alpha-proteobacterial species examined, the conservation of CtrA binding motifs was evolutionarily constrained, with greater conservation of *S. meliloti* CtrA binding sites in organisms that are either more closely related to *S. meliloti* or have more similar lifestyles.

In Chapter 3, I describe the role of the cell cycle in a specific *S. meliloti* cellular differentiation event that occurs during symbiosis with *M. sativa.* In order to differentiate into a nitrogen-fixing bacteroid, *S. meliloti* must undergo endoreduplication of the genome, which requires a de-coupling of DNA replication and cell division and therefore an interesting deviation from the normal cell cycle program. In *C. crescentus,* CtrA negative regulates DNA replication initiation by

binding to and silencing the origin of replication. If this mechanism of cell cycle control is conserved in *S. meliloti,* the cell cycle regulated silencing of the origin would need to be permanently relieved for endoreduplication to occur. To explore the hypothesis that specific regulation of the essential master cell cycle regulator CtrA must occur to allow for endoreduplication, I tested the effects of depletion of CtrA in *S. meliloti* in collaboration with Emmanuele Biondi. We discovered that CtrA depletion results in elongated and branched cells with endoreduplicated genomes, suggesting that down-regulation of CtrA could be a method to produce these phenotypes in bacteroids during symbiosis. This is consistent with the previous finding that CtrA is nearly completely absent from bacteroid cells (Appendix B). Further supporting the importance of proper regulation of CtrA in *S. meliloti* during symbiosis, we discovered that, although *C. crescentus ctrA* expressed under its own promoter can complement *S. meliloti ctrA* during free-living growth, it cannot complement during symbiosis (2). Suspecting that either the *C. crescentus ctrA* promoter region or the *C. crescentus* CtrA protein could regulated properly in *S. meliloti* during symbiosis, we tested the symbiotic efficiency of two strains expressing either *C. crescentus ctrA* from the *S. meliloti ctrA* promoter (BM557) or *S. meliloti ctrA* from the *C. crescentus ctrA* promoter (BM561). The lack of severe symbiotic defect in either of these strains poses a regulatory paradox begging the question of how the *C. crescentus ctrA* promoter region or coding region alone can be largely sufficient for symbiosis when paired with complimentary *S. meliloti ctrA* coding or promoter region, but when combined cause such a severe symbiotic defect.

**How does CtrA regulate cell cycle progression in *S. meliloti*?**

Previous studies have demonstrated that CtrA is essential in *S. meliloti* and results presented in these new experiments demonstrate that depletion of CtrA results in serious cell cycle defects and eventually loss of viability. Furthermore, my microarray cell cycle gene expression analysis of synchronized cultures of *S. meliloti* revealed the importance of transcriptional regulation of cell cycle regulation in *S. meliloti* and identified many putative CtrA target genes that demonstrate cell cycle regulated gene expression. The genes identified by my analysis include genes controlling the important cell cycle functions of flagella biosynthesis, cell division and regulation of DNA replication, but the specific action of CtrA on these putative target genes needs to be verified *in vivo.*

***Does CtrA regulate flagella biogenesis and chemotaxis during the cell cycle?*** My gene expression microarray studies revealed that the expression of genes required for flagella biosynthesis and chemotaxis in *S. meliloti* is cell cycle regulated and restricted to the later stages of the cell cycle, which is has also been observed in *C. crescentus* (1). In *C. crescentus,* CtrA directly activates the expression of flagella and chemotaxis genes in predivisional cells by binding the upstream regulatory regions of these genes and activating their transcription (3). This direct regulation does not appear to be conserved in *S. meliloti,* as my binding motif analysis of genes with cell cycle regulated transcripts revealed that CtrA binding motifs are only present in the promoter regions of the flagellin genes *flaABCD* (Fig. 2.5). However, I did identify putative CtrA binding sites in the promoter region of *rem,* which is a regulator of motility during exponential growth in *S. meliloti* (4). During exponential

growth of *S. meliloti* Rem is activated by VisNR and directly activates the expression of class II flagellar genes (*flg, flh, fli, mot*), which then activate the transcription of class III genes (*che, fla*). The CtrA binding motifs present upstream of *rem* in *S. meliloti* are well conserved in the other alpha-proteobacteria we surveyed (Figure 2.5). It therefore seems likely that CtrA integrates cell cycle regulated control of the expression of these motility genes by regulating timing of *rem* transcription during the cell cycle.

The cell cycle regulated control of the expression of flagellar and chemotaxis genes by CtrA in *S. meliloti* has yet to be shown directly. A simple experiment to show this would be to visualize flagella in *S. meliloti* after depletion of CtrA. If CtrA was necessary for expression genes required for flagella biosynthesis, then *S. meliloti* depleted of CtrA should have less or no peritrichously localized flagella. Furthermore, the presence of CtrA binding motifs in the upstream regulatory region of the *rem* gene does not directly prove that CtrA regulates the transcription of *rem.* To test this, these binding sites must be experimentally verified either *in vitro* by DNA footprinting assays or *in vivo* by chromatin IP experiments, such as ChIP-seq. A ChIP-seq experiment would be incredibly informative, as it would not only help verify putative CtrA binding sites identified in ours and previous analysis, but might also identify new transcriptional targets of CtrA (5, 6). To discern whether CtrA serves as an activator or repressor of flagella and chemotaxis gene expression, microarray gene expression studies should be performed in *S. meliloti* depleted of CtrA, perhaps using BM49 described in Chapter 3 or a temperature sensitive allele of CtrA as was used in similar studies in *C. crescentus* (1).

***How is CtrA involved in regulation of the timing of cell division in S. meliloti?*** In addition to regulating the expression of flagella and chemotaxis genes in *C. crescentus,* CtrA also regulates the timing of septum formation through regulation of the transcription of *ftsZ* and *ftsW,* genes required for the cell division apparatus (3). CtrA directly activates the transcription of *ftsW,* but CtrA regulation of *ftsZ* transcription is more complicated as CtrA both activates and represses *ftsZ* transcription at different times in the cell cycle (3, 7). The CtrA binding motifs found in the promoter regions of *ftsZ* and *ftsW* in *C. crescentus* are not conserved in *S. meliloti (*Figure 2.5). Instead, CtrA binding motifs are present in the upstream regulatory regions of *S. meliloti* division genes *ftsK* and *minCD.* Interestingly, all organisms we surveyed that contain homologs of the gene encoding MinC, which is part of the Min system for regulation of septum formation, also have conserved CtrA binding motifs in the promoter region of *minC* (Figure 2.5). *C. crescentus* does not have homologs of the Min system (*minCDE*) and instead uses MipZ to regulated the location of the septum during division (8). In *S. meliloti* and *E. coli,* however the MinCDE proteins act together to inhibit Z ring formation at the poles and ensure that the contractile Z ring is placed at mid-cell (9, 10). Although the *minCDE* genes are transcribed as an operon, our data indicate that *minC* expression greatly precedes that minDE, which could be explained by a RIME element in the intergenic region between *minC* and *minD* (10, 11). Nonetheless, the conservation of CtrA binding motifs in the promoter region of the *minCDE* operon strongly suggests may regulate their expression during the cell cycle (Fig. 2.5). The ChIP-seq experiment or DNA footprinting assays are needed to verify that these sites are indeed bound by

CtrA in *S. meliloti* and transcriptional profiling if *S. meliloti* depleted of CtrA will elucidate whether CtrA acts to induce or repress the expression of the *minCDE* operon.

***Is CtrA a negative regulator of DNA replication initiation in S. melioti?*** An important role of CtrA in *C. crescentus* is silencing of the origin of replication in swarmer cells. CtrA binds five sites on the origin of replication and thereby prevents initiation of DNA replication by the initiation protein DnaA (12). The presence of these binding sites has not been confirmed in the *S. meliloti* origin although preliminary *in silico* analyses indicate that they may be absent. The phenotype of highly elevated DNA content induced upon depletion of CtrA in *S. meliloti* suggest that CtrA may negatively regulate DNA replication initiation in *S. meliloti,* but this phenotype could also be explained by the loss of CtrA activity causing a block in cell division. The previously mentioned ChIP-seq experiment to look for CtrA binding sites in the *S. meliloti* genome would help to determine the presence of CtrA regulatory sites in the *S. meliloti* origin of replication.

**Mechanisms of CtrA regulation during the *S. meliloti* free-living cell cycle and during symbiosis.**

Much is not understood about the regulation of CtrA activity in *S. meliloti.* In *C. crescentus* the activity of CtrA is subject to a complex regulatory circuit including different modes of transcriptional and post-transcriptional regulation(13, 14). Initial work, including single gene studies and bioinformatics analysis, had begun to outline the modes of CtrA regulation in *S. meliloti*, but much was left to learn about CtrA regulation in *S. meliloti.* The results of my microarray analysis of cell cycle gene

expression in *S. meliloti* suggest that *ctrA* may undergo a different mechanism of transcriptional regulation in *S. meliloti* as observed in *C. crescentus* since *S. meliloti ctrA* expression did not peak at the same point in the cell cycle as *C. crescentus ctrA.* My work has also indicated that, unlike in *C. crescentus,* degradation of CtrA in *S. meliloti* is likely to be essential. In addition, symbiotic assays I performed with *S. meliloti* expressing *C. crescentus ctrA* indicate that *S. meliloti*-specific regulation of CtrA is crucial during symbiosis. Additional work is required to further elucidate the mechanisms of CtrA regulation in both the free-living cell cycle and during symbiosis with *M. sativa.*

***Is CtrA phosphorylation governed by the same mechanism in S. meliloti as in C. crescentus?*** One of the most important modes of regulation of CtrA activity in *C. crescentus* is via cell-type dependent phosphorylation and proteolysis. Both the phosphorylation and proteolysis of CtrA are controlled by a phosphorelay centered on the membrane associated histidine kinase CckA. Activation of CckA by DivL in the swarmer cell compartment stimulates the kinase activity of CckA and leads to the phosphorylation of CtrA and CpdR through the ChpT phosphotransferase (13). This both activates CtrA because phosphorylated CtrA has a higher affinity for its DNA targets (15). Phosphorylated CpdR is quickly degraded by the protease complex ClpXP (16). This leads to the stabilization of CtrA because active CpdR stimulates CtrA degradation by ClpXP (16). In stalked cells the activation of CckA by DivL is prevented by the phosphorylated response regulator DivK and CckA instead acts as a phosphatase siphoning phosphoryl groups back up the phosphorelay resulting in unphosphorylated CtrA and CpdR (13). The histidine kinase DivJ and the

phosphatase PleC act to regulate the phosphorylation status of DivK in each cell type (13). Un-phosphorylated CpdR activates the proteolysis of CtrA by a complex mechanism involving the second messenger cyclic di-GMP (17), which alleviates the repression of the origin by CtrA and allows of DNA replication initiation in stalked cells.

The genes involved in this CtrA regulatory network are well conserved in *S. meliloti,* but the conservation of their function has not fully been tested (6). As in *C. crescentus,* phosphorylated DivK acts negatively on CtrA and is localized exclusively to the old cell pole (stalked pole in *C.crescentus*) (18). Unlike in *C. crescentus,* both DivK phosphorylation and de-phosphorylation are essential in *S. meliloti* (Appendix B). Also *S. meliloti* contains CbrA, an additional cognate kinase to DivK besides DivJ that is not present in *C. crescentus* (19). Both the *S. meliloti ΔdivJ-ΔcbrA* double mutant and the *ΔpleC* mutant are inviable (Appendix B). *In vivo* phosphorylation experiments have also indicated that these factors have conserved kinase (*divK, cbrA,* divJ) and phosphatase (*pleC* ) activities (19) (Appendix B). These data suggest that although these factors have similar functions in CtrA regulation in *S. meliloti,* the specific wiring of the regulatory network may be divergent from that of *C. crescentus.* The cell synchronization method described in this thesis will make it possible to determine when these regulatory proteins are present during the *S. meliloti* cell cycle via Western blot analysis. It will also be possible to determine the phosphorylation pattern of these two-component regulators during the *S. meliloti* cell cycle now that pure populations of *S. meliloti* in different stages of the cell cycle can be obtained.

***Is regulated proteolysis of CtrA essential in S. meliloti?*** Data presented in Chapter 3 indicate that unlike *C. crescentus,* cell cycle regulated proteolysis of CtrA may be essential in *S. meliloti* (16). In *C. crescentus, ctrADD* and *ctrAΔM3* alleles produce stable versions of CtrA that are resistant to proteolysis by ClpXP (16). We constructed correspnding *S. meliloti* versions of these alleles, but were not able to successfully introduce them to *S. meliloti* (Chapter 3). This indicates that the putative stable CtrA alleles*, ctrADD* and *ctrAΔM3* are lethal in *S. meliloti* and suggests that regulated proteolysis of CtrA by ClpXP is essential. Additional experiments need to be performed to lend stronger support to this theory. The phenotypes produced by expression of *S. meliloti ctrADD* and *ctrAΔM3* from a tightly regulated inducible promoter should be assessed. If severe cell cycle defects are observed upon induction of a stable allele of *ctrA,* then it is likely that CtrA proteolysis is indeed essential. To test if CtrA proteolysis is dependent on ClpXP in *S. meliloti,* both the phenotype and CtrA levels in *S. meliloti* depleted of ClpX should be assessed. Cell synchronization can also be utilized to monitor CtrA, CpdR1 and ClpXP protein levels during the cell cycle to gain a better understanding of the timing of CtrA proteolysis.

***How is ctrA transcriptionally regulated during the cell cycle and symbiosis?*** It has been previously shown that *S. meliloti ctrA* shares a similar promoter structure as *C. crescentus ctrA* with transcription initiating from two separate promoters P1 and P2 (2, 20). DNase footprinting analysis in *S. meliloti* demonstrated that *C. crescentus* CtrA can bind to five sites in the *S. meliloti ctrA* promoter region including the -35 regions of P1 and P2 as well as the +1 region of

P1 and the -70 and -150 regions of P2 (2). In *C. crescentus* CtrA is transcribed from the P1 and P2 promoters at different points during the cell cycle (20). After the initiation of DNA replication, *ctrA* transcription is activated at low levels from the P1 promoter by the transcriptional regulator GcrA. Once CtrA expression begins from P1, CtrA binds the -35 region of the P2 promoter with high affinity to activate high levels of transcription from P2 (20). It has also been shown that CtrA binds the -10 region of the P1 promoter with lower affinity to repress transcription from P1 (20). It is possible that a similar mechanism controls the transcription of *S. meliloti ctrA* although the presence of five CtrA binding sites in the *S. meliloti ctrA* promoter suggests possible differences in regulation. In fact, my gene expression analysis in synchronous cultures of *S. meliloti* revealed that *ctrA* transcription is activated later in the cell cycle and not as strongly in *S. meliloti* than *C. crescentus.* To assess if *S. meliloti ctrA* is transcribed at different points in the cell cycle from the P1 and P2 promoters, transcriptional *lacZ* fusions to the two promoters of *S. meliloti* CtrA should be constructed and their activity should be monitored in synchronized *S. meliloti* culture.

My work has also demonstrated that *S. meliloti*-specific regulation of CtrA is required during symbiosis. Although *C. crescentus ctrA* can complement *S. meliloti ctrA* in the free living state, *C. crescentus ctrA* expressed from its own promoter region cannot complement during symbiosis. Subsequent experiments trying to discern the contribution of differences in transcriptional or post-translational regulation to this inability to complement during symbiosis raised more questions than they answered. Only relatively subtle symbiotic defects were seen in *S. meliloti*

strains expressing *C. crescentus* CtrA from the *S. meliloti ctrA* promoter region or vice versa. This poses the question of how a promoter region and a coding region that function relatively well individually during symbiosis, are no longer sufficient for symbiosis when combined. A complex regulatory mechanism of CtrA activity and expression during symbiosis is likely at work. It is possible that both the *C. crescentus ctrA* promoter region and coding region cannot be properly regulated during symbiosis and the redundancy present in the CtrA regulatory network protects against loss of one of these mechanisms of control, but not both. It is also possible that the *S. meliloti ctrA* mRNA is specifically regulated during symbiosis and, when the entire mRNA is derived from *C. crescentus ctrA,* that regulation is lost or perhaps the *C. crescentus ctrA* mRNA is degraded *in planta* and therefore non-functional. The mechanisms that control CtrA activity during symbiosis are still unclear, but will be elucidated by continued study of the *S. meliloti ctrA* regulatory network.

## References


1. Laub MT, McAdams HH, Feldblyum T, Fraser CM, & Shapiro L (2000) Global analysis of the genetic network controlling a bacterial cell cycle. *Science* 290(5499):2144-2148.
2. Barnett MJ, Hung DY, Reisenauer A, Shapiro L, & Long SR (2001) A homolog of the CtrA cell cycle regulator is present and essential in Sinorhizobium meliloti. *Journal of bacteriology* 183(10):3204-3210.
3. Laub MT, Chen SL, Shapiro L, & McAdams HH (2002) Genes directly controlled by CtrA, a master regulator of the Caulobacter cell cycle. *Proceedings of the National Academy of Sciences of the United States of America* 99(7):4632-4637.
4. Rotter C, Muhlbacher S, Salamon D, Schmitt R, & Scharf B (2006) Rem, a new transcriptional activator of motility and chemotaxis in Sinorhizobium meliloti. *Journal of bacteriology* 188(19):6932-6942.
5. Schluter JP*, et al.* (2013) Global mapping of transcription start sites and promoter motifs in the symbiotic alpha-proteobacterium Sinorhizobium meliloti 1021. *BMC genomics* 14:156.
6. Brilli M*, et al.* (2010) The diversity and evolution of cell cycle regulation in alpha-proteobacteria: a comparative genomic analysis. *BMC systems biology* 4:52.
7. Kelly AJ, Sackett MJ, Din N, Quardokus E, & Brun YV (1998) Cell cycle-dependent transcriptional and proteolytic regulation of FtsZ in Caulobacter. *Genes & development* 12(6):880-893.
8. Thanbichler M & Shapiro L (2006) MipZ, a spatial regulator coordinating chromosome segregation with cell division in Caulobacter. *Cell* 126(1):147-162.
9. Errington J, Daniel RA, & Scheffers DJ (2003) Cytokinesis in bacteria. *Microbiology and molecular biology reviews : MMBR* 67(1):52-65, table of contents.
10. Cheng J, Sibley CD, Zaheer R, & Finan TM (2007) A Sinorhizobium meliloti minE mutant has an altered morphology and exhibits defects in legume symbiosis. *Microbiology* 153(Pt 2):375-387.
11. Newbury SF, Smith NH, & Higgins CF (1987) Differential mRNA stability controls relative gene expression within a polycistronic operon. *Cell* 51(6):1131-1143.
12. Quon KC, Yang B, Domian IJ, Shapiro L, & Marczynski GT (1998) Negative control of bacterial DNA replication by a cell cycle regulatory protein that binds at the chromosome origin. *Proceedings of the National Academy of Sciences of the United States of America* 95(1):120-125.
13. Tsokos CG & Laub MT (2012) Polarity and cell fate asymmetry in Caulobacter crescentus. *Current opinion in microbiology* 15(6):744-750.
14. Collier J, McAdams HH, & Shapiro L (2007) A DNA methylation ratchet governs progression through a bacterial cell cycle. *Proceedings of the National Academy of Sciences of the United States of America* 104(43):17111-17116.

15. Siam R & Marczynski GT (2000) Cell cycle regulator phosphorylation stimulates two distinct modes of binding at a chromosome replication origin. *The EMBO journal* 19(5):1138-1147.
16. Iniesta AA, McGrath PT, Reisenauer A, McAdams HH, & Shapiro L (2006) A phospho-signaling pathway controls the localization and activity of a protease complex critical for bacterial cell cycle progression. *Proceedings of the National Academy of Sciences of the United States of America* 103(29):10935-10940.
17. Abel S*, et al.* (2011) Regulatory cohesion of cell cycle and cell differentiation through interlinked phosphorylation and second messenger networks. *Molecular cell* 43(4):550-560.
18. Lam H, Matroule JY, & Jacobs-Wagner C (2003) The asymmetric spatial distribution of bacterial signal transduction proteins coordinates cell cycle events. *Developmental cell* 5(1):149-159.
19. Sadowski C, Wilson D, Schallies K, Walker G, & Gibson KE (2013) The Sinorhizobium meliloti sensor histidine kinase CbrA contributes to free-living cell cycle regulation. *Microbiology*.
20. Domian IJ, Reisenauer A, & Shapiro L (1999) Feedback control of a master bacterial cell-cycle regulator. *Proceedings of the National Academy of Sciences of the United States of America* 96(12):6648-6653.